TWO-PHOTON SENSITIVE PROTECTING GROUPS FOR BIOLOGICAL APPLICATION

Karolina Anna Korzycka

St Cross College

Under the supervision of Prof. H. L. Anderson FRS

A thesis submitted to the board of the faculty of mathematical, physical & life sciences in partial fulfilment of the requirements for the degree of *Doctor of Philosophy* of the University of Oxford.

Trinity Term 2015

to Mikhail

ACKNOWLEDGEMENTS

„Innovation occurs at the boundaries between mind sets, not within the provincial territory of one knowledge and skill base" – Dorothy Leonard Barton

First and foremost I would like to acknowledge Prof. Harry Anderson who accepted me as his student. Harry, I wish to thank you for giving me the opportunity to explore the field of uncaging in your group and for providing me with a good balance between freedom and guidance during my Ph.D. Many results presented in this thesis would not have been achieved if not for multiple collaborations pursued within and outside the TOPBIO network (funded by the European Comission under the Marie Curie Initial Training Network), such as with Prof. Lucia Flamigni (photophysics), Prof. Alex Rebane (two-photon measurements) and Prof. Ole Paulsen (electrophysiology). Many thanks go to all other members of the network who I very much enjoyed meeting every couple of months at their research institutions.

I am very grateful to all my students: Joanna, Wilf and Eduardo. Not only did you provide me with loads of useful materials but, more importantly, you taught me everything that I know about building trust and mentorship. Fred, Adina, Yu and Golnaz – you opened my eyes for the essence of collaborative studies and were incredibly accommodating. I am also highly appreciative to Philip – for your contribution in laying foundations for the two-photon uncaging project, teaching me by example how to remain calm when things went wrong and patting me on the shoulder when things went right.

Many massive thanks go to the members of the Anderson group who created a very welcoming and friendly environment. I am truly grateful to Patrick and Julien − you two put a lot of effort to make the group's life vivid and kept me highly amused at work and during a great number of social events. I am pleased I had a chance to enjoy my time in the lab (and outside the department) with all of you: Sophie, Arjen, James W., Guzman, Cécile, Martin, Nun, Levon, René, Renee, Johnatan, Pengpeng, Christiane, Pablo, Kanok, Frank, Christie, Beth, Sarah, Kuoren, James R., Ismael and Tim. Special thanks must go to some Slavic spirits: Dima, Igor and Wojtek who made me feel a little bit less homesick. I am also obliged to everyone who made it possible for me to have a meal in each of 37 Colleges (and nibbles in the Hall of All Souls College). Some people claimed I could never do it!

I cannot imagine my time in Oxford without Michelle, Peter and Felix – thank you for being such good friends, bringing so much joy and care. I am also forever indebted to Ania and Edyta, who were always willing to lend an ear and supported me over the distance.

I must acknowledge my earlier chemistry teachers, Prof. M. Kozieł and Prof. E. Sochacka, whose guidance and passion led me to choose chemistry as a career. Nevertheless, I would have never got so far without the coaching and inspiration that I received from Serghei and Mikhail.

Finally, I want to thank my family. Mamo, Tato - dziękuję za wyrozumiałość, słowa otuchy i wsparcie, na które mogłam bezwarunkowo liczyć w każdej chwili; bez Was ta praca by nie powstała. Nie mogę też zapomnieć o wpływie moich dziadków, których dziś już z nami nie ma, a którzy byli moimi największymi kibicami.

TWO-PHOTON SENSITIVE PROTECTING GROUPS FOR BIOLOGICAL APPLICATION

Karolina Korzycka, St Cross College, University of Oxford

D.Phil. Thesis, Trinity Term 2015

Abstract

Caged compounds are a class of photosensitive reagents used to stimulate cells with spatial control down to a sub-cellular level, and millisecond temporal control. They comprise of biologically important molecule which is modified with a photolabile protecting group. In the absence of light, caged compounds are physiologically silent but irradiation with light induces the release of biologically active species. Illumination under two-photon conditions is particularly advantageous as it enables restriction of the photolysis volume to ~1 fL and it provides deeper penetration into scattering samples.

This thesis reports the development of new protecting groups for two-photon uncaging in neuroscience. Mechanistically, the deprotection in these novel groups is designed to operate *via* an intramolecular photoinduced electron transfer (PeT) between the absorbing unit (electron-donor) and the release module (electron-acceptor). The modular design of these cages ensures separation of absorption and release steps, and allows each process to be tuned and optimized independently.

Chapter 1 provides an introduction to the two-photon absorption phenomenon and a historic overview of the uncaging technique. It also discusses recent advances in the development of two-photon sensitive probes used in neuroscience.

Chapter 2 describes the exploration of molecular designs for novel protecting groups. A two-photon absorbing dye (electron-donor; fluorene dye) and three different release units (electron-acceptors; nitrobenzyl, pyridinium and phenacyl) were identified as suitable building blocks for the current project. Efficiency of the intramolecular electron transfer between chosen units was evaluated using model dyads which constitute covalently linked electron-donor and acceptor species.

Chapter 3 is devoted to the synthesis and photophysical evaluation of nitrobenzyl-based protecting group.

Chapter 4 describes the preparation of pyridinium-derived protecting group and demonstrates PeT-mediated release of tryptophan and GABA under one- and two-photon excitation. Hydrolytic instability of pyridinium esters is highlighted.

Chapter 5 reports the synthesis, hydrolytic stability and one-photon uncaging efficiency of phenacyl-based derivatives.

Chapter 6 discusses properties of developed caged compounds and compares them with other compounds reported in literature. It contains overall conclusions and outlook for the current project.

Chapter 7 details the experimental procedures and the characterization of compounds synthesized during this work.

PUBLICATIONS

Papers:

1. "*Two-photon sensitive protecting groups operating via intramolecular electron transfer: uncaging of GABA and tryptophan*"
K. A. Korzycka, P. M. Bennett, E. J. Cueto-Diaz, G. Wicks, M. Drobizhev, M. Blanchard-Desce, A. Rebane and H. L. Anderson, *Chem. Sci.*, 2015, **6**, 2419.

2. *"Model dyads for 2PA uncaging of a protecting group via photoinduced electron transfer"*
A. I. Ciuciu, K. A. Korzycka, W. J. M. Lewis, P. M. Bennett, H. L. Anderson and L. Flamigni, *Phys. Chem. Chem. Phys.*, 2015, **17**, 6554.

Posters:

1. *"Two-photon PeT mediated uncaging of aminoacids"*
K. A. Korzycka, P. M. Bennett and H. L. Anderson, presented at "Challenges in Organic Chemistry", ISACS14, Royal Society of Chemistry Conference, Shanghai, China, August 2014

2. *"Two-photon uncaging for biological application"*
K. A. Korzycka, P. M. Bennett and H. L. Anderson, presented at the Second Year Poster Presentations, Oxford, University of Oxford, England, October 2013

3. *"Two-photon uncaging for biological application"*
K. A. Korzycka, P. M. Bennett and H. L. Anderson, presented at "Photonic meets biology", Summerschool, Hersonissos, Crete, Greece, September 2013

Awards:

1. *Astra-Zeneca* Award at the Third Year Graduate Lecture Symposium, Department of Chemistry, University of Oxford, October 2014.

2. *Chemical Science* Poster Prize at the ISACS14 International Conference in Shanghai, China, August 2014.

3. *Eli Lilly* postgraduate award for achievements during the first year of a chemistry Ph.D., University of Oxford, October 2012.

ABBREVIATIONS AND SYMBOLS

δ_a – two-photon absorption cross-section

δ_u – two-photon uncaging cross-section

ΔG^* − activation energy

ΔG_{ET} – Gibbs free energy of electron transfer

ε − extinction coefficient

λ − reorganization energy (in Marcus theory); wavelength (in spectroscopy)

μ - micro

ϕ_u – uncaging quantum yield

A – acceptor; absorption

Ac – acetyl

aCSF – artificial cerebrospinal fluid

ATP – adenosine triphosphate

BEF - bisethynyl fluorene

BET – back electron transfer

bs – broad singlet

^{13}C NMR – carbon nuclear magnetic resonance

Cbz – carboxybenzyl

d – doublet

D – donor

DBU - 1,8-diazabicyclo[5.4.0]undec-7-ene

DCM – dichloromethane

DIPA – *N, N*-diisopropylamine

DIPEA – *N, N*-diisopropylethylamine

DNA – deoxyribonucleic acid

DMAP – *N,N*-dimethylpyridin-4-amine

DMSO – dimethyl sulfoxide

E_{CS} – energy of charge-separated state

E_{00} – excited state energy

E_{OX} – oxidation potential

E_{RED} – reduction potential

EDC – *N*-(3-Dimethylaminopropyl)-*N*′-ethylcarbodiimide hydrochloride

EGTA – ethylene glycol tetraacetic acid

ESI – electrospray ionization

Et$_3$N – trimethylamine

EtOH – ethanol

Fc – ferrocene

Fig – figure

FRET – Förster resonance energy transfer

GABA – γ-aminobutyric acid

Glu – glutamate

GM – Göppert-Mayer

^{1}H NMR – proton nuclear magnetic resonance

HEPES - 4-(2-hydroxyethyl)-1-piperazineethanesulfonic acid

Hex – hexyl

HOMO – highest occupied molecular orbital

HPLC – high-performance liquid chromatography

I_F – intensity of fluorescence

Ind – 3-indolepropionic acid

IR – infrared

k_{ET} – rate of the electron transfer

k_{BET} – rate of the back electron transfer

k_{REL} – rate of the release of protected moiety

LUMO – lowest unoccupied molecular orbital

m – meta

m – mili; multiplet

M – molarity; molecular ion

MALDI – matrix-assisted laser desorption/ionization

MeCN – acetonitrile

MeOH – methanol

Na2GTP – guanosine 5′-triphosphate sodium salt hydrate

NBS – *N*-bromosuccinimide

Non – nonyl

o – ortho

OPA – one-photon absorption

p – para

PBS – phosphate-buffered saline

PeT – photoinduced electron transfer

Ph – phenyl

ppm – parts per million

QX-314 – lidocaine *N*-ethyl bromide

Ref – reference

s – singlet

S_0 – singlet ground state

S_1 – lowest singlet excited state

SCE – standard calomel electrode

S_N2 – bimolecular nucleophilic substitution

t – tert; triplet

TBAF – tetra-n-butylammonium fluoride

TBDMSCl – tert-butyldimethylsilyl chloride

TFA – trifluoroacetic acid

THF – tetrahydrofuran

TIPS – triisopropylsilane

TMS – trimethylsilyl

TPA – two-photon absorption

UV – ultra violet

TABLE OF CONTENTS

Chapter 1

Introduction

The ultimate goal of molecular biologists is to elucidate the mechanisms of complex cellular processes and develop methods to control them. Particular attention is paid to recognizing the role of receptors, specialized structures that allow cells to receive external stimuli. Conveniently, the use of small-molecule synthetic probes allows researchers to gain insight into the mechanistic aspects of this kind of cellular stimulation. The work presented in this thesis is aimed at extending the toolbox available to neurophysiologists to investigate the communication between neurons. The following introduction covers the principle of signal transmission in neuronal networks (Fig. 1) and briefly highlights common research methods presently used in neuroscience. Two-photon uncaging is reviewed in more detail to report on the development of the two-photon sensitive compounds. Finally, a new design strategy is proposed to overcome limitations of currently available probes for two-photon uncaging.

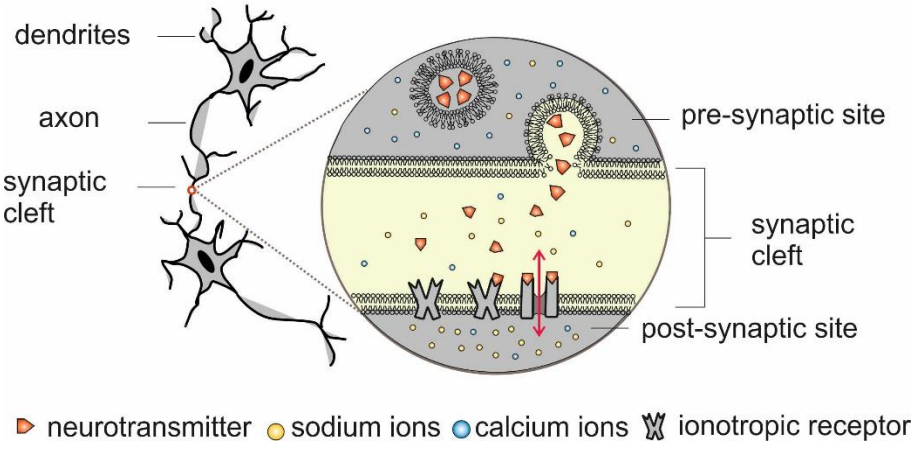

Figure 1. Schematic presentation of neurotransmission. Membrane depolarization spreads in the direction dendrite → axon and results in activation of voltage-gated calcium channels. The influx of calcium ions into the pre-synaptic site of the axon initiates a vesicular liberation of messengers (neurotransmitters). Released neurotransmitters diffuse to the post-synaptic density of the dendrite where they bind to the ligand-gated receptors. Upon binding, transmembrane ion-channels change their conformation and allow for the transport of ions inside and outside the cell. Figure adapted from ref. 3, Published by The Royal Society of Chemistry.

1.1 The role of neurotransmitters and action potential in synaptic activity

The essential mechanism of information transfer between neurons operates through a regenerative, self-propagating change in the potential of the membrane, termed action potential.[1] The electric signal is propagated in one direction, from dendrite to axon and mediated by messengers (neurotransmitters) across the junction between the dendrites and axons of connected neurons (synaptic cleft) as shown in Figure 1.[2] There are six distinct stages in the generation and propagation of the action potential (Fig. 2a).[4]

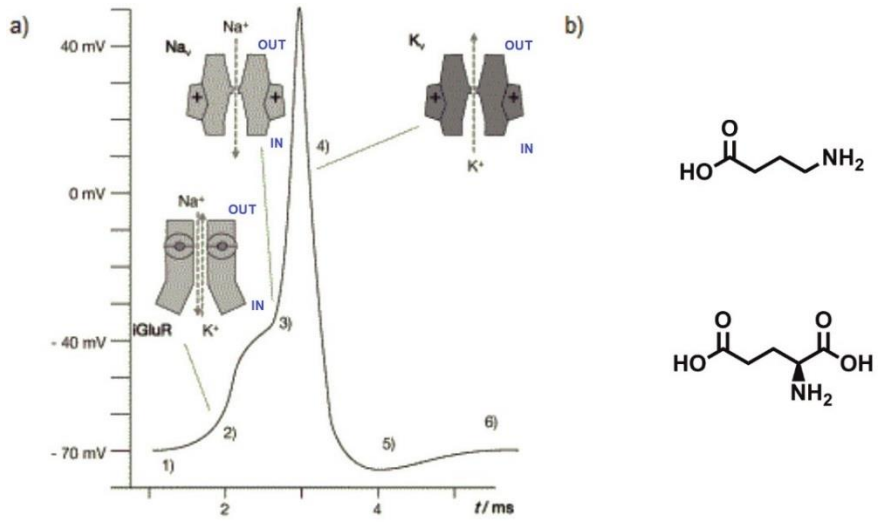

Figure 2. **a)** Stages of action potential evoked by binding of the excitatory neurotransmitter glutamate: *1* – neurons at resting state, *2* – activation of ligand-gated receptors, influx of sodium ions, *3* – activation of voltage-gated receptors, influx of sodium ions, *4* – deactivation of sodium channels, activation of voltage-gated potassium ion channels, the outward flow of potassium ions, *5* **–** undershoot: the value of the membrane potential is below the value in the resting state, *6* – neuron at resting state. Adapted with permission from ref.4. Copyright © 2011 WILEY-VCH Verlag GmbH & Co. KGaA, Weinheim. **b)** Structures of the main inhibitory and excitatory neurotransmitters in central nervous system, γ-aminobutyric acid (GABA) and L-glutamate, respectively.

Adenosine triphosphate (ATP) driven potassium and sodium pumps sustain the resting potential of neuronal membrane at –70 mV and the process of signal transmission starts with activation of ligand-gated ion channels. Neurotransmitters that bind to distinct types of ionotropic channels (Fig. 2b) initiate opening of pores and allow for the flow of sodium ions into the cell. Influx of sodium ions leads to a change of membrane potential up to –40 mV followed by the opening of voltage-gated sodium channels. As more sodium ions flow into the cell, the potential of the membrane is even

further depolarized and reaches +50 mV. At this stage, sodium channels are deactivated and voltage-gated potassium channels open to allow for the outward flow of potassium ions. Consequently, the membrane reaches a potential below its resting state (undershoot) and is brought back to –70 mV by ion pumps.

The shape, rate and pattern of action potential vary across different types of neurons and ion channels. Moreover, the stimulation of neuronal activity is possible through diverse mechanisms.[5-7] Nevertheless, a wide range of tools enables researchers to carry out experiments with resolution down to the single cell level and to manipulate remotely the activity of desired network components.

1.2 Light-induced remote manipulation of neuronal activity

Techniques that are currently used in neuroscience to regulate neuronal activity remotely address both ion channels and neurotransmitters (Fig. 3).[8-10]

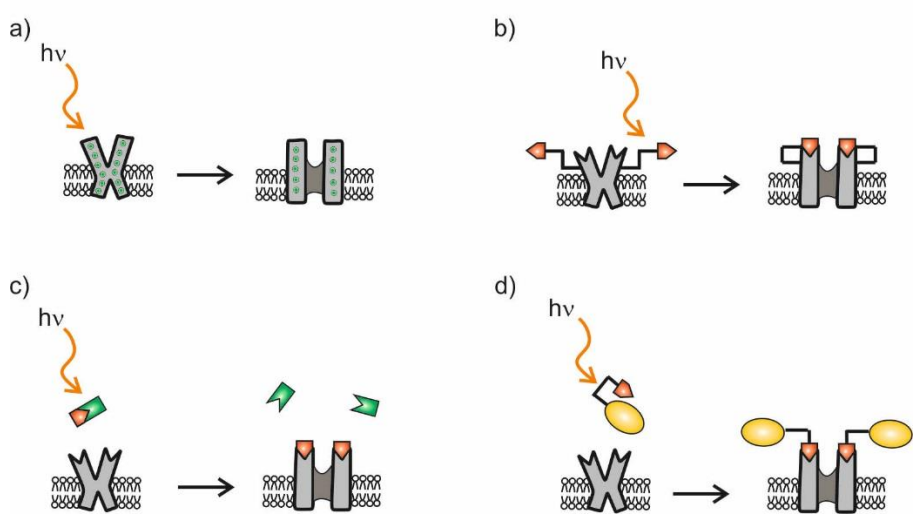

Figure 3. The strategies used to open the ion channels in neurons with use of light. **a)** The exogenous light-gated ion channels are expressed in neurons. Upon illumination, the light-sensitive domain in the ion channel undergoes conformational changes and exerts force to open the channel and allow for the transport of ions in both directions across the plasma membrane of the cell. **b)** Ligand-gated receptors are covalently attached to the matching ligands *via* the photosensitive linkers. Illumination of the cell results in photoisomerization of the linker and allows for binding of the ligand to its receptor. Upon the ligand-receptor recognition, the ion channel changes its structural conformation to enable the transport of ions through the cellular membrane. **c)** Ligand is not recognized by the receptor as its key functional group is covalently attached to the protecting group. Upon the absorption of light, the protecting group is cleaved and the liberated ligand binds to the matching receptor, thereby regulating the activity of the related ion-channel. **d)** Binding of the ligand to its receptor is constrained by steric hindrance imposed by a large substituent attached to the ligand. Absorption of light leads to the photoisomerization of the linker connecting the ligand with the substituent and induces conformational changes in the probe. Upon this transformation, the ligand is able to bind to its receptor and activate the corresponding ion channel.

Control over ion channels is exerted by means of genetic manipulation and application of light-sensitive compounds. The first method, optogenetics, takes advantage of the expression of exogenous light-activated ion channels in neurons (Fig. 3a).[11,12] Upon absorption of light, transmembrane proteins of microbial origin induce conformational changes in ion channels resulting in their opening. Alternatively, "chemical genetics" employs photoswitchable ligands, which are covalently tethered to the transmembrane receptors (Fig. 3b).[3,8-10] Irradiation induces isomerization of a linker that allows for the interaction of the ligand with the active site of the receptor. The ion channel opens upon the binding of the ligand to the receptor.

A second strategy uses neurotransmitters. In the uncaging method, a physiologically active compound is liberated from its inactive "caged precursor" (Fig. 3c).[13] The inactive analogue is obtained by modification of the physiologically relevant compound with a covalently attached, photolabile protecting group, and this structural alteration prevents the molecule from binding to receptors. Irreversible removal of the protecting group is triggered by light and enables the interaction of the organic molecule with the targeted receptor. Upon binding, the related ion channel undergoes structural changes and allows for the transport of ions through the cellular membrane. In another approach, photoswitches are used as conjugates of neurotransmitters (Fig. 3d).[3] These derivatives comprise a neurotransmitter and a covalently attached photoswitchable side, which enables controlled changes of the conjugate conformation. Only one geometry of the switch allows for receptor-neurotransmitter recognition and this can be reversibly activated and deactivated.
The abovementioned methods are complementary and the choice of the used technique is dictated by the purpose and scope of studies. In neuroscience, uncaging (Fig. 3c) has been used to study the role of neurotransmitters, second messengers[14] and calcium ions[15] to examine the fundamental processes that underlie communication between neurons. The benefit of this technique comes from the fact that this method enables the investigation of the native cellular machinery without the need for genetic manipulations. The invention of photolabile protecting groups dates back to 1960s, however their application in neuroscience has gained prominence in 2000s.

1.3 Historic overview of uncaging: from one to two-photon induced photolysis

The precedent finding of Barltrop and Schofield in 1962 (removal of carboxybenzyl (Cbz) group from the amino group of glycine upon irradiation at 254 nm) ushered in a new era of studies on protecting groups.[16] Light-sensitive protecting groups have continued to gain importance as tools for investigating the role of physiologically active compounds, ever since they were first applied in a biological system in 1978.[17] Kaplan, Forbush and Hoffman's seminal work on caged ATP laid the foundations for the field of uncaging and drew attention to the potential of this new research technique (Fig. 4a).

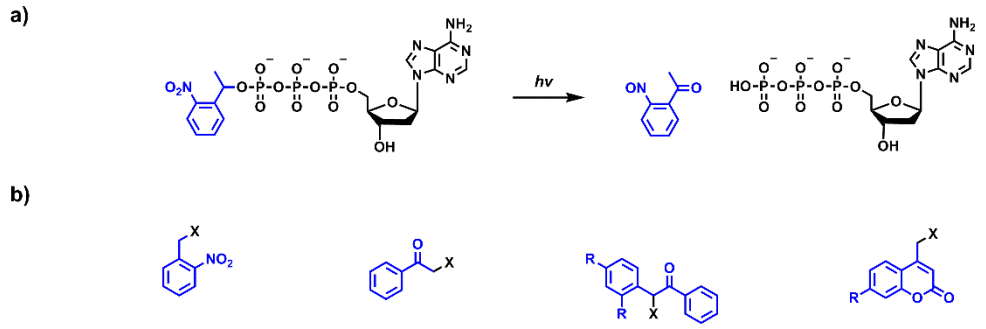

Figure 4. a) Photolysis of P^3-1-(2-nitro)phenylethyl caged ATP.[17] Upon irradiation, the protecting group (drawn in blue) is cleaved and the physiologically relevant molecule (ATP) is liberated. **b)** Structures of common photolabile protecting groups developed for one-photon uncaging: *o*-nitrobenzyl, phenacyl, benzoinyl and coumarinyl. X = leaving group.

A number of ultraviolet and visible light cleavable cages have been developed[18-23] (Fig. 4b) to allow for rapid control over spatially and temporally resolved photorelease of various biomolecules, including caged nucleic acids, proteins, cellular signaling molecules and messengers, hormones, lipids and membranes, both *in vitro* and *in vivo*.[24-26] The utility of photolabile protecting groups stems from their cleavage conditions, as light can be orthogonal to intracellular processes. Although ultraviolet light has a damaging effect on DNA, light of infrared wavelengths is not harmful to cells and can deeply penetrate tissue, which is relatively transparent between 650-950 nm. The depth of optical penetration depends on the type of the tissue and the used wavelength. For example, in the brain, light reaches depths of 0.9-2.5 mm at 633-834 nm.[27] Nevertheless, under one-photon irradiation with infrared light, molecules do not gather enough energy to undergo bond-breaking events.

In the 1990s, the concept of uncaging was extended to take advantage of two-photon absorption (TPA),[28] a nonlinear optical phenomenon in which excitation occurs by the simultaneous absorption of two photons, each having half the energy of that required for the corresponding one-photon process.

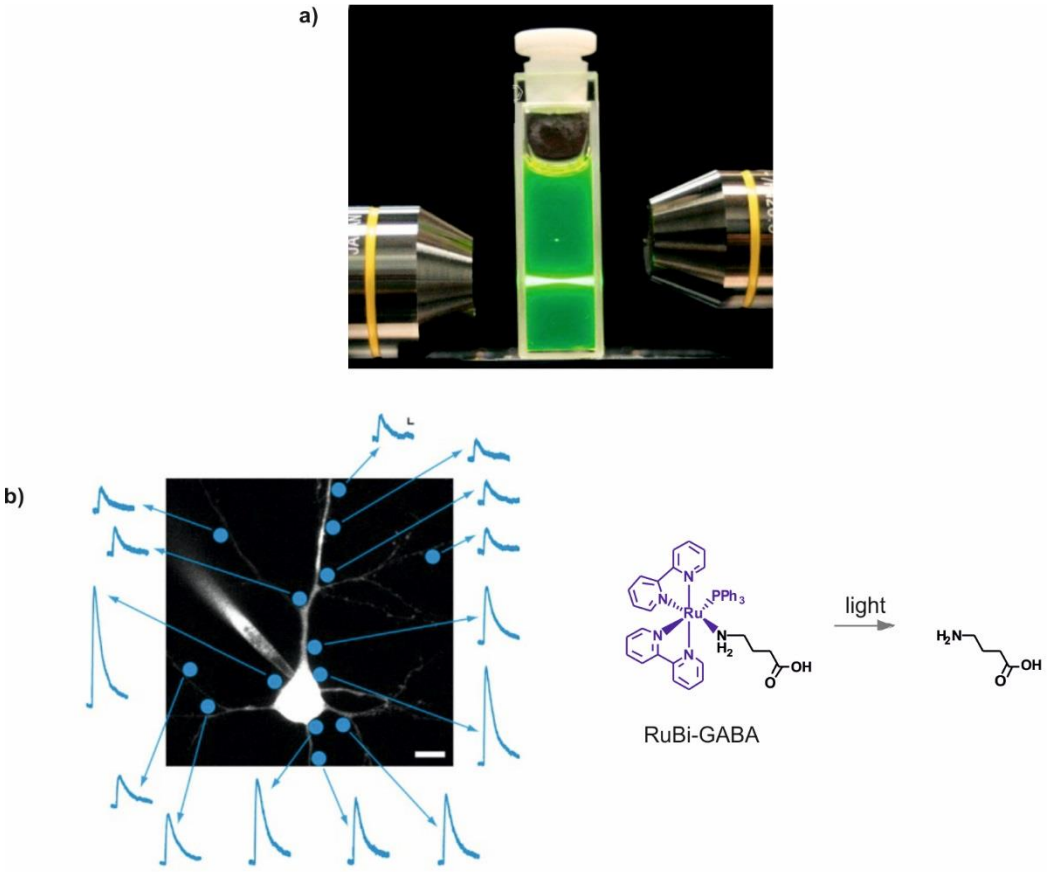

Figure 5. a) Comparison of excitation volume induced upon one- and two-photon absorption. Fluorescence induced by one-photon process (visible light) occurs in a volume with a shape of an hourglass, whereas excitation volume for two-photon process (infrared light) is confined to a spot. Adapted with permission from ref. 38. Copyright © 2012 WILEY-VCH Verlag GmbH & Co. KGaA, Weinheim. **b)** Example of an uncaging experiment aimed at mapping of GABA-ergic receptors. Photolysis was initiated by one-photon absorption (473 nm), whereas imaging was performed under two-photon excitation (950 nm, upon filling the neuron with Alexa 594).GABA was liberated from RuBi-GABA at points marked as blue circles. One-photon photolysis was carried out point by point by moving a laser spot. The patch-clamp recordings of the inhibitory post synaptic potential (blue traces) allowed one to conclude on the position of studied receptors. Adapted from ref. 35. Copyright © 2008 Rial Verde Zayat, Etchenique and Yuste.

The first application of TPA in biology has been made by Denk, Strickler and Webb.[199] They built the first laser scanning microscope based on the two-photon excited florescence and also suggested the possibility of using TPA in uncaging experiments. Four years later, Denk realized this idea and induced photorelease of an agonist of nicotinic receptors with infrared light.[29] Under two-photon excitation conditions, the photolysis is spatially restricted, resulting in tight three-dimensional control over the drug administration (Fig. 5a). Therefore, this technique is particularly valued in

neuroscience as it enables selective stimulation of sub-cellular domains in single neurons within their multilayer circuits *in vivo* and in acute brain slices.[30-34] Photolysis of caged neurotransmitters allowed the distribution of receptors to be mapped within specific divisions of single cells and for investigating synaptic connectivity (Fig 5b).[35] Moreover, wavelength-selective uncaging of orthogonally protected neurotransmitters (two-colour uncaging) opens the door to the simultaneous stimulation of synapses by two different ligands.[36,37]

1.4 Two photon uncaging: current challenges

The main challenge in establishing two-photon uncaging as a powerful and ubiquitous method in biological research is the development of compatible photolabile protecting groups. Despite the remarkable success of experimental neurophysiology with currently available caged compounds, [29-36] the full capacity of the two-photon uncaging method has not been explored yet. The limited scope of reliable probes reveals that this technique is still in its infancy.

Most protecting groups optimized for one-photon uncaging cannot be used in two-photon photolysis experiments because they display low efficiency under two-photon excitation. Their chromophores lack the specific features required for efficient TPA.[39, 40] In a classical approach, the protecting group plays two roles: absorbs light and releases the protected compound. If a protecting group does not absorb light efficiently, it does not collect enough energy to break bonds and liberate caged species. A consequence of poor absorption is a poor yield of the activated compound. This obstacle can be overcome by increasing the laser power (to enforce uncaging) and the concentration of the probe (to ensure critical concentration of physiologically relevant compounds that are obtained upon photolysis). On the other hand, much effort has been made to develop probes that efficiently absorb two photons of infrared light and undergo a subsequent bond-scission with high yield, at a laser power that is not harmful for cells. Although the design features of two-photon absorbers are well understood and can be rationalized, the development of two-photon sensitive protecting groups is still a field where success results from trial and error.

1.5 Two-photon absorption - physical background and chromophore design

A prerequisite for TPA-initiated bond-breaking is efficient absorption of light. TPA requires instantaneous interaction of a molecule with two photons and thus the probability of excitation increases with the square of the light intensity. Therefore TPA occurs only in beams of high photon density, which are conveniently generated by focused pulsed lasers. An advantage of the quadratic dependence of TPA on the light intensity is that absorption is limited to the focal volume. As light intensity decreases quadratically in the function of the distance (z) from the focal volume, the probability of TPA outside the focus is proportional to z^{-4}.[40] Consequently, scattered photons do not have sufficient energy to induce photolysis and uncaging is not observed out of the plane of focus.

The mechanism of two-photon excitation involves the formation of a virtual state, which is generated upon interaction of the molecule with the first photon. Transition to the excited state depends on the structure of the chromophore and selection rules are related to the symmetry of orbital wavefunctions (Fig. 6).

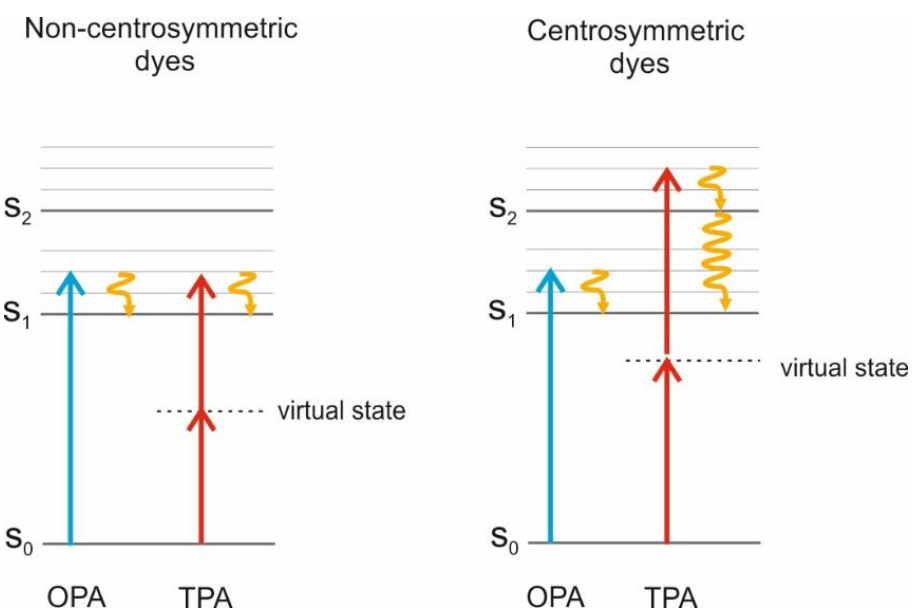

Figure 6. Schematic representation of TPA (red arrows) and OPA (blue arrows) in non-centrosymmetric dyes (left) and centrosymmetric dye (right). Initial excited state relaxed to the lowest excited state upon internal conversion (yellow arrows).

For non-centrosymmetric chromophores OPA (one-photon absorption) and TPA lead to the same excited state. Therefore, light required for a TPA-promoted $S_0 \rightarrow S_1$ transition has approximately twice

the wavelength of light necessary to access S_1 by OPA. In contrast, centrosymmetric dyes are promoted to different excited states as a result of OPA and TPA. Consequently, the observed maximum wavelength of TPA does not match double the maximum wavelength of OPA. Irrespective of the nature of the initial excited state, chromophores undergo internal conversion and further chemistry proceeds from the lowest excited state (Kasha's rule).

The parameter that quantifies the ability of the molecule to undergo two-photon excitation is the TPA cross-section, δ_a [GM] (1 GM = 10^{-50} cm^4 s $photon^{-1}$), and for organic molecules its value ranges from several GM (for small aromatic platforms) to ~200 000 GM (porphyrin oligomers). The relationship between the structure of the chromophore and its TPA cross-section has been thoroughly studied.[28,41,42] In general, TPA-cross section depends on the degree of redistribution of π-electrons and generation of transition dipole moments upon excitation. Charge displacement, in turn, is facilitated in coplanar chromophores with π-conjugated chains and donor-acceptor segments. Studies have shown that in linear chromophores, δ_a is higher for quadrupolar push-pull systems (D-π-A-π-D) than for dipolar (D-π-A), where D: electron-donor, A: electron-acceptor (Fig. 7). Moreover, systems with terminal donors (D-π-D; D-π-A-π-D) have higher δ_a than systems with terminal acceptors (A-π-A; A-π-D-π-A) and nitrogen-based groups are better terminal donors than oxygen-based groups. An important parameter is the number of π-electrons. TPA cross-section increases with conjugation, up to a critical length, at which the system loses coplanarity and charge displacement occurs only within limited distances.

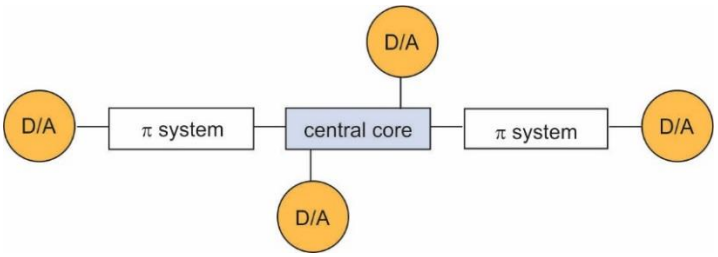

Figure 7. Typical design of two-photon absorbing dye. Adapted with permission from ref. 43. Copyright © 2008 WILEY-VCH Verlag GmbH & Co. KGaA, Weinheim.

1.6 Requirements for protecting groups used in neuroscience - parameters quantifying uncaging

In addition to the need for a compound to have excellent absorption properties, there is a long list of requirements that caged compounds have to fulfil to become useful in experiments in living cells.[44] For application in neuroscience, caged compounds have to be soluble in water without the necessity of adding co-solvents, such as DMSO and acetonitrile. In addition, protected species have to be resistant to hydrolysis in aqueous buffers at pH 7.2-7.4, preferably in aCSF (artificial cerebrospinal fluid) saturated with CO_2 at 30-37 °C. Commercially available compounds are reported to remain intact for weeks in solutions of physiological pH, although the composition of buffers is not always identical with that used in experiments with cells. The activity of caged compounds should be reduced below detection limits until photolysed. Nonetheless, many neurotransmitters in their caged form display off-target behavior and exhibit antagonistic effects upon GABA-A receptors at ~0.1 mM concentration (tonic inhibition). This issue poses a limitation to induce a signal transmission with mM concentration of the probe (assuming 100% uncaging; phasic stimulation).[45] Furthermore, bond scission should be faster than the biological process under investigation and any by-products formed upon uncaging should not be toxic.

The efficiency of protecting groups is measured against a set of parameters. Physiologically relevant compounds should be liberated in high chemical yield [%], which reflects the ratio between the amount of the compound released and amount of photolysed precursor. Moreover, the process of uncaging can be divided into two steps: light absorption and bond scission. The efficiency of absorption is quantified by the TPA cross-section (δ_a), whereas the quantum yield of uncaging (ϕ_u) measures the efficiency of photo-induced bond scission. The typical quantum yield of uncaging of widely used protected compounds is 0.1. Quantum yields for one- and two-photon initiated processes are assumed to be equal because the photochemical reaction generally proceeds from the same lowest excited state (Kasha's rule).[46,47] Moreover, higher excited states have much shorter lifetimes. A figure of merit reflecting the overall sensitivity of a protecting group to two-photon uncaging is the two-photon uncaging cross-section δ_u, which is a product of the TPA cross-section and the one-photon

uncaging quantum yield ($\delta_u = \delta_a\phi_u$). A high TPA-cross section can compensate a low uncaging quantum yield, however it is desirable to maximize the efficiency of both processes. Typically, δ_u values reported to date lie between 0.05 and 2.5 GM. Considering the diffusion and depletion of the caged species from the focal volume, it has been estimated that for biological applications, δ_u should lie between 3-30 GM to ensure efficient two-photon absorption at laser power levels harmless to living cells and release of the neurotransmitter in the concentration required to induce a biological response.[48]

1.7 Overview of two-photon protecting groups for neuroscience

Since the first use of TPA in uncaging,[29] much effort has been made to develop compounds with better absorption profiles. There are three main strategies that have been explored to prepare highly sensitive two-photon cages:

i) searching for genuinely novel protecting groups with high TPA

ii) extension of the chromophore of pre-existing uncaging platforms

iii) adding spatial separation between the absorption and cleavage steps.

Each approach presents unique advantages and limitations which are discussed in the following sections.

1.7.1 Searching for genuinely novel protecting groups with high TPA

In general, an ideal candidate for a protecting group suitable for biological application is a small platform displaying excellent absorption (δ_a ~ tens of GM) and release properties (ϕ_u ~ 1). Not only does the small size of the caging unit simplify the synthesis but it also facilitates transport of the probe through membranes. Therefore early efforts were aimed to design new chromophores that possess both high δ_a and ϕ_u. Consideration of the structural factors enhancing TPA cross-section (π-conjugated, coplanar systems with electron donating and accepting groups) led to a rational design of small protecting groups with improved TPA. This category includes such families of caging groups as *o*-nitrobenzyl,[49] nitroindolinyl (**NI**,[200] **MNI**,[32,50,51] **MDNI**,[52] **CDNI**[36,53], **DPNI**[54,55]), 2-(2-nitrophenyl)propyl,[56] *o*-hydroxycinnamate (***o*-HCA**),[57,58] coumarinyl (**Bhc**,[59] **DECM**[60]),

inorganic metal complexes (**RuBi**)[35,61,62] and quinoline (**BHQ**,[63,64] **DMAQ**[65,66]) (Table 1). Extensive studies of structure-property relationship (usually including a series of small aromatic platforms with various substitution patterns) resulted in the development of useful protecting groups with two-photon uncaging cross-section δ_u of only 0.06−2.0 GM.

Table 1. Properties of two-photon sensitive protecting groups.

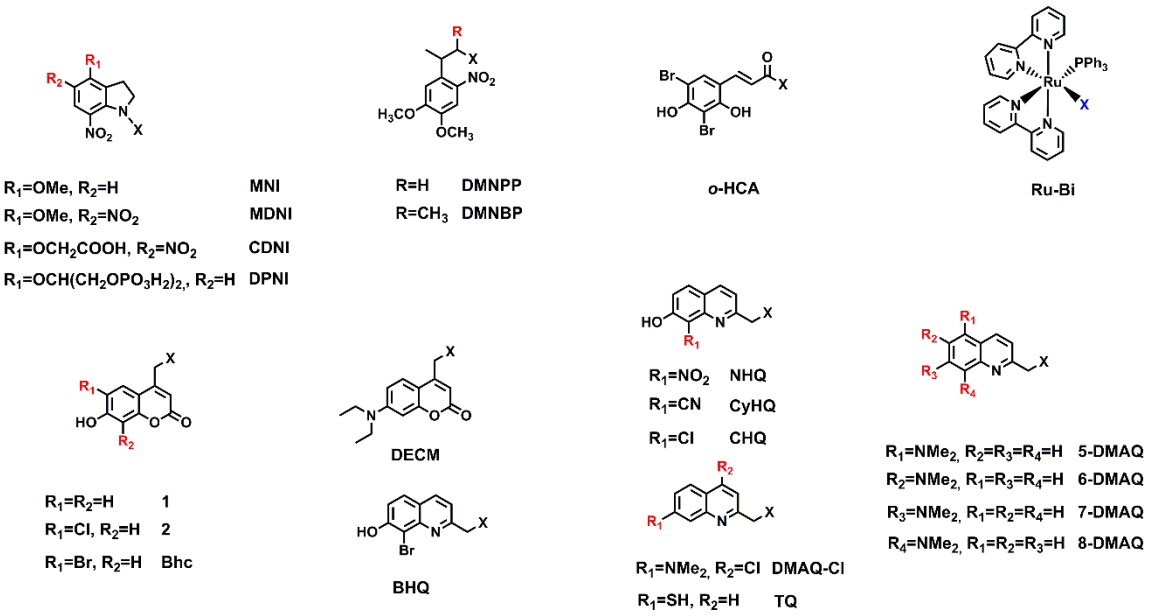

Protecting group	X – Leaving group	δ_u [GM] / λ [nm]	ϕ_u	Comments	Ref.
MNI-Glu	Glutamate (amide)	0.06 /730	0.085		32
MDNI-Glu	Glutamate (amide)	0.06/720	0.47		52
CDNI-Glu	Glutamate (amide)	0.06/720	0.5		36, 53
DPNI-GABA	GABA (amide)	n.d.	0.085	Hydrolytically stable	54,55
DMNPB	Glutamate (ester)	0.098 /720	0.26	Release yield >95%	56
	Benzoic acid	1.17 /740		Release yield >95%	56
DMNPP	Benzoic acid	n.d	n.d	Release yield: 60%	56
***o*-HCA**	Ethanol	1.6 / 750	n.d	ϕ_u=1.6 GM – *in vivo*, 0.6 GM - *in vitro*	57, 58
		0.6 / 750			
RuBi-Glu	Glutamate (*N*-coordinated)	0.14 /800	0.13	Hydrolytically stable	61, 62
RuBi-GABA	GABA (*N*-coordinated)	n.d	n.d		35
Bhc-OAc	Acetate	1.99 /740	0.037		59
Bhc-Glu	Glutamate (ester)	0.89 /740	0.019	Hydrolytically unstable	59
Bhc-Glu	Glutamate (carbamate)	0.95 /740	0.019	Hydrolytically stable	59
DECM	Glutamate (ester)	n.d.	0.1	Hydrolytically stable	59
BHQ	Acetate	0.59/740	0.29		64
BHQ	Benzoic acid	0.64 /740	0.30	Release yield: 60-70%	63
BHQ	Piperonylic acid	0.76 /740	0.32	Release yield: 60-70%	63
8-DMAQ-OAc	Acetate	0.67 /730	0.17	Highest δ_a in the series	66
8-DMAQ-Glu	Glutamate (ester)	n.d	n.d	Hydrolytically unstable	66

n.d. – not determined

MNI-glutamate became the most common protected glutamate and has been used in multiple studies despite its low δ_u of 0.06 GM at 730 nm. [32,50,51] It allows action potentials to be evoked in individual neurons, although it is not a useful probe to study neuronal circuits: **MNI-Glu** is a strong GABA-ergic antagonist (it blocks GABA-ergic responses).[61] Interestingly, the **DPNI** protecting group is specifically tailored for GABA because **NI-GABA** displays such a strong off-target effect that renders the probe impractical.[54,55] To date, **MNI-Glu** serves as a reference compound and the utility of new caged neurotransmitters is evaluated against the **MNI** protecting group. Several trials aimed at improving the properties of nitroindolinyl platform. Ellis-Davies *at al* reported that the presence of an additional nitro group in **MDNI-Glu**[52] and **CDNI-Glu**[36,53] facilitates the release of glutamate and leads to 5.5 times higher quantum yield of uncaging. However, in separate studies, Papageorgiou *at al* found only a 2.5 fold improved sensitivity of the dinitroindoline (due to a greater near UV absorption coefficient) but no change of quantum yield.[201] Furthermore, unlike the mononitroindoline, the release of glutamate was only 60-70% of stoichiometric and the photolysis reaction generated nitroindoline as well as nitrosoindoline byproducts, suggesting a mechanistic difference.

Optimization of protecting groups is a challenging task. Not only does any alteration in the structure influence the release and absorption steps but the quantum yield of uncaging also depends on the leaving group. Furthermore, some protecting groups suffer from low chemical yield of uncaging and undergo side reactions upon excitation. Subtle variations in the design of related protecting groups may significantly influence their properties, as illustrated in the following review of novel caging units for two-photon photolysis (Table 1). For instance, the structure of derivatives of dimethoxy-nitrophenyl group (**DMNPB** and **DMNPP**) differ only by a methyl substituent in α-position to the leaving group. However, photolysis of **DMNPB** leads to nearly quantitative release of benzoic acid, whereas **DMNPP** undergoes reactions competitive to uncaging and gives only 60% of the desired product.[56]

A study related to the substitution pattern within the *o*-hydroxycinnamic platform (***o*-HCA**) clearly shows that protecting groups displaying the best photophysical parameters (δ_u) within the considered series might never be useful caging groups due to their low aqueous solubility or stability.[57]

Moreover, an experiment carried out with ***o*-HCA** caged ethanol in zebrafish embryo shows that δ_u measured *in vivo* (1.6 GM at 750 nm) is nearly three times higher than value obtained *in vitro* (0.6 GM at 750 nm).[57,58] A non-fluorescent *o*-hydroxycinnamic ester transforms into fluorescent coumarin as a result of uncaging and allows the concentration of released moiety to be quantified in real-time in *in vivo* studies. The authors of this study evaluated the changes in fluorescence before and after the uncaging event. Their quantitative results indicate that the two-photon uncaging cross-section strongly depends on the location of the probe in intracellular organelles.

Ruthenium-bipyridine complexes (**Ru-Bi**) of *N*-coordinated GABA[35] and glutamate[61,62] exhibit excellent stability and remarkably fast photocleavage (50 ns for RuBi-Glu) but the greatest advantage of **RuBi-Glu** is that it displays reduced off-target effects. In contrast to **MNI-Glu**, **RuBi-Glu** (300 μM) allows the studies of inhibitory circuits to be carried out.

Historically, halogenated 7-hydroxycoumarin was the first caging platform with δ_u above 1 GM.[59] The cleavage of this compound proceeds from the triplet state, formation of which is promoted by presence of heavy atoms (in the order Br (**Bhc**) > Cl (**2**) > H (**1**)). Systematic studies on **Bhc** group provide an excellent example of how the uncaging quantum yield varies with the leaving group. Acetic acid (**Bhc-OAc**) is liberated with nearly double quantum yield than glutamate from its ester (**Bhc-Glu**). The difference between ϕ_u for glutamate caged as ester and carbamate is negligible but disparity in hydrolytic stability is staggering, rendering carbamate resistant to hydrolysis over six days. At the same time this hydrolytic stability comes at a price of slower release, as the initially liberated carbamic acid undergoes decarboxylation over a few ms to give free glutamate.

Structurally similar to **Bhc**, esters of 8-bromo-7-hydroxyquinoline (**BHQ**) display good aqueous stability and δ_u ~ 0.6 GM at 740 nm.[63,64] Experiments show that the 7-hydroxy group is involved in the cleavage of **BHQ** platform, however uncaging does not proceed from the triplet state. These findings allow for the replacement of the bromine atom by an electron-withdrawing substituent to facilitate deprotonation of the hydroxyl group. Systematic studies on the influence of the substitution pattern have been conducted for the quinoline family (**NHQ**, **CyHQ**, **CHQ**, **TQ**, **DMAQ-Cl**)[65] but none of the alternative structures is more photo-sensitive than **BHQ-OAc**.[64] Within *N*,*N*-dimethyl

amine substituted derivatives, **8-DMAQ** was found to be the most efficient protecting group.[66] Unfortunately, its glutamate derivative, **8-DMAQ-Glu,** is hydrolytically unstable and thus impractical for physiological experiments.

From all of the probes discussed in this section, only nitroindolinyl- and RuBi-caged neurotransmitters have become commercially available and found application in experiments in living cells. None of the other designs held sufficient advantages to become new benchmark. The shortcoming of the presented design strategy is that small chromophores display relatively low δ_a.

1.7.2 Extension of a chromophore

Another common strategy for preparing protecting groups with enhanced TPA cross-section is to extend the π-system of a pre-existing protecting platform and modulate the strength of electron-donating/accepting substituents. Dipolar, quadrupolar and octupolar architectures have been explored for functionalizing established caging groups such as coumarin, *o*-nitrobenzyl, 2-(*o*-nitrophenyl)propyl, phenacyl and quinoline with vinyl, phenyl, styryl, dihydronaphthalenyl, thienyl, fluorenyl and triphenylamine groups (Table 2-5). The strategy of incorporating an existing protecting group into a conjugated D-π-A system led to a dipolar protecting group within the 2-(*o*-nitrophenyl)propyl series with a record δ_u of 11 GM at 800 nm.[67] However, as absorption and bond scission are inherently related, any alteration in the caging group influences both δ_a and ϕ_u. Therefore some structurally modified cages, such as BNSF (δ_u of 5 GM at 800 nm, 65% yield of uncaging) suffer from light-induced side reactions or decreased yield of release, compared to their parent protecting units.[43]

Coumarin

Despite the efforts of several research groups, coumarin does not prove adaptable for extension (Table 2). Decoration of coumarin by a vinyl substituent (**DEAC-450**, **3**) does not enhance δ_u but instead, gives access to a protecting group with a red-shifted peak of TPA.[68,69] **DEAC-450** undergoes efficient photolysis at 900 nm offering two-photon two-colour (i.e. wavelength orthogonal) uncaging when paired with nitroindolinyl cages that are cleaved with shorter wavelengths (720 nm). Although

all of these compounds display antagonism towards GABA-A receptors, this effect is more pronounced for carboxylic acid (**DEAC-450**) than PEG decorated coumarin **3**. Both GABA-esters exhibit high aqueous stability at pH 7.4 in PBS buffer.[68,69]

Table 2. Properties of two-photon sensitive protecting groups derived from coumarin.

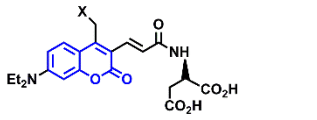

DEAC-450

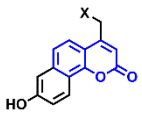

4

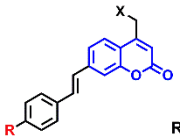

R=H 6

R=OCH_2CH_3 7

R=NMe_2 8

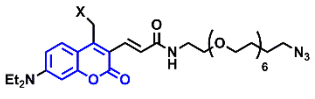

3

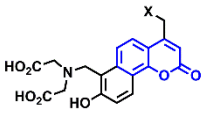

5

Protecting group	X – Leaving group	δ_u [GM] / λ [nm]	ϕ_u	Comments	Ref.
DEAC-450	Glutamate (ester)	0.5*/900	0.39	* value estimated	68
DEAC-450	GABA (ester)	n.d.	n.d.	Hydrolytically stable	69
3	GABA (ester)	n.d.	n.d.	Hydrolytically stable	69
4	Glutamate (ester)	0.3* /750	0.006	*estimated; uncaging in CD_3OD	70
5	Glutamate (ester)	n.d.	n.d.	Hydrolytically unstable	70
6	4-methoxybenzyl alcohol	n.d.	n.d.		71
7	4-methoxybenzyl alcohol	n.d.	n.d.		71
8	4-methoxybenzyl alcohol	0.26 /800	0.00083		71

n.d. – not determined

Regardless of significant changes in the coumarin architecture, insertion of the phenyl ring into the coumarin platform **4**, **5** does not bring radical improvements in two-photon properties (δ_a ~50 GM) of the caging group.[70] Moreover, poor aqueous stability of **5** in HEPES buffer (pH 7.4) and poor solubility of **4** exclude these probes from application in living cells. As a result of another study, coumarin is conjugated with styryl derivatives and built into a D-π-A system.[71] Modulation of donor/acceptor properties of the aromatic platforms **6**-**8** yield a dye with improved absorption properties. A chromophore with enhanced TPA cross-section (δ_a =309 GM) is found to be the one bearing *N*,*N*-dimethyl-amine **8**. Because of its very low quantum yield of release, **8** has two-photon uncaging cross-section of merely 0.23 GM at 800 nm.

o-Nitrobenzyl and phenacyl

Attempts to utilize *o*-nitrobenzyl and phenacyl groups employ conjugation of these platforms with small electron-donating substituents (Table 3). A series of caging groups with *o*-nitrobenzyl backbone has been investigated by Jullien.[49] Studied compounds include benzyl-substituted derivatives **9** and *o*-nitrobenzyl cores conjugated with a phenyl ring **10**-**12**. Obtained protecting groups display uncaging cross-section comparable to **MNI-Glu**, i.e. between 0.015 and 0.065 GM at 750 nm. *o*-Nitrobenzyl, when incorporated into 1,2-dihydronaphtalene derived push-pull chromophore **13**-**14**, shows enhanced TPA cross section of 150 GM but the uncaging quantum yield is reduced to 0.01 at 680 nm.[72] The main obstacle to adapt *o*-nitrobenzyl group is its very low quantum yield of uncaging once its π-system is altered.

Table 3. Properties of two-photon sensitive protecting groups derived from *o*-nitrobenzyl and phenacyl.

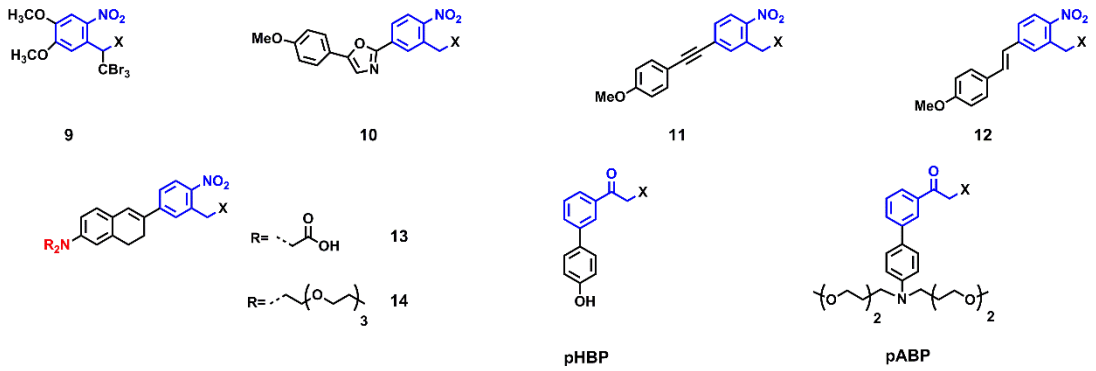

Protecting group	X– Leaving group	δ_u [GM] / λ [nm]	ϕ_u	Comments	Ref.
9	Coumarin	0.065 /750	0.013		49
10	Coumarin	0.040 /750	0.001		49
11	Coumarin	0.050 /750	0.001		49
12	Coumarin	0.020 /750	0.001		49
13, **14**	Glutamate (ester)	1.2*/680	0.01	* value estimated	72
pHBP	GABA (ester)	0.24 /740	0.21	Half life at pH 7.4 (PBS) -10 h	73
pABP	GABA (ester)	n.d	0.015	Half life at pH 7.4 (PBS) -10 h	73

n.d. – not determined

Efforts made to adapt the phenacyl group are equally unsatisfactory. The conversion of phenacyl into D-π-A system was achieved upon substitution with phenyl derivatives bearing amino (**pABP**) and hydroxyl (**pHBP**) groups.[73] GABA is liberated from **pHBP** nearly quantitatively (chemical yield) but with low δ_u of 0.24 GM, whereas only 55% of GABA is released despite full conversion of **pABP**.

Moreover, both caged GABA esters show low hydrolytic stability with half-life of 10 h at pH 7.4 (PBS). Further development of *o*-nitrobenzyl and phenacyl groups has been abandoned.

2-(*o*-Nitrophenyl)propyl

To date, 2-(*o*-nitrophenyl)propyl platform have proved the most adaptable towards chromophore extension (Table 4).

Table 4. Properties of two-photon sensitive protecting groups derived from 2-(*o*-nitrophenyl)propyl.

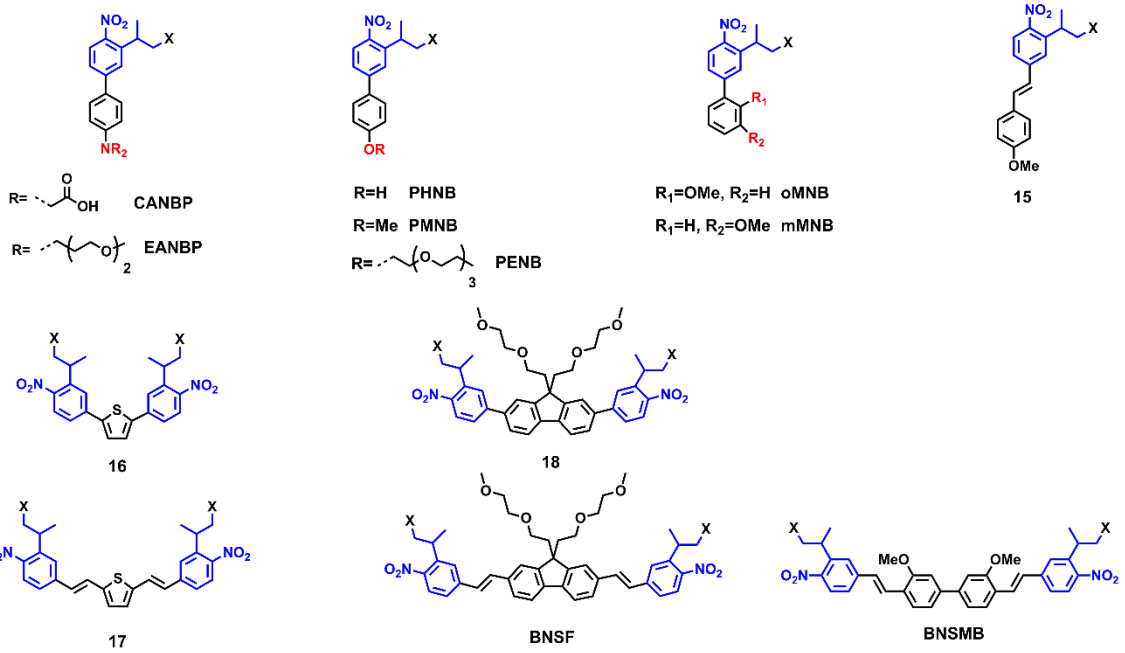

Protecting group	X – Leaving group	δ_u [GM] / λ [nm]	ϕ_u	Comments	Ref.
CANBP	GABA (ester)	7.4 /800	0.15	Hydrolytically stable (pH 7.4, PBS)	67
EANBP	GABA (ester)	11 / 800	0.15	Hydrolytically stable (pH 7.4, PBS)	67
PHNB	Glutamate (ester)	n.d	n.d.	10% of released glutamate	74
PMNB	Glutamate (ester)	3.2 /740	0.1		74
PENB	Glutamate (ester)	3.2 /740	0.09		73
mMNB	Glutamate (ester)	1.8 /740	n.d		73
oMNB	Glutamate (ester)	2.2 /740	n.d		73
15	Glutamate (ester)	n.d.	n.d.	48% of released glutamate	74
16	Glutamate (ester)	3.1 /740	0.29	100% of released glutamate	75
17	Glutamate (ester)	n.d	n.d.	5% of released glutamate	75
18	Glutamate (ester)	n.d.	n.d	60% of released glutamate	75
BNSF	Glutamate (ester)	5.0 /800	0.25	65% of released glutamate	43
BNSMB	Glutamate (ester)	0.9 /800	0.3	60% of released glutamate	43

n.d. – not determined

Within the dipolar series, 2-(*o*-nitrophenyl)propyl constitutes a biphenyl chromophore which is decorated with various substituents. The highest values of δ_u are obtained for cages bearing nitrogen-based electron-donating substituents (**CANBP** and **EANB** with δ_u 7.4 GM and 11 GM respectively at 800 nm).[67] Both protecting groups release GABA quantitatively upon photolysis (chemical yield) and display high aqueous stability at pH 7.4. Oxygen-substituted analogues demonstrate slightly worse photophysical properties. Only **PHNB** (bearing hydroxyl group) undergoes competitive photo-induced reactions and exhibit low chemical yield of uncaging (5%). For ether derivatives δ_u depends on the substitution pattern and lies between 1.8 − 3.2 GM at 740 nm (the highest value is obtained for *p*-isomer, **PMNB**). The analogue of **PMNB**, with central vinyl bridge **15**, shows significantly worse properties such as remarkably decreased chemical yield of liberated product (48%).[73,74]

Thienyl (**16**, **17**),[75] fluorenyl (**18**, **BNSF**) and biphenyl (**BNSMB**)[43] chromophores have been used to build quadrupolar caging groups. Here, nearly all platforms are consumed by side reactions and display chemical yield of release ~60%. Nevertheless, the high quantum yield of uncaging and TPA cross-section compensate for this disadvantage to ultimately give δ_u within 0.9-5.0 GM at 800 nm.

These examples clearly show how difficult the rational design of protecting groups is. A substitution pattern developed for one platform is not necessarily the optimal one for a close derivative. It is very hard to predict the presence of reactions that compete with uncaging. Hence, structure-property studies have not yet offered general guidelines that are applicable to construction of all caging platforms.

Quinoline

An original approach to the design of protecting groups has been demonstrated by an attempt to employ an octupolar chromophore (Table 5).[76] A systematic study on structure-properties relationship was carried out on dipolar, quadrupolar and octupolar derivatives of quinoline. Triphenylamine was chosen as a core for quadrupolar caging group since derivatives of triphenylamine display TPA cross-section between 30-1080 GM.[77] These studies reveal that TPA cross-section is significantly higher for octupolar protecting groups than for corresponding analogues with dipolar architecture (**19** – 480 GM at 730 nm, **20** – 163 GM at 750 nm), but the opposite order is true for ϕ_u. Enhanced conjugation in

octupolar chromophores leads to relaxation processes that compete with uncaging. Unfortunately, values of ϕ_u are not only far below these reported for simple quinolines[63,66] but also render proposed protecting groups highly impractical (ϕ_u ~10^{-4} – 10^{-6}). Interestingly, quadrupolar derivative of fluorene **23** performed the worst in the investigated series, with TPA cross-section of 75 GM at 710 nm and ϕ_u ~10^{-6}.

Table 5. Properties of two-photon sensitive protecting groups derived from quinoline.

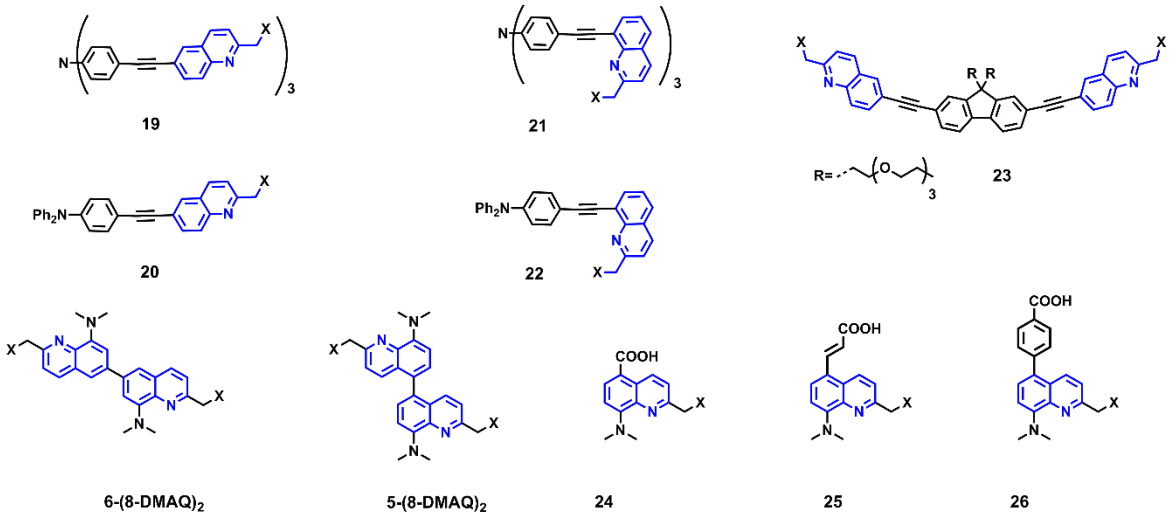

Protecting group	X – Leaving group	δ_u [GM] / λ [nm]	ϕ_u	Comments	Ref.
19	Acetate	n.d	7.0×10^{-6}	δ_a = 480 GM (730 nm)	76
20	Acetate	n.d	1.1×10^{-4}	δ_a = 163 GM (750 nm)	76
21	Acetate	n.d	n.d.	δ_a= 390 GM (710 nm)	76
22	Acetate	n.d	2.0×10^{-4}	δ_a = 110 GM (710 nm)	76
23	Acetate	n.d	1.7×10^{-6}	δ_a = 75 GM (710 nm)	76
6-(8-DMAQ)$_2$	Acetate	0.07 /730	0.093		78
5-(8-DMAQ)$_2$	Acetate	0.4 /730	0.066		78
24	Acetate	0.11 /730	0.32	Highly water soluble <50 mM	79
25	Acetate	0.25 /730	0.21		79
26	Acetate	2.0 / 730	0.14		79

n.d. – not determined

Pioneering effort has been made to understand the influence of symmetry on the uncaging efficiency of quinoline-derived quadrupolar probes.[78] Two centrosymmetric probes **5-(8-DMAQ)$_2$** and **6-(8-DMAQ)$_2$** undergo slower photorelease of acetic acid than the parent protecting group **8-DMAQ** (Table 1) and both probes display low values of two-photon uncaging cross-section: 0.07 and 0.4 GM at 730 nm, respectively. This outcome stems from the deviation from C_2-symmetry; in reality

quinoline dimers are not coplanar but have a conformation of a twisted diaryl system. The difference in two-photon uncaging cross-section between **5-(8-DMAQ)$_2$** and **6-(8-DMAQ)$_2$** is accounted for as a substituent effect, which has been explored in the following studies. Attempts to incorporate quinoline into D-π-A system yielded protecting groups with two-photon uncaging cross-sections of 0.11 - 2.0 GM at 730 nm.[79]

To use the chromophore extension strategy efficiently, one has to balance inherently related absorption and cleavage steps. This problem is very well illustrated with the *o*-nitrobenzyl and quinoline families. In most cases, enhanced TPA-cross section in these platforms comes at a price of significantly lower uncaging quantum yield than for their respective parent protecting groups. Extended systems indeed undergo efficient two-photon absorption as charge-displacement is facilitated by π-conjugated substituents. Nevertheless, the lowest excited state of such platforms either decays in a competitive pathway or its energy is too low to drive the bond cleavage.

1.7.3 Adding spatial separation between the absorption and cleavage steps

Considering the limitations of the design strategies discussed in the last section, several attempts have been made to explore alternative approaches, in which the absorption and release steps are decoupled. Since it has proved extremely difficult to enhance δ_a while preserving a high value of ϕ_u, further development of protecting groups utilized spatial separation of absorption and cleavage. In such caging platforms, absorption and release steps occur in distinctive units, which are held in close proximity to each other by means of a covalently attached linker. The strategy relies on sensitized deprotection, in which light is absorbed by an antenna chromophore and the excited state decays by energy or electron transfer to the protecting group, liberating the caged species. Sensitized uncaging takes advantage of a substantial difference between absorption properties of the peripheral chromophore and a poorly absorbing protecting group. It also relies on efficient interaction between the antenna and the protecting group (either in the form of electron or energy transfer) to improve the quantum yield of release, compared to the quantum yield achieved upon direct excitation of the caging group. Irrespective of the operating mechanism, migration of the excited state energy allows for initiating reactions in molecules that are otherwise unable to harvest light efficiently.

The following two sections cover the principles of energy and electron transfer, and provide a review of protecting groups which are designed to work according to these mechanisms.

Energy transfer

There are two mechanisms that allow an excited donor to transfer energy to an acceptor: dipole-dipole interaction (Förster resonance energy transfer, FRET) or electron exchange (Dexter mechanism, Fig. 8).[80,81]

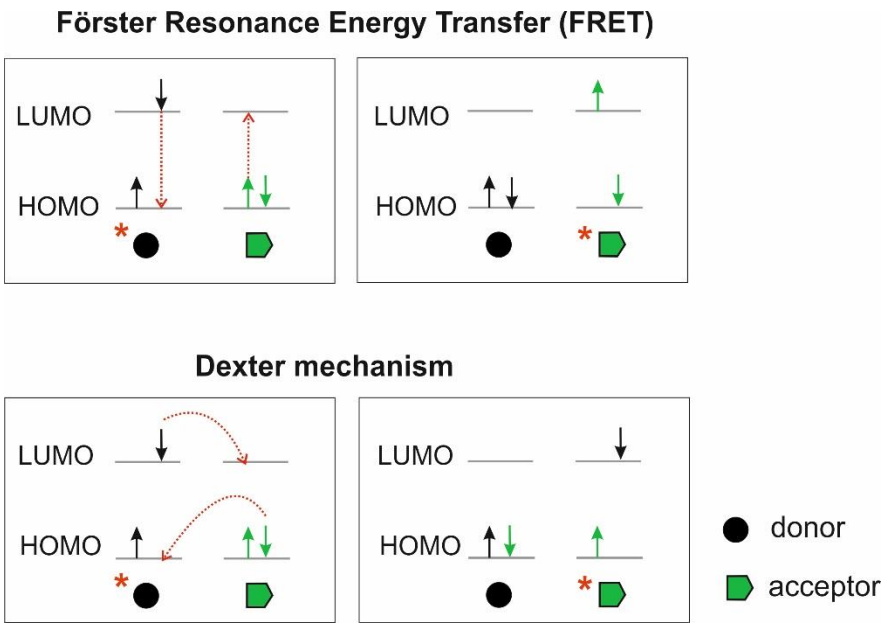

Figure 8. Förster and Dexter mechanism of energy transfer. In Förster Resonance Energy Transfer (FRET) electrons in donor and acceptor move within orbitals of their native electron shell. Energy transfer occurs as a result of coupling between electric fields induced by simultaneous electronic transitions in donor and acceptor. In Dexter mechanism (electron exchange) electrons are transferred between LUMO-LUMO and HOMO-HOMO of donor and acceptor.

FRET is a through space (1-10 nm distance range)[82] interaction between a donor in the excited state and acceptor in the ground state (Fig. 8). Although a fundamental requirement for FRET to occur is the overlap of the emission spectrum of the donor with the absorption spectrum of the acceptor, emission and subsequent absorption of a photon do not take place. The mechanism of energy transfer is based on the interactions of dipoles that are formed upon transitions LUMO → HOMO in donor and HOMO → LUMO in acceptor (Fig. 8). Each dipole induces its own electric field and affects the partner. The electric fields are coupled to each other and therefore decay of the excited state of the donor and excitation of the acceptor are simultaneous. The rate of FRET (k_{FRET}, Equation 1) depends

on many factors, such as the aforementioned spectral overlap of emission and absorption of donor and acceptor $J(\lambda)$, quantum yield of the donor ϕ_D, lifetime of excited donor $_D$, orientation of partner molecules κ and the distance between them r.[82] The interaction is independent of the environment and solvatation shell as long as the solvent does not change the spectral properties of reactants.

$$k_{FRET} = \frac{1}{\tau_D}\left(\frac{R_0}{r}\right)^6 \qquad (1)$$

$$R_0^6 = \frac{9ln(10)\kappa^2\phi_D}{128\pi^5 N n^4} J(\lambda) \quad (2)$$

Equation 1. Rate constant of Förster Resonance Energy Transfer, k_{FRET}, where τ_D is the lifetime of excited donor in the absence of acceptor, r is the distance between the donor and acceptor, R_0 is Förster distance (distance at which efficiency of FRET is 50% and typically lies between 20-60 Å). **Equation 2.** Förster distance, R_0, where κ^2 is the orientation factor, ϕ_D is quantum yield of the donor in the absence of acceptor, N is Avogadro number, n is refractive index of the medium and $J(\lambda)$ is an overlap integral. R_0 can be calculated based on experimentally determined data mentioned in Equation 2 and κ^2 is assumed as 2/3 if the chromophores are randomly oriented with respect to each other.

In electron exchange (Dexter interaction) two electrons are exchanged simultaneously: one between HOMO-HOMO and the other between LUMO-LUMO of donor and acceptor (Fig. 8). As a result of this concerted exchange the donor returns to the ground state and the acceptor is promoted to the excited state. Similarly to FRET, the Dexter mechanism also requires overlap of emission and absorption spectra but additionally overlap of orbitals is needed. Both singlet-singlet and triplet-triplet state interactions can be involved in energy transfer process.

Irrespective of the mechanism of energy transfer, the fate of the excited acceptor is determined by its photophysical properties. The energy gained upon excitation of the molecule can be dissipated as heat, released radiatively or used to initiate a reaction, such as a rearrangement or bond scission. The latter is anticipated in excited acceptors applied in sensitized deprotection.

The concept of sensitized uncaging, in which two spatially separated steps of photorelease are linked by intramolecular energy transfer was first demonstrated for one-photon photolysis. Systematic studies were carried out for triplet-triplet sensitized liberation of thymidine from thioxanthone−2-(*o*-nitrophenyl)propyl conjugate (Table 6, **27**).[83,84] Quantum yields of deprotection ranged between 0.09-0.42 depending on the linker, substitution pattern and excitation wavelength. Separate series of

experiments showed that the photosensitivity of nitroindol protecting group is increased six times as a result of assembly with benzophenone (**28**).[85] Attempts to evaluate the utility of chimeric structure **28** in living cells were not possible because of precipitation of the probe in media containing Ca^{2+} ions. An extensive set of troubleshooting experiments revealed that this precipitation was related to the presence of benzophenone bearing phosphate substituents. It was found that aqueous solubility can be maintained upon replacement of the phosphate group with aspartic acid (**29**).[86] This example clearly shows that protecting groups have to fulfill many requirements and all the structural features of the probe need to be optimized to avoid undesirable interactions with other species present in biological samples.

Recently, the strategy of energy transfer mediated release has been implemented in two-photon uncaging systems. Examples include intermolecular (bimolecular) energy transfer in isopropylthioxanthone−2-(*o*-nitrophenyl)propyl used in the fabrication of DNA microarrays (**30**, δ_u of 0.86 GM at 766 nm)[87] and intramolecular FRET in fluorene-cored systems aimed at application in neuroscience (**31**-**36**).[88,89] In the latter a fluorene derived antenna gives rise to a quadrupolar system comprising either nitroindol (**31**, **32**)[88] or 4,5-dimethoxy-2-nitrobenzyl protecting groups (**33**-**36**).[89] Although the values of two-photon uncaging cross section are still modest (0.5 GM at 730 nm for **32** and 0.11-0.25 GM at 730-800 nm for **33**-**36**) they show a significant enhancement compared to δ_u of their parent release groups (which for **MNI-Glu** is 0.06 GM at 720 nm[32] and for 4,5-dimethoxy-2-nitrobenzyl acetate 0.03 GM at 740 nm[59]). Low values of δ_u obtained for structures **31**-**36** result from inefficient energy transfer and low uncaging quantum yield of the parent protecting units. Therefore the advantage of two-photon absorbing dye with high δ_a was not fully displayed in these systems. Further research is focusing on the use of protecting groups with red-shifted absorption profile to improve spectral overlap with the fluorene chromophore and to give higher yield of uncaging.

Table 6. One- and two-photon sensitive protecting groups operating through energy transfer mechanism.

One-photon sensitized deprotection

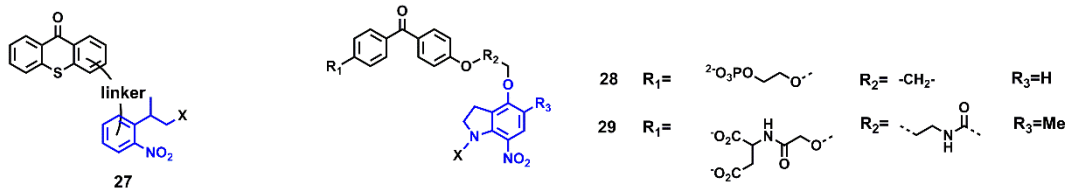

Two-photon sensitized deprotection

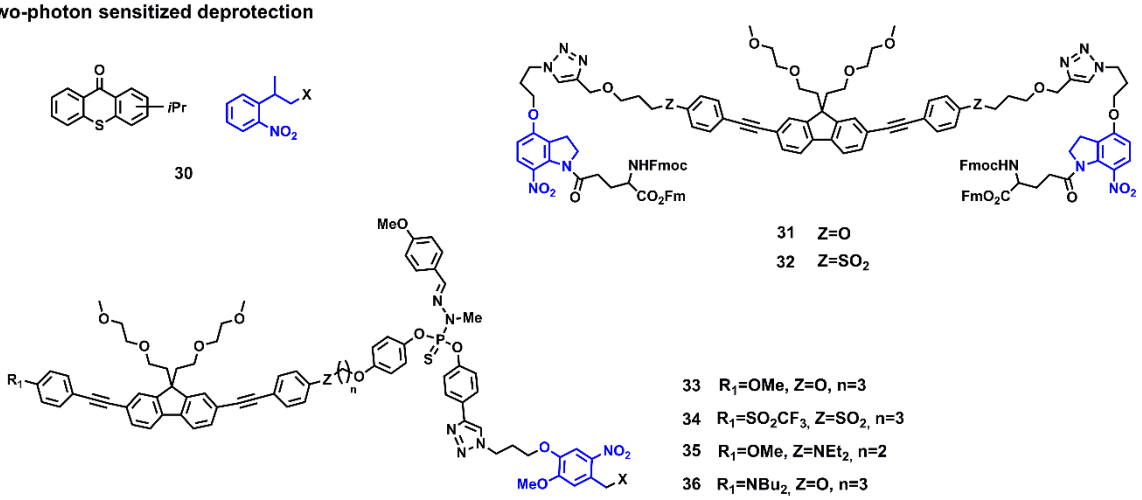

Protecting group	X – Leaving group	δ_u [GM] / λ [nm]	$\phi_{ET}{}^a$	Comments	Ref.
31	Glutamate[b]	n.d.	0.85	δ_a = 42 GM (710 nm)	88
32	Glutamate[b]	0.5 /730	0.88	δ_a = 76 GM (720 nm)	88
33	Acetate	0.11 /730	0.38	δ_a = 50 GM (750 nm)	89
34	Acetate	0.12 /730	0.17	δ_a = 110 GM (730 nm)	89
35	Acetate	0.1 /750	0.11	δ_a = 160 GM (750 nm)	89
36	Acetate	0.25 /800	0.05	δ_a= 310 GM (800 nm)	89

a – yield of energy transfer; *b* – Glutamate was released as Fmoc-Glu(OH)-OFm; n.d. – not determined.

Electron transfer

An alternative method of linking spatially separated absorption and release steps is to connect them through photoinduced electron transfer (PeT).[80,81, 91-93] In PeT the term "donor" refers to the species giving an electron away and "acceptor" to the molecule which receives this electron. Although both donor and acceptor can play the role of light absorbing species, in the following discussion only the case when the electron donor acts as an antenna will be considered. [94]

The mechanism of PeT mediated uncaging is shown in Figure 9.[23] The electron-donor plays the role of a light-harvesting platform, whereas the acceptor unit serves as a protecting group. Upon excitation, the donor transfers an electron to the acceptor (k_{ET}) to give a charge-separated state. PeT occurs efficiently only if it is faster than other pathways of deactivation of the excited state: non-radiative decay, fluorescence or intersystem-crossing. The radical cation and anion formed as a result of PeT are active species and can undergo further transformation such as fragmentation that leads to the release of the protected moiety (k_{REL}).[95] The choice of the release unit is crucial, as not all acceptors initiate bond-breaking events upon one-electron reduction. Moreover, bond cleavage occurs only if it is faster than the charge recombination. Therefore long-lived charge-separated states are desirable as they facilitate subsequent transformation of radicals. The main reaction that competes with uncaging is the decay of the charge-separated state to the ground, or low-lying triplet state, through back electron transfer (BET, k_{BET}).

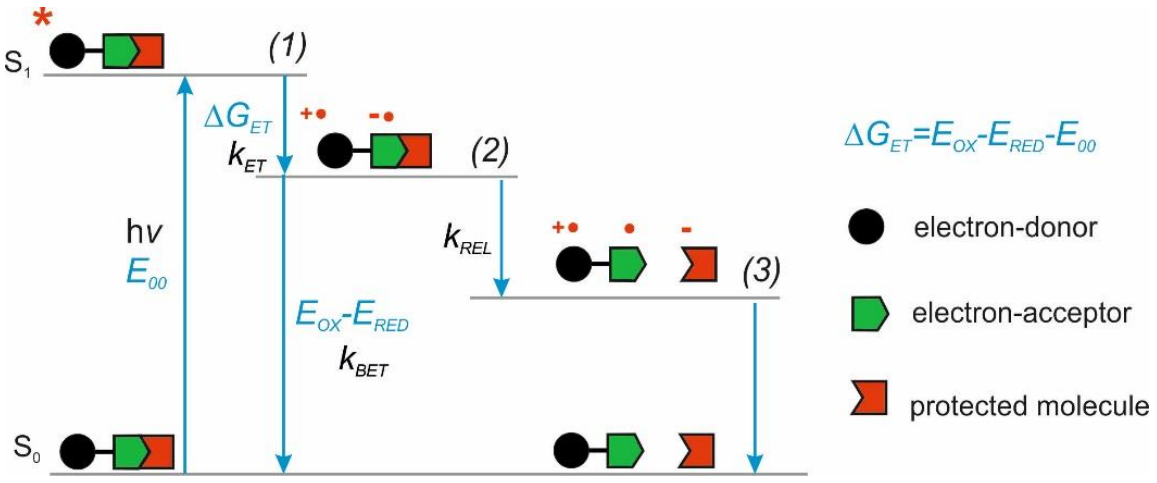

Figure 9. Mechanism of PeT mediated uncaging. Light absorption generates a photosensitizer-based excited state (*1*), which is quenched by electron transfer (k_{ET}) to the release group. The resulting charge-separated state (*2*) decays by σ-bond cleavage (k_{REL}) to liberate protected molecule (*3*). Charge recombination (k_{BET}) can compete with uncaging reaction.

The fundamental requirement for efficient PeT is that the Gibbs free energy (ΔG_{ET}) for the process must be negative (Equation 3).[96] The energy of the singlet excited state of the dye (E_{00}) must be greater than the energy cost of transferring an electron from the donor to the acceptor, i.e. greater than the difference between the oxidation potential of the donor (E_{OX}) and the reduction potential of the acceptor (E_{RED}), corrected by the Coulombic stabilization of the charges. The excited state energy (E_{00})

is defined as the energy of transition between the lowest vibrational level of the ground and excited states, and can be estimated from the point of overlap between the absorption and emission spectra. The oxidation potential of the donor (E_{OX}) and reduction potential of the acceptor (E_{RED}) can be measured electrochemically.

$$\Delta G_{ET} = N_A \{e[E_{OX} - E_{RED}] + w(D^{+\cdot}A^{-\cdot}) - w(DA)\} - E_{00} \quad (3)$$

$$w(D^{+\cdot}A^{-\cdot}) = \frac{z(D^{+\cdot})z(A^{-\cdot})e^2}{4\pi\varepsilon_0\varepsilon_r a}; w(DA) = \frac{z(D)z(A)e^2}{4\pi\varepsilon_0\varepsilon_r a} \quad (4)$$

Equation 3. Gibbs free energy of photoinduced electron transfer, where E_{00} is the singlet excited state of the dye, E_{OX} is oxidation potential of the donor, E_{RED} is reduction potential of the acceptor, N_A is the Avogadro constant, e is the elementary charge, $w(D^{+\bullet}A^{-\bullet})$ and $w(DA)$ are terms that factor in electrostatic interaction in the products and reactants. **Equation 4.** Coulombic attraction between donor and acceptor, where ε_0 is the vacuum permittivity, ε_r is the dielectric constant of the solvent, a is the distance of charge separation and z(D/A) is charge of the species (D: donor; A: acceptor).

The photophysical parameters of the probe, such as the rate of PeT and BET, can be modulated by variation in the length of the bridge connecting donor and acceptor and the structure of electron-acceptor. The lifetime of the charge-separated state can be prolonged, to some extent, by choosing a suitable linker joining a given pair of donor and acceptor. The electron transfer (forward and back) occurs more slowly over large distances and consequently the lifetime of the charge-separated state is extended. The dependence of the rate constant of PeT on the center to center distance between the donor and the acceptor depends on the mechanism of electron transfer. In general, this relationship is exponential[97-99] but there are several reports of systems in which the rate of PeT depends inversely on the length of the bridge and this is attributed to a multistep hopping mechanism.[100,101] Equally important is the structure of the linker. Rigid spacers are desirable as they hold donor and acceptor away from each other. In such systems electron transfer can be mediated either by solvent or occur through the bonds of the rigid bridge which provides its orbitals (δ, σ*, π or π*) as tunnels (*super exchange mechanism*). Flexible linkers might allow for through-space interactions between reactants and rapid electron transfers resulting in a short lifetime of charge-separated state.

One can also advance the efficiency of forward electron transfer and reduce the rate of competing back electron transfer ($k_{ET} > k_{BET}$) by modulating ΔG. The Marcus model establishes a quadratic dependence of the rate constant k on the free energy of PeT reaction ΔG (Equation 5, 6; Fig. 10).[102,103]

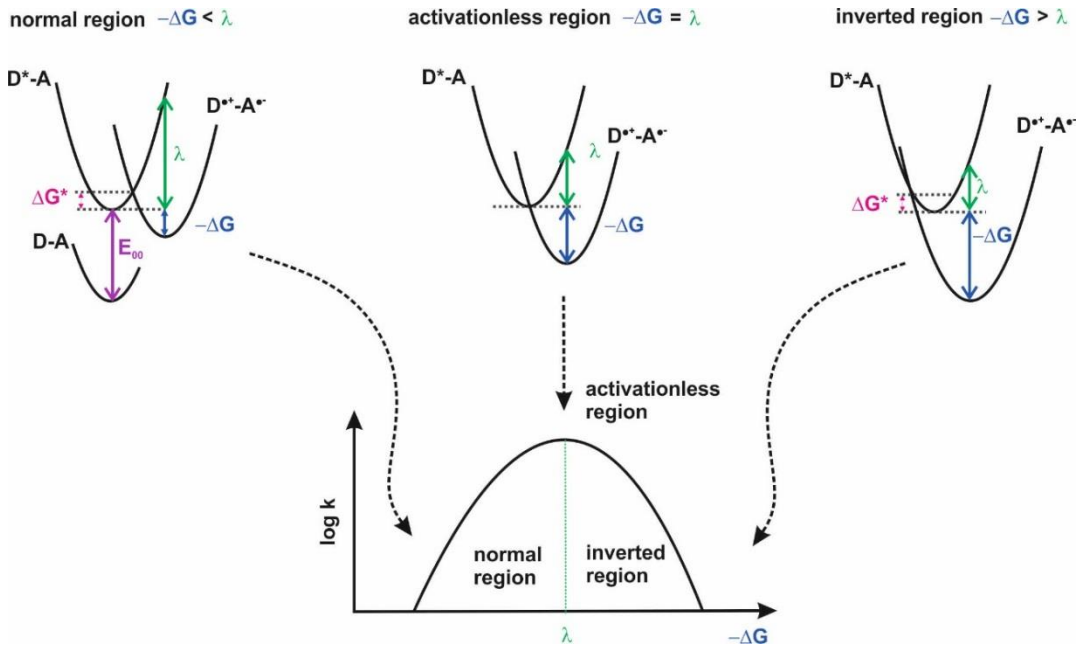

Figure 10. **Top:** Parabolas representing Gibbs free energy of reactants and products as a function of nuclear coordinates for electron transfer reactions. Parabolas reflect overall energy of reacting molecules and their surrounding solvation shell. In normal region Gibbs free energy is larger than reorganization energy, in contrast to the inverted region, where $-\Delta G > \lambda$. **Bottom:** Dependence of the electron transfer rate constant on the exothermicity of reaction: rate constant increases with exothermicity in normal region, reaches maximum for $-\Delta G = \lambda$ and decreases in inverted region.

$$\Delta G^* = \frac{(\Delta G+\lambda)^2}{4\lambda} \quad (5)$$

$$k = Aexp\left(-\frac{\Delta G^*}{k_B T}\right) \quad (6)$$

Equation 5. Activation energy of electron transfer reaction ΔG^*, where ΔG is free energy of the reaction, λ is reorganization energy. **Equation 6.** Rate constant of electron transfer reaction, where A is a pre-exponential factor dependent on the nature of the reaction, k_B is Boltzmann constant and T is the temperature.

Key assumptions of Marcus theory are that electron transfer occurs when geometry of donor and acceptor match and that reactants and products have the same parabolic potential energy surface, shifted on a reaction coordinate. Marcus factors in the reorganization energy, λ which is required for the structural rearrangement of the reactants and their solvation shell: substrates need to obtain the

conformation of products and the surrounding solvent molecules have to change their orientation to stabilize the ions formed. The theory also predicts that the rate of PeT increases with exothermicity but only for $-\Delta G < \lambda$ (Marcus normal region). The reaction reaches maximum rate for $-\Delta G = \lambda$ (activationless region) and slows down when $-\Delta G > \lambda$ (Marcus inverted region). Typically, forward electron transfer is less exothermic than charge recombination ($\Delta G_{ET} < \Delta G_{BET} = E_{OX} - E_{RED}$ in Fig. 9). Consequently, forward electron transfer usually lies in the Marcus normal region and back electron transfer occurs in the Marcus inverted region. By carefully selecting a donor−acceptor pair, for which $-\Delta G$ is sufficiently negative, the energy of the charge separated state can be increased. In this way back electron transfer is pushed even more to the inverted region and proceeds more slowly relative to the forward electron transfer. As a result, the lifetime of the charge separated state is extended, allowing the radical anion to undergo further reactions and liberate protected species.

Release mediated through PeT has not been thoroughly explored in the field of two-photon uncaging. Although several examples of PeT sensitized one-photon deprotection are reported in the literature, there are very few examples of rational design of protecting groups operating *via* PeT. Covalently linked donor−acceptor systems were investigated with use of phenacyl[104] and *N*-alkyl-4-picolinium (pyridinium)[105] as acceptor units in one-photon photolysis studies. In a series of comparative experiments, deprotection was carried out for separated and covalently linked donor−acceptor pairs, such as *N*,*N*-dimethylaniline−phenacyl **37**, anthracene−phenacyl **35** and carbazole−pyridinium **39** (Fig. 11). The carboxylic acid was efficiently released in each case when electron-donor and electron-acceptor were unlinked. However, in the series of fixed assemblies, only *N*,*N*-dimethylaniline−phenacyl **37** liberated carboxylic acid. The difficulties encountered in other systems highlight the challenges related to intramolecular electron transfer. In the case of anthracene **38** back electron transfer followed by intersystem crossing prevented the bond scission from taking place. Uncaging was completely unsuccessful because the radical cation decayed to lower-lying triplet state. The lifetime of the charge separated state of the fixed carbazole−pyridinium pair **39** was too short to allow bond scission to occur and back electron transfer was the prevalent process.

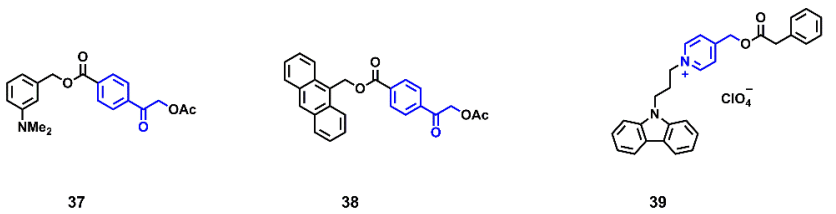

37 38 39

Figure 11. Structures of primary protecting groups operating through PeT mediated mechanism.

To the best of our knowledge, two-photon sensitive protecting groups that operate through PeT have not been reported in the literature. However, unpublished studies were carried out in Prof. Seth Marder's group (Georgia Institute of Technology). Experiments were conducted by Dr Jing Wang and the results were presented in her Ph.D. thesis.[106] A two-photon absorbing dye **40** with δ_a of 1050 GM at 730 nm was selected as an electron donor,[107] whereas phenacyl caging unit served as electron acceptor (Fig. 12). Ester **41**, ether **42** and unsubstituted model phenacyl **43** were employed to investigate the influence of the linker on the deprotection. Acetic acid was chosen as a model protected carboxylic acid. Efficiency of uncaging was evaluated only under one-photon excitation. In bimolecular photolysis experiments (performed for each phenacyl derivative in the presence of the model dye **40**) no acetic acid was liberated in the case of ester **41.** Under identical conditions uncaging proceeded successfully for ether **42** and unsubstituted analogue **43**. The same result was observed when covalently linked donor−acceptor assemblies were photolysed. Ester derivative **44** remained intact and ethers **45** and **46** released desired acid. The author hypothesized that this disparity could be explained in terms of electron-donating effect of ester linker which impedes photorelease. The relationship between the position of caging unit and the efficiency of deprotection was also carefully examined. Additional experiments showed that substitution of the central π-bridge of the chromophore **45** resulted in two times higher yield of released acid than in the case of derivative **46** in which phenacyl was attached to the terminal electron donating group.

Protecting groups designed to operate *via* PeT have shown notable promise; although no two-photon deprotection experiments were carried out, the proof-of-concept one-photon photolysis proceeded smoothly and yielded free acetic acid in nearly quantitative chemical yield (92% for **45**).

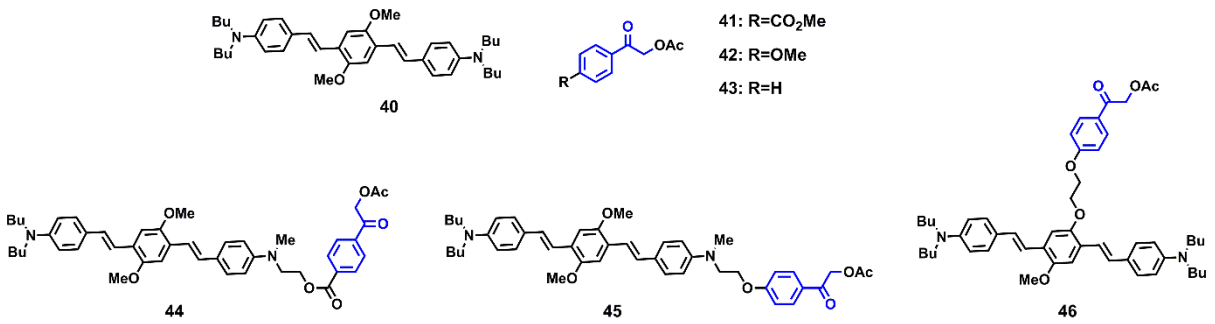

Figure 12. Structures of model compounds and two-photon sensitive protecting groups designed to liberate protected molecules upon PeT.[106]

1.8 Aim of the project: towards two-photon, PeT mediated uncaging

The examples presented in the previous sections show that modular design holds significant advantages over other design strategies but also brings new challenges. As absorption and cleavage steps are independently tuned, and dyes are available with δ_a of up to 10,000 GM and higher, this approach, in theory, may result in combinations of donor and acceptor units that give rise to protecting groups with unprecedentedly high δ_u. Furthermore, modular design provides opportunities to improve stability and aqueous solubility of probes without affecting their absorption properties. Nevertheless, initial attempts to develop protecting groups for PeT and energy transfer mediated photorelease yielded cages with $\delta_u < 1$ GM. In the long-term perspective this approach shows some promise but the optimal molecular design remains a field of exploration. The current challenge in the development of highly sensitive caging groups relates to the determination of the antenna−release unit pairs that cooperate with each other efficiently.

The aim of this project was to study PeT-mediated uncaging in a two-photon excitable system. Drawing upon previously reported designs, a protecting group that is activated *via* intramolecular PeT between a photoexcited electron-donor (a TPA dye with high δ_a) and an electron-acceptor (pre-existing release unit, Fig.13) was devised. The objective was to explore alternative architectures and scrutinize the structure-property relationships for several combinations of donor−acceptor pairs. A particular goal of this project was to develop probes that are water-soluble and apply them to studies in live cells. Due to the special attention paid by neuroscientists to the neurotransmitter GABA,

we decided to extend the available research toolbox by preparing a series of the protected analogues of GABA. The structure of a preliminary synthetic target is shown in Figure 13.

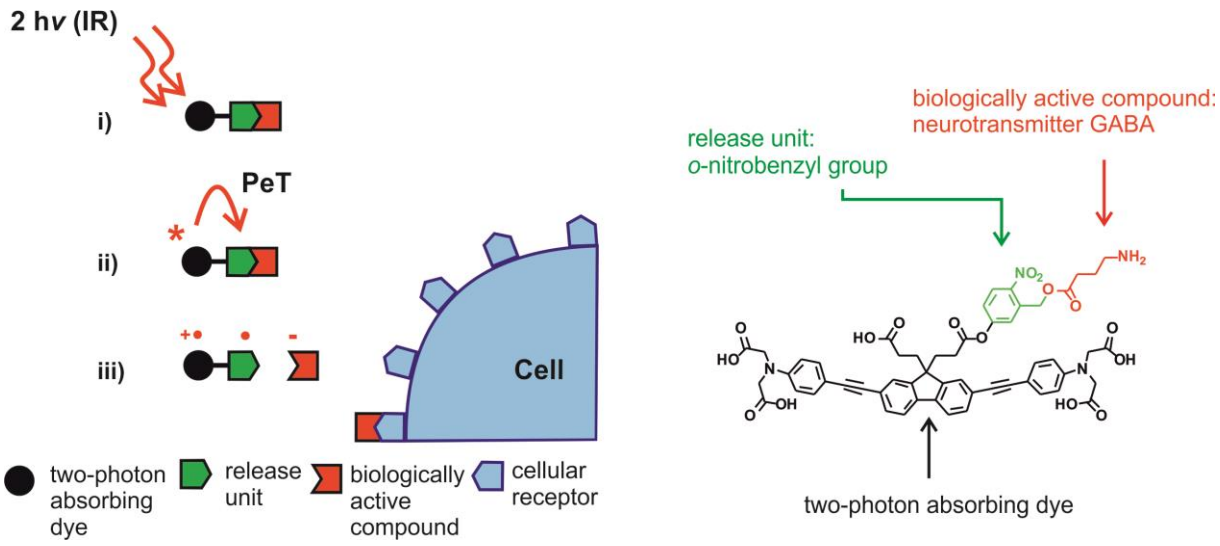

Figure 13. Left: Concept of a photolabile protecting group operating *via* photoinduced electron transfer. Upon two-photon excitation (*i*) the dye unit donates an electron to the release unit (*ii*), which undergoes photochemical reaction and liberates the drug (*iii*). Adapted with permission from ref. 3, Published by The Royal Society of Chemistry. **Right**: Structure of the first synthetic target.

It was critical to choose an antenna with high TPA cross-section which is also appropriate for biological studies, including future applications as a membrane-permeable probe. A symmetric fluorene-based dye with alkylated aniline terminal donors connected with the core *via* the acetylene bridge (D-π-A-π-D) presented an ideal candidate for this project (**47**, Fig. 14). It combines a relatively simple design with a reported TPA cross-section of 1200 GM at 705 nm.[108]

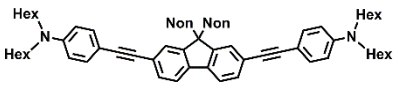

47

Figure 14. Structure of the parent chromophore employed as an antenna and electron–donor.[108]

Initial studies focused on the evaluation of *o*-nitrobenzyl platform as the electron acceptor. Further work presented in this thesis is a continuation of research started by Dr Philip Bennett[109] and explores the utility of phenacyl and pyridium units.

o-Nitrobenzyl group and its nitrobenzylic derivatives are the most common photolabile protecting groups and were used in numerous biological experiments to protect and efficiently release carboxylic

acids, phosphates, alcohols and amines upon direct irradiation.[18] Although they were never demonstrated to release protected compounds upon PeT there are several examples in which halides,[110,111] ketones[112,113] and amines[114] were liberated as a result of cathodic deprotection (Scheme 1). Electrochemical studies revealed that the cleavage of carbon-halogen bond proceeds through a stepwise mechanism, in which the initially formed radical anion fragments to yield a nitrobenzyl radical and a halogen anion. Presence of the electron-withdrawing group lowers the reduction potential and facilitates electron transfer, but in most cases removal of the protecting group is accompanied by side reactions and yields vary with the temperature, solvent and pH.

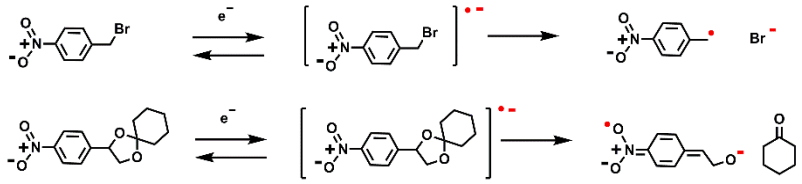

Scheme 1. The mechanism of fragmentation of *p*-nitrobenzyl bromide[111] and *p*-nitro-1,3-dioxolane[112] induced by electrochemical reduction.

Phenacyl group has been reported to release carboxylic acids, phosphates and alcohols not only upon direct illumination with ultraviolet light but also as a result of PeT.[115-117] The mechanism of deprotection involves formation of the radical anion of phenacyl ester and the radical cation of the sensitizer upon one-electron reduction (Scheme 2). The radical anion undergoes fragmentation of the α−C−O bond to give a phenacyl radical and a carboxylate anion. Neutral phenacyl ester is formed as a result of proton abstraction from the sensitizer. Moreover, phenacyl esters have been photolysed under physiological conditions. Upon direct illumination, GABA and glutamate were released from their *p*-hydroxyphenacyl esters in rat[118] and mice[119] brain cortical slices respectively and bradykinin (an inflammatory mediator)[120] was liberated in rat dorsal root ganglion (DRG) neurons.

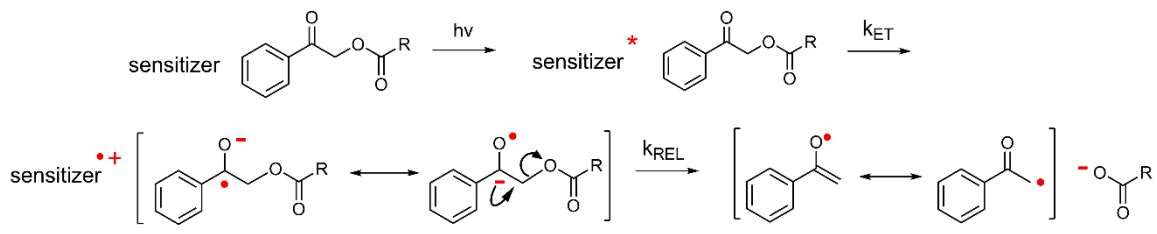

Scheme 2. The mechanism of fragmentation of phenacyl ester induced by photoinduced electron transfer.[116]

Picolinium esters, which are the precursors of the pyridinium group, were originally used in solid-phase peptide synthesis[121-124] and removed upon cathodic cleavage.[125] Their *N*-methylated derivatives possess a relatively low reduction potential (-1.1 V vs SCE)[126] and were proven to release carboxylic acids upon inter- and intramolecular PeT.[126-130,185] Removal of the pyridinium group proceeds through the intermediate pyridyl radical, which is generated upon PeT from the excited state of the sensitizer. Subsequent fragmentation of the C−O bond leads to the release of carboxylate and formation of radical cation (Scheme 3). *N*-methyl pyridinium protecting group has never been adopted for application under strictly physiological conditions.

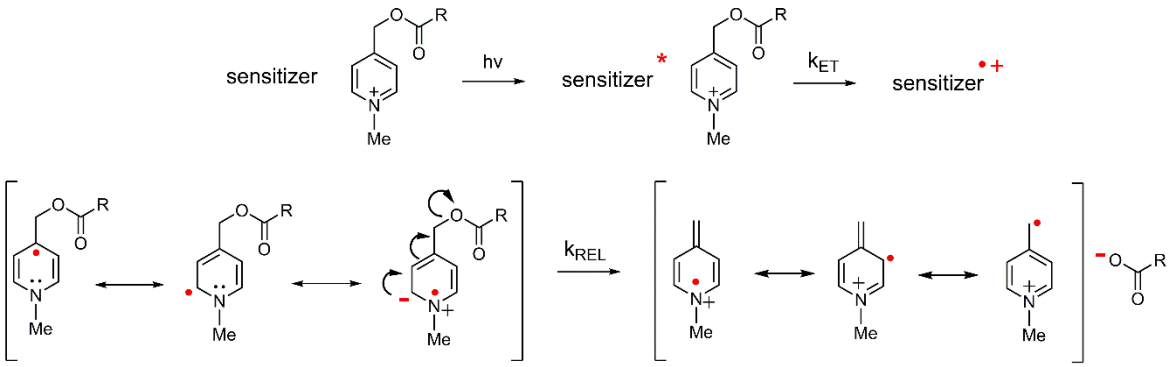

Scheme 3. The mechanism of fragmentation of *N*-methyl picolinium ester induced by photoinduced electron transfer.[126]

Chapter 2

The molecular design of protecting groups

A four-stage approach has been pursued in the development of two-photon sensitive protecting groups for PeT mediated deprotection (Fig. 15). The first and second steps involved optimization of the electron-donor and the electron-acceptor. The electron-donor was chosen based on literature reports, whereas a pool of alternative structures was investigated to identify a suitable electron-acceptor. In the third stage, an array of model compounds was synthesized, in which donor and acceptor were covalently linked. Numerous photophysical attributes of these compounds were studied to assess the feasibility and efficiency of intramolecular electron transfer. Finally, the release properties of the developed protecting groups were evaluated during one-photon photolysis of the model caged carboxylic acids. The collected data permitted assessment of the utility of the novel protecting groups and helped to direct further development. The results presented in this chapter refer to the first three stages of the design process.

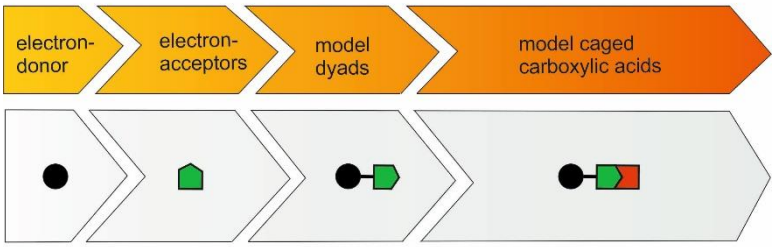

Figure 15. Schematic outline of the research strategy adopted for the development of two-photon sensitive protecting groups operating through PeT.

2.1 Selection of the electron-donor

2.1.1 Synthesis of the model electron donor (first generation)

The studies began with the choice of a suitable electron-donor that would efficiently undergo two-photon excitation. As outlined in Section 1.8, a symmetric banana-shaped bisethynyl fluorene dye

(**BEF**) has been chosen as the precursor for the backbone of the electron-donor. Compound **47** displays δ_a of 1200 GM at 720 nm and an excited state energy (S_1) of 3.07 eV.[108] Structure **47** could be functionalized by the replacement of nonyl (Non) and hexyl (Hex) chains with a suitable linker connecting the dye with the release unit and substituents enhancing aqueous solubility. Bis-propionic carboxylates were introduced at position *9* of the fluorene to permit for covalent attachment of the electron-acceptor unit (**48**, Fig. 16). The original Hex chains were replaced with carboxyethyl substituents to aid aqueous solubility. Model compound **48** was designed to evaluate electrochemical properties of this class of compounds and investigate the range of its aqueous solubility.

Figure 16. The structure of fluorene-based dyes.

A retrosynthetic analysis of **48** (Scheme 4) presented the Sonogashira coupling as a key step in the preparation of the model dye. By allowing preparation of the core and the aniline unit separately, the convergent synthesis provided a convenient access to a range of analogues.

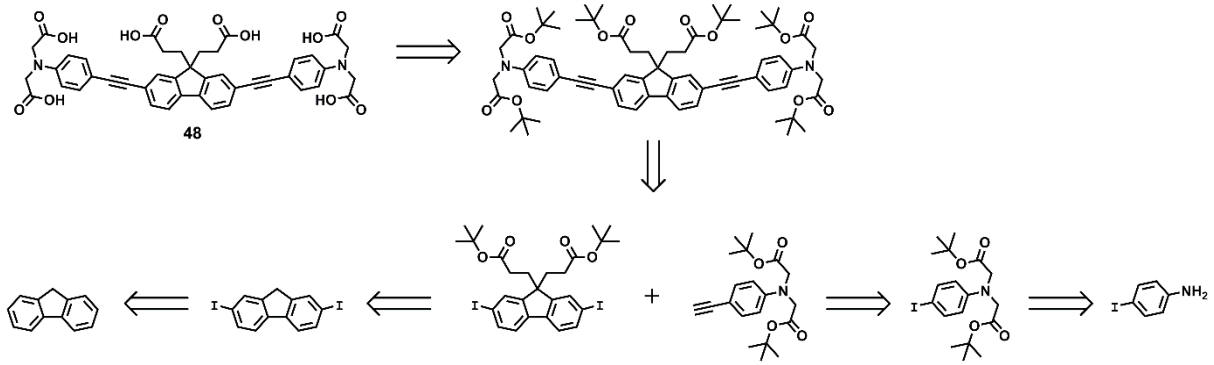

Scheme 4. Retrosynthetic analysis of a fluorene-based dye.

The synthesis of compound **48** was developed by Dr Philip Bennett[109] and started with regioselective 2,7-iodination of fluorene with elemental iodine in the presence of periodic and sulfuric acid (Scheme 5).[131] The next step involved a base-catalyzed Michael addition of fluorene **49** to *t*-butyl acrylate to give 9-alkyl functionalized core **50**.[132] The alkylation of *p*-iodoaniline with bromo-*t*-butyl acetate yielded derivative **51**, which was subsequently coupled with TMS-acetylene to give **52**. The final

aniline component **53** was obtained upon treatment of **52** with TBAF. Cross-coupling between **50** and **53** generated the ester precursor **BEF-tBu**. The *t*-butyl ester deprotection, to yield free carboxylic acids, proved irreproducible. Attempts to hydrolyze the *t*-butyl esters under acidic conditions resulted only in decomposition of the starting material. Moreover, solubility studies of **48** carried out by Dr Bennett showed that six carboxylic groups do not provide sufficient solubility at pH 7.4 and 1 mM solution could be obtained only in buffers at pH >12.[106] Due to the difficulties encountered during the synthesis of compound **48**, its analogue **BEF-tBu** was treated as a model for photophysical and electrochemical studies as well as it was used in initial bimolecular uncaging experiments (Chapter 3, Section 3.1).

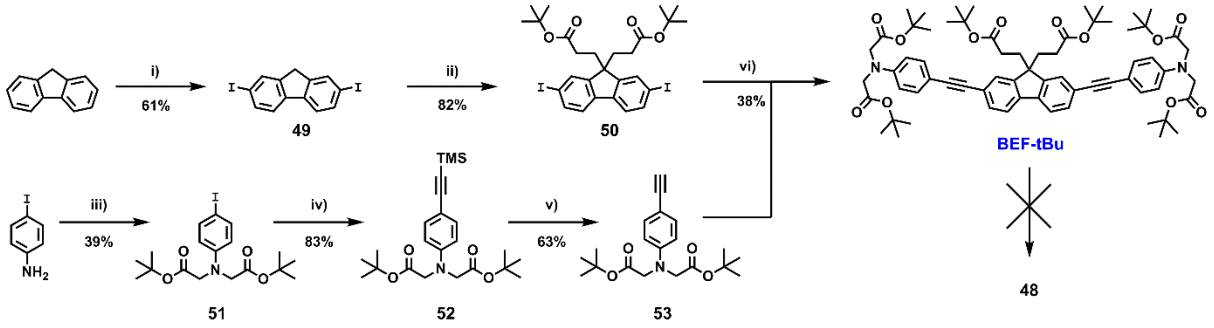

Scheme 5. Synthetic route to **48**. Reagents and conditions: i) I_2, H_5IO_6, AcOH, H_2SO_4, H_2O, 80 °C, 4 h, ii) *t*-butyl acrylate, TBAF, THF, 20 °C, 2 h, iii) bromo-*t*-butyl acetate, Na_2CO_3, DMF, 100 °C, 24 h, iv) TMS-acetylene, $Pd(OAc)_2$, PPh_3, CuI, DIPA, 20 °C, 16 h, v) TBAF, THF, 20 °C, 15 min, vi) **53**, $Pd(OAc)_2$, PPh_3, CuI, DIPA, 20 °C, 1 h.

2.1.2 Photophysical properties of the electron-donor (first generation)

The one-photon absorption and emission spectra of **BEF-tBu** in THF are shown in Figure 17. The fluorene-based dye exhibits a strong absorption in the range 300-400 nm with its maximum at 378 nm ($\varepsilon = 9.0 \pm 0.2 \times 10^4\ M^{-1} \cdot cm^{-1}$) and fluorescence with a maximum at 437 nm and quantum yield $\phi_f = 0.42$ (referenced to quinine in 0.5 M H_2SO_4). The energy required for the transition from the lowest vibrational level of the ground state to the lowest vibrational level of the first singlet excited state (excited state energy, E_{00}) was determined from the intersection of the emission and absorption spectra and is 3.06 eV (406 nm).

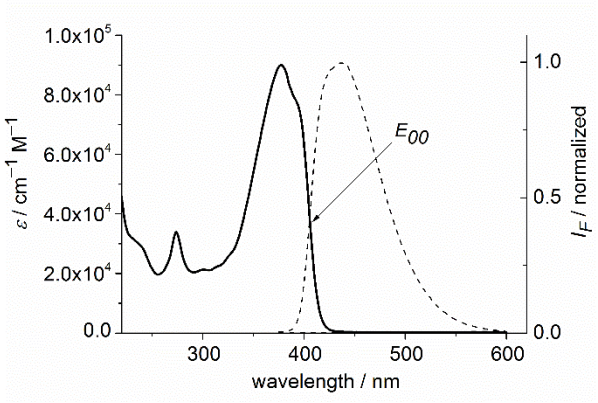

Figure 17. Absorption (solid line) and normalized emission (dashed line) spectra of **BEF-tBu** at 20 °C in THF. Excitation wavelength: 366 nm.

The electrochemical properties of **BEF-tBu** were investigated by cyclic voltammetry and square wave analyses (Fig. 18). Measurements were carried out in DCM with 0.1 M Bu_4NPF_6 (electrolyte) and ferrocene (internal reference). Cyclic voltammetry experiments revealed that **BEF-tBu** undergoes an irreversible oxidation and square wave analysis permitted the accurate determination of the first oxidation potential E_{OX} = 0.55 V vs Fc/Fc^+.

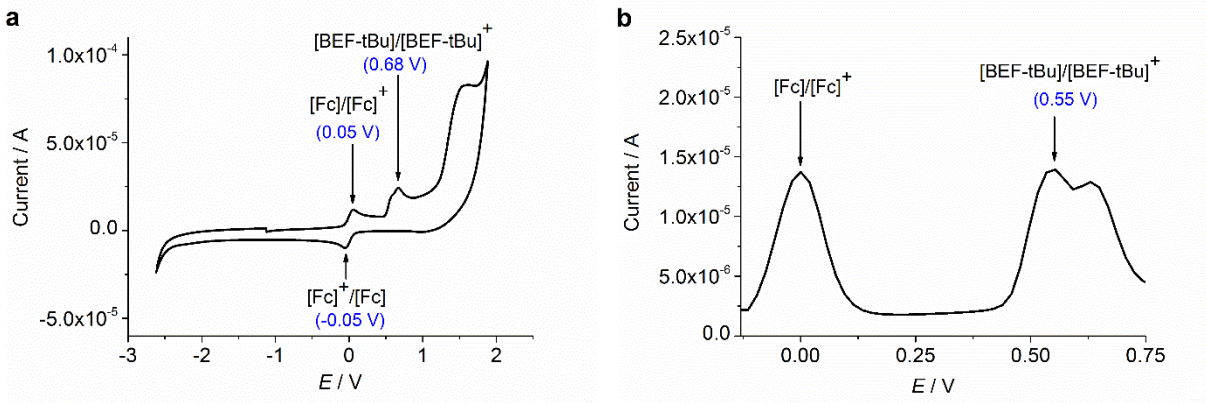

Figure 18. Electrochemistry of the model electron donor **BEF-tBu**; **a)** cyclic voltammogram with ferrocene as internal reference, **b)** square wave voltammogram with ferrocene as internal reference, corrected to Fc/Fc^+ = 0 V. The results show that the first oxidation potential of **BEF-tBu** is 0.55 V vs Fc/Fc^+ (in DCM, with 0.1 M Bu_4NPF_6 as supporting electrolyte).

E_{00} and E_{OX} were used to solve a simplified Equation 3 (page 27, Gibbs energy ΔG_{ET} of photoinduced electron transfer without Coulombic contribution). Calculations showed that electron transfer is energetically favored between **BEF-tBu** and release platforms with a reduction potential $E_{RED} > -2.51$ V. These results suggested that fluorene-based dye **BEF-tBu** is a suitable electron donor in the novel

uncaging system, however its lack of aqueous solubility presented a critical issue for biological application.

2.1.3 Synthesis of the electron-donor (second generation)

An obvious strategy to improve the aqueous solubility of the dye was to decorate it with substituents that would enhance its solubility but not alter the absorption profile or electrochemical properties of the chromophore. Polyethylene glycol chains have been widely used to aid aqueous solubility of organic compounds.[133] Their low *in vitro* toxicity and chemical inertness conferred additional advantages, therefore the ethyl carboxylates in compound **BEF-tBu** were replaced with methyl ether hexaethylene glycol chains. Moreover, the carboxylate linker in positon *9* of the fluorene core was transformed to alcohol to facilitate further functionalization of the dye with the acceptor units. The structure of the second generation of the water-soluble model dye, **BEF-OH**, is presented in Figure 19.

BEF-OH

Figure 19. Model fluorene-based dye **BEF-OH**.

Conceptually, the preparation of **BEF-OH** followed the same synthetic strategy as preparation of **BEF-tBu**, with Sonogashira coupling between the aniline and fluorene components employed as the key reaction (Scheme 6). The heptaethylene glycol functionalized aniline **58** was synthesized in four steps. The synthetic sequence utilized regioselective iodination of *N*, *N*'-phenyldiethanoloamine with elemental iodine in pyridine to give **55**,[134] which was coupled to TIPS-protected acetylene resulting in **56**. The TIPS protecting group was chosen over TMS because it proved more resistant to the strongly basic conditions necessary for alkylation of the diethanol chains with the tosylate **54** to generate **57**. Removal of TIPS group with TBAF gave the aniline unit **58**. The key fluorene intermediate **60** was obtained upon hydrolysis of *t*-butyl esters with trifluoroacetic acid followed by the reduction of the carboxylic acid **59**. The alcohol **60** was converted to TBDMS ether **61** and coupled to the readily prepared aniline component **58** to generate **BEF-OTBDMS**. The treatment of **BEF-OTBDMS** with TBAF resulted in deprotection of the alcohol groups and yielded **BEF-OH**. The revised synthetic

route employed fluorene derivative **60** in the key Sonogashira coupling with **58** and gave **BEF-OH** with higher yield compared to the earlier route (Scheme 6).

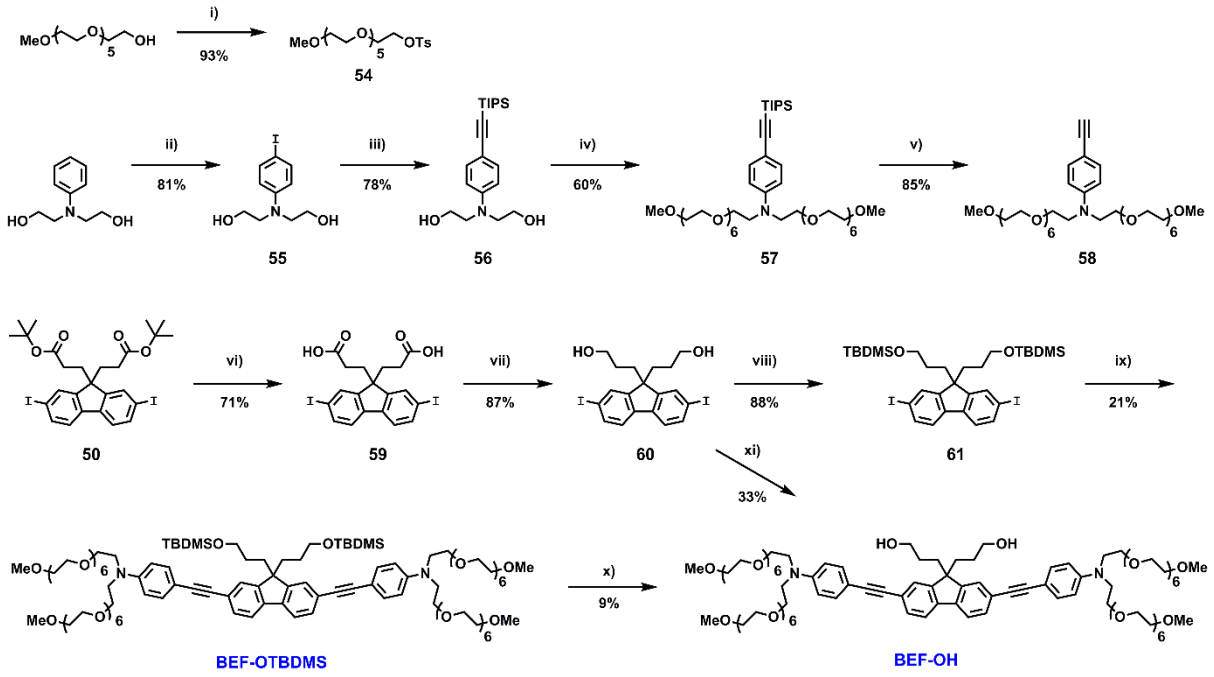

Scheme 6. Synthetic route to **BEF-OH**. Reagents and conditions: i) *p*-TsCl, Et_3N, DCM, 0 °C → 20 °C, 16 h, ii) I_2, pyridine, 0 °C → 20 °C, 16 h, iii) TIPS-acetylene, $Pd(OAc)_2$, PPh_3, CuI, DIPA, 50 °C, 16 h, iv) **54**, NaH, THF, reflux, 48 h, v) TBAF, THF, 20 °C, 12 h, vi) TFA, DCM, 20 °C, 16 h, vii) BH_3·THF, THF, 0 °C → 20 °C, 1 h, viii) TBDMSCl, imidazole, DMF, 20 °C, 4 h, ix) **58**, $Pd(OAc)_2$, PPh_3, CuI, DIPA, 50 °C, 2 h, x) TBAF, THF, 20 °C, 5 h, xi) **58**, $Pd(OAc)_2$, PPh_3, CuI, DIPA, MeCN, 20 °C, 3 h. Adapted with permission from ref. 3. Published by The Royal Society of Chemistry.

2.1.4 Photophysical properties of the electron donor (second generation)

One-photon absorption and emission spectra

The one-photon absorption and emission spectra of **BEF-OH** and **BEF-OTBDMS** were recorded in a wide range of solvents and are shown in Figure 20. The heptaethylene glycol decorated dyes exhibit almost identical absorption properties as their precursor **BEF-tBu**. Comparison of the absorption spectra in THF (Fig. 20a) reveals that characteristic features are maintained across the family of compounds and variation of substituents on the nitrogen atom only insignificantly altered the strong absorption band between 300 nm and 400 nm. The maximum of absorption is redshifted by 2 nm for **BEF-OH** (to 380 nm) and remains unchanged for **BEF-OTBDMS** with respect to **BEF-tBu**. The shape of spectra matches well within all derivatives. Therefore the extinction coefficient ($\varepsilon = 9.0 \pm 0.2 \times 10^4$ M^{-1} cm^{-1}), which was experimentally determined for **BEF-tBu**, was used for all second

generation dyes. The attempts to determine extinction coefficient of the oily (and difficult to weigh out) second generation of dyes gave inaccurate and irreproducible results.

Comparison of the absorption spectra of **BEF-OH** in a range of solvents confirmed that the one-photon absorption properties of **BEF-OH** are independent of solvent polarity (Fig 20b).

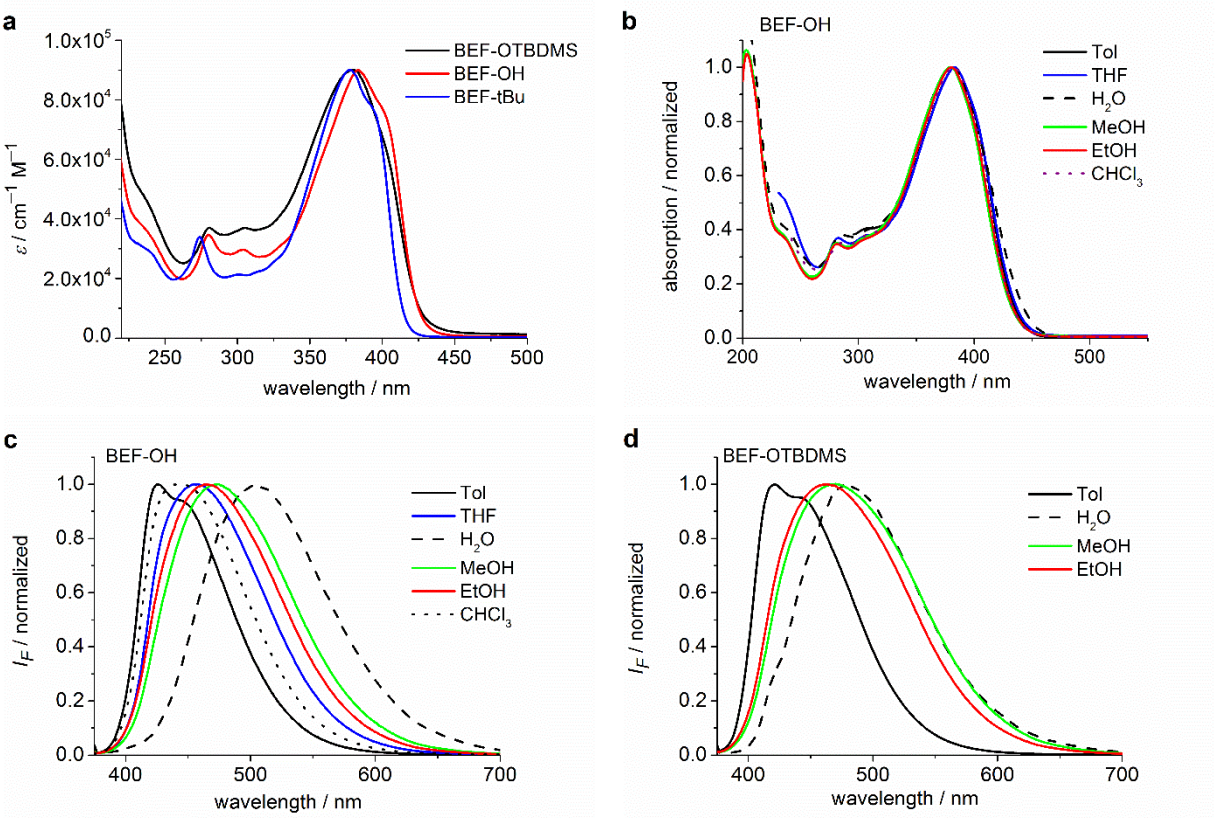

Figure 20. One-photon absorption (top) and emission (bottom) spectra recorded for model electron donors**. a)** overlaid absorption spectra of **BEF-OH**, **BEF-OTBDMS** and **BEF-tBu** in THF, **b)** absorption spectra of **BEF-OH**, **c)** emission spectra of **BEF-OH**, **d)** emission spectra of **BEF-OTBDMS**. Fluorescence spectra were recorded with excitation wavelength 366 nm.

Fluorescence properties, however, were affected by the solvent environment (Fig. 20c). The luminescence spectra are structured only in toluene, whereas in other solvents the emission is broad, with peak width increasing with solvent polarity. Furthermore, the emission spectra of **BEF-OH** and **BEF-OTBDMS** display a strong solvatochromic effect, more pronounced for **BEF-OH** than **BEF-OTBDMS** (Fig. 20c-d and Table 7). The spectrum of **BEF-OH** in water is red-shifted by almost 80 nm with respect to the emission in toluene, whereas for the **BEF-OTBDMS** derivative, the same change in solvent polarity results in a 60 nm shift. Bathochromic shifts in the luminescence spectra of the fluorene dyes have been accounted for by symmetry breaking and the formation of a polar excited

state, which is stabilized in polar solvents.[135] Both derivatives exhibit strong fluorescence in organic solvents, with average quantum yields ϕ_f = 0.4 (referenced to quinine in 0.5 M H_2SO_4, Table 7) but ϕ_f falls to 0.1 in water. The excited state energy E_{00}, which is estimated at the intersection of the normalized emission and absorption spectra, strongly depends on the solvent and model compound that is considered. For **BEF-OH**, E_{00} ranges from 3.02 eV (toluene) to 2.85 eV (water), whereas for **BEF-OTBDMS** 3.06 (toluene) - 2.95 eV (water). The average value of the excited state energy for the fluorene-based dyes was estimated as 2.95 eV.

Table 7. Photophysical properties for the model electron donors **BEF-OH** and **BEF-OTBDMS**; ϕ_f – fluorescence quantum yield, $\lambda_{em,max}$ – maxima of fluorescence emission, n.d – not determined.

Solvent	$\lambda_{em,max}$ / nm		ϕ_f[a]	
	BEF-OH	**BEF-OTBDMS**	**BEF-OH**	**BEF-OTBDMS**
Toluene	426	420	0.43	0.43
$CHCl_3$	444	n.d.	0.48	n.d
THF	458	n.d	0.43	n.d
EtOH	463	462	0.41	0.5
MeOH	474	468	0.42	0.41
H_2O	502	478	0.10	0.05

[a] The absolute fluorescence quantum yield was determined with reference quinine in 0.5 M H_2SO_4;[136] n.d. – not determined; excitation wavelength: 366 nm.

Two-photon absorption spectra

The two-photon absorption spectra of **BEF-OH** and **BEF-OTBDMS** were recorded in H_2O and EtOH, respectively by Geoffrey Wicks (Prof. Alexander Renabe's group at Montana State University, USA, Fig. 21). The TPA cross-section was measured by two-photon excited fluorescence with fluorescein (in buffer, at pH 11) used as a reference compound.[202,203] The TPA maxima are 1150 GM at 700 nm (for **BEF-OTBDMS** in EtOH) and 1100 GM at 715 nm (for **BEF-OH** in water). These cross-sections are similar to those reported previously for closely related dyes. [108,137] The spectrum is slightly broader and red-shifted in water, but the spectra are similar, revealing that the TPA is largely insensitive to the solvent environment. In both solvents, there is a shoulder in the TPA spectrum at twice the wavelength of the one-photon allowed $S_0 \rightarrow S_1$ transition (Fig. 22). However, the TPA spectra

are dominated by peaks corresponding to the one-photon forbidden, two-photon allowed higher-energy electronic or vibronic transitions. This behavior is similar to that reported for quadrupolar chromophores (D-π-A-π-D), the symmetry of which slightly deviates from ideally centrosymmetric.[108]

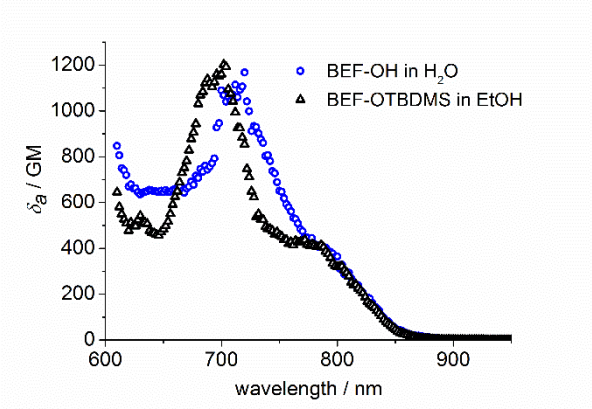

Figure 21. Two-photon absorption spectra recorded for **BEF-OH** (in H_2O) and **BEF-OTBDMS** (in EtOH). Spectra were recorded by Geoffrey Wicks (Prof. Alexander Renabe's group at Montana State University, USA). The TPA cross-section was measured by two-photon excited fluorescence with fluorescein (in buffer, at pH 11) used as a reference compound.[202,203] Adapted with permission from ref. 3. Published by The Royal Society of Chemistry.

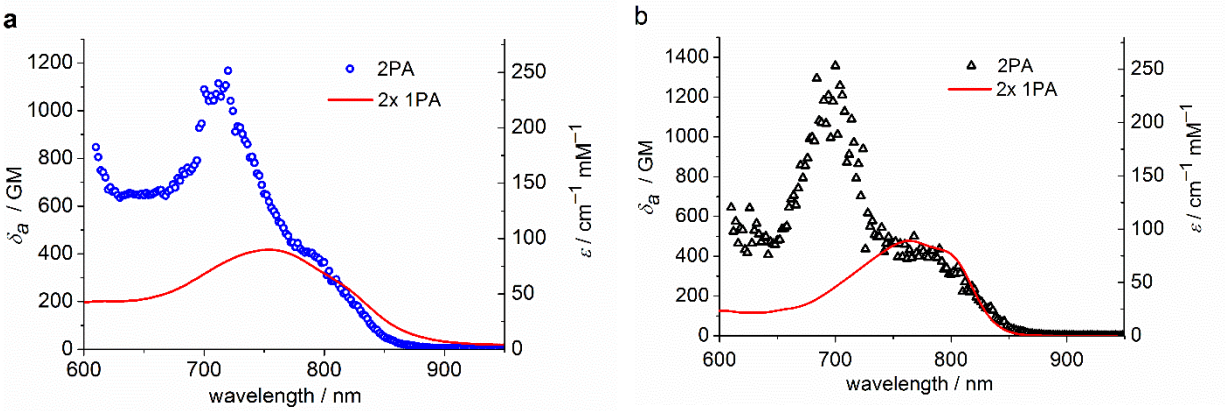

Figure 22. Two-photon absorption spectra (circles and triangles) overlaid with double-wavelength one-photon absorption spectra (red line); a**)** absorption spectra of **BEF-OH** in H_2O, **b)** spectra of **BEF-OTBDMS** in EtOH. Spectra were recorded by Geoffrey Wicks (Prof. Alexander Renabe's group at Montana State University, USA). Adapted with permission from ref. 3. Published by The Royal Society of Chemistry.

Electrochemical measurements

BEF-OH was chosen as a model dye for electrochemical studies. The properties of **BEF-OH** were investigated using cyclic voltammetry and square-wave experiments in THF. Similarly to **BEF-tBu**, **BEF-OH** displayed irreversible oxidation, however at a lower potential than its *t*-butyl ester analogue. Square wave experiments determined E_{OX} as 0.36 V vs Fc/Fc^+ in THF with 0.1 M Bu_4NPF_6 (Fig. 23). This disparity in oxidation potentials between **BEF-tBu** and **BEF-OH** can be explained by the

influence of substituents on the nitrogen atom. The ester derivative **BEF-tBu** bears electron rich substituents therefore it displays higher oxidation potential than **BEF-OH,** which is decorated with glycol chains.

The introduction of heptaethylene glycol chains in **BEF-OH** did not improve aqueous solubility as dramatically as expected. **BEF-OH** still tended to aggregate in water at millimolar concentrations, resulting in broad signals in ^{1}H NMR in D_2O. Nevertheless, it was anticipated that upon linking with a cationic neurotransmitter, the solubility of the protecting group would be improved.

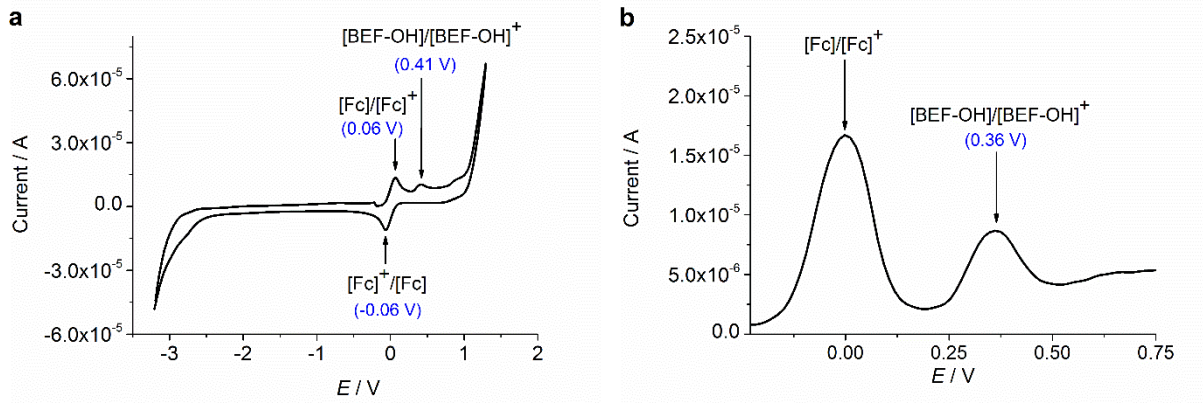

Figure 23. Determination of electrochemical properties of the model electron donor **BEF-OH**; **a)** cyclic voltammetry with ferrocene as internal reference, **b)** square wave voltammogram with ferrocene as internal reference, corrected to Fc/Fc^+ = 0 V. The results show that the first oxidation potential of **BEF-OH** is 0.36 V vs Fc/Fc^+ (in THF, with 0.1 M Bu_4NPF_6).[3] Published by The Royal Society of Chemistry.

Overall, the fluorene-based dye offered many advantages and was a suitable candidate for use in a novel protecting group for PeT-mediated uncaging. The excellent absorption properties, reflected in high extinction coefficient (ε = 9.0 ± 0.2 × 10^4 $M^{-1}\cdot cm^{-1}$) and TPA cross-section above 1000 GM proved that **BEF-OH** is a good two-photon absorbing chromophore. A relatively high energy of the excited state E_{00} (average value of 2.95 eV) and low oxidation potential (0.36 V for derivative with enhanced aqueous solubility) confirmed that the fluorene-based chromophore had potential for use as a light-harvesting antenna and electron-donor to trigger bond scission.

2.2 Selection of the electron-acceptor

The second stage of the design process required the identification of a suitable electron-acceptor. The critical factor for efficient PeT between donor and acceptor is negative Gibbs free energy ΔG_{ET}. The

energetic criterion however, was not the only condition that a useful caging platform had to meet. An applicable electron-acceptor would undergo faster than charge recombination, clean and efficient fragmentation upon electron transfer, leading to the deprotection and release of the molecule. Moreover, it was desirable to use such a combination of donor/acceptor that the fluorene dye would be the only absorbing species at wavelengths longer than 300 nm. Although this feature was not essential, it would allow the active role of the electron-donor to be demonstrated by its selective excitation. The initial candidates: phenacyl, pyridinium and *o*-nitrobenzyl platforms have been reported in the literature to undergo bond-scission upon one-electron reduction, as outlined in Section 1.8. The electrochemical behavior of pyridinium and phenacyl derivatives bearing protected carboxylic acids was initially investigated by Dr Philip Bennett.[109] These platforms have been revisited in the current systematic studies.

Considering various connection of the release units with the dye, ester- and ether-substituted phenacyl and nitrobenzyl derivatives were investigated. Structures of model compounds selected to evaluate electrochemical and photophysical properties of chosen platforms are presented in Figure 24 and include: methyl 4-acetylbenzoate (**Phen-COOMe**), 4′-methoxyacetophenone (**Phen-OMe**), *N*-methylpyridinium salt (**Pyr**), methyl 4-nitrobenzoate (**NB-COOMe**) and 1-methoxy-4-nitrobenzene (**NB-OMe**). Model compounds did not bear any substituents that could undergo cleavage during electrochemical experiments. The electron acceptors used in this study are not uncaging groups by themselves, but they can be easily elaborated into uncaging groups.

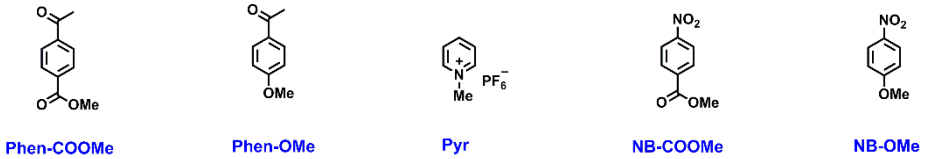

Figure 24. Structures of release platforms.

2.2.1 The synthesis of model release units

The phenacyl and nitrobenzene derivatives presented in Figure 24 were commercially available whereas **Pyr** was synthesized according to the route presented in Scheme 7. Pyridine was methylated

with methyl iodide to give an iodide salt **62** which in the next step was converted to hexafluorophosphate salt **Pyr**. The ion exchange was essential to ensure an absorption cut-off at 300 nm because methyl pyridinium iodide exhibits a charge-transfer absorption band at ~350 nm.

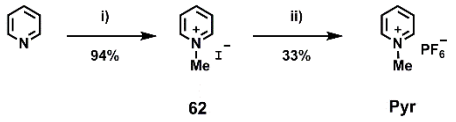

Scheme 7. Synthesis of **Pyr**. Reagents and conditions: i) MeI, THF, 20 °C, 3h, ii) H_2O/NH_4PF_6, MeOH, 4 °C, 1h.

2.2.2 Photophysical properties

The photophysical properties of the model electron-acceptors were investigated in THF and their normalized absorption spectra are presented in Figure 25. All platforms exhibit absorption within ultraviolet region with maxima ranging from 248 nm to 306 nm and extinction coefficients between ~ 5 000 - 25 000 M^{-1} cm^{-1} (Table 8). The most desirable properties are displayed by the pyridinium group with a sharp cut-off in absorption at 280 nm. Absorption spectra of *o*-nitrobenzyl and phenacyl platforms extend beyond 300 nm, and the use of lamp with a broad emission spectrum (300-400 nm) poses risk of initiating bond cleavage via direct excitation of these release units. Nevertheless, absorption above 300 nm is an issue only in one-photon photolysis. Overlap in absorption spectra is of negligible importance under two-photon excitation as the TPA cross-sections of the phenacyl, nitrobenzyl and pyridinium platforms are insignificant.

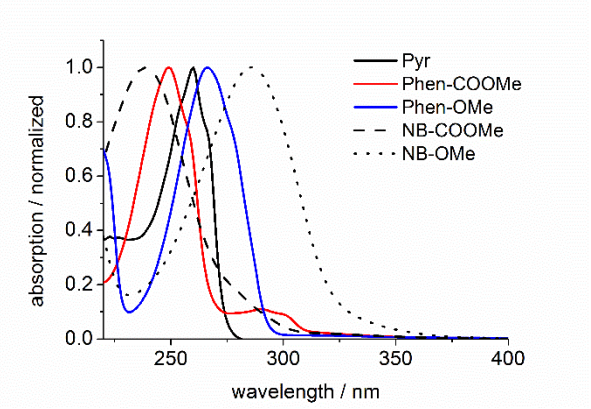

Figure 25. Normalized absorption spectra of model electron-acceptors in THF.

Table 8. Photophysical and electrochemical properties of model electron-acceptors in THF. $\lambda_{abs,\,max}$ – maxima of one-photon absorption, ε - molar extinction coefficients at $\lambda_{abs,\,max}$, E_{RED} – reduction potential, ΔG_{ET} –Gibbs free energy calculated for the forward electron transfer from **BEF-OH** to each caging platform.

Compound	$\lambda_{abs,\,max}$ / nm	ε / M^{-1} cm^{-1}	E_{RED}[a] / V	ΔG_{ET}[b] eV
Phen-COOMe	248	$21.9 \pm 0.1 \times 10^3$	−2.18	−0.44
Phen-OMe	266	$23.1 \pm 0.2 \times 10^3$	−2.92	+0.30
Pyr	260	$4.95 \pm 0.05 \times 10^3$	−1.76	−0.86
NB-COOMe	258	$16.3 \pm 0.4 \times 10^3$	−1.47	−1.15
NB-OMe	306	$13.7 \pm 0.1 \times 10^3$	−1.82	−0.80

[a] Reduction potentials were measured with use of cyclic voltammetry and square wave experiments; potentials are reported with reference to the Fc/Fc^+ [b] ΔG_{ET} was calculated according to Equation 3. The Coulombic term has been neglected. Following values were used: E_{OX} = 0.36 V, E_{00} in THF = 2.98 eV.

2.2.3 Electrochemical properties

The electrochemical properties of the model electron-acceptors were investigated by cyclic voltammetry and square wave experiments. All reduction potentials are collected in Table 8 and corresponding voltammograms are presented in Figures 26 and 27. The model compounds were studied in THF with 0.1 M Bu_4NPF_4 as supporting electrolyte, with ferrocene as internal reference.

Single cathodic peaks were observed in the case of **Pyr** and **Phen-OMe** and were unambiguously attributed to an irreversible reduction (Fig. 26a, 26e respectively). The accurate value of the reduction potential was determined by square wave experiments and was found at −2.92 V for **Phen-OMe** and −1.78 V for **Pyr** vs Fc/Fc^+ (Fig. 26b, 26f). **Phen-COOMe** underwent two quasi-reversible reductions, the first of which occurred at −2.18 V (Fig. 26g). **NB-COOMe** displayed similar behavior with its first reduction potential at −1.47 V (Fig. 27a-b). The quasi-reversible reduction of the ether derivative **NB-OMe** occurred at −1.82 V (Fig. 27c-d). Considering the irreversibility of the reduction process, **Pyr** and **Phen-OMe** seemed the most promising candidates to serve as uncaging platforms to facilitate efficient release process.

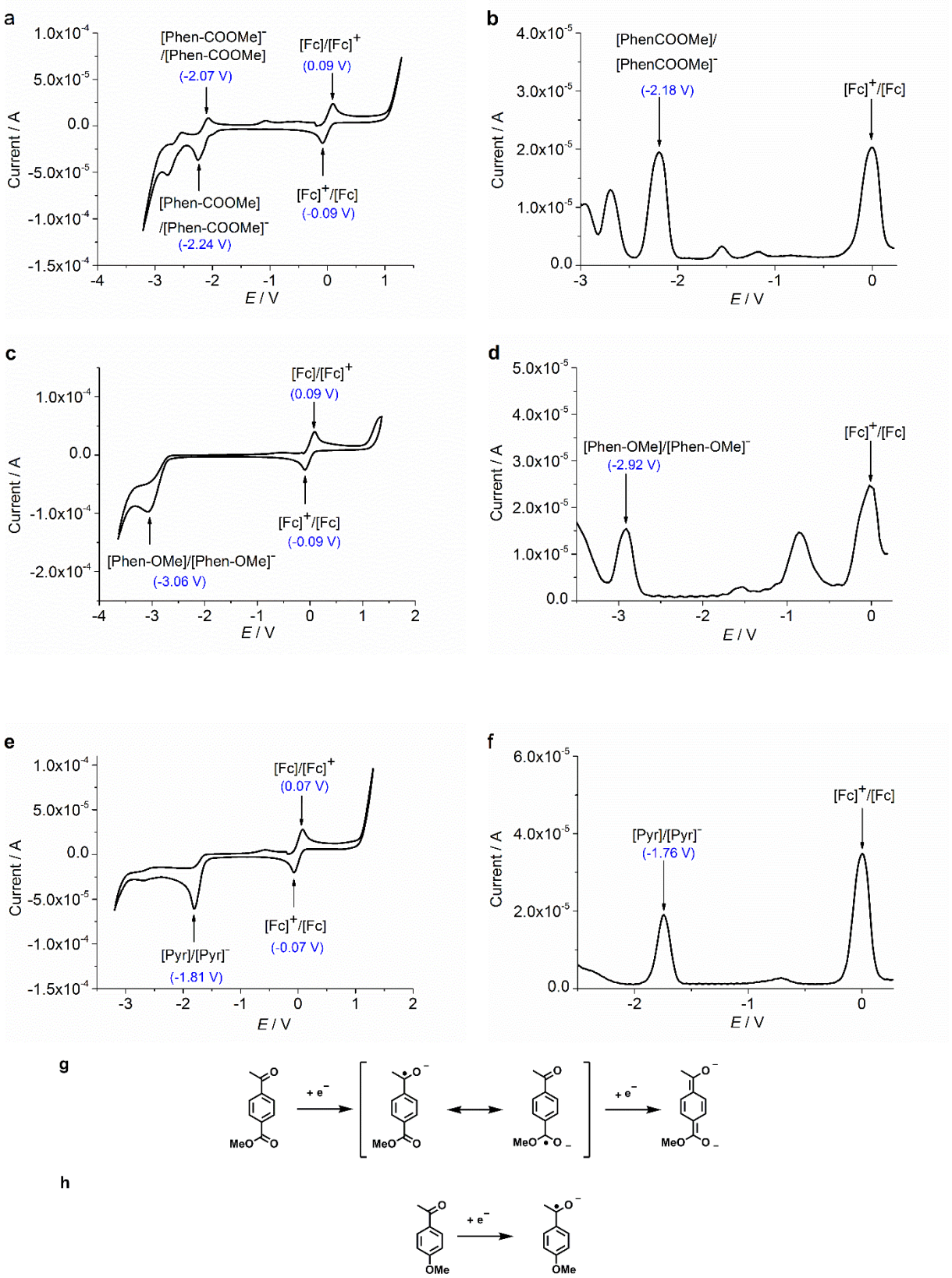

Figure 26. Determination of the electrochemical properties of model electron-acceptors; **a**, **c**, **e** – cyclic voltammograms, **b**, **d**, **f** - square-wave voltammograms. Measurements were carried out in THF with 0.1 M Bu_4NPF_6 vs Fc/Fc^+. The results show that the first reduction potentials of the investigated compounds are as follows: **Phen-COOMe**: −2.18 V, **Phen-OMe**: −2.92 V, **Pyr**: −1.76 V. Species obtained upon **g**) two-electron reduction of **Phen-COOMe**, **h**) one-electron reduction of **Phen-OMe**.[138] Adapted by permission of the PCCP Owner Societies.

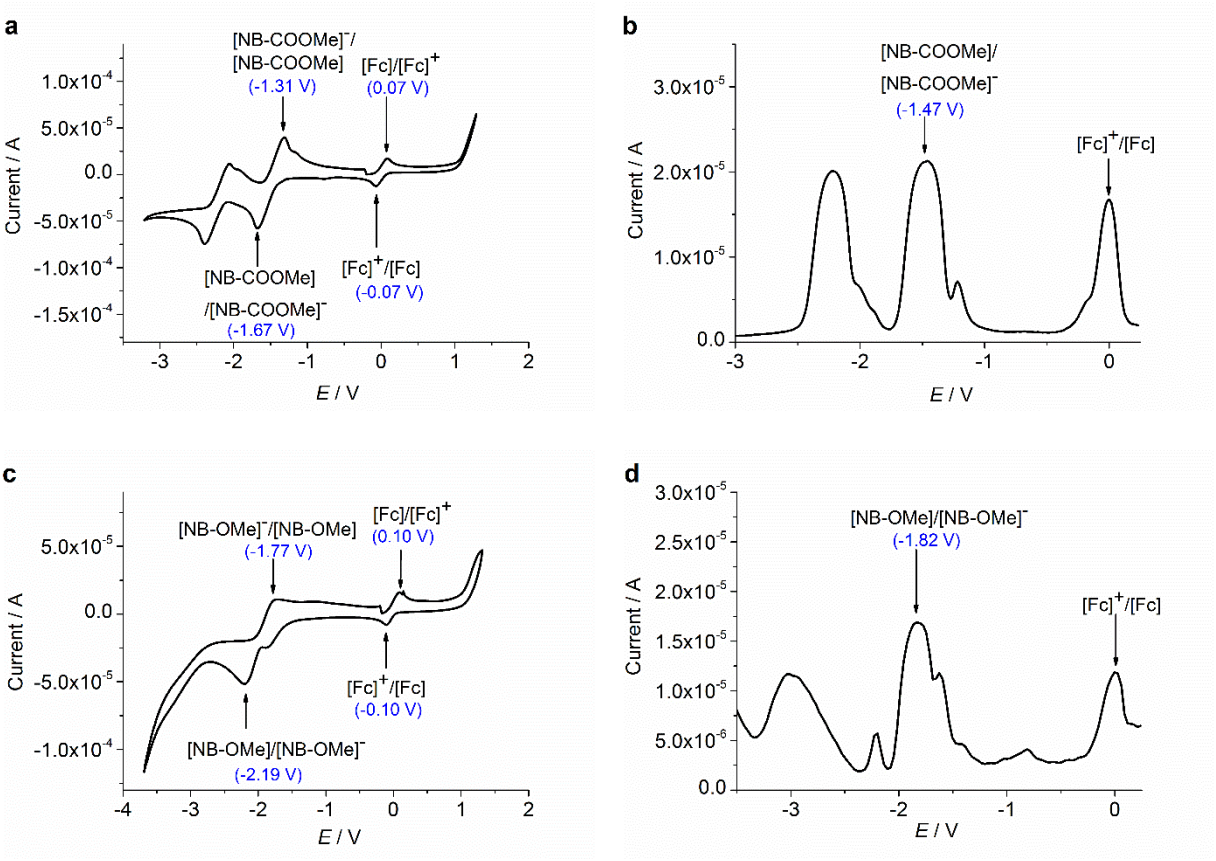

Figure 27. Determination of the electrochemical properties of model electron-acceptors. Left column – cyclic voltammograms, right column - square-wave voltammograms. Measurements were carried out in THF with 0.1 M Bu_4NPF_6 vs Fc/Fc^+. The results show that the first reduction potentials of the investigated compounds are as follows: **NB-COOMe**: −1.47 V, **NB-OMe**: −1.82 V.[138] Adapted by permission of the PCCP Owner Societies.

2.2.4 Thermodynamics of Electron Transfer

The reduction potentials that were measured in the previous section were used to evaluate the possibility of electron transfer from **BEF-OH** to each of the studied acceptors. The driving force for PeT was calculated rather crudely, according to Equation 3, with omission of the Coulombic term (see later). Results are collated in Table 8. The phenacyl group displayed the poorest performance among all the families considered. The calculated Gibbs energy for electron transfer from **BEF-OH** to **Phen-OMe** was positive (+0.30 eV), rendering the process unfavourable, whereas the driving force for the reduction of **Phen-COOMe** was only ΔG_{ET} = −0.44 eV. From the thermodynamic perspective, **NB-COOMe** was the most promising candidate with ΔG_{ET} = −1.15 eV. However, as discussed in Section 2.2.2, it was expected that a fraction of caged carboxylic acid would be released upon direct excitation of *o*-nitrobenzyl. On the other hand, the pyridinium group **Pyr** appeared a much better

candidate for the designed system. Not only does it have a sufficiently negative ΔG_{ET} (−0.86 eV) but due to the cut-off in absorption at 280 nm, uncaging with **Pyr** was expected to proceed exclusively by an electron transfer mechanism.

Owing to the multiple conformations of the final probe (Fig. 13b) and the resulting variation in distance between the donor and acceptor moieties, the Coulombic term was neglected in the previous calculations. To evaluate the contribution of the electrostatic attraction between components of the probe to the Gibbs free energy for photoinduced electron transfer, ΔG_{ET} for **Phen-COOMe** and **NB-COOMe** derivatives was calculated for the model structures presented in Figure 28. The electron-donor and electron-acceptor were separated by C-3 alkyl chain linker and the distance between separated charges *a* was estimated as a center-to-center distance between the fluorene unit and release platform. To simplify the calculations, model compounds were used, bearing methyl substituents on the aniline nitrogen atoms and acetic acid esters on the release platforms. Molecular mechanics simulations and distance measurements were performed in HyperChem 8 using the MM+ forcefield. The distance measured between donor and acceptor was 8.7 Å for **NB-COMe** and 9.5 Å for **Phen-COOMe**. Thus the term *w*(DA) was estimated to be −0.22 eV for **NB-COOMe** and −0.20 eV for **Phen-COOMe**. This value of the Coulombic term is an approximation, as the distance between the donor and acceptor varies across possible conformations and introduces high uncertainty.

Figure 28. Model structure for calculation of the distance between the fluorene and release units: **left** – **NB-COOMe**, **right** – **Phen-COOMe**. Centers of the fluorene-dye and release unit are represented by green balls. Simulations were performed by Dr Arjen Cnossen (Prof. Harry Anderson's group, University of Oxford).[3] Published by The Royal Society of Chemistry.

However, this term proved relatively significant. Although no simulations for the derivative of **Phen-OMe** were made, it was hypothesized that electrostatic attraction between oxidized donor and reduced acceptor would stabilize the system and be enough to make ΔG_{ET} negative. In the case of the

pyridinium-based systems, the Coulombic term is zero because electron transfer does not result in formation of a charge-separated state but only in the migration of a pre-existing charge. Nevertheless, these calculations provided a guide for the selection of matching components and construction of an efficient probe. Consideration of the electrostatic forces between the donor and acceptor unit did not change the overall observation that platforms with a high reduction potential show moderate ΔG_{ET}.

In order to rationally design a protecting group operating *via* PeT it was desirable to evaluate efficiency of electron transfer in covalently linked donor-acceptor pairs (model dyads). Such systems presented more reliable models for the final protecting groups and could be experimentally evaluated.

Efficient forward electron transfer was not the only issue that had to be considered. As highlighted in Section 1.7 (page 26), fast charge recombination is the main reaction that competes with uncaging in PeT-mediated release. Therefore, an investigation of a set of model dyads was started to help identify design features that slow down the rate of back electron transfer. Considering the values of ΔG_{ET} and trying to maintain structural diversity across models, three caging platforms were chosen for further studies: **Pyr**, **NB-COOMe** and **Phen-COOMe**. The following section reports on photophysical investigation of three dyads, consisting of the same electron-donor attached to three different electron-acceptors; **BEF-Pyr**, **BEF-NB** and **BEF-Phen** (Fig 29).

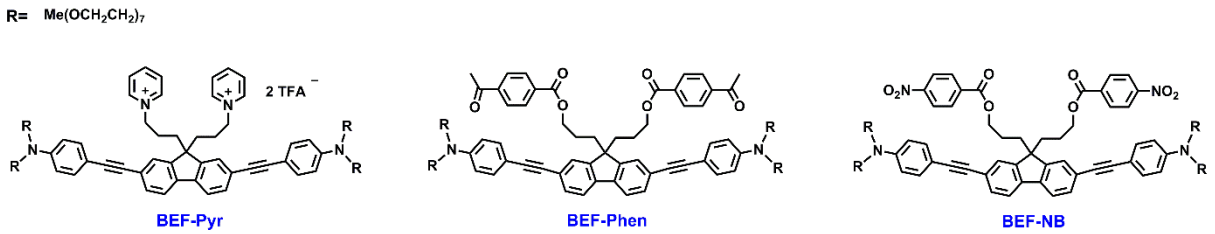

Figure 29. Structures of the model dyads designed for the investigation of intramolecular PeT.

2.3 Dyads - models to investigate the intramolecular electron transfer

Three dyads, **BEF-Pyr**, **BEF-Phen** and **BEF-NB**, were prepared in order to gain an insight into the dynamics of intramolecular charge separation and charge recombination, both of which affect the yield of uncaging. An extended study of PeT in model compounds representing donor-acceptor units of the novel protecting groups was performed by Dr Adina Ciuciu and Prof. Lucia Flamigni (ISOF-CNR,

Bologna, Italy) and has been published.[138] The synthesis of **BEF-NB** was carried out by Wilfred Lewis, a summer student in Prof. Harry Anderson's group.

2.3.1 Synthesis of the dyads

The synthetic strategy towards the model dyads was similar to the previous approaches. The divergent route started with readily available dialcohol **60** which was esterified with 4-acetoxybenzoic acid and 4-nitrobenzoic acid to give functionalized cores **63** and **64**, respectively. The preparation of pyridinium-decorated core **66** employed conversion of the dialcohol **60** into the dimesylate **65** followed by reflux in pyridine. In the final sequence of the synthesis the Sonogashira cross-coupling of the functionalized cores with aniline unit **58** was applied. The last step of the synthesis proceeded quantitatively to give **BEF-Pyr**, **BEF-Phen** and **BEF-NB**. However, multiple attempts to isolate dyads and remove minor impurities (starting material **58** and the product of its homocoupling) from the samples resulted in a decrease of the overall yield to ~15%.

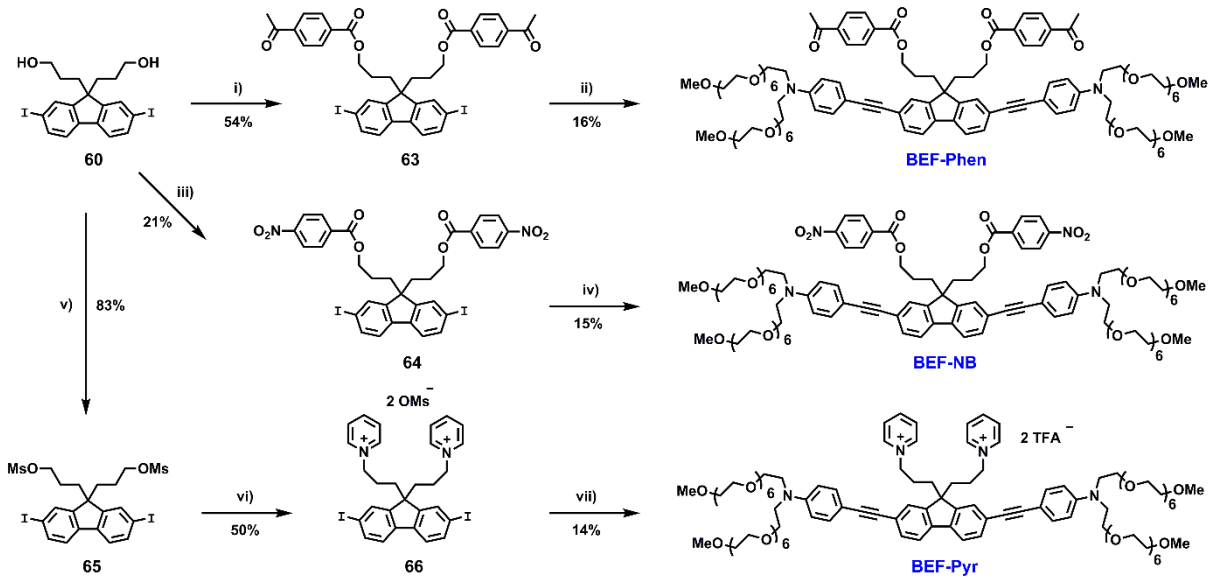

Scheme 8. Synthesis of BEF-Pyr. Reagents and conditions: i) 4-acetoxybenzoic acid, EDC, DMAP, DCM, 20 °C, 2 h, ii) **58**, $Pd(OAc)_2$, PPh_3, CuI, DIPA, MeCN, 20 °C, 2 h, iii) 4-nitrobenzoic acid, EDC, DMAP, THF, MeCN, 20 °C, 16 h, iv) **58**, $Pd(OAc)_2$, PPh_3, CuI, DIPA, MeCN, 20 °C, 2 h, v) MsCl, Et_3N, DCM, 0 °C → 20 °C, 1 h, vi) pyridine, 115 °C, 16 h, vii) **58,** $Pd(OAc)_2$, PPh_3, CuI, DIPA, MeCN, 20 °C, 2 h.[138] Adapted by permission of the PCCP Owner Societies.

2.3.2 Electrochemical properties of the model dyads

The electrochemical behavior of the model dyads was investigated with cyclic voltammetry and square wave experiments (Table 9). All measurements were carried out in THF with 0.1 M Bu_4NPF_6

and potential values were reported with reference to ferrocene. Overall, oxidation and reduction potentials of the dyads differed by ± 0.02 V from the values determined for the models **BEF-OH**, **Pyr**, **NB-COOMe**, **Phen-COOMe** (Table 8). These deviations were accounted for by the experimental errors. Electrochemical data confirmed a weak electronic coupling between components in the ground state.

Table 9. Electrochemical properties of model dyads. Measurements were conducted in THF with 0.1 M Bu_4NPF_6 against Fc/Fc^+.[138] Reproduced by permission of the PCCP Owner Societies.

Compound	E_{RED} / V	E_{OX} / V
BEF-Pyr	−1.78	0.38
BEF-NB	−1.51	0.37
BEF-Phen	−2.20	0.36

2.3.3 Photophysical properties of the model dyads

Photophysical studies carried out by Dr A. Ciuciu and Prof. L. Flamigni aided construction of the energy level diagrams for **BEF-Pyr**, **BEF-NB** and **BEF-Phen** (Fig. 31). The characterization of the excited species was possible due to the comparative investigation of separated components of each dyad, i.e. **BEF-OH**, **Pyr**, **NB-COOMe**, **Phen-COOMe.** All measurements were carried out in methanol (MeOH), which mimics physiological conditions, and toluene, a non-polar solvent.

Absorption and emission spectra

The absorption spectra of the dyads maintain characteristic features of the constituent parts (Fig. 30a-c) and imply that donor and acceptor molecules do not interact with each other in the ground state. The strong emission of the fluorene dye in the dyads was reduced to below 1% in MeOH and to 8%-0.5% in toluene, compared to the quantum yield of parent **BEF-OH** (original quantum yields are presented in Table 10). Since FRET from the excited dye to any of the acceptors was not possible (absorption spectra of electron-acceptors do not overlap with the emission spectrum of **BEF-OH**), the reduced fluorescence indicated occurrence of PeT.

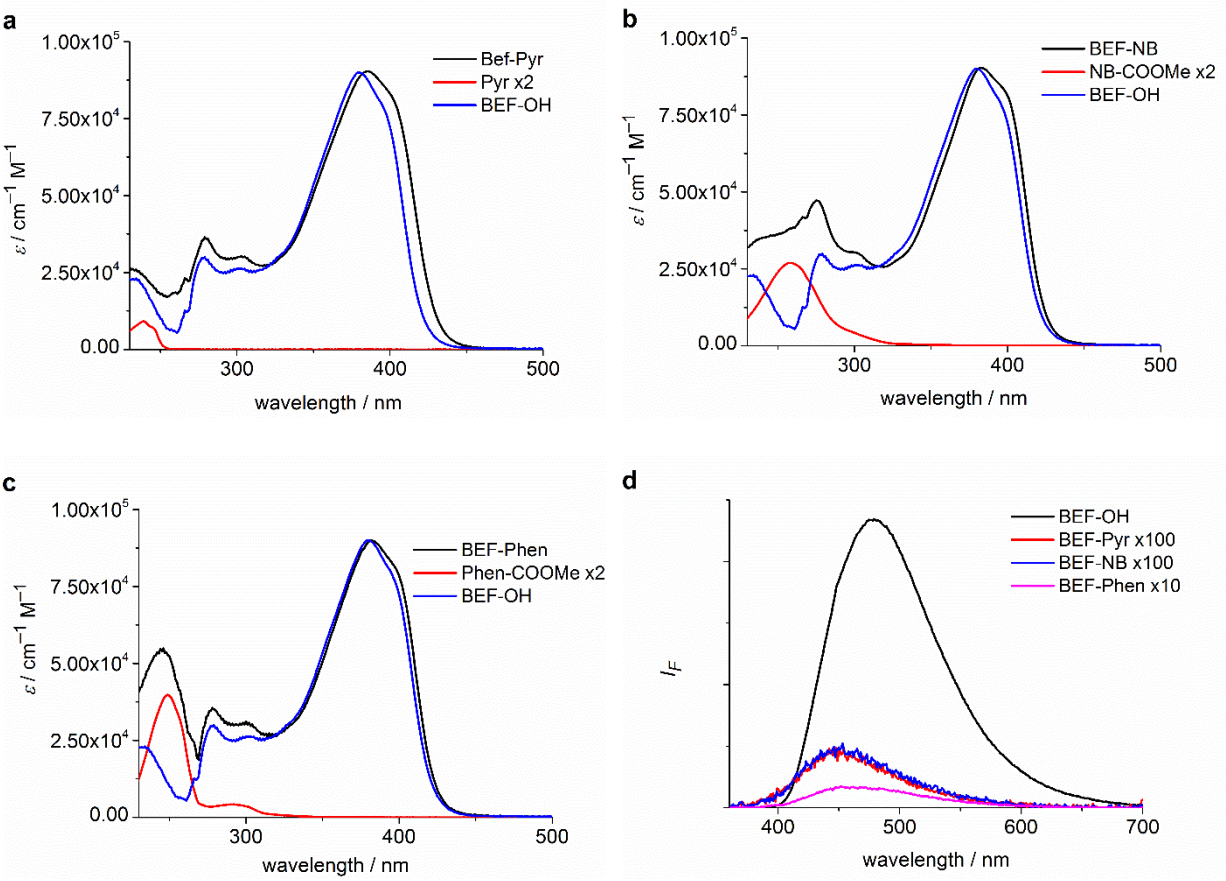

Figure 30. a-c: Absorption spectra of dyads overlaid with spectra of their constituent units (multiplied as indicated). Recorded in MeOH; **d**: Fluorescence spectra of the model **BEF-OH** and model dyads (multiplied as indicated). Excitation wavelength: 350 nm. Spectra were recorded by Dr Adina Ciuciu from ISOF-CNR, Bologna, Italy.[138] Reproduced by permission of the PCCP Owner Societies.

2.3.4 Photoinduced electron transfer

The dyads and models representing their constituent parts have been characterized. Time-resolved fluorescence, detection of phosphorescence and transient absorption experiments allowed excited states to be identified and their lifetimes to be measured. Precise determination of several values was not possible due to the limits of instrumental resolution or uncertainty introduced by estimation of Coulombic term. Therefore, the following discussion of the photoinduced process is limited to a qualitative comparison between dyads.

The energy levels of the excited states were determined by luminescence experiments at 77 K. The energy of the singlet state of the fluorene dye in the dyads is ~ 2.90 eV in toluene and MeOH and the triplet state energy is ~ 2.13 eV. The energies of the charge-separated states, E_{CS}, were derived from the electrochemical measurements (Table 9, 10) by the addition of the energy required to oxidize the

donor and reduce the acceptor ($E_{CS} = E_{OX} - E_{RED}$). The oxidation and reduction potentials were determined in THF and no corrections were introduced in the estimation of the energy levels of charge-separated states in MeOH. This led to the energy levels of 2.16 eV for **BEF-Pyr**, 1.88 eV for **BEF-NB** and 2.56 eV for **BEF-Phen**. It is known that corrections calculated with the Weller equation overestimate the energy of ion pairs in non-polar solvents.[139] Therefore, the energies of the charge-separated states in toluene were approximated by adding 0.3 eV, which is the typical value of the nuclear reorganization energy for organic molecules with π-systems in toluene.[140] As a result, the following energies were obtained in toluene: 2.46 eV for **BEF-Pyr**, 2.18 eV for **BEF-NB** and 2.86 eV for **BEF-Phen** (Fig. 31).

Table 10. Photophysical properties of the model **BEF-OH** and dyads measured in MeOH and toluene. Values were determined at room temperature unless stated otherwise. ϕ_f – fluorescence quantum yield, E_{S1} – energy of the relaxed excited state, E_{T1} – energy of triplet state, E_{CS} – energy of charge-separated state, ΔG_{ET} – Gibbs free energy of forward electron transfer, k_{ET} – rate of the forward electron transfer, ΔG_{BET} – Gibbs free energy of back electron transfer, k_{BET} – rate of the charge recombination.

	BEF-OH		**BEF-Pyr**		**BEF-NB**		**BEF-Phen**	
	MeOH	Toluene	MeOH	Toluene	MeOH	Toluene	MeOH	Toluene
ϕ_f [a]	0.48	0.52	0.001	0.003	0.001	0.002	0.003	0.04
E_{S1}[b] /eV	2.89	2.94	2.86	2.90	2.88	2.90	2.91	2.91
E_{T1}[b] /eV	2.26	2.43	2.16	2.16	–	2.17	–	2.18
E_{CS} /eV	–	–	2.16	2.46	1.88	2.18	2.56	2.86
ΔG_{ET}[c] /eV	–	–	−0.70	−0.44	−1.0	−0.72	−0.35	−0.05
k_{ET} /s^{-1}	–	–	6.6×10^{10}	4.0×10^{10}	5.5×10^{10}	5.0×10^{10}	2.2×10^{10}	1.4×10^{10} 1.5×10^{9}
ΔG_{BET} /eV	–	–	−2.16	−2.46	−1.88	−2.18	−2.56	−2.86
k_{BET} /s^{-1}	–	–	3.3×10^{10}	4.0×10^{9}	3.3×10^{10}	5.5×10^{9}	1.6×10^{10}	6.2×10^{8}

[a] Fluorescence quantum yield was determined against quinine sulfate in 0.5 M H_2SO_4, [b] Data from measurements at 77 K, [c] The values of calculated ΔG_{ET} differ from these presented in Table 8. This inconsistency stems from the deviations in the measured red-ox potentials in the model compounds and dyads and E_{00} (here, E_{S1}) for **BEF-OH**. Data were collected by Dr Adina Ciuciu from ISOF-CNR, Bologna, Italy.[138] Adapted by permission of the PCCP Owner Societies.

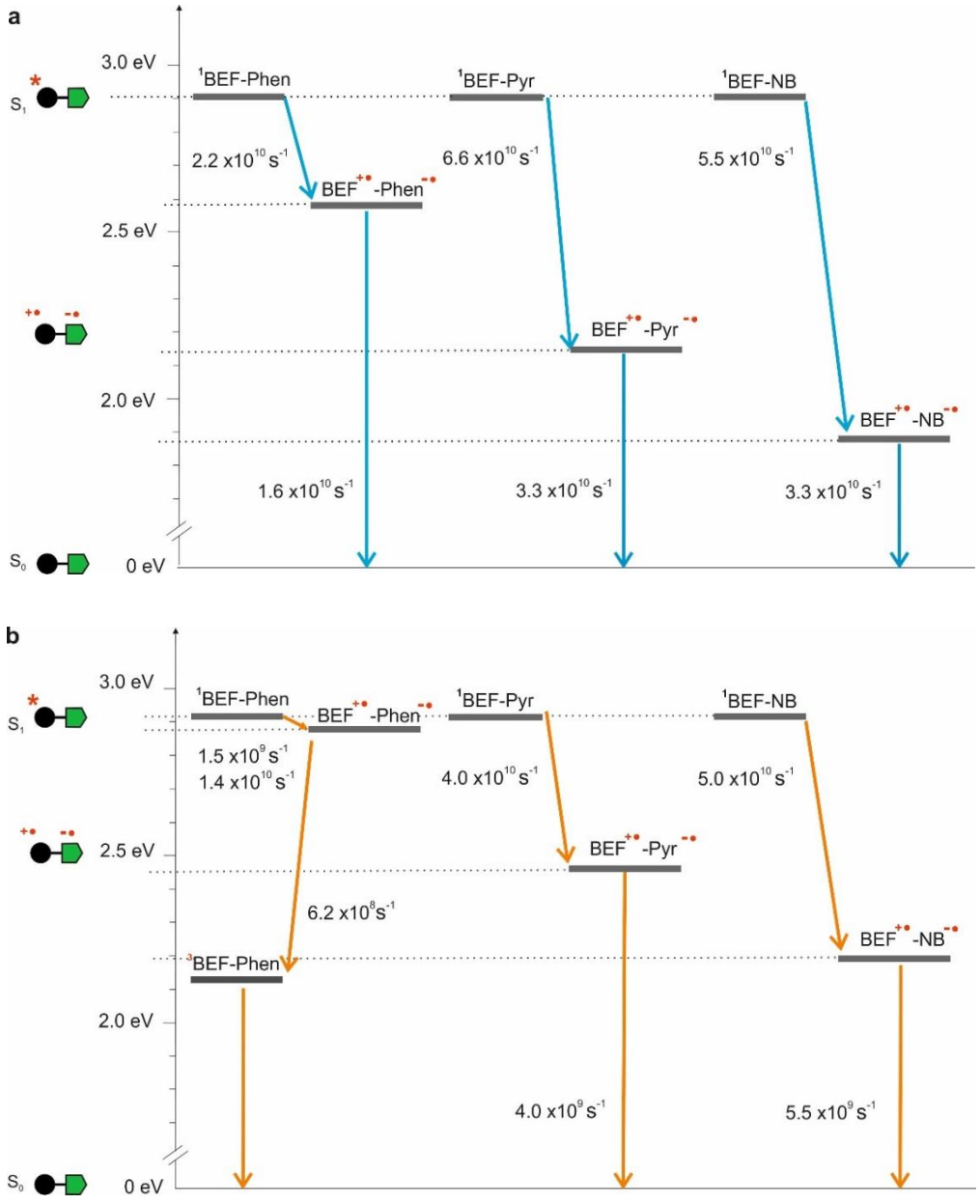

Figure 31. Schematic energy-level diagrams of **BEF-Phen**, **BEF-Pyr** and **BEF-NB** in **a)** MeOH and **b)** in toluene. Based on the data collected by Dr Adina Ciuciu from ISOF-CNR, Bologna, Italy.[138] Adapted by permission of the PCCP Owner Societies.

Time-resolved fluorescence experiments allowed the lifetime of the singlet excited states to be determined and Equation 7 was applied to calculate the rate of charge separation, k_{ET}.

$$k_{ET} = \frac{1}{\tau} - \frac{1}{\tau_0} \qquad (7)$$

Equation 7. The rate constant of PeT, k_{ET}, expressed as the relation between the lifetime of the excited donor in the model τ_0 and excited donor incorporated into the dyad τ.

From a formal point of view, in the case of **BEF-Pyr**, charge relocation rather than charge separation was observed. However, to focus on comparison of the dyads in the current discussion, the term "charge separation" and "charge recombination" will be used with respect to **BEF-Pyr** as well. In MeOH, PeT occured at rates 6.6 $\times 10^{10}$ s^{-1} for **BEF-Pyr**, 5.5$\times 10^{10}$ s^{-1} for **BEF-NB** and 2.2$\times 10^{10}$ s^{-1} for **BEF-Phen** and was driven by the Gibbs free energy ($\Delta G_{ET} = E_{OX} - E_{RED} - E_{00}$) of −0.70 eV, −1.0 eV and −0.35 eV for **BEF-Pyr**, **BEF-NB** and **BEF-Phen**, respectively. Charge separation was comparably fast in toluene, with k_{ET} (and ΔG_{ET}) determined to be as follows: 4.0$\times 10^{10}$ s^{-1} (−0.44 eV) for **BEF-Pyr**, 5.0$\times 10^{10}$ s^{-1} (−0.72 eV) for **BEF-NB** and 1.4$\times 10^{10}$ s^{-1} and 1.5$\times 10^{9}$ s^{-1} (−0.05 eV) for two conformers of **BEF-Phen**. In both solvents the forward electron transfer occured in the Marcus normal region because the rate of the charge-sepration increased with the growing exergonicity (Fig. 32). **BEF-Pyr** and **BEF-NB** lie in the activationless area, as a change of ΔG_{ET} (−0.7 eV vs −1.0 eV in MeOH) had little impact on the rate constant of electron transfer (6.6$\times 10^{10}$ s^{-1} vs 5.5$\times 10^{10}$ s^{-1}).

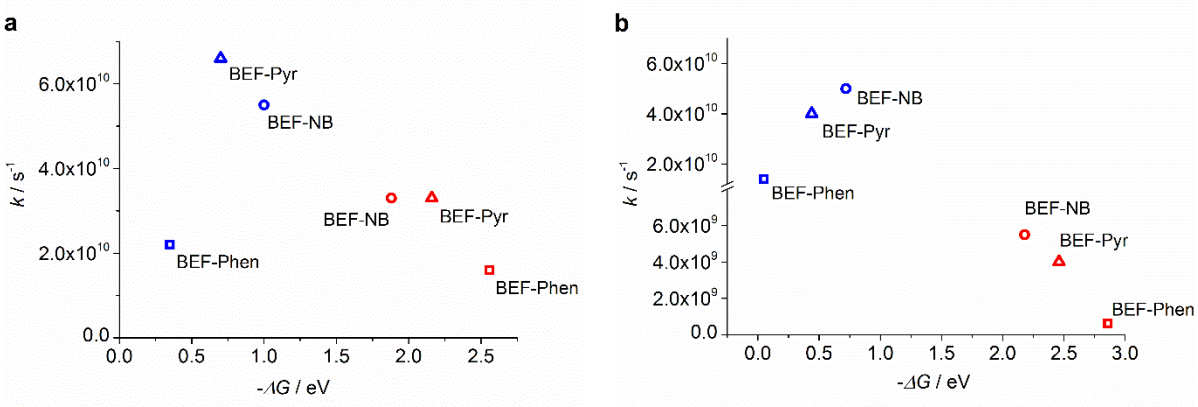

Figure 32. The rates of the forward (blue) and back (red) electron transfer in the function of **–***ΔG*. Squares - **BEF-Phen**, triangles – **BEF-Pyr**, circles – **BEF-NB**; **a** – data collected in MeOH, **b** – data collected in toluene.[138] Adapted by permission of the PCCP Owner Societies.

Charge recombination rates, k_{BET}, were established by transient absorption experiments. In MeOH, the determination of the lifetimes of **BEF-Pyr** and **BEF-NB** was limited by the instrumental resolution (30 ps) and the rates of charge recombination were estimated as 3.3$\times 10^{10}$ s^{-1}. The lifetime of **BEF-Phen** was measured as 60 ps to give k_{BET} of 1.6$\times 10^{10}$ s^{-1}. Charge recombination was driven by following energetics: −2.16 eV for **BEF–Pyr**, −1.88 eV for **BEF–NB** and −2.56 eV for **BEF–Phen**. The relation between the driving force of the charge recombination and its rate constant suggested that

BET occurs in the Marucs inverted region in MeOH. Similar observations were made for measurements in toluene (Fig. 32). The rates of charge recombination (and ΔG_{BET}) were determined to be as follows: 4.0×10^{9} s^{-1} (−2.46 eV) for **BEF-Pyr**, 5.5×10^{9} s^{-1} (−2.18 eV) for **BEF-NB** and 6.2×10^{8} s^{-1} (−2.86 eV) for **BEF-Phen**. The data show that BET proceeded nearly ten times slower in the apolar solvent than in the polar one. Interestingly, in contrast to **BEF-Pyr** and **BEF-NB**, charge recombination in **BEF-Phen** in toluene led to the triplet state. Decay of the excited state of the model **BEF-OH** to the triplet state was estimated to occur with ~48% efficiency. In the dyad, this level was populated more efficiently *via* the charge recombination pathway.

2.4 Conclusions and outlook

Photochemical characterization of the dyads allowed us to gain insight into electron transfer processes in the prototypes of the developed protecting groups. The electron transfer proceeded from the lowest excited state of the fluorene-dye and based on the fluorescence quenching in the dyads, the efficiency of PeT was close to unity. PeT occured with rate constants of the order of 10^{10} s^{-1} and lay in the Marcus normal region. In contrast, charge recombination took place in the Marcus inverted region. Unfortunately, in a polar solvent BET was of the same order of magnitude as PeT (k_{BET} = 10^{10} s^{-1}). These results were attributed to the flexibility of the bridge. Despite the electronic separation, donor and acceptor could come into close contact through space. This explanation was supported by the fact that in another phenacyl-based system with a less flexible bridge the lifetime of the charge-separated state was ~10^{-7} s (acetonitrile), in contrast to that measured in the current study 6.0×10^{-11} s (MeOH).[104] In the light of these data, the best performance in terms of suppressed BET was displayed by **BEF-Phen**, for which the lifetime of the charge-separated state was the longest in a polar solvent. Unfortunately, considering a lifetime of the charge-separated state of 60 ps and a C−O bond cleavage occurring at a timescale of 8 ns,[141] the uncaging quantum yield was estimated to be 1% at best. Despite these disappointing results, the dyads **BEF-Pyr**, **BEF-Phen** and **BEF-NB** were transformed into the respective protecting groups (Chapters 3-5). The aim of the further work was to investigate the advantages and limitations of the chosen design strategy. .

Chapter 3

o-Nitrobenzyl-derived protecting groups

Consideration of the photophysical properties of model dyads led to the conclusion that, among the studied compounds, PeT is the fastest for the *o*-nitrobenzyl derived protecting group. But it was also found that charge recombination is comparably fast and therefore a low (below 1%) quantum yield of uncaging was expected. Regardless of the dynamics of the intramolecular electron transfer, it is worth noting that the *o*-nitrobenzyl group has never been demonstrated to liberate protected species via PeT mechanism. To enable a rapid evaluation of the release through PeT, bimolecular uncaging experiments were planned (Scheme 9). It was anticipated that photolysis of a solution containing a mixture of an electron-donor and electron-acceptor would verify whether *o*-nitrobenzyl is a suitable release unit for the current project. We aimed to address the question of PeT-mediated uncaging by means of a simple experiment that does not require sophisticated model compounds. For this purpose, release platforms, **NB-OMe** and **NB-COOMe** (Chapter 2, Fig. 24) were elaborated into protecting groups for carboxylic acids to give propanoates (**67**, **68**) and acetates (**70**, **71,** Scheme 10).

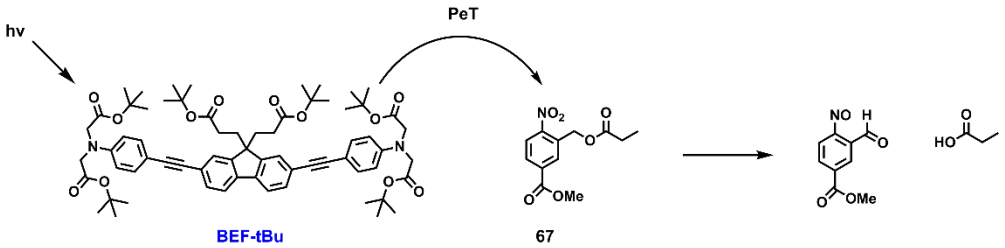

Scheme 9. Schematic presentation of the bimolecular uncaging experiment in which a solution containing an electron-donor **BEF-tBu** and electron-acceptor **67** is irradiated. It was expected that light would be predominantly absorbed by **BEF-tBu** which would donate an electron to **67** and lead to the liberation of propionic acid.

3.1 Intermolecular uncaging experiments

3.1.1. Synthesis of model protected carboxylic acids

The synthesis of model caged propanoates and acetates for bimolecular uncaging experiments is shown in Scheme 10. The route towards protected esters **67** and **69** commenced with the acid catalyzed conversion of 3-methyl-4-nitrobenzoic acid into methyl ester **71** upon boiling in MeOH. Bromination of **71** with NBS in benzylic position gave inseparable mixture of **72**, starting material **71** and dibrominated products. The resulting material was directly used in the next step in which the bromine atom was displaced with propanoate and acetate to yield desired **67** and **69**, respectively. The formation of ether derivatives **68** and **70** followed a three-step procedure, involving esterification of 5-hydroxy-2-nitrobenzaldehyde with Me_2SO_4 and subsequent reduction of aldehyde **73** with $NaBH_4$ in MeOH to give **74**. Respective propanoate **68** and acetate **70** were obtained upon treatment of **74** with corresponding acyl chlorides in the presence of Et_3N and DMAP.

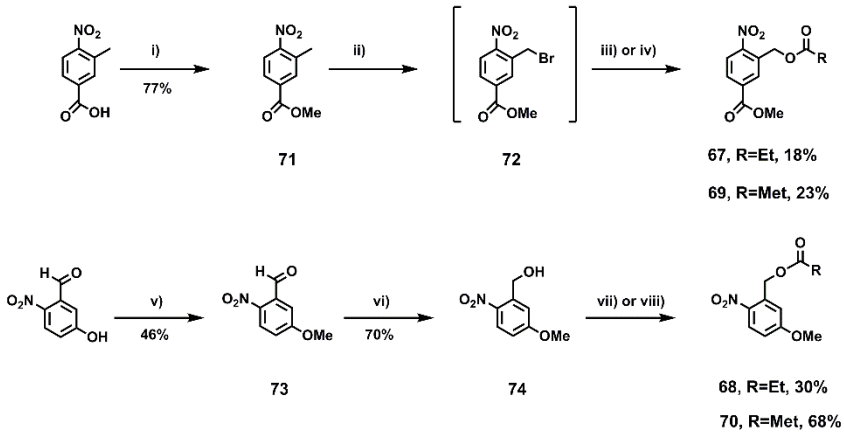

Scheme 10. Synthesis of the caged acetates and propanoates. Reagents and conditions: i) MeOH, H_2SO_4, reflux, 16 h, ii) NBS, benzoyl peroxide, CCl_4, reflux, 48 h, iii) NaOAc, DMF, 70 °C, 24 h, iv) propionic acid, K_2CO_3, DMF, NaI, 80 °C, 1 h, v) Me_2SO_4, EtOH, NaOH, H_2O, 50 °C, 16 h, vi) $NaBH_4$, MeOH, 0 °C → 20 °C, 1 h, vii) acetyl chloride, DMAP, Et_3N, THF, 20 °C, 16 h, viii) propionyl chloride, Et_3N, DCM, 20 °C, 1 h.

3.1.2 Electrochemical properties

Protected acetates **69** and **70** were used in electrochemical measurements to investigate the influence of additional substituents on the reduction potential of release units. Cyclic voltammetry and square wave experiments were carried out in THF with 0.1 M Bu_4NPF_6 against Fc/Fc^+ as an internal reference. Both ether **70** and ester **69** displayed E_{RED} almost identical to their precursors, **NB-OMe** and

NB-COOMe (page 49, Fig. 27), with −1.77 V for ether and −1.43 V for ester. Moreover, cyclic voltammetry provided evidence for reductive cleavage of acetates. In addition to peaks observed already for **NB-OMe** and **NB-COOMe (**Fig. 27), voltammograms presented in Figure 33a-b showed extra signals (pointed with arrows in dotted line traces). Importantly, these peaks appeared only if the potential was swept from more negative values than E_{RED} of release units and scanning proceeded with the rates of 0.1-0.5 V/s. The observed peaks were assigned to products of uncaging which are reduced before they diffuse away from the electrode. In contrast, the discussed peaks did not appear if the rate of potential sweep was lower than 0.1 V/s or the return scan finished at the potential more negative than the E_{RED} pointed with arrows (Fig. 33, solid lines).

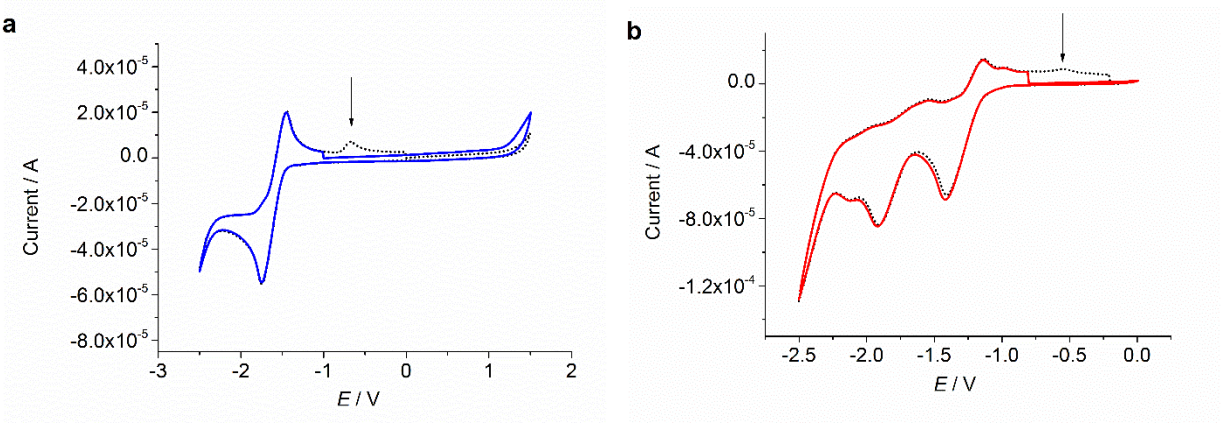

Figure 33. Voltammograms of **a)** ether **70** and **b)** ester **69** caged acetates recorded in THF with 0.1 M Bu_4NPF_6 at the scan rate 0.1 V/s. The direction of scanning was towards the positive first vertex followed by the negative second vertex and back to the value of the starting potential. Solid lines present traces for which scanning began at potential value more negative than required for the reduction of the highligted peak. Dotted lines present traces for which scanning began at potential value more positive than required for the formation of the peak pointed with an arrow. The peak at ~ −0.5 V appeared only at the return cycyle suggesting that it is a reduced product of electrochemical uncaging.

3.1.3 Photolysis experiments

Bimolecular uncaging experiments (Scheme 9) were carried out to evaluate if PeT sensitised one-photon deprotection is feasible for the identified donor/acceptor pairs. In intermolecular uncaging experiments, a 1 : 1 mixture of model dye **BEF-tBu** and ester **69** (or ether **70**) in THF was irradiated with a broad source of light (300-400 nm). The photolysis experiments were performed at 0.5 mM concentration of each component and the progress of deprotection was monitored by NMR. Control experiments involved irradiation of protected acids in the absence of the electron-donor. The fact that

the absorption of the *o*-nitrobenzyl platform overlapped with the emission of the irradiation lamp proved to be a severe barrier to interpret results. Liberation of propionic acid was observed in both uncaging and control samples and for this reason the active role of the electron-donor could not be proven. It is noteworthy that in a system where electron-donor and acceptor are separated, reactants need to form a diffusive encounter within a lifetime of the excited state of the donor.[80,142] Moreover, considering a random distribution of reactants at the time of excitation, the process becomes time and distance dependent. Therefore high concentrations of reaction partners are required to allow for the bimolecular reaction. The shortcomings of performing experiments at ~ mM concentration is that transmittance of a solution is equal to zero. Therefore irradiation resulted in direct absorption of light by the nitrobenzyl group and liberation of acid also in control samples.

3.2 Intramolecular uncaging experiments

One-photon bimolecular uncaging experiments highlighted the drawback of the *o*-nitrobenzyl for which absorption exceeds 300 nm and overlaps with the emission of irradiation lamp. At mM concentration the rate of uncaging depends only on the light intensity and the quantum yield, but not on the molar absorption coefficient. Therefore one could not take advantage of the fact that the extinction coefficient of a fluorene dye is ~10 times higher than for the release units at 300-320 nm. Under such conditions it was difficult to elucidate the mechanism of the cleavage and evaluate the utility of *o*-nitrobenzyl platform. A facile way to circumvent the problem of significant absorption of the caging platform is to perform photolysis at μM concentration of reactants. However, at this concentration the probability that the excited electron donor would collide with the caged acid is relatively low. Therefore it is necessary to tether the electron-donor to the release unit. Consequently, the choice of the model compound is dictated by the capacity of analytical methods used to monitor the progress of photolysis. L-Tryptophan (**Trp**) was selected as a model caged amino acid due to the presence of an indole chromophore that allows release to be quantified by HPLC, with UV detection. Importantly, absorption of tryptophan does not occur at $\lambda > 300$ nm and no FRET is possible from the excited **BEF-OH** (Fig. 34).

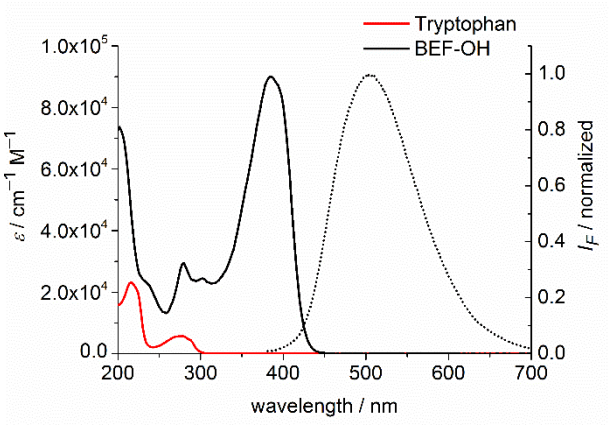

Figure 34. Absorption spectra (solid lines) of tryptophan and **BEF-OH** and normalized emission spectrum (dotted line) of **BEF-OH** in H_2O. Excitation wavelength 366 nm.

Given that the ester derivative, **BEF-NB**, has been already thoroughly investigated in Section 2.3 (pages 52-58), the studies of *o*-nitrobenzyl family focused on the further exploration of the ester-linked protecting groups. Moreover, the maximum of absorption of the ester is shifted to shorter wavelengths than the ether and better separated from the fluorene absorption region (Fig. 25). Photolysis of **BEF-NB-Trp** was aimed to investigate whether the intramolecular electron transfer leads to the release of the protected species (tryptophan, Fig. 35). To compare the course of deprotection operating through PeT and direct excitation, a control experiment was planned in which **NB-Trp** would be used a model compound (Fig. 35).

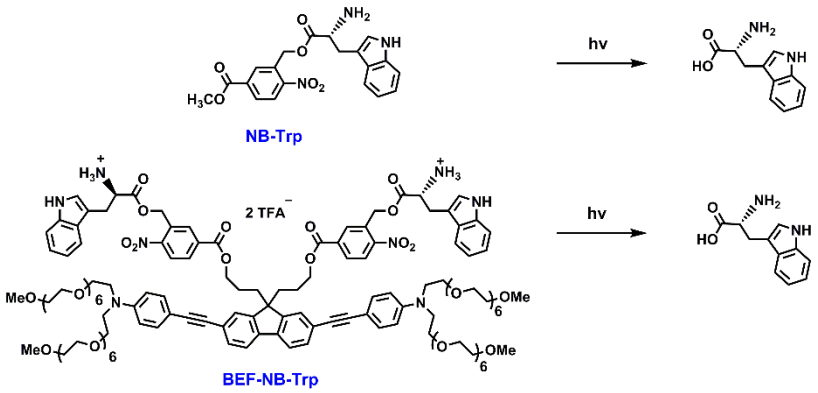

Figure 35. Schematic presentation of the uncaging experiments of **BEF-NB-Trp** and **NB-Trp**. Both experiments were conducted at the identical concentration of caged tryptophan and illumination conditions.

3.2.1 Synthesis of caged compounds for intramolecular PeT

The synthesis of **BEF-NB-Trp** and model **NB-Trp** is shown in Scheme 10.

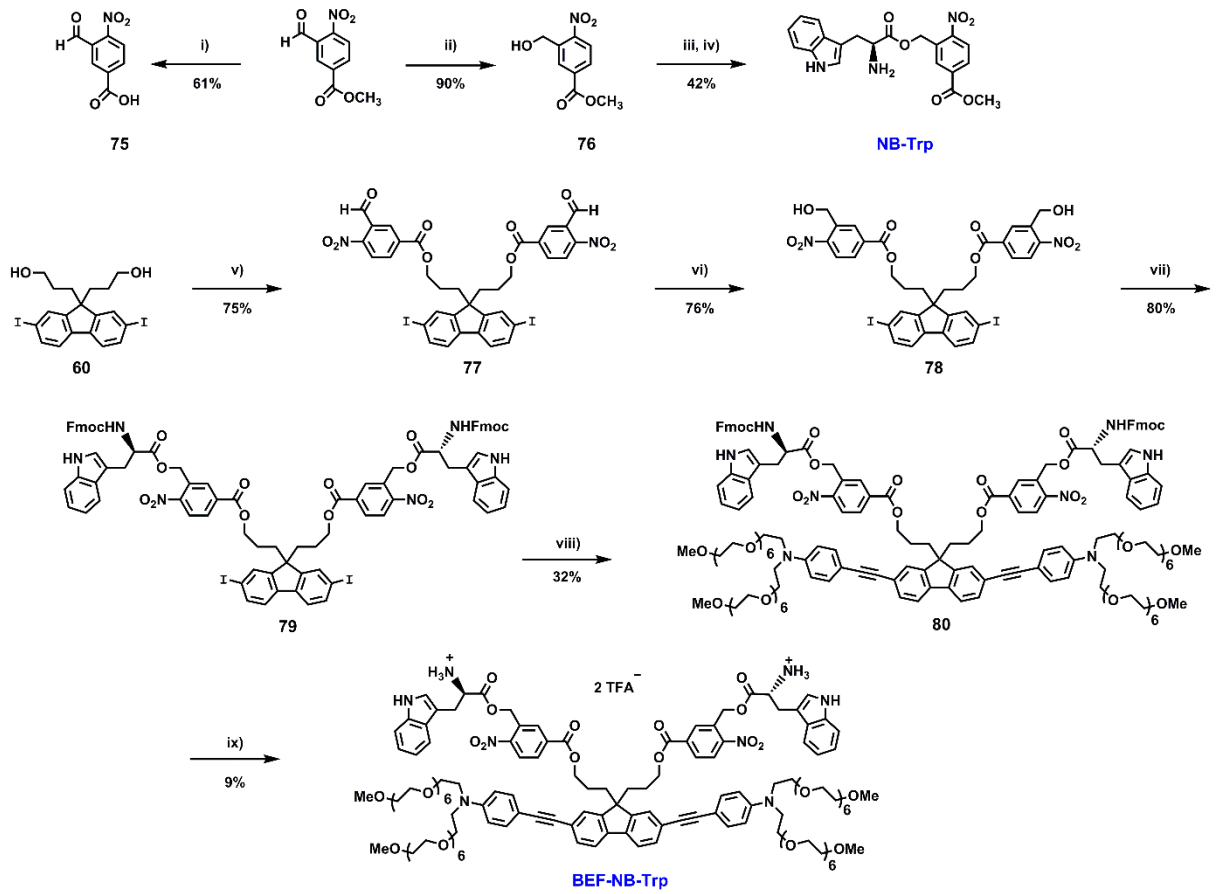

Scheme 11. Scheme 11. Synthesis of **BEF-NB-Trp** and **NB-Trp**. Reagents and conditions: i) conc. H_2SO_4, H_2O, 100 °C, 24 h, ii) $NaBH_4$, MeOH, 0 °C → 20 °C, 1 h, iii) N_α-Fmoc- L -tryptophan, EDC, DMAP, DCM, 20 °C, 2 h, iv) piperidine, MeCN, v) **75**, EDC, DMAP, DCM, 20 °C, 2 h, vi) $NaBH_4$, MeOH, 0 °C → 20 °C, vii) Fmoc-Trp-OH, EDC, DMAP, DCM, 20 °C, 48 h, viii) **58**, $Pd(OAc)_2$, PPh_3, CuI, DIPA, DCM, 20 °C, 2 h, ix) piperidine, MeCN, 20 °C, 2 h, then purified with 0.1% TFA solvent system.[3] Published by The Royal Society of Chemistry.

The route towards **BEF-NB-Trp** commenced with the acid-catalyzed hydrolysis of methy-3-formyl-nitrobenzoate to give **75**. Coupling of **75** with **60** in the presence of EDC and DMAP furnished a functionalized core **77** which was subsequently exposed to $NaBH_4$ in MeOH to deliver alcohol **78**. The preparation of **79** was achieved by treatment of **78** with N_α-Fmoc-L-tryptophan, EDC and DMAP. Substituted aniline **58** was coupled to **79** under usual Sonogashira conditions to yield in **80**. The final step involved removal of the Fmoc protecting groups and purification with TFA-buffered solvent to give the trifluoroacetate salt of **BEF-NB-Trp**. The synthesis of model **NB-Trp** started from the reduction of methy-3-formyl-nitrobenzoate with $NaBH_4$ to form an alcohol **76**. Conversion of **76** into the tryptophan ester was achieved in two steps by coupling with N_α-Fmoc-L-tryptophan in the presence of DMAP and EDC followed by the removal of Fmoc groups upon treatment with piperidine.

3.2.2 Photophysical properties

The absorption spectra of **BEF-NB-Trp** and **NB-Trp** in H_2O are shown in Figure 36. Each spectrum displays characteristic features of its constituents. The spectrum of **BEF-NB-Trp** is dominated by the fluorene-band in the range 300-450 nm whereas absorption of **NB-Trp** exceeds 300 nm. The rational of this comparison was to demonstrate the difference in extinction coefficients of absorbing species at 300-400 nm. It was expected that upon irradiation with a broad source of light (300-400 nm, peak 350 nm) tryptophan would be liberated from both samples, **BEF-NB-Trp** and **NB-Trp**. Considering absorption properties, the liberation of tryptophan from **NB-Trp** was anticipated to proceed with slower rate than in the case of **BEF-NB-Trp**.

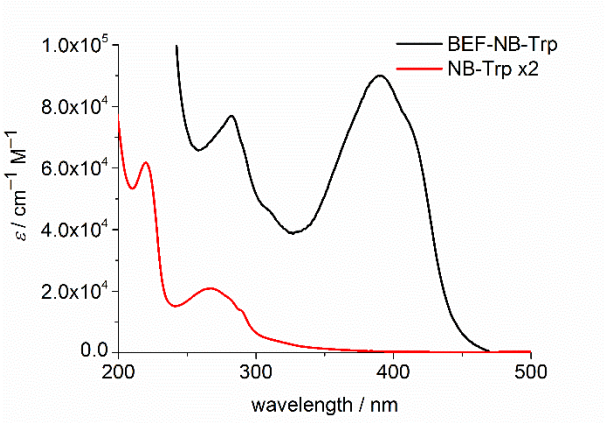

Figure 36. Absorption spectra of **BEF-NB-Trp** and **NB-Trp** (multiplied by two) in H_2O at 20 °C.

3.2.3 Photolysis experiments

Photolysis of **BEF-NB-Trp** was tested in a range of solvents (5 μM concentration in H_2O, $NaHCO_3$-based artificial cerebrospinal fluid [$NaHCO_3$-aCSF], MeCN, MeOH and THF) using a broad UV-A light source (300–400 nm; peak: 350 nm), but no release of tryptophan was observed. Photochemical decomposition of **BEF-NB-Trp** occurred, but it did not result in the formation of free tryptophan (Fig. 37a-c). The same outcome was observed when irradiation was carried out at 280 nm in an effort to selectively excite the *o*-nitrobenzyl unit in the **BEF-NB-Trp**. Analysis of the reaction mixture proved problematic as HPLC chromatograms did not reveal the formation of any other products of photolysis. Tryptophan was liberated cleanly in 75% yield only by the hydrolysis of **BEF-NB-Trp** in the dark over 40 h (2 μM concentration in $NaHCO_3$-based aCSF buffer, Fig 37d). The

irradiation of **NB-Trp** (the concentration of **NB-Trp** in the control experiments was doubled because each **BEF-NB-Trp** bears two caged units; 10 μM in H_2O and phosphate-buffered saline [PBS] at pH 7.4) consistently resulted in 35 ± 3% yield of liberated tryptophan suggesting that a competitive reaction also took place. Similarly to **BEF-NB-Trp**, no other peaks were observed by HPLC. Over the course of performed uncaging experiments, it became apparent that the excitation of the fluorene-dye in the system containing an *o*-nitrobenzyl unit leads to the degradation of the whole compound. Full consumption of **BEF-NB-Trp** (5 μM concentration) required only 30 min of irradiation, whereas 210 min of photolysis were necessary to degrade **NB-Trp** (10 μM concentration). The mechanism of this reaction and the fate of the starting material remained unclear. The energy transfer from excited **BEF-OH** to tryptophan has been ruled out since the emission spectrum of **BEF-OH** does not overlap with the absorption spectrum of tryptophan (Fig. 34). Also electron transfer from **BEF-OH** to tryptophan does not seem possible since both compounds undergo a facile oxidation rather than reduction.[143]

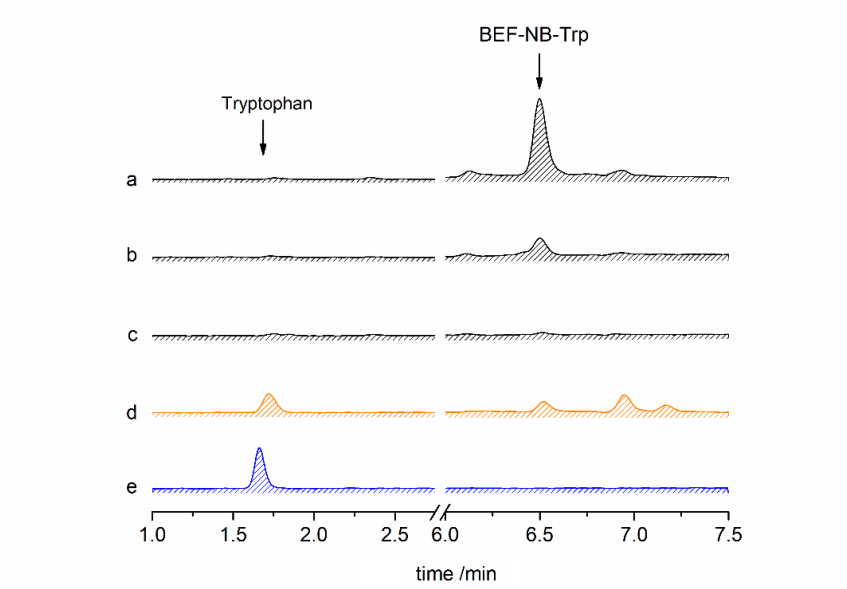

Figure 37. HPLC chromatograms (Zorbax SB column, HPLC method *1*, detection at 220 nm) of: **a) BEF-NB-Trp** (5 μM, H_2O) before photolysis, after **b)** 15 min and **c)** 30 min of irradiation with 300-400 nm (350 nm peak); **d) BEF-NB-Trp** (2 μM, $NaHCO_3$-aCSF) after 40h of hydrolysis in the dark, 75% of tryptophan was liberated, **e)** free tryptophan (4.8 μM, H_2O).

3. 2.4 Conclusions and outlook

The observed results indicated that *o*-nitrobenzyl unit was not a suitable candidate for a release platform for PeT mediated uncaging. Therefore further exploration of this design has been abandoned and attention was turned to the investigation of the pyridinium unit.

Chapter 4

Pyridinium-derived protecting groups

The second design of the protecting group for PeT-mediated uncaging employed a combination of the fluorene dye as an electron-donor and pyridinium as an electron-acceptor. Data acquired for the model dyad **BEF-Pyr** (Chapter 2) suggested that in the polar solvent (MeOH) the forward electron transfer in this system was the fastest within the whole family of investigated compounds. The ratio between the rates of the forward (k_{ET}) and back and electron transfer (k_{BET}) was 2.0 and was also the highest among prepared dyads. Therefore compound **BEF-Pyr** studied in Chapter 2 was converted into the protecting group by replacing the pyridinium group with 4-pyridinium methanol. The efficiency of this cage has been assessed by Dr Philip Bennett with the protected neurotransmitter GABA, **BEF-Pyr-GABA**, in a series of one-photon irradiation experiments (Fig. 38).[3,109]

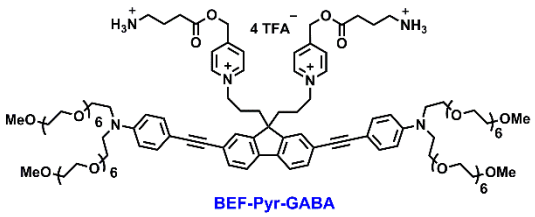

Figure 38. The structure of the caged neurotransmitter GABA, **BEF-Pyr-GABA**, which has been used to evaluate the uncaging properties of the pyridinium derived system and caged acetic acid, **Pyr-OAc**, used in the preliminary stability studies of pyridinium esters. Compounds were synthesized by Dr Philip Bennett. [3, 109]

The high aqueous solubility of **BEF-Pyr-GABA** facilitated photolysis at mM concentration in D_2O and allowed the progress of the reaction to be monitored by ^1H NMR spectroscopy (Fig. 39). The developed protecting group has been demonstrated to release GABA upon one-photon irradiation (300-400 nm, 350 nm peak) in nearly quantitative chemical yield. Two GABA molecules were released from each molecule of **BEF-Pyr-GABA**, which showed that the BEF chromophore is able to undergo two cycles of photoreduction.

The quantum yield of uncaging ϕ_u was determined with ferric oxalate actinometry and by comparison with the commercially available DPNI-GABA, which has ϕ_u of 0.085.[54] It was found that the fast back electron transfer from the charge-shifted state results in an overall quantum efficiency of uncaging of ϕ_u = 0.009 ± 0.004. Nevertheless, due to the high value of the TPA cross section δ_a (1100 GM at 700 nm), the calculated two-photon uncaging cross section for **BEF-Pyr-GABA** was $\delta_u = \delta_a\phi_u$ = 10 ± 3 GM at 700 nm, which is comparable to the highest previously reported value of 11 GM for the 2-(*o*-nitrophenyl)propyl caged GABA.[67]

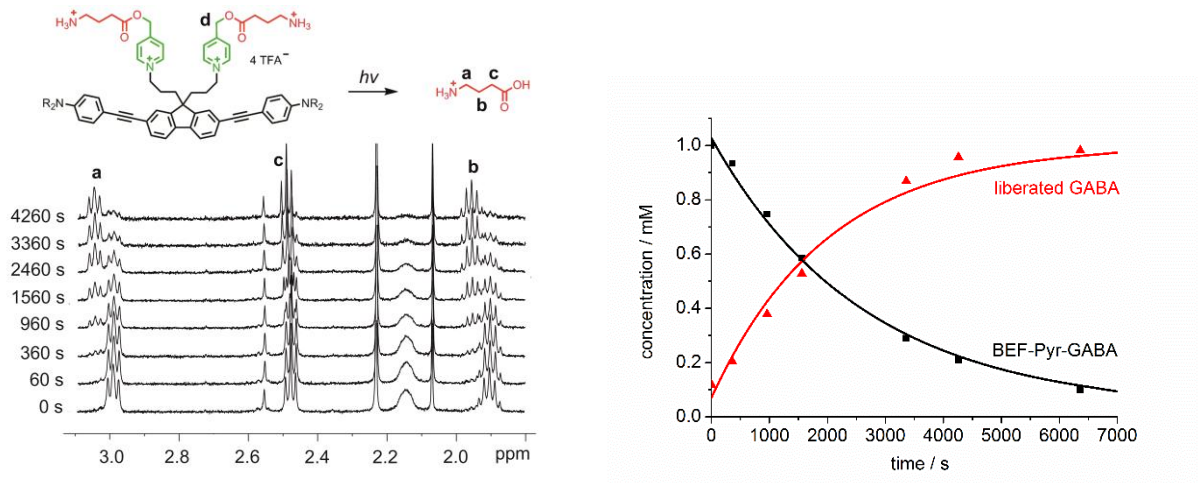

Figure 39. Left: ^{1}H NMR spectra from a representative uncaging experiment, which shows the disappearance of caged-GABA signals with a concurrent increase of a new set of multiplets later found to be free GABA (signals "a-c"). The decrease in intensity of signal "d" (5.29 ppm) is not shown; **Right:** The change in concentration of **BEF-Pyr-GABA** (black squares) and free GABA (red triangles) over time. Mono-exponential fitting curves were applied to the data (lines). Concentration of free GABA and **BEF-Pyr-GABA** were determined by integration of signal "c" and "d" respectively relative to *t*-butanol. The presence of free GABA was confirmed by doping an irradiated solution with an authentic sample, which resulted in no new signals and an increase in the intensity of the suspected GABA signals. Measurements were carried out by Dr Philip Bennett. Reproduced with permission from ref. 3. Published by The Royal Society of Chemistry.

4.1 Evaluation of hydrolytic stability of BEF-Pyr-GABA

The excellent photophysical properties of **BEF-Pyr-GABA** encouraged further examination of the probe under physiological conditions. For this reason, **BEF-Pyr-GABA** was handed over to the research group of Prof. Ole Paulsen (Department of Physiology, Development and Neuroscience, University of Cambridge) to test the performance of the probe under two-photon excitation in the proximity of cultured neurons. During the course of the initial studies with cells, it became apparent

that **BEF-Pyr-GABA** (0.06-0.2 mM concentration, in $NaHCO_3$-aCSF buffer) undergoes rapid hydrolysis. The concentration of free GABA in freshly prepared and administered samples was high enough to evoke changes in the membrane potential even before the irradiation event. This instability appeared to render the probe unusable for further biological testing. Interestingly, a control experiment which was carried out in unbuffered D_2O (90 min, 25 °C) did not reveal any hydrolysis of **BEF-Pyr-GABA**.[3] Moreover, stability studies of a model pyridinium caged acetate (**Pyr-OAc**, Fig. 38) conducted by Dr Bennett in PBS-buffered D_2O (pD 7.4, 48 h, 38 °C) did not account for the immediate hydrolysis of the GABA-pyridinium ester.[109] Finally, the contamination of the sample with free GABA was investigated and refuted. At this stage, the reasons for the instability during the biological tests remained unclear.

Due to the limited availability of **BEF-Pyr-GABA**, attempts to rationalize the rapid hydrolysis of the probe started with the investigation of the model compound **Pyr-GABA** (Scheme 12). **Pyr-GABA** presents a constituent unit of the final structure and was easily prepared according to the route in Scheme 12. The synthesis utilized a three-step sequence, starting with the coupling of 4-pyridinemethanol with Boc-GABA in the presence of EDC and DMAP to give **81**.[109] Alkylation with methyl iodide yielded **82** which upon treatment with formic acid afforded desired **Pyr-GABA**.

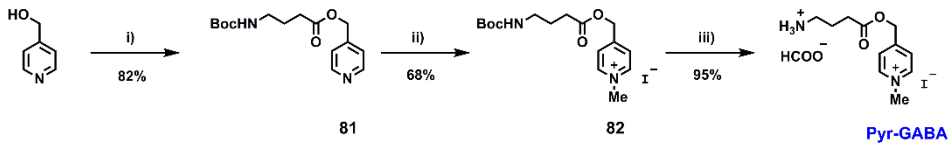

Scheme 12. Synthetic route towards the model compound **Pyr-GABA**. Conditions: i) Boc-GABA-OH, EDC, DMAP, THF, MeCN, 20 °C, 16 h, ii) MeI, MeOH, 60 °C, 16 h, iii) HCOOH, 20 °C, 3 h.

The analytical method that was used to assess the stability of **Pyr-GABA** was dictated by the photophysical properties of the compound. Due to the high polarity of the caged GABA and the difficulties encountered with finding a suitable HPLC method, the progress of the hydrolysis reaction was monitored by ^1H NMR. The model (~1 mM concentration, in PBS-buffered D_2O, pD 7.4) proved surprisingly stable, with only 15% of material hydrolyzed over 9.5 h at 25 °C (Fig. 40a). Results of this experiment did not reflect the behavior of **BEF-Pyr-GABA** at the same pH in aCSF-buffer. This

finding suggested that the stability of GABA esters is sensitive to pH and to the composition of the buffer.

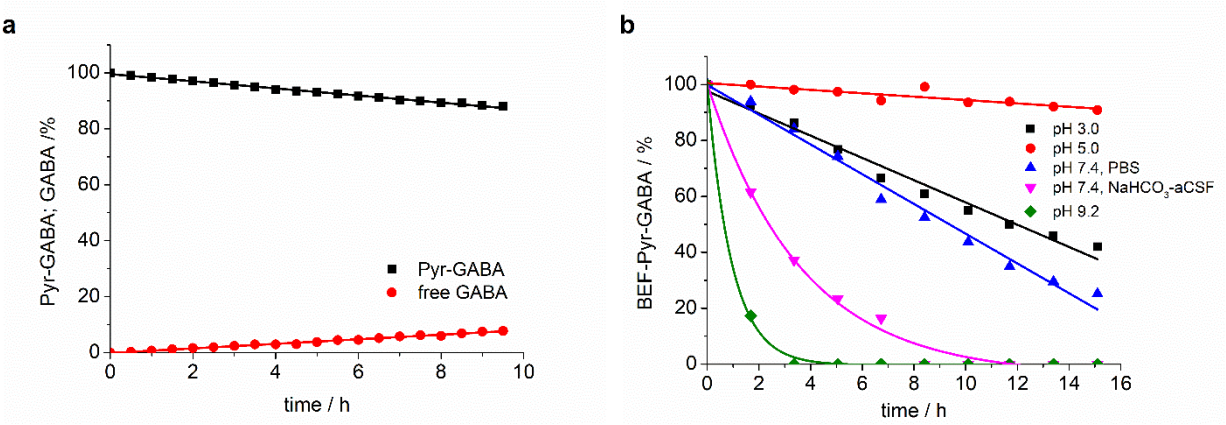

Figure 40. a) The stability studies of **Pyr-GABA** (~1 mM in PBS-buffered D_2O, pH 7.4) monitored by ^1H NMR. **Pyr-GABA** and free GABA were quantified upon integration of signals corresponding to NH_3-$\underline{CH_2}$- relative to the D_2O peak; **b)** Stability of **BEF-Pyr-GABA** at varying pH (2 µM, pH 3.0, 5.0 - sodium citrate/citric acid buffer (black and red, respectively), pH 7.4 - PBS buffer (blue), $NaHCO_3$-aCSF buffer (pink), pH 9.2 - sodium carbonate/sodium bicarbonate (green)). Changes in concentration of **BEF-Pyr-GABA** were determined by HPLC with respect to the integration of the starting material at time = 0 min, with detection at 220 nm. Mono-exponential fitting curves were applied to the data. All experiments were carried out at 20-25°C.

To verify this hypothesis, **BEF-Pyr-GABA** was scrutinized in a set of experiments performed in aqueous buffers at pH 3.0 – 9.2 (Fig. 40b) and monitored by HPLC. It was not possible to follow hydrolysis in these buffers by ^1H NMR spectroscopy due to the high concentration of inorganic salts and carboxylic acids in prepared solutions (see Chapter 7, Section 7.5 for the composition of buffers). Unfortunately, the HPLC method of monitoring this reaction was limited to the observation of the decrease in starting material. Since GABA lacks a chromophore to absorb ultraviolet light, the release of this aminoacid could not be quantified. For this reason, hydrolysis of **BEF-Pyr-GABA** could not be distinguished from other decomposition processes. As expected, results showed that the hydrolysis of **BEF-Pyr-GABA** was very fast at basic pH and slow under acidic conditions. Interestingly, the rate of the depletion of the compound at pH 5.0 was slower than at pH 3.0. The reasons for this divergent result were not investigated at this stage (see page 77). Most importantly, depending on the buffer content, a staggering disparity in the stability of **BEF-Pyr-GABA** was observed at pH 7.4. The half-life in PBS buffer (2 µM concentration) was 10 h, whereas in $NaHCO_3$-aCSF it was reduced to 2.5 h. In a separate series of experiments, an extensive set of troubleshooting tests was carried out.

The preparation of eight versions of aCSF-buffer (each missing a single component) allowed HCO_3^- to be identified as the detrimental component of the mixture. Therefore $NaHCO_3$ was replaced with HEPES [4-(2-hydroxyethyl)-1-piperazineethanesulfonic acid], which is an alternative component of standard buffers used in neuroscience. The stability of **BEF-Pyr-GABA** (20 µM concentration) in an array of buffers at pH 7.4 is shown in Figure 41. Under these conditions, the half-life of **BEF-Pyr-GABA** was found to be *ca*. 15 h in PBS-buffer and 1.5 h in $NaHCO_3$-aCSF. In contrast, the half-life of the probe was extended to *ca*. 50 h HEPES-aCSF.

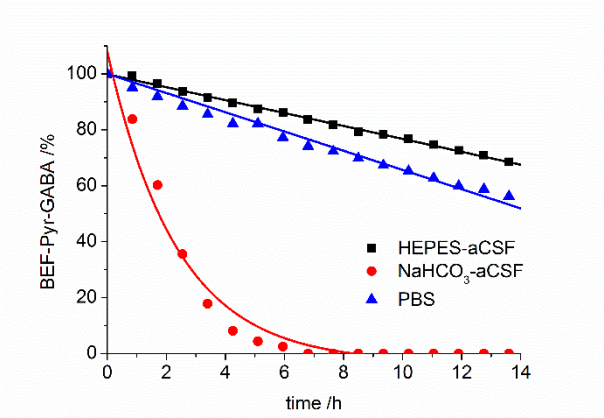

Figure 41. Stability of **BEF-Pyr-GABA** (20 µM) in aqueous buffers at pH 7.4 at 20 °C; HEPES-aCSF (black), $NaHCO_3$-based aCSF (red), PBS (blue). Changes in concentration of **BEF-Pyr-GABA** were determined by HPLC with respect to the integration of the starting material at time = 0 min, with detection at 220 nm. Mono-exponential fitting curves were applied to the data. The half-lives of the probe (PBS – 15 h, $NaHCO_3$-acSF – 1.5 h, HEPES-acSF – 50 h) were estimated by extrapolation of the fitting curves. Reproduced with permission from ref. 3. Published by The Royal Society of Chemistry.

These observations highlighted the necessity of evaluating the stability of caged compounds under conditions identical to those of the final target application. The mechanism by which bicarbonate catalyzes this hydrolysis reaction was not investigated, but the hydrolysis of α-amino acid esters under similar conditions has been attributed to a CO_2-mediated carbamate formation and intramolecular cyclization (Fig. 42).[144,145] The low hydrolytic stability of GABA-pyridinium esters in standard $NaHCO_3$-aCSF buffer posed a limitation for the use of these compounds under strictly physiological conditions that would need to be addressed in future molecular designs. Nevertheless, HEPES-aCSF was applied in the preliminary uncaging experiments in patch-clamped neurons, as outlined in the following section.

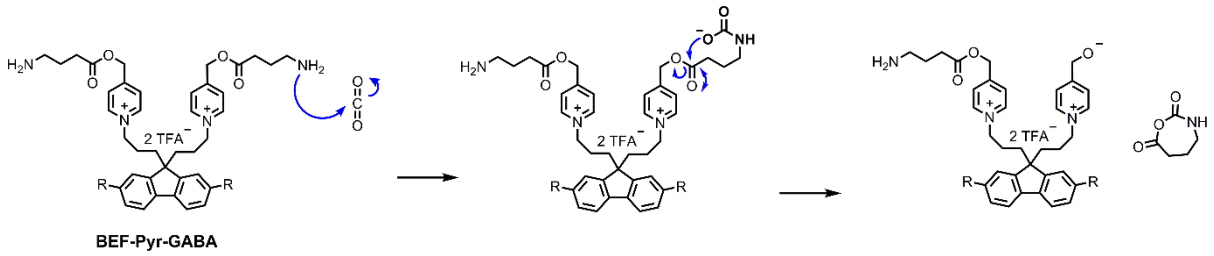

Figure 42. Proposed mechanism of hydrolysis of **BEF-Pyr-GABA** in the presence of CO_2.

4.2 Two-photon uncaging of BEF-Pyr-GABA

The preliminary experiments described in this section were carried out by Dr Yu Zhang in Prof. Ole Paulsen's laboratory at the University of Cambridge. The release of GABA from **BEF-Pyr-GABA** (0.01-2 mM in HEPES-aCSF) was tested in the proximity of cultured rat cortical neurons upon two-photon excitation at 720 nm (300 fs, Ti:sapphire laser; 2–5 ms duration, 5 mW). Whole-cell patch-clamp recordings were used to monitor changes in the membrane potential and cells were imaged under two-photon excitation upon filling with Alexa-594 (20 µM) at 800 nm. The scope of this experiment was limited due to the small amounts of **BEF-Pyr-GABA** that were available at the time.

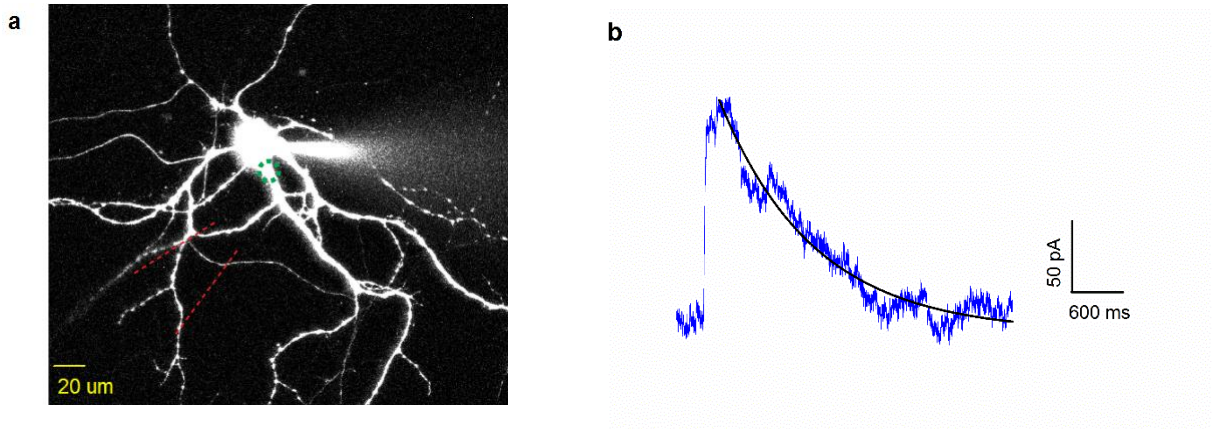

Figure 43. Two-photon uncaging of **BEF-Pyr-GABA** in cultured rat cortical neurons. **a)** Two-photon fluorescence image of the patch-clamped rat cortical neuron filled with Alexa-594 (20 µM, 800 nm). Cells were irradiated above the soma (indicated by a green circle) and **BEF-Pyr-GABA** (2 mM) was administrated locally by puffing with a second patch pipette (red lines). **b)** Average of 10 current traces recorded for the cell after the photolysis of **BEF-Pyr-GABA** at 720 nm, 2-5 ms, 5 mW (Ti:sapphire laser, 300 fs). All experiments were carried out at 20-25°C. Recorded by Dr Yu Zhang from Prof. Ole Paulsen's group (University of Cambridge).

In the presence of **BEF-Pyr-GABA**, two-photon irradiation of the neuron above the soma (indicated by the dashed green circle on Figure 43a) resulted in the repetitive light activation of the cell and generation of outward currents (Fig. 43b). The kinetics of the changes in membrane potential were consistent with activation of GABA-A receptors, indicating GABA release from **BEF-Pyr-GABA**. These initial experiments demonstrated two-photon sensitivity of the developed protecting group, however further experiments are needed to assess the performance of **BEF-Pyr-GABA** against commercially available probes, such as DPNI-GABA[54] or RuBi-GABA.[35]

4.3 Demonstration of the PeT mechanism of deprotection

The family of BEF-derived protecting groups has been designed to operate through an intramolecular electron transfer between the photoexcited electron-donor and an electron-acceptor to achieve efficient release of physiologically active compounds (Figure 44a). To prove that photo-cleavage of the new protecting group is sensitized by the absorption of the fluorene-based dye, rather than by direct excitation of the pyridinium unit, the efficiency of uncaging was investigated as a function of irradiation wavelength. Specifically for this purpose, caged tryptophan, **BEF-Pyr-Trp** was prepared (Fig 44b). This compound has a significant advantage over **BEF-Pyr-GABA**; changes in the concentration of the starting material and the liberated species (tryptophan) could be directly quantified at μM concentration by UV detection.

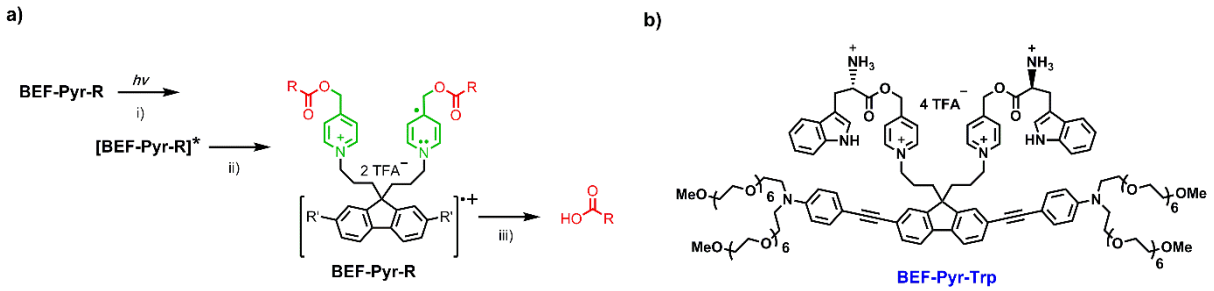

Figure 44. a) Schematic representation of the mechanism of uncaging in the BEF-Pyr protecting group: i) light absorption generates a photosensitizer-based singlet state, which is quenched by electron transfer to the release group, ii) the resulting charge-shifted state decays by bond cleavage to liberate the physiologically active carboxylic acid; **b)** Structure of **BEF-Pyr-Trp**, a compound designed for the wavelength dependent uncaging experiments. Adapted with permission from ref. 3. Published by The Royal Society of Chemistry.

4.3.1 Synthesis of BEF-Pyr-Trp

The synthesis of **BEF-Pyr-Trp** exploited the strategy used in the preparation of **BEF-NB-Trp** (Section 3.2.1) and involved the decoration of the core with the release unit followed by the extension of the chromophore (Scheme 13).

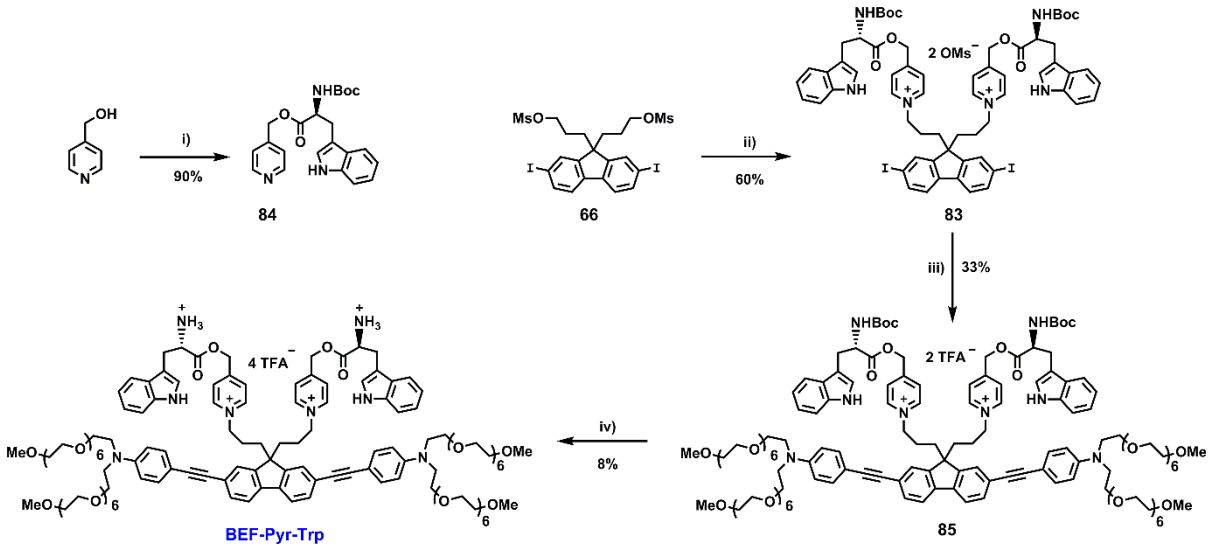

Scheme 13. Synthetic route towards **BEF-Pyr-Trp**. Conditions: i) N_α-Boc-L-tryptophan, EDC, DMAP, MeCN, 20 °C, 16 h, ii) **84**, MeCN, 100 °C, 24 h, iii) **58**, $Pd(OAc)_2$, PPh_3, CuI, DIPA, DCM, MeCN, 20 °C, 2 h, then purification in TFA-buffered solvent, iv) HCO_2H, TIPS-H, 20 °C, 1 h, then purification in TFA-buffered solvent. Adapted with permission from ref. 3, Published by The Royal Society of Chemistry.

The formation of functionalized core **83** involved substitution of the mesylate groups in the readily available **66** with picoline caged tryptophan **84** which was synthesized by coupling of 4-pyridinemethanol with N_α-Boc-L-tryptophan in the presence of EDC and DMAP. The synthesis of the chromophore unit was accomplished by connecting **83** with the aniline unit **58** under Sonogashira reaction conditions. The resulting compound **85** was subjected to formic acid to remove the Boc groups, followed by the reverse-phase column chromatography in TFA-buffered solvent to yield **BEF-Pyr-Trp** as a TFA-salt. The low yield of the last step was attributed to the acid-catalyzed decomposition of the product during the purification. Use of non-buffered solvent system did not give desired purity of the product.

4.3.2 Stability studies of BEF-Pyr-Trp

At the early stage of the studies on **BEF-Pyr-Trp**, the HPLC analysis revealed that the background (dark) hydrolysis occurred on a 1 h timescale and could therefore not be neglected during the photochemical cleavage experiments. To find optimal conditions for limited hydrolysis, the stability of **BEF-Pyr-Trp** was examined in aqueous media at pH 3.0-9.2 (Fig. 45).

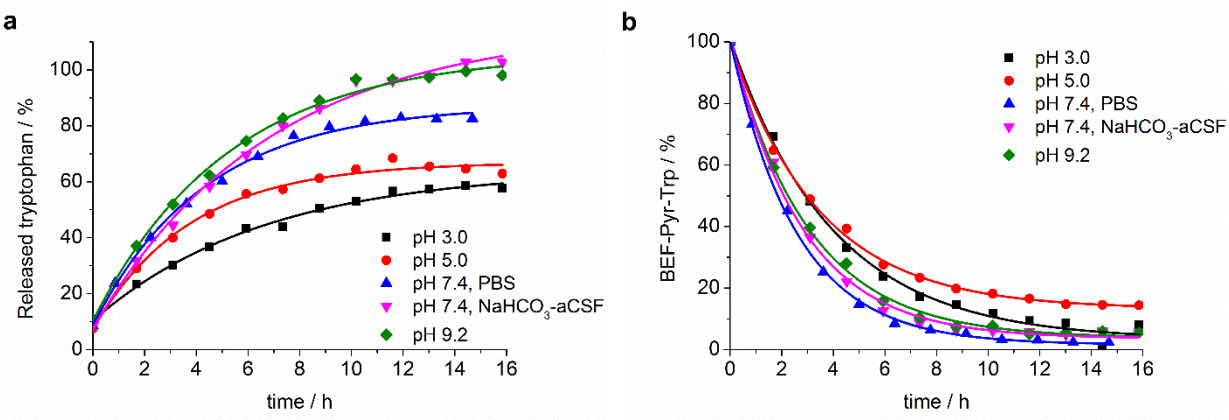

Figure 45. Stability of **BEF-Pyr-Trp** (2 µM, pH 3.0, 5.0 - sodium citrate/citric acid buffer (black and red, respectively), pH 7.4 - PBS buffer (blue), $NaHCO_3$-aCSF buffer (pink), pH 9.2 - sodium carbonate/sodium bicarbonate (green)). Changes in concentration of **a)** free tryptophan were determined by HPLC with use of a calibration curve prepared for tryptophan (1.24-6.20 µM concentration) with detection at 220 nm Changes in concentration of **b) BEF-Pyr-Trp** were determined by HPLC relative to the integration of its corresponding peak at time = 0 min, with detection at 375 nm. Analyzed samples contained 7% of free tryptophan at time = 0 min Mono-exponential fitting curves were applied to the data. All experiments were carried out at 20-25°C. Reproduced with permission from ref. 3. Published by The Royal Society of Chemistry.

This series of experiments showed that hydrolysis was suppressed at strongly acidic pH 3.0. However, under these conditions the percentage of released tryptophan (Fig. 45a) did not match the percentage of consumed **BEF-Pyr-Trp** at the corresponding time points. After 16 h, 90% of **BEF-Pyr-Trp** was consumed, whereas the concentration of tryptophan reached only 60%. This observation indicated that additional processes are leading to the depletion of **BEF-Pyr-Trp**. At acidic pH, hydrolysis may compete with another side reaction resulting in the degradation of the starting material without the release of tryptophan. The HPLC analysis did not reveal the formation of any other products and ^{1}H NMR measurements were not feasible because **BEF-Pyr-Trp** gave broad ^{1}H NMR spectra at mM concentrations in D_2O, presumably due to aggregation. In contrast to **BEF-Pyr-GABA**, the composition of the buffer at pH 7.4 was not relevant, and starting material was depleted with identical

rate constant in PBS and $NaHCO_3$-aCSF-buffered solutions. The stability of **BEF-Pyr-Trp** was influenced only by the pH of the medium.

In order to gain insight into the factors affecting the acid-catalyzed decomposition of **BEF-Pyr-Trp**, the stability of several related structural motifs was studied. Model compounds presented constituent units of **BEF-Pyr-Trp** and their structures are shown in Figure 46. The synthesis of **BEF-OH** and **BEF-Pyr** has been described in Chapter 2 (page 40 and 52) whereas the preparation of **Bu-Pyr** and **Pyr-Trp** was accomplished according to the Scheme 14. The methyl ester of tryptophan, **MeO-Trp**, was commercially available.

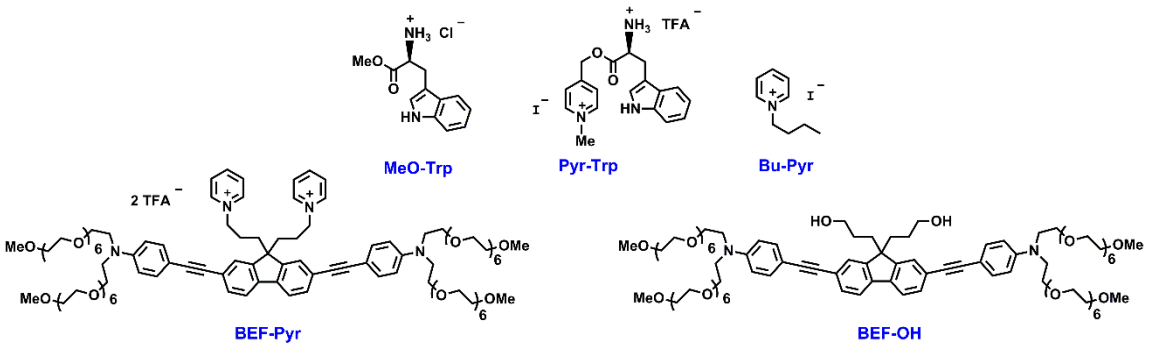

Figure 46. Structures of model compounds used in the systematic stability studies of **BEF-Pyr-Trp**.

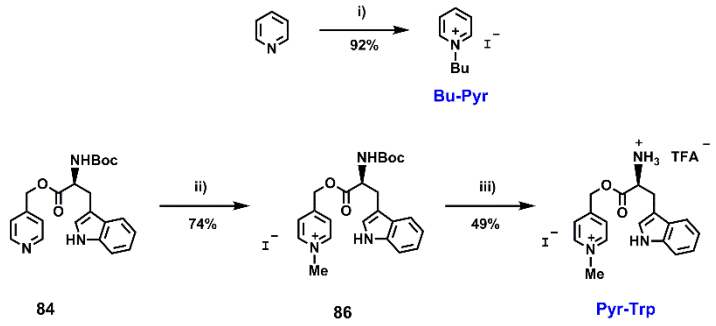

Scheme 14. The synthetic routes towards model compounds **Bu-Pyr** and **Pyr-Trp**. Conditions: i) 1-iodobutane, MeOH, 55 °C, 16 h, ii) MeI, MeOH, 55 °C, 72 h, iii) TFA, THF, 20 °C, 1 h. Adapted with permission from ref. 3, Published by The Royal Society of Chemistry.

The preparation of **Bu-Pyr** was completed in one-step by refluxing pyridine with 1-iodobutane. The synthesis of **Pyr-Trp** commenced with readily available tryptophan ester **84** which was *N*-alkylated with methyl iodide to give **86** and subsequently treated with TFA to remove the Boc group.

The stability of the abovementioned compounds was examined in aqueous buffers at pH 3.0-9.2, using HPLC to analyze the outcomes. The results showed that the BEF-chromophore underwent decomposition in acidic media but remained intact at physiologically relevant pH, as demonstrated for **BEF-Pyr** and **BEF-OH** (Fig. 47a-b). These observations were consistent with the results previously shown for **BEF-Pyr-GABA** in Figure 40b, in which the probe was depleted faster at pH 3.0 than at pH 5.0. The products and the mechanism of this reaction have not been investigated at this point. The experiments that were carried out with model **Bu-Pyr** showed that the *C–N* bond joining the release unit and alkyl chain is resistant over the range of tested conditions (Fig. 47c).

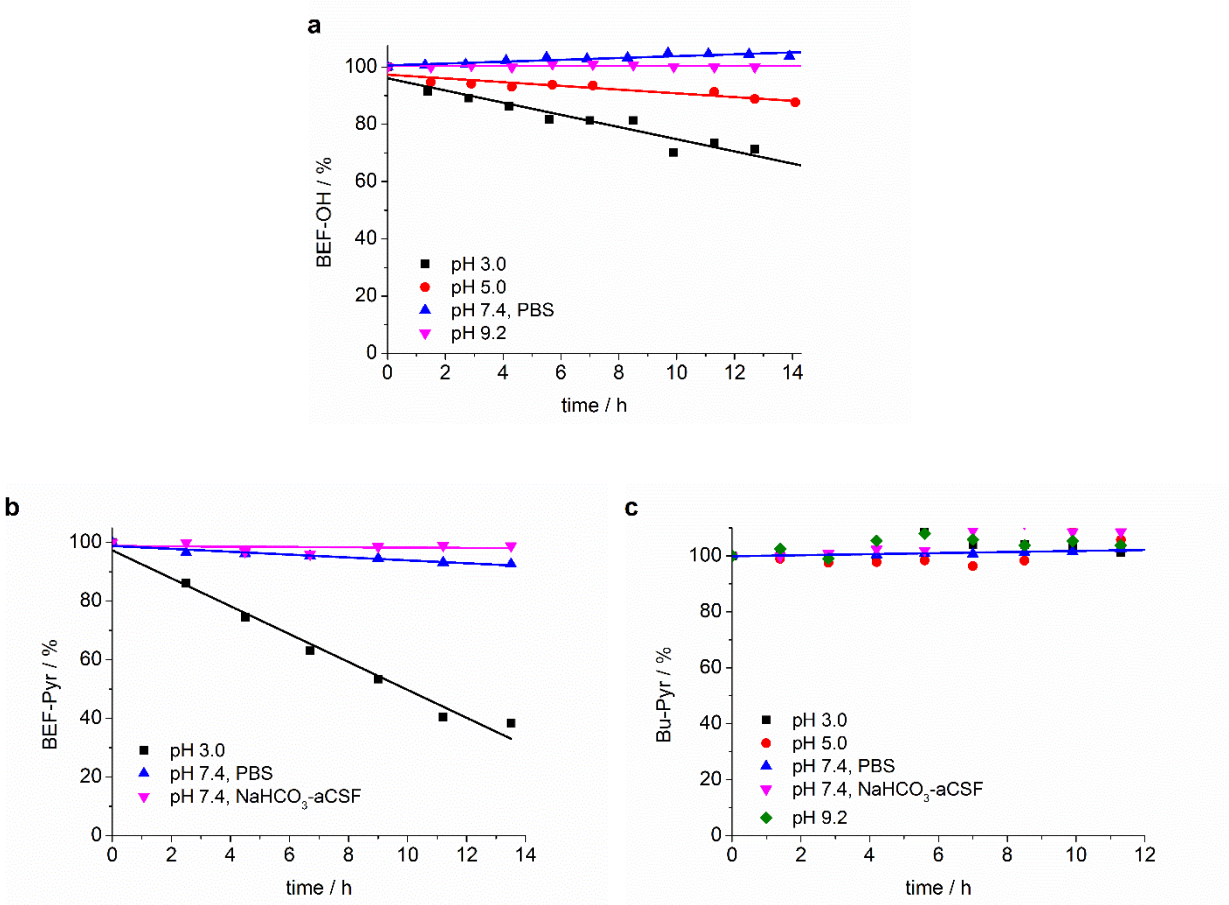

Figure 47. The stability studies of **BEF-Pyr-Trp** model compounds **BEF-OH**, **BEF-Pyr** and **Bu-Pyr**. Experiments were carried out at 20-25 °C, at a range of pH: 3.0-9.2 (pH 3.0, 5.0 - sodium citrate/citric acid buffer (black and red, respectively), pH 7.4 - PBS buffer (blue), $NaHCO_3$-aCSF buffer (pink), pH 9.2 - sodium carbonate/sodium bicarbonate (green)). Samples concentrations were 1.5-20 µM. Changes in the concentration of the studied compounds were determined by HPLC with detection at 220 nm and 375 nm and were calculated relative to the integration of **BEF-OH**, **BEF-Pyr** and **Bu-Pyr** peaks at t = 0 min. Mono-exponential fitting curves were applied to the data.

Tryptophan was released quantitatively from **Pyr-Trp** upon hydrolysis at physiological and basic pH. This observation was confirmed by a ^{1}H NMR study of **Pyr-Trp** (~1 mM concentration, in PBS-buffered D_2O, pD 7.4, not shown), in which exclusive formation of free tryptophan was observed. However, under acidic conditions, the amount of **Pyr-Trp** that was consumed did not match the amount of liberated tryptophan (within 7 h 15% of starting material was consumed and only 4% of tryptophan released, Fig. 48a-b). In contrast, the methyl ester of tryptophan **MeO-Trp** did not hydrolyze at pH 3.0 and 5.0 (Fig. 48c-d). The reason for this discrepancy remained unclear since the HPLC analysis did not reveal the formation of any new peaks. Nevertheless, all further experiments were carried out at pH 3.0 due to the suppressed hydrolysis.

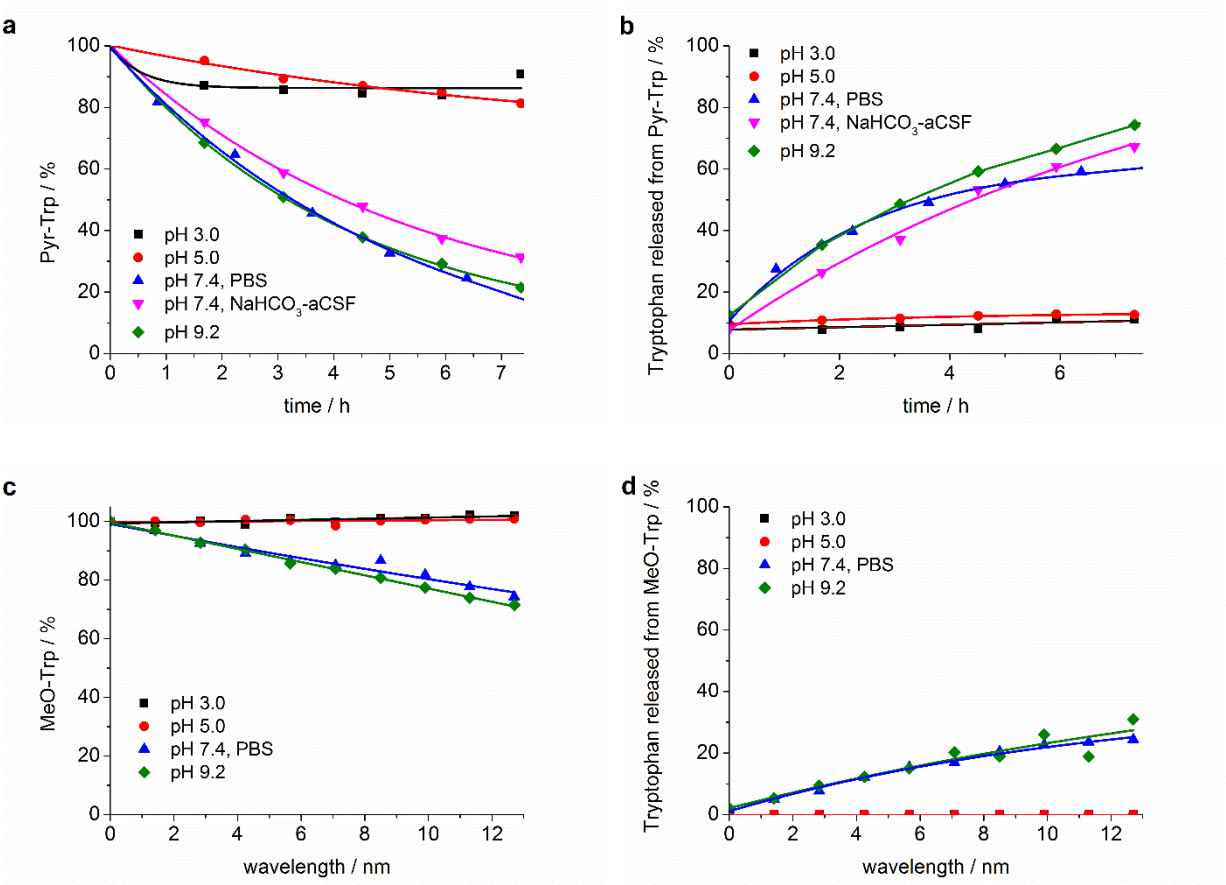

Figure 48. Stability studies of **BEF-Pyr-Trp** model compounds **Pyr-Trp** and **MeO-Trp.** Experiments were carried out at 20-25 °C, at a range of pH: 3.0-9.2 (pH 3.0, 5.0 - sodium citrate/citric acid buffer (black and red, respectively), pH 7.4 - PBS buffer (blue), $NaHCO_3$-aCSF buffer (pink), pH 9.2 - sodium carbonate/sodium bicarbonate (green)). Samples concentrations were 3-4 µM. Changes in the concentration of the studied compounds and free tryptophan were determined by HPLC with detection at 220 nm. Tryptophan was quantified according to the calibration curve prepared for free tryptophan (1.24-6.20 µM concentration), whereas changes of concentration of **Pyr-Trp** and **MeO-Trp** were calculated relative to the integration of their corresponding peaks at t = 0 min. Mono-exponential fitting curves were applied to the data.

4.3.3 Uncaging quantum yield of BEF-Pyr-Trp

The absorption spectra of **BEF-Pyr-Trp** and its respective constituents **Pyr** (Fig. 24), tryptophan and **BEF-OH** in H_2O and THF, are shown in Figure 49. A close examination of the spectra show that **BEF-Pyr-Trp** can be selectively excited at the chromophore unit with 300-400 nm irradiation wavelength. This distinctive separation of the fluorene absorption band, together with a high difference in its intensity, compared to the bands of the other monomer subunits, made **BEF-Pyr-Trp** particularly useful in attempts to demonstrate PeT-mediated uncaging mechanism.

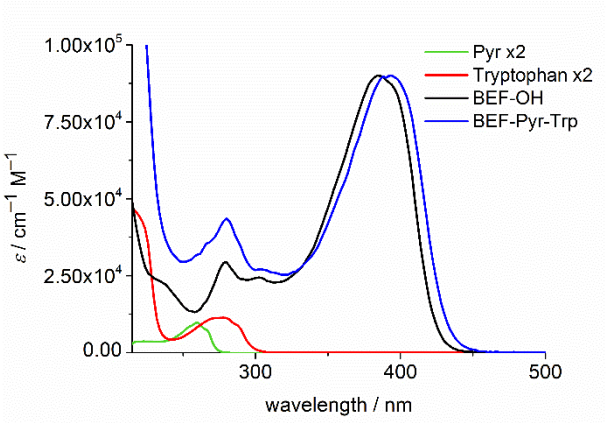

Figure 49. Absorption spectrum of **BEF-Pyr-Trp** (in H_2O) overlaid with the spectra of its constituent building blocks: **BEF-OH**, tryptophan (in H_2O) and **Pyr** (in THF). The absorption spectra of **Pyr** and tryptophan were doubled as each **BEF-Pyr-Trp** molecule bears two equivalents of these species. Spectra were recorded at 20 °C.

The uncaging properties of **BEF-Pyr-Trp** were evaluated in a series of one-photon irradiation experiments, the progress of which was monitored by HPLC. All samples were photolyzed in solutions at pH 3.0. When irradiation was performed with a powerful source of light, such as a Rayonet RMR-600 (300–400 nm, 350 nm peak, photon flux: $1.89 \pm 0.04 \times 10^{16}$ photons s^{-1}), the complete photolysis of **BEF-Pyr-Trp** (< 10 μM concentration) proceeded rapidly (< 2 min) and with high chemical yields (83 ± 2%). No photochemically-generated byproducts were detected. The quantum yield of uncaging for **BEF-Pyr-Trp** was determined under moderate illumination conditions (using a fluorimeter) to allow for a gradual photo-cleavage. A solution of **BEF-Pyr-Trp** (1.5 μM, pH 3.0) was irradiated at 360 ± 5 nm and photorelease of tryptophan was quantified by HPLC. Due to the previously described stability issues, it was not possible to obtain a tryptophan-free sample and all freshly prepared solutions contained on average 7.0 ± 0.5% of free tryptophan (relative

to the maximum expected value). Moreover, within 3800 s, the tryptophan concentration rose to 14.5 ± 1.0% in control samples stored in the dark. For this reason, a special protocol was designed to take account of competing background hydrolysis and acid-catalyzed decomposition of **BEF-Pyr-Trp**. The concentration of tryptophan liberated exclusively upon uncaging (net tryptophan) was obtained by subtracting the concentration reached in control samples from the photolysis experiments (Fig. 50b).

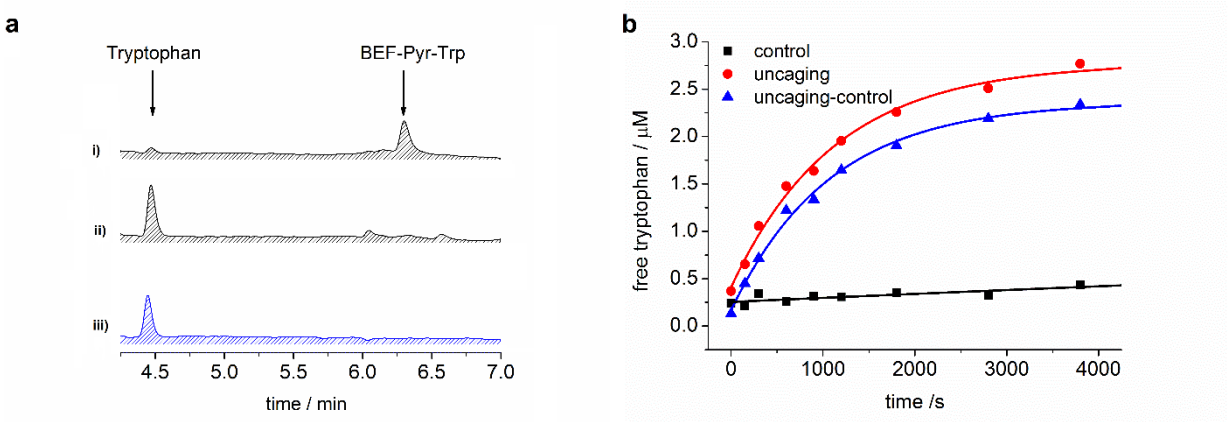

Figure 50. a) HPLC chromatograms (Eclipse XDB column, HPLC method *2*, detection at 220 nm) of **i) BEF-Pyr-Trp** (1.77 µM, sodium citrate/citric acid buffer, pH 3.0) before photolysis, after **ii)** 10 min of irradiation with 300-400 nm (350 nm peak); photolysis resulted in 80% yield of uncaging (2.8 µM concentration of tryptophan) **iii)** free tryptophan (2.5 µM, H_2O); **b)** The change in concentration of tryptophan upon photolysis of **BEF-Pyr-Trp** at pH 3.0 and at 360±5 nm (fluorimeter); red circles–photolyzed sample, blue squares–control samples stored in the dark, black triangles – net concentration of tryptophan released upon uncaging. The concentration of tryptophan was determined by HPLC according to the calibration curve prepared for free tryptophan (1.24-6.20 µM concentration). Figure 50b was reproduced with permission from ref. 3. Published by The Royal Society of Chemistry.

The release of tryptophan followed first order reaction kinetics and the rate of uncaging was determined to be $9.3 \pm 0.8 \times 10^{-4}$ s^{-1}. The photon flux of the fluorimeter at 360 nm was measured with ferric oxalate actinometry and was $3.30 \pm 0.5 \times 10^{15}$ photons s^{-1} (Chapter 7, section 7.4.1).[146,147] The uncaging quantum field was calculated according to Equation 7 to give 0.0025 ± 0.0006.[148] Consequently, two-photon uncaging cross-section ($\delta_u = \delta_a \times \phi_u$; δ_a = 1000 GM at 720 nm for **BEF-OH** in H_2O, Chapter 2, page 43) for **BEF-Pyr-Trp** at 720 nm was estimated as only δ_u 2.5 ± 0.6 GM.

$$\phi_u = \frac{kcVN_A}{f(1-10^{-A})} \qquad (7)$$

Equation 7. Equation used in calculating one-photon uncaging quantum yield ϕ_u where k - release rate constant under investigated illumination conditions, c - concentration of the photolysed solution, V- volume of the photolysed solution, N_A – Avogadro number, f - number of photons administrated by the source of light, A - absorption of the irradiated solution at the photolysis wavelength.

It is known that the quantum yield of uncaging depends on the leaving group but the reasons for the nearly four-fold difference in ϕ_u between **BEF-Pyr-Trp** and **BEF-Pyr-GABA** (ϕ_u = 0.009) are unclear. This disparity might stem from the fact that **BEF-Pyr-Trp** is depleted by competitive reactions at pH 3.0.

4.3.4. Wavelength-dependent uncaging

The spectra shown in Figure 49 clearly demonstrate that irradiation at 300-400 nm results in excitation of the electron-donor unit. Therefore, the amount of released tryptophan should be proportional to the extinction coefficient of the fluorene dye, if photo-cleavage is exclusively PeT-mediated. To demonstrate that liberation of tryptophan results from the absorption of the fluorene-based dye, rather than by direct excitation of pyridinium unit, the efficiency of uncaging was evaluated for a set of irradiation wavelengths. For this purpose, solutions of **BEF-Pyr-Trp** (~1.5 μM, pH 3.0) were photolyzed at 340, 360, 380, 400 and 420 nm for 3800 s. The plot for an example uncaging experiment is presented in Figure 50b and the chemical yield of uncaging at each wavelength is given in Table 11. The extent of uncaging correlates closely with the absorption spectrum of the BEF chromophore, confirming the active role of the fluorene dye in uncaging and PeT mediated release of tryptophan from **BEF-Pyr-Trp** (Fig. 51).

Table 11. The yield of uncaging obtained upon 3800 s of photolysis of 1.35–1.77 μM **BEF-Pyr-Trp** solutions in citric acid/ citrate buffer (pH 3.0).[3] Published by The Royal Society of Chemistry.

Wavelength	**Tryptophan concentration − measured / μM**	**Tryptophan concentration −expected[a] / μM**	**Chemical yield of uncaging / %**
340	1.58	3.00	52
360	2.33	3.54	65
380	2.15	2.40	89
400	1.77	2.40	73
420	1.3	3.54	36

[a] – The expected concentration of tryptophan was calculated based on the measured absorbance of **BEF-Pyr-Trp** at 393 nm, with an extinction coefficient 90 000 M^{-1} cm^{-1} and 0.9 factor to correct for the purity of each sample.

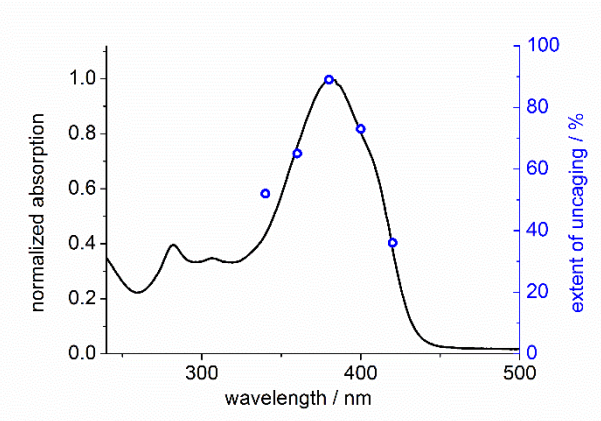

Figure 51 Normalized absorption spectrum of **BEF-Pyr-Trp** in citric acid/sodium citrate buffer (pH 3.0) (black line) plotted with the extent of photolysis, expressed as the yield of released tryptophan upon 3800 s of irradiation of **BEF-Pyr-Trp** at 340–420 nm (blue circles). Reproduced with permission from ref. 3. Published by The Royal Society of Chemistry.

4.4 Conclusions and outlook

The pyridinium-derived protecting group has been demonstrated to release the neurotransmitter GABA and amino acid L-tryptophan upon irradiation with light at wavelengths 340–420 nm, in aqueous solution in nearly quantitative chemical yields. This group exhibits a highly efficient charge-transfer between the electron-donor and acceptor (~99%, based on the fluorescence quenching, Chapter 2, Section 2.3.3) but the fast back electron transfer from the charge-shifted state reduced the overall quantum efficiency of uncaging to around 1% in **BEF-Pyr-GABA** and 0.25% in **BEF-Pyr-Trp**. Consequently, when combined with the TPA cross-section, the two-photon uncaging cross-section of the **BEF-Pyr** protecting group was 10 ± 3 GM for GABA and 2.5 ± 0.6 GM for tryptophan. Wavelength-dependent uncaging experiments confirmed the electron-transfer mediated release of caged tryptophan with the efficiency of release proportional to the extinction coefficient of the fluorene dye within 340–420 nm. A key objective for future experiments will be to apply an electron donor–acceptor pair for which the back electron-transfer is suppressed, so that bond-scission becomes the main decay pathway. Another crucial point for future studies will be to identify a release unit with enhanced resistance to hydrolysis as the susceptibility of pyridinium esters to this decomposition pathway led to practical difficulties for uncaging studies in aqueous media.

Chapter 5

Phenacyl-derived protecting group

Data collected in Chapter 2 showed that from a thermodynamic point of view, PeT was the most favored for *o*-nitrobenzyl and pyridinium derived systems, with $\Delta G = -1.0$ eV for **BEF-NB** and −0.70 eV for **BEF-Pyr** (Table 10). Unfortunately, as demonstrated in Chapter 3 and 4, *o*-nitrobenzyl and pyridinium based protecting groups suffer from disadvantages typical for caging units: low quantum yield, hydrolytic susceptibility and the presence of side reactions. On the other hand, initial studies on the phenacyl group revealed that PeT could occur from the fluorene dye only to the ester-linked release unit with $\Delta G = -0.40$ eV. Bimolecular uncaging studies previously performed by Dr Philip Bennett were inconclusive and results varied with the solvent used in the photolysis experiments.[109] Nevertheless, fluorescence of **BEF-Phen** was almost fully quenched indicating that efficient PeT took place (Chapter 2, Table 10).[138]

Despite a low driving force for the electron transfer, several literature reports support the hypothesis that a phenacyl group could be used successfully as the release unit in a two-photon sensitive protecting group for biological applications. Firstly, phenacyl has been already applied in the liberation of glutamate from its *p*-hydroxyphenacyl ester in rat brain cortical slices and no hydrolytic instability was highlighted.[119] Secondly, it was reported that phenacyl released acetic acid quantitatively upon intramolecular electron transfer.[104] Therefore we decided to evaluate one-photon uncaging properties of the phenacyl derived system with a model caged tryptophan, **BEF-Phen-Trp**, and then test the performance of the developed platform under two-photon excitation conditions with GABA analogue **BEF-Phen-GABA** (Fig. 52).

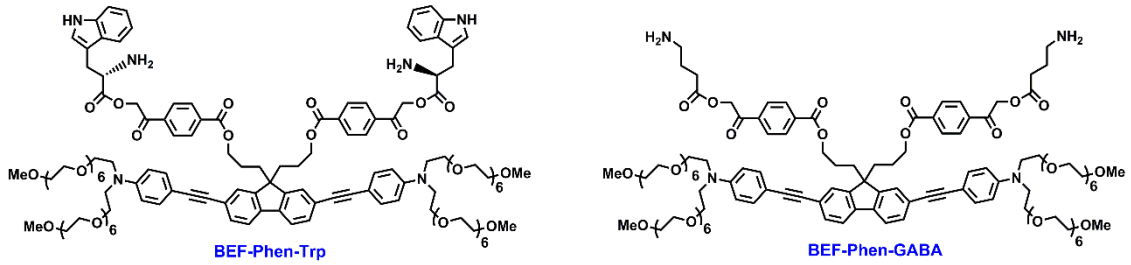

Figure 52. Structures of compounds designed to evaluate uncaging properties of the **BEF-Phen** group: caged tryptophan (**BEF-Phen-Trp**) and GABA (**BEF-Phen-GABA**).

5.1 Stability studies of model compounds

5.1.1. Synthesis of model protected carboxylic acids

Guided by the experience from the work on the pyridinium protecting group, studies on phenacyl derivatives began with the evaluation of hydrolytic stability of phenacyl esters. Tryptophan and GABA were selected as model carboxylic acids to be protected with a phenacyl group. Tryptophan was of particular interest due to its utility in HPLC monitored one-photon uncaging experiments (Chapter 4, Section 4.3.2) whilst GABA was chosen for its biological activity and applicability in the future two-photon liberation in the proximity of neurons (Chapter 4, Section 4.2). The structures of the model compounds designed for the stability studies are shown in Figure 53.

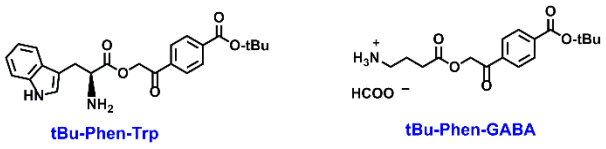

Figure 53. Structures of the model caged phenacyl compounds for HPLC-monitored stability studies: **tBu-Phen-GABA** and **tBu-Phen-Trp**.

Syntheses of phenacyl esters reported in the literature employed conversion of α-brominated ketones into esters via S_N2 bromide displacement.[118-120,149-151] Therefore the synthetic strategy towards target compounds **tBu-Phen-GABA** and **tBu-Phen-Trp** relied on a common intermediate **88**, that permitted access to a variety of phenacyl derivatives (Scheme 15).

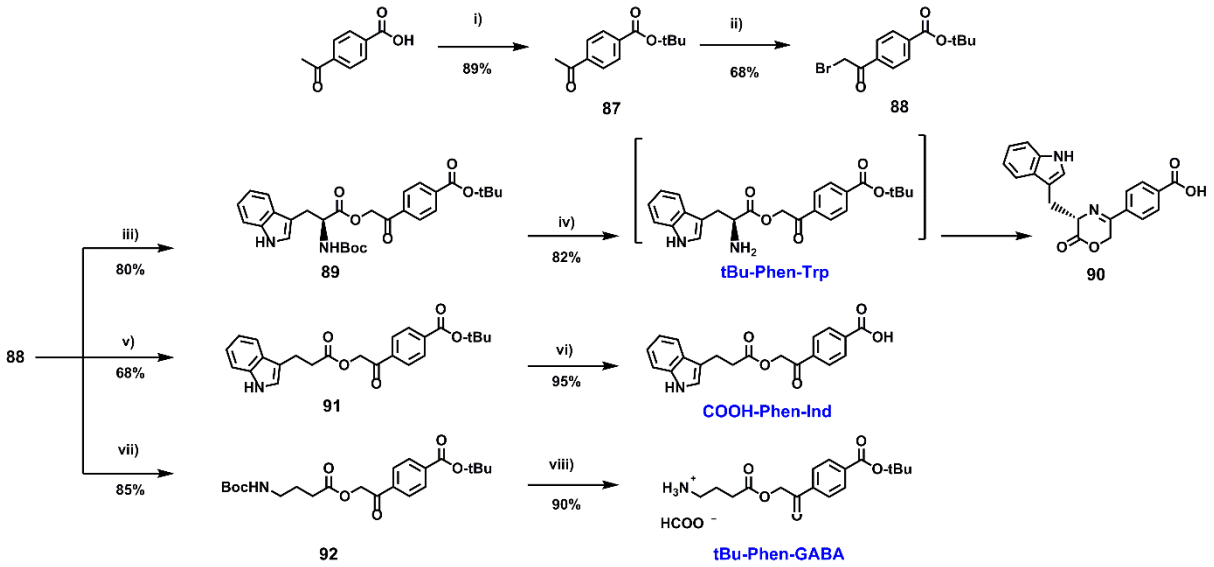

Scheme 15. i) di-tert-butyl-dicarbonate, DMAP, *t*-BuOH, 20 °C, 6 h, ii) Br_2, $CHCl_3$, 0 °C → 20 °C, 1 h, iii) N_α-Boc-L-tryptophan, DBU, MeCN, 13 °→ C 20 °C, 16 h, iv) HCOOH, 20 °C, 6 h, v) 3-indolepropionic acid, DIPEA, MeCN, 20 °C, 16 h, vi) HCOOH, 20 °C, 2 h, vii) Boc-GABA-OH, DBU, MeCN, 20 °C, 16 h, viii) HCOOH, 20 °C, 30 min.

The two-step sequence towards **88** started from the protection of the carboxylic group of commercially available 4-acetylbenzoic acid by treatment with di-*tert*-butyl-dicarbonate and DMAP in *t*-BuOH. This reaction afforded ester **87**, which was subsequently brominated with elemental bromine to furnish the desired α-halogenated ketone. Bromine displacement by N_α-Boc-L-tryptophan in the presence of DBU followed by the removal of Boc group by treatment with formic acid resulted in the formation of **tBu-Phen-Trp**, as was confirmed by mass spectrometry of the crude reaction mixture. In solution (DMSO-d_6, D_2O), **tBu-Phen-Trp** spontaneously cyclized to form 3,6-dihydro-2*H*-1,4-oxazin-2-one **90**. The structure of compound **90** was elucidated using mass spectrometry and comparison of ^{13}C NMR chemical shifts (δ_C) with those reported in the literature for 3,6-dihydro-2*H*-1,4-oxazin-2-one derivative.[152] The attack of the free amino group on the ketone group to form a 6-membered ring posed a limitation for protection of α−aminoacids. Similar observations have been reported for benzoin carbamates.[153] The issue of this intramolecular reaction was overcome by the use of an alternative structure, 3-indolepropionic acid (**Ind**), which possesses the indole chromophore but lacks the amino group. Through this approach, the absorption properties of tryptophan could be preserved whilst cyclization was avoided. The new model compound for HPLC-monitored uncaging, **tBu-Phen-Ind** was prepared from readily available common intermediate **88**, which was treated with 3-indolepropionic acid in the presence of DIPEA. Unfortunately, ester **91** resulting from the bromide

displacement proved insoluble in H_2O even at concentrations lower than 10 μM. Therefore it was hydrolyzed using formic acid to give final model compound **COOH-Phen-Ind**, which was more soluble in water due to the presence of free carboxylic acid**.**

The synthesis of the GABA analogue, **tBu-Phen-GABA**, was carried out according to the same two-step protocol, generating intermediate **92** upon bromide displacement from **88** with Boc-protected GABA followed by the treatment of **92** with formic acid.

5.1.2 Stability studies of model phenacyl esters

Model compounds **COOH-Phen-Ind** and **tBu-Phen-GABA** present building blocks of **BEF-Phen-Ind** and **BEF-Phen-GABA**. The hydrolytic stability of each model compound was studied to enable the identification of design flaws at an early stage.

The stability of all model compounds was screened by HPLC in aqueous media at physiologically relevant pH 7.4, in PBS and $NaHCO_3$-aCSF buffers (Fig. 54). It was found that **COOH-Phen-Ind** was more resistant to hydrolysis in PBS buffer (as was best quantified by the half-life, 18 h) than in $NaHCO_3$-aCSF (8 h, 20 μM concentration of the caged compound). In contrast, the studies revealed that **tBu-Phen-GABA** was too unstable for practical application. Its half-life ranged between 1 h and 2.5 h in $NaHCO_3$-aCSF and PBS respectively (45 μM concentration).

The analysis did not permit a direct comparison between GABA and **Ind** esters. First of all, experiments were carried out at different concentrations. Secondly, the phenacyl units bore different substituents; the deprotonated carboxylic acid in **COOH-Phen-Ind** might decrease the electrophilic nature of the carbonyl group and enhance its hydrolytic stability. Nevertheless, these studies highlighted limitations related to the choice of carboxylic acids: the α-aminoacid could not be protected with a phenacyl unit and the GABA ester proved susceptible to hydrolysis.

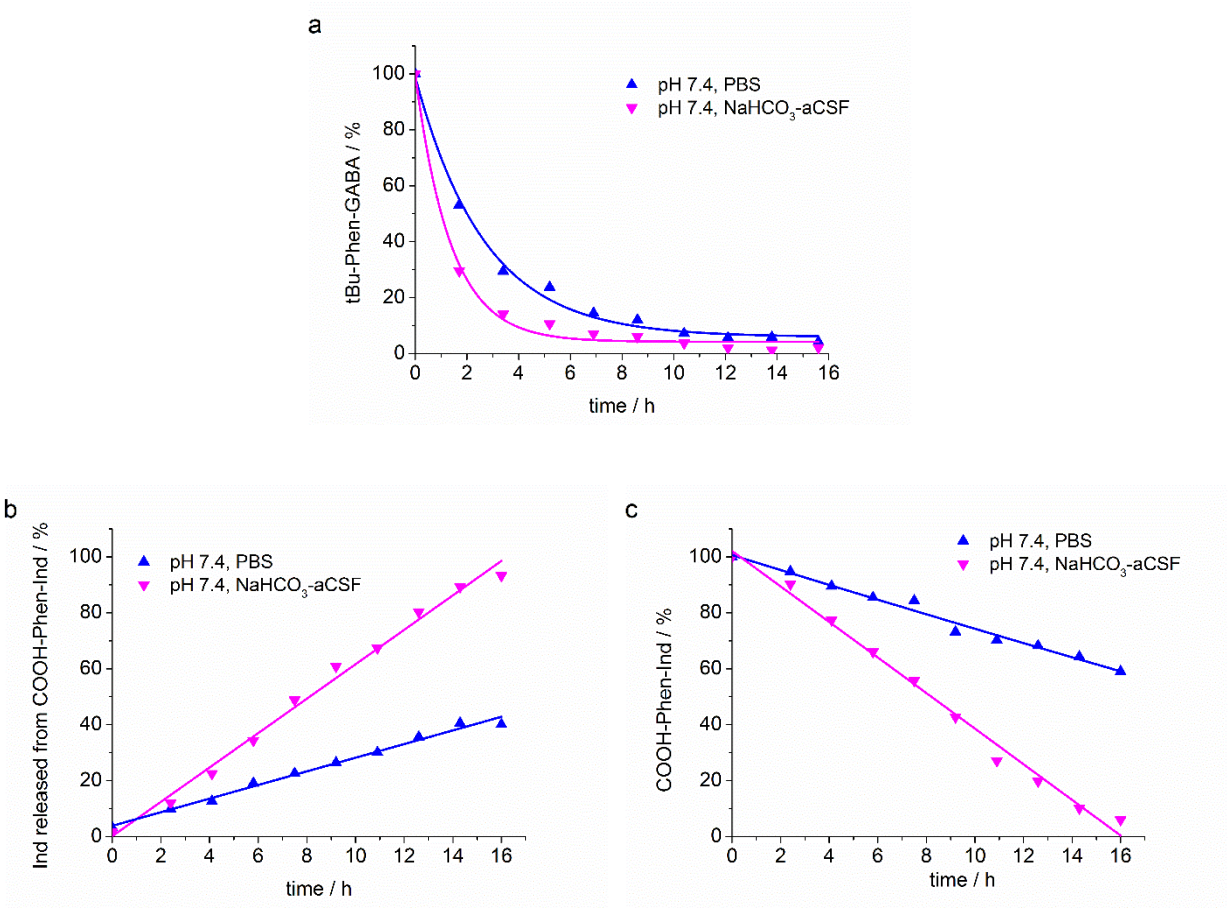

Figure 54. HPLC-monitored stability studies of phenacyl caged compounds **a) tBu-Phen-GABA** (45 µM) and **b-c) COOH-Phen-Ind** (20 µM) in aqueous buffers at pH 7.4: PBS and $NaHCO_3$-aCSF. Depleted amount of **COOH-Phen-Ind** matches amount of released **Ind**, indicating that no other processes than hydrolysis take place under investigated conditions. Experiments were carried out at 20 °C. Data was fitted to mono-exponential decay curve.

To investigate the role of the substituent born by the aromatic ring on the stability of GABA esters, three additional derivatives were prepared: **OH-Phen-GABA**,[119] **OMe-Phen-GABA** and **COOH-Phen-GABA** and their resistance to hydrolysis was compared with that of **tBu-Phen-GABA**.

The synthesis of phenacyl caged GABAs is shown in Scheme 16. In the case of **OMe-Phen-GABA** and **OH-Phen-GABA**, commercially available α-bromoketones were converted to Boc-GABA esters **93** and **94** respectively and the desired products were obtained upon Boc-deprotection under acidic conditions. **COOH-Phen-GABA** was obtained as a result of the prolonged (compared to the synthesis of **tBu-Phen-GABA**, when reaction had to be stopped after 30 min) exposure of **92** to formic acid. Unfortunately, this compound proved soluble only in acetic acid and was of no use in the following experiments.

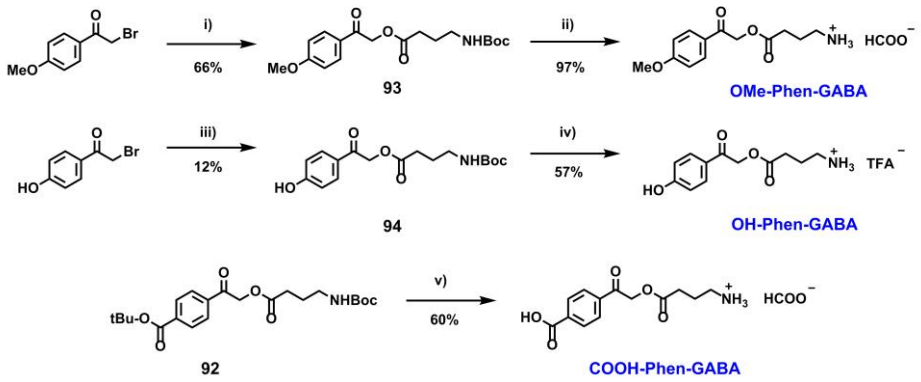

Scheme 16. Synthesis of model phenacyl caged GABA for HPLC-monitored stability studies **OH-Phen-GABA** and **OMe-Phen-GABA**. Reagents and conditions: i) Boc-GABA-OH, DBU, MeCN, 20 °C, 16 h, ii) TFA, 20 °C, 16h, iii) Boc-GABA-OH, DBU, MeCN, 20 °C, 16 h, iv) HCOOH, 20 °C, 3 h, v) HCOOH, 20 °C, 16 h.

The stability of **OH-Phen-GABA** and **OMe-Phen-GABA** at pH 7.4 was studied by HPLC (Fig. 55). The hydrolytic resistance at physiological pH decreased in the order **OH-Phen-GABA** > **OMe-Phen-GABA** > **tBu-Phen-GABA**. These results indicate that the susceptibility of GABA esters to hydrolysis was directly related to electron-donating nature of the substituent born by the aromatic ring. The rate of hydrolysis is the lowest for the analogue bearing the most powerful electron-donating group (hydroxyl, **OH-Phen-GABA**, half-life in $NaHCO_3$-aCSF: 10 h, 75 µM concentration, Fig. 55). In contrast, the derivative with the electron-withdrawing group hydrolyzes rapidly (ester, **tBu-Phen-GABA**, half-life in $NaHCO_3$-aCSF: 1 h, 45 µM concentration, Fig. 54a). It should be noted that all samples decomposed faster in $NaHCO_3$-aCSF than in PBS buffered solutions which indicated that not only pH but as well the components of the buffer influenced the stability of GABA derivatives. A similar observation was already made for **BEF-Pyr-GABA** (Chapter 4, Section 4.1). It was demonstrated that the presence of HCO_3^- ions accelerated hydrolysis of **BEF-Pyr-GABA** and the use of HEPES-aCSF resulted in a longer half-life of the probe. In the case of **OH-Phen-GABA**, the replacement of HCO_3^- with HEPES culminated in nearly complete suppression of hydrolysis (Fig. 55a). In the light of the current experiments it became evident that the HCO_3^- -induced hydrolysis of GABA esters is not specific to pyridinium derivatives but is applicable to GABA esters in general.

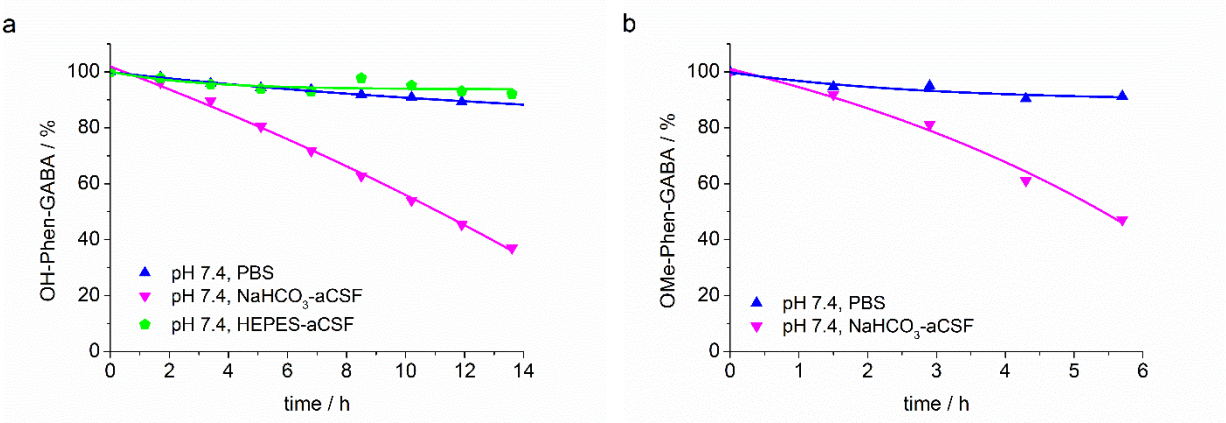

Figure 55. Stability studies of phenacyl caged GABA. **a)** Stability of **OH Phen-GABA** (75 µM) and **b) OMe-Phen-GABA** (22 µM) in aqueous buffers at pH 7.4: PBS, $NaHCO_3$-aCSF and HEPES-aCSF. Progress of the hydrolysis reaction was monitored by HPLC. Experiments were carried out at 20 °C. Data was fitted to mono-exponential decay curve.

The literature provides very few examples of successful caged compounds in which GABA was protected as an ester: **CANBP**, **EANBP**,[65] **pHBP**, **pABP**,[73] **3**, **DEAC450-GABA**[69] (Fig. 56). None of these compounds was evaluated in $NaHCO_3$-aCSF and available data only demonstrate their stability in PBS buffer Nevertheless, **CANBP**, **EANBP**, **DEAC450-GABA** and various analogues of **OH-Phen-GABA**[118,154] were successfully used in uncaging experiments carried out in brain slices in $NaHCO_3$-aCSF solutions (Fig. 56). Therefore, to conclude how the stability of GABA esters in $NaHCO_3$-aCSF varies with the structure of the caging platform, a thorough screen of available compounds should be carried out.

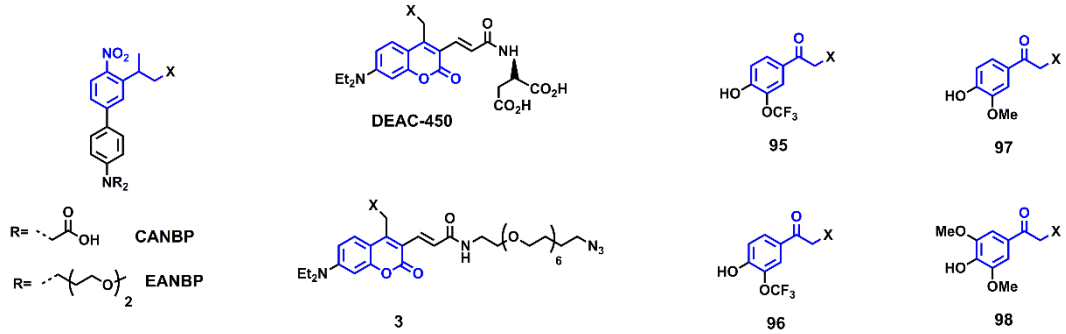

Figure 56. Structures of caged GABA esters used in uncaging experiments in brain slices, in $NaHCO_3$-aCSF. X = $OC(O)CH_2CH_2CH_2NH_2$.

In conclusion, experiments conducted in this section identified 3-indolepropionic acid (**Ind**) as a suitable molecule for further studies on the intramolecular PeT mediated uncaging. For this reason, **Ind** was incorporated into the structure of two-photon sensitive system, as outlined in the Scheme 17.

In contrast, due to the rapid hydrolysis, GABA could not be used with a protecting group in which phenacyl and fluorene are connected through the ester bond. Despite the fact that an ether linker suppressed the rate of GABA release (as demonstrated for **OMe-Phen-GABA**), experiments carried out in Section 2.2.4 showed that PeT from fluorene to methoxy-substituted phenacyl (**Phen-OMe**) were not thermodynamically favored. Nevertheless, the abovementioned results did not take account of the Coulombic term and electrostatic interaction between charged components may result in negative ΔG for the electron transfer. However, due to the fact that ΔG is expected to be only slightly negative, the efficiency of the electron transfer between fluorene and methoxy-substituted phenacyl is expected to be at best as for the ester-linked **BEF-Phen**.

5.2 Intramolecular uncaging experiments

5.2.1 Synthesis of BEF-Phen-Ind

The synthesis of **BEF-Phen-Ind**, a compound designed for intramolecular uncaging experiments, was accomplished according to the route in Scheme 17. The previously used modular approach was pursued, in which readily available **63** (Chapter 2, Section 2.3.1) was brominated to give **99** and subsequently functionalized with 3-indolepropionic acid to furnish **100**. In the last step, the chromophore unit was extended by reacting fluorene derivative **100** with substituted aniline **58** to deliver the desired product. Sonogashira coupling proceeded quantitatively but mechanical losses during the purification step resulted in a low (7%) yield of **BEF-Phen-Ind**.

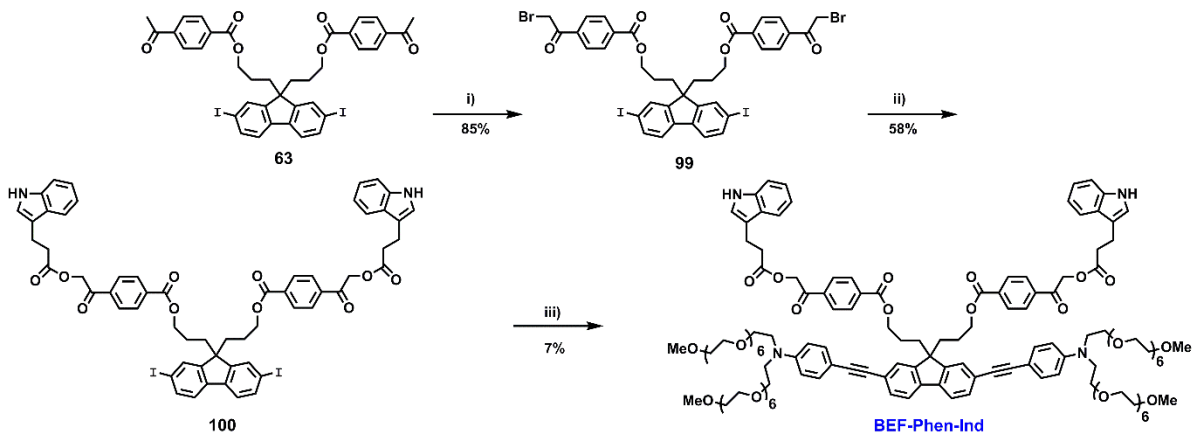

Scheme 17. Synthesis of **BEF-Phen-Ind**. Reagents and conditions: i) Br_2, $CHCl_3$, 0 °C → 20 °C, ii) 3-indolepropionic acid, DBU, THF, 20 °C, 16 h, iii) 58, $Pd(OAc)_2$, PPh_3, CuI, DIPA, DCM, 20 °C, 3 h.[3] Published by The Royal Society of Chemistry.

5.2.2 Spectral properties of BEF-Phen-Ind

Absorption spectra of **BEF-Phen-Ind** and its constituent units **COOH-Phen-Ind** and **Ind** in H_2O are presented in Figure 57. Previous studies revealed that electron-donor and electron-acceptor in covalently linked systems are electronically separated and each unit preserves their individual properties. Therefore the extinction coefficient of **BEF-Phen-Ind** was not determined experimentally but assumed to be the same as for **BEF-tBu**, $\varepsilon_{385} = 9.0 \pm 0.2 \times 10^4$ M^{-1} cm^{-1}. It was expected that large errors would be introduced to the values determined experimentally for an oily compound like **BEF-Phen-Ind** (similarly to **BEF-OH** in Chapter 2, page 42). Figure 57 shows that the spectrum of **BEF-Phen-Ind** is dominated by the two-photon absorbing dye, which is the main component that absorbs at 350 nm. It is noteworthy that the phenacyl unit does absorb in this region as well, but its extinction coefficient is only 2% of that of the fluorene dye. It was anticipated that 3-indolepropionic acid released upon irradiation at 350 nm would result from PeT mediated uncaging if photolysis is conducted at ~10 μM concentration. At higher concentrations of components, absorption by phenacyl unit would result in uncaging regardless of the presence of the fluorene dye (see bimolecular uncaging studies on nitrobenzyl derivatives, Section 3.1.3, page 61).

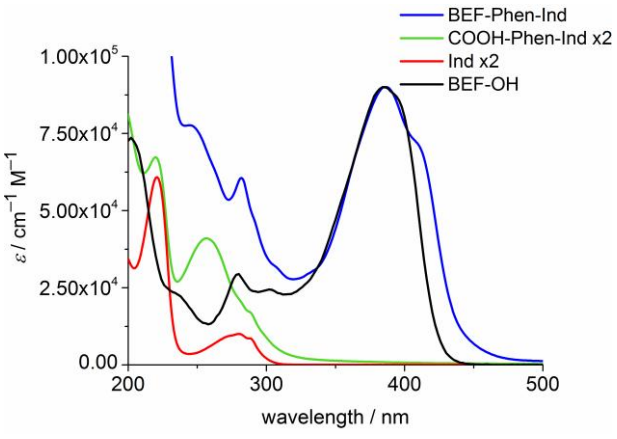

Figure 57. Absorption spectra of **BEF-Phen-Ind** overlaid with spectra of 3-indolepropionic acid (**Ind**, $\varepsilon_{279} = 5.0 \times 10^3$ M^{-1} cm^{-1}) and **COOH-Phen-Ind** ($\varepsilon_{256} = 20.5 \times 10^3$ M^{-1} cm^{-1}) in H_2O. The absorption spectra of **Ind** and **COOH-Phen-Ind** were doubled as each **BEF-Phen-Ind** molecule bears two equivalents of these species. Spectra were recorded at 20 °C.

5.2.3 One-photon photolysis of BEF-Phen-Ind

The uncaging of **BEF-Phen-Ind** (4.5-17 μM concentration in H_2O) was evaluated by irradiation at 300-400 nm (350 nm peak, Rayonet RMR-600) and subsequent HPLC analysis of the photolyzed samples. Initial one-photon photolysis experiments showed that uncaging of **BEF-Phen-Ind** proceeded significantly slower than that of **BEF-Pyr-Trp** (Chapter 4, Section 4.3.2). A solution of **BEF-Phen-Ind** (4.5 μM in H_2O) required 12 min of irradiation, in contrast to **BEF-Pyr-Trp** (~10 μM in H_2O) which was fully consumed in less than 2 min under the same illumination conditions. This discrepancy in the rates of photorelease could be accounted for by differences in Gibbs free energy of electron transfer ΔG_{ET} between the phenacyl and pyridinium systems. Studies of model dyads (Chapter 2, Section 2.3.4) revealed that PeT occurred in the Marcus normal region and the slowest rate of PeT was displayed by phenacyl, the platform with the lowest $\Delta G_{ET.}$ Initial uncaging experiments also showed that **Ind** was liberated with only 20 ± 1% chemical yield (Figure 58). The concentration of indole did not change upon prolonged irradiation (another 8 mins) which confirmed the photostability of the liberated product. These results indicated the presence of a competing reaction that led to the photoinitiated decomposition of **BEF-Phen-Ind**. Similar to the *o*-nitrobenzyl and pyridinium systems, HPLC analysis of photolyzed solutions did not reveal formation of any new peaks. For this reason, ^{1}H NMR was employed to gain information about the fate of the probe. Unfortunately, **BEF-Phen-Ind** (~1 mM concentration) was not soluble in D_2O even when 20% of DMSO-d_6 (v/v) was added. No sign of uncaging was observed even after 5 h of irradiation of the sample in pure DMSO-d_6. The plausible explanation for such photostability could be that either forward electron transfer is thermodynamically unfavorable in DMSO or the rate of the charge recombination is faster than the rate of PeT.

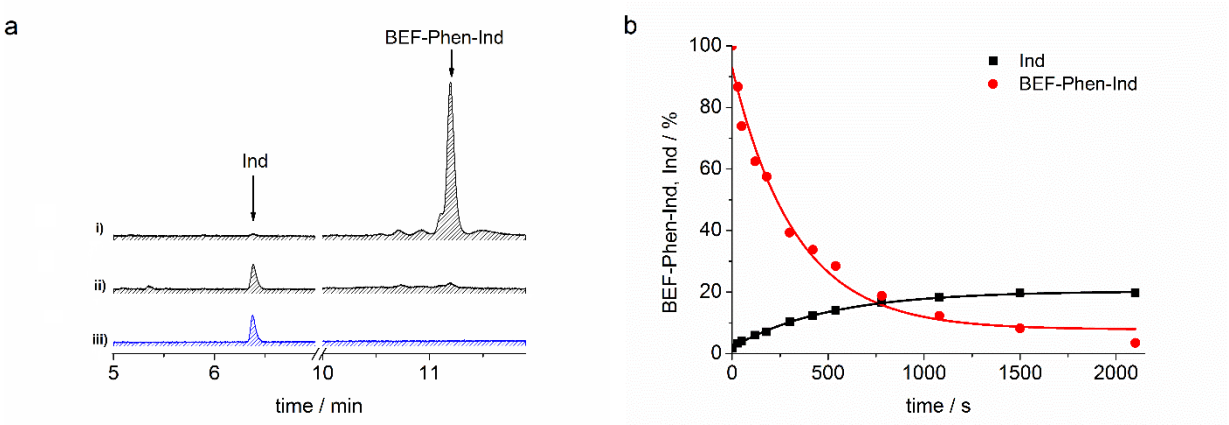

Figure 58. a) HPLC chromatograms (Eclipse XDB column, HPLC method *2*, detection at 220 nm) of **i) BEF-Phen-Ind** (17 μM,H_2O) before photolysis, **ii)** after 2100 s of irradiation at 300-400 nm (350 nm peak); photolysis resulted in 20% yield of uncaging (6.7 μM concentration of **Ind**), **iii)** free **Ind** (6.9 μM, H_2O); **b)** The change in concentration of **Ind** and **BEF-Phen-Ind** upon photolysis at 300-400 nm (350 nm peak) in H_2O; red circles–photolyzed **BEF-Phen-Ind**, black squares–**Ind** released upon uncaging. The concentration of **Ind** and **BEF-Phen-Ind** was determined by HPLC, by detection at 220 nm and 375 nm respectively. Concentration of **Ind** was measured according to the calibration curve prepared for free **Ind** (concentrations 1.4 – 20.7 μM), whereas changes of concentration of **BEF-Phen-Ind** were calculated relative to the integration of their corresponding peaks at t = 0 min. Data was fitted to mono-exponential decay curve. Figure 58b was adapted with permission from ref. 3. Published by The Royal Society of Chemistry.

The one-photon uncaging quantum yield of **BEF-Phen-Ind** was determined using ferric oxalate actinometry.[146,147] The number of photons going into the reaction vessel (emission: 300-400 nm, peak 350 nm) was determined as $1.89 \pm 0.04 \times 10^{16}$ photons s^{-1}. A solution of **BEF-Phen-Ind** (17 μM, H_2O) was irradiated for 2100 s and the progress of the reaction was monitored by HPLC (Fig. 58a). Control samples of **BEF-Phen-Ind** stored in the dark showed that within the experiment time the sample underwent insignificant hydrolysis which was neglected. Changes in the concentration of **BEF-Phen-Ind** and **Ind** during the photolysis are presented in Figure 58b. Upon irradiation, **Ind** was released consistently with 20% chemical yield. Monoexponential curves were fitted to the data which permitted determination of the release rate constant of **Ind**, $k_{REL} = 1.99 \pm 0.08 \times 10^{-3}$ M^{-1} s^{-1}. The uncaging quantum yield was calculated according to Equation 7 (Chapter 4, page 80) to give $\phi_u = 0.0022 \pm 0.0001$. The two-photon uncaging cross-section δ_u was estimated as 2.4 ± 0.1 GM at 700 nm ($\delta_u = \delta_a \times \phi_u$, $\delta_a = 1100$ GM at 700 nm).

5.3 Conclusions and outlook

In this chapter the uncaging properties of a **BEF-Phen** based protecting group have been assessed. Photophysical evaluation was carried out for **BEF-Phen-Ind**, which bore 3-indolepropionic acid as a caged molecule. In comparison with the **BEF-Pyr** derived protecting group described in Chapter 4, **BEF-Phen** displayed a poor performance. The limited scope of substrates that could be caged (due to the reactivity of the ketone group), the low chemical yield of photorelease (20%) and the susceptibility to hydrolysis under physiological conditions made ester linked phenacyl platforms unattractive release units.

Chapter 6

Conclusions and outlook

Caged compounds, which are comprised of physiologically important molecules modified with photolabile protecting groups, provide useful tools for elucidating complex cellular processes. The development of new probes meets the existing need for the extension of the toolbox that is used to utilize the full capacity of the two-photon uncaging. The primary goal of the project described in this thesis was to evaluate the possibility of developing protecting groups in which absorption and release steps are separated and could be optimized independently. Mechanistically, these novel cages were designed to liberate physiologically active compounds *via* PeT following simultaneous absorption of two photons at near-infrared wavelengths.

6.1 Results

The family of caged compounds investigated during this work possessed the same symmetric fluorene-based chromophore with a two-photon absorption cross-section of 1100 GM at 715 nm as an electron-donor and three different release platforms. Electron transfer was energetically favored for the following electron-acceptors: *N*-pyridinium (calculated energy of electron transfer: −0.86 eV), phenacyl (−0.44 eV) and *p*-nitrobenzene (−1.15 eV, Chapter 2). Properties of novel protecting groups were studied with use of their tryptophan and 3-indolepropanoic acid esters: **BEF-Pyr-Trp**, **BEF-Phen-Ind**, **BEF-NB-Trp (**Fig. 56). Tryptophan and 3-indolepropanoic acid were selected as model protected molecules due to their excellent photophysical properties (no absorption beyond 300 nm, preventing energy transfer to the fluorene dye, ε = 5 700 M^{-1} cm^{-1} at 280 nm), allowing the release of acid to be quantified by HPLC. Additionally, *N*-pyridinium group was used to cage neurotransmitter GABA, **BEF-Pyr-GABA**.[109]

The performance of the compounds was evaluated in one-photon irradiation experiments and assessed against a set of key indicators, such as chemical yield of uncaging, quantum yield of uncaging ϕ_u and two-photon uncaging cross-section δ_u (Fig. 59).

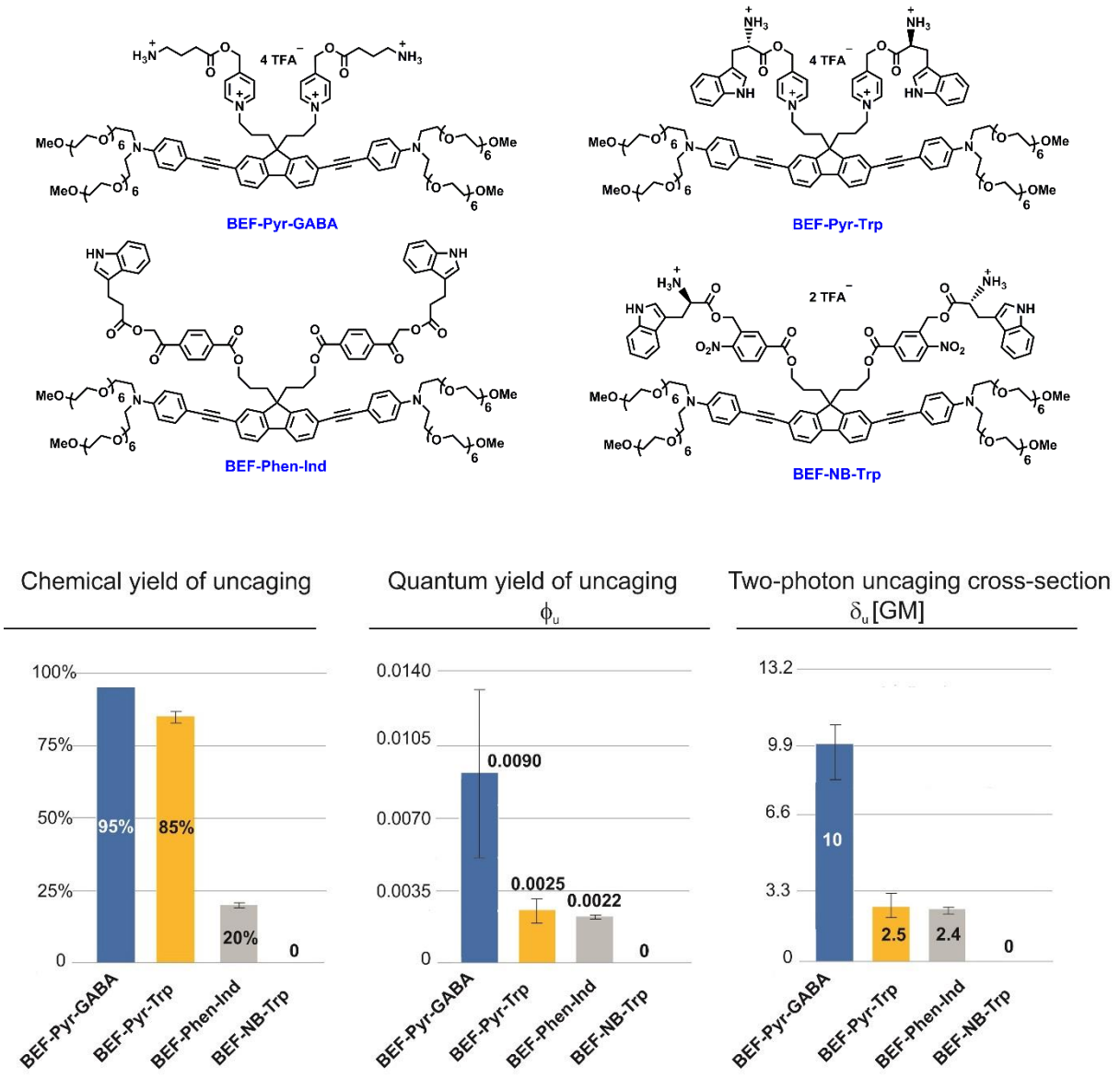

Figure 59. Structures and photophysical properties of a family of protecting groups developed to release caged species upon PeT. Photolysis conditions: **BEF-Pyr-GABA**: 1 mmol, D_2O, 300-400 nm, 350 nm peak; **BEF-Pyr-Trp**: 1.77 µM, sodium citrate/citric acid buffer, pH 3.0, 360 nm; **BEF-Phen-Ind**: 17 µM, H_2O, 300-400 nm, 350 nm peak. Conditions of photolysis (buffered solution, pH, source of light and wavelength) were dictated by the stability of protected compounds, rate of uncaging and method employed to monitor progress of the reaction. The error bars represent standard error.

Considering the abovementioned photophysical parameters, the *N*-pyridinium group displayed the best properties. GABA and tryptophan were liberated from their respective esters with >95% and 83 ± 2% chemical yield. Also, the quantum yield of uncaging was the highest within this series, with

0.009 ± 0.004 for **BEF-Pyr-GABA** and 0.0025 ± 0.0006 for **BEF-Pyr-Trp**. The product of the two-photon absorption cross-section δ_a and quantum yield ϕ_u gave the two-photon uncaging cross-section δ_u ($\delta_u = \delta_a \times \phi_u$) of 10 ± 3 GM at 700 nm for **BEF-Pyr-GABA** and 2.5 ± 0.6 GM at 720 nm for **BEF-Pyr-Trp**. These values are within the order of magnitude required for experiments with cells.[48] One-photon photolysis of phenacyl-protected 3-indolepropionic acid (**BEF-Phen-Ind**) resulted in 20 ± 1% chemical yield and 0.0022 ± 0.0001 quantum yield of uncaging, corresponding to the two-photon uncaging cross-section of 2.4 ± 0.1 GM at 700 nm. The remaining 80% of starting material was consumed in a competitive photo-initiated reaction, the nature of which was not determined. No uncaging was observed upon irradiation of nitrobenzyl protected tryptophan, **BEF-NB-Trp**. Despite exploring a range of photolysis conditions, exposure to light was only deleterious to the starting material and no tryptophan was released.

N-Pyridinium caged GABA not only performed better than other BEF-derived probes but it proved to be second best in comparison with other caged neurotransmitters reported in literature, with respect to the two-photon sensitivity (Fig. 60). Nevertheless, the value of the two-photon uncaging cross-section is only a fraction of the capacity that could be displayed with the currently pursued design strategy. The limiting factor for all BEF-derived protecting groups is the dominating back electron transfer. This deficiency is reflected in the quantum yield of uncaging which for BEF-probes (ϕ_u = 0.0022-0.009) falls short of the average value displayed by other cages (Fig. 60).

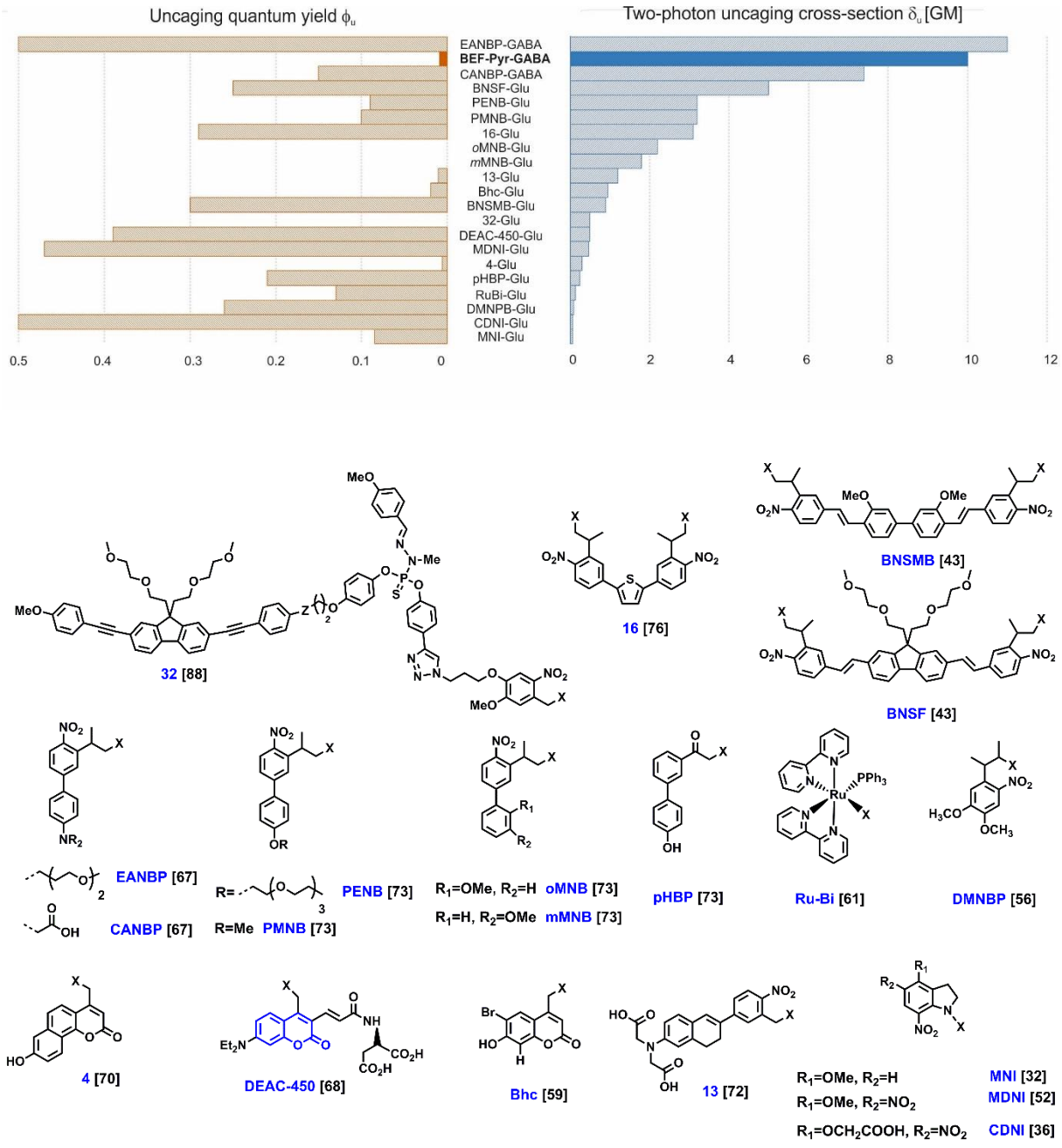

Figure 60. Comparison of **BEF-Pyr-GABA** with caged neurotransmitters reported in the literature. X= GABA or glutamate; uncaging quantum yield of ***o*MNB-Glu**, ***m*MNB-Glu** and **32-Glu** was not determined; values of two-photon uncaging cross section were estimated for: **4-Glu**, **13-Glu** and **DEAC-450**. Numbers in square brackets are literature references.

6.2 Outlook

The advantage of a modular design is that certain deficiencies of the probe can be addressed independently by altering the structures of respective building blocks. All BEF-derived protecting groups suffered from a fast back electron transfer. This obstacle could be overcome by replacing a

flexible linker with a rigid connection so that donor and acceptor units would not be able to come in physical contact.[109] Consequently, uncaging quantum yield and two-photon uncaging cross-section should increase.

The pyridinium derivative proved the most promising candidate for further optimization. The analogues of **BEF-Pyr** group underwent clean photolysis, in contrast to their **BEF-NB** and **BEF-Phen** counterparts, which in addition to uncaging were depleted by light-induced side reactions. Unfortunately, the major drawback of **BEF-Pyr** esters was their hydrolytic instability. A facile way to circumvent this problem could be caging aminoacids as carbamates. The structure of corresponding protected GABA (**BEF-Pyr-CONH-GABA**) is shown in Figure 61. The release of various amines from their respective *N*-picolinium esters has been already demonstrated.[155] The only drawback of this strategy is that decarboxylation of the liberated carbamic acid occurs within a millisecond timescale and its rate depends on pH of the medium.[59,156] In comparison, the kinetics of activation of GABA-ergic receptors vary with their structural composition and concentration of GABA[157,158] but in general, inhibitory post synaptic currents are evoked within 0.5-5 ms and decay within tens to hundreds of milliseconds.[159] It means that release of amines from carbamates might be too slow for application in neuroscience.

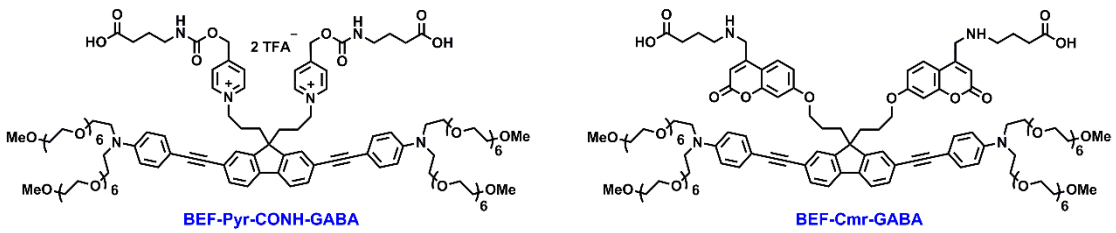

Figure 61. Alternative structures of protecting groups for PeT-mediated release of GABA: **BEF-Pyr-CONH-GABA** and **BEF-Cmr-GABA**.

An alternative is to liberate amines *via* a direct *C*−*N* bond cleavage (**BEF-Cmr-GABA**, Fig. 61). Couraminylmethylamine has been reported to release primary and secondary amines upon *C*−*N* bond scission following intramolecular electron transfer between amine and coumarin units.[160] The reduction potential of 7-methoxycoumarin is −1.62 V vs NHE,[161] (−2.25 V vs Fc)[162], which is of the same order as for the phenacyl ester described in Chapter 5 (E_{RED} of **Phen-COOMe**: −2.18 V vs Fc).

In conclusion, selection of suitable components to construct protecting groups operating *via* PeT is a challenging task. For the successful pair of donor and acceptor not only does the forward electron transfer occur in high yield but charge-separated state is long-lived enough to permit subsequent photochemistry. Importantly, the release unit has to undergo bond cleavage upon one-electron reduction. This criterion narrows the pool of existing caging groups that could be adopted in this design. Therefore, FRET-mediated release might provide more opportunities for sensitized deprotection. It is also desirable that absorption bands of all components are well separated to ensure selective excitation of building units. Lastly, the developed construct must not hydrolyze under physiological conditions.

Despite all the complications, regarding multistep synthesis and strenuous efforts made to find an optimal structure, sensitized uncaging seems to offer access to protecting groups with unprecedentedly high two-photon sensitivity.

Chapter 7

Experimental procedures

7.1 General methods

All solvents and reagents were purchased from commercial suppliers (Fisher or Sigma-Aldrich). Anhydrous THF, DCM and MeCN were obtained by passing solvents through a column of activated alumina. Diisopropylamine (DIPA), triethylamine (Et_3N) and piperidine were distilled from CaH_2. All other reagents were used as supplied by commercial agents. Analytical thin layer chromatography *TLC* was carried out on Merck silica gel 60 F_{254} aluminum supported plates and visualized by absorption of UV light. Flash column chromatography was performed with VWR silica gel 60 applying pressure of N_2. Size exclusion chromatography was carried out with use of Bio-rad Bio-beads S-X1. HPLC separation was conducted on an Agilent 1100 system equipped with a G1315B diode array detector, a G1311A quaternary pump and a G1316A fraction collector. Analytical HPLC was performed with C18 5 μm, 4.6 × 150 mm Eclipse XDB-C18 column (Agilent) and C18 5 μm, 2.1 × 50 mm Zorbax SB-C18 column (Agilent) using 1 mL min^{-1} flow and stepwise gradient at 40 °C. Semi-preparative purification was carried out with use of C8 5 μm, 9.4 × 250 mm Eclipse XDB-C8 column (Agilent) and 3 mL min^{-1} solvent flow. The chromatographic separations were monitored in the range 190–900 nm.

HPLC method 1:

Time [min]	H_2O (0.1% TFA) [v/v, %]	MeCN [v/v, %]
0.00	95	5
9.00	0	100
11.00	0	100

HPLC method 2

Time [min]	H_2O (0.1% TFA) [v/v, %]	MeCN [v/v, %]
0.00	95	5
9.00	0	100
18.00	0	100

HPLC method 3:

Time [min]	H_2O (0.1% TFA) [v/v, %]	MeCN [v/v, %]
0.00	50	50
3.00	20	80
5.00	0	100
10.00	0	100
10.01	50	50
12.00	50	50

HPLC method 4:

Time [min]	H_2O (0.1% TFA) [v/v, %]	MeCN [v/v, %]
0.00	100	0
20.00	0	100

ESI measurements were performed operating in positive or negative mode on a Waters LCT Premier (LRMS) or Bruker μTOF (HRMS) from acetonitrile solutions. MALDI-ToF mass spectrometry was carried out using a Micromass MALDI micro MX spectrometer and following matrices: dithranol (**1,8,9-anthracenetriol)**, DTCB (*trans*-2-[3-(4-*tert*-butylphenyl)-2-methyl-2-propenylidene]malononitrile), CHCA (α-cyano-4-hydroxycinnamic acid). ESI spectra for **BEF-NB-Trp** and **BEF-Pyr-Trp** were measured at the EPSRC National Mass Spectrometry service (Swansea) using the positive nano-electrospray on the LTQ Orbitrap XL.

NMR spectra were acquired at ambient temperature with Bruker instruments DPX200 (200 MHz), DPX250 (250 MHz), DPX400 (400 MHz), AV400 (400 MHz), DRX500 (500 MHz). Chemical shifts for the ^{1}H-NMR and ^{13}C spectra are reported with $CDCl_3$ or DMSO-d_6 as reference. Data are displayed as follows: chemical shift δ (ppm), multiplicity, integration and coupling constants *J* (Hz).

7.2 Synthetic procedures

2,7-Diiodofluorene (49)[163]

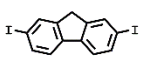

49

This known compound was prepared according to the literature procedure.[163] To a solution of fluorene (2.0 g, 12 mmol) in a mixture of acetic acid (32 mL), conc. H_2SO_4 (1 mL), H_2O (6.5 mL)

was heated to 95 °C. After starting material dissolved the mixture was cooled to 80 °C and iodine (2.1 g, 8.3 mmol) and periodic acid (0.92 g, 4.0 mmol) were added and stirred for 1 h. The precipitate was filtered, washed with saturated aqueous solution of $NaHCO_3$, then H_2O followed by the recrystallization from hexane. 2,7-Diiodofluorene was obtained in 60% yield (3.0 g, 7.23 mmol).

^{1}H NMR (400MHz, $CDCl_3$): δ 3.84 (s, 2H), 7.50 (d, *J*=8.0 Hz, 2H), 7.70 (d, *J*=8.0 Hz, 2H), 7.88 (s, 2H). Data were in agreement with those previously reported.[163]

di-*tert*-Butyl 3,3'-(2,7-diiodo-9*H*-fluorene-9,9-diyl)dipropionate (50)[132]

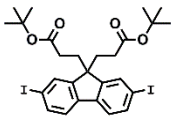

50

This known compound was prepared according to the literature procedure.[132] 2,7-Diiodofluorene (6.0 g, 14.3 mmol) was dissolved in THF (300 mL) and a solution of TBAF (1.0 M in THF, 28.7 mL, 28.7 mmol) was added. After 5 min of stirring, *tert*-butylacrylate (7.5 mL, 52.0 mmol) was added and mixture was stirred for 3 h at room temperature. The solvent was evaporated to dryness and desired compound was isolated using column chromatography. Petroleum ether – DCM in gradient 0-30% of DCM were used as eluents and 7.53 g (11.17 mmol, 77%) of **50** as yellow solid were obtained.

^{1}H NMR (400MHz, $CDCl_3$): δ 1.30 (s, 18H), 1.44 (m, 4H), 2.27 (m, 4H), 7.40 (d, *J*=8 Hz, 2H), 7.66 (m, 4H); ^{13}C NMR (100 MHz, $CDCl_3$): δ 28.0, 29.8, 34.3, 53.9, 80.3, 93.8, 121.7, 132.2, 136.9, 139.7, 149.9, 172.1, *m/z* EI-MS+ 674.0389, $[M]^+$, $C_{27}H_{32}I_2O_4$, requires 674.0390 (100%). Data were in agreement with those previously reported.[132]

di-tert-Butyl 2,2'-((4-iodophenyl)azanediyl)diacetate (51)

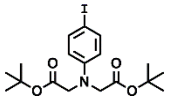

51

This novel compound was prepared according to the literature procedure.[109] 4-Iodoaniline (10.0 g, 45.7 mmol), *tert*-butyl bromoacetate (29.3 mL, 183.0 mmol), sodium carbonate (24.15 g, 228.0 mmol) were suspended in DMF (100 mL) and degassed by nitrogen bubbling for 20 min. Afterwards the mixture was heated to 100 °C for 48 h under nitrogen. The solid was filtered off and discarded. The DMF solution was diluted with water (100 mL) and extracted with DCM (200 mL). The organic phase was washed with water (200 mL), dried over $MgSO_4$ and evaporated to dryness. The product was isolated by column chromatography using petroleum ether–ethyl acetate in gradient 0-1.5% as the eluent to yield in 8.04 g (18.0 mmol, 39%) of **51** as a white solid.

^{1}H NMR (400MHz, $CDCl_3$): δ 1.46 (s, 18H), 3.97 (s, 4H), 6.37 (d, *J*=9 Hz, 2H), 7.46 (d, *J*=9 Hz, 2H); ^{13}C NMR (100MHz, $CDCl_3$): δ 28.0, 54.4, 79.2, 81.8, 114.5, 137.7, 147.7, 169.6; *m/z* ESI-MS+ 470.07, $[M+Na]^+$,$C_{18}H_{26}INNaO_4^+$, requires 407.08 (100%).

di-*tert*-Butyl 2,2'-((4-((trimethylsilyl)ethynyl)phenyl)azanediyl)diacetate (52)

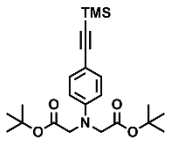

52

This novel compound was prepared according to the modified literature procedure.[164] Compound **51** (2.0 g, 4.5 mmol), $Pd(OAc)_2$ (200 mg, 0.89 mmol), PPh_3 (461 mg, 1.75 mmol) and CuI (190 mg, 0.99 mmol) were placed in a Schlenk flask. The system was flushed with nitrogen and distilled diisopropyl amine (20 mL) was added. The reaction mixture was degassed by two freeze-thaw cycles and trimethylsilylacetylene (1.9 mL, 13.44 mmol) was added. Another freeze-thaw cycle was run and the mixture was stirred at 50 °C overnight. After cooling to room temperature, the reaction mixture was diluted with diethyl ether (20 mL) and washed with water (20 mL), saturated aqueous solution of ammonium chloride (40 mL) and again with water (40 mL). The organic layer was dried over $MgSO_4$ and evaporated to dryness. The product was isolated by column chromatography using hexane-ethyl acetate in gradient 0-15% as the eluents to yield **52** in 1.1 g (2.6 mmol, 57%) of white solid.

^{1}H NMR (500MHz, $CDCl_3$): δ 0.22 (s, 9H), 1.45 (s, 18H), 4.00 (s, 4H), 6.50 (d, *J*=9 Hz, 2H), 7.33 (d, *J*=9 Hz, 2H); ^{13}C NMR (125 MHz, $CDCl_3$): δ 0.1, 28.0, 54.4, 81.7, 91.6, 105.9, 111.7, 111.8, 133.1, 148.0, 169.7; *m/z* ESI-MS+ 857.38, $[2M+Na]^+$, $C_{46}H_{70}N_2NaO_8Si_2^+$, requires 857.46 (100%).

di-*tert*-Butyl 2,2'-((4-ethynylphenyl)azanediyl)diacetate (53)

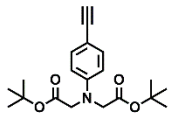

53

This novel compound was prepared by analogy with a reported procedure.[165] A THF solution (5 mL) of compound **52** (1.1 g, 2.6 mmol) was treated with a solution of TBAF (1.0 M in THF, 7.8 mL, 7.8 mmol) and stirred at room temperature for 4 h. The solvent was evaporated to dryness and pure compound was isolated using column chromatography. Hexane-ethyl acetate in gradient 0-7% of ethyl acetate were used as eluent and 0.56 g (1.6 mmol, 63%) of **53** as a white solid were obtained.

^{1}H NMR (400MHz, $CDCl_3$): δ 1.50 (s, 18H), 2.98 (s, 1H), 4.03 (s, 4H), 6.50 (d, *J*=9 Hz, 2H), 7.34 (d, *J*=9 Hz, 2H); ^{13}C NMR (100 MHz, $CDCl_3$): δ 28.0, 54.4, 75.1, 81.9, 84.3, 110.7, 111.8, 133.3, 148.3, 169.7; *m/z* ESI-MS$^+$ 713.30, $[2M+Na]^+$, requires 713.37 (100%).

BEF-tBu[109]

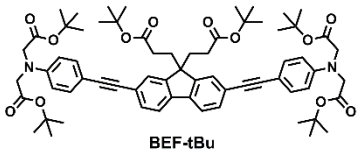

This compound was prepared according to the modified literature procedure.[109] Compound **50** (212 mg, 0.3 mmol) and **53** (250 mg, 0.7 mmol), $Pd(OAc)_2$ (2 mg, 0.009 mmol), PPh_3 (4 mg, 0.015 mmol) and CuI (1.0 mg, 0.005 mmol) were placed in a Schelenk tube and the system was flushed with nitrogen. Distilled DIPA (2 mL) was added and reaction mixture was degassed by three freeze-thaw cycles. Reaction was stirred at room temperature for 1 h. After this time diethyl ether (10 mL) was added and organic phase was washed with water (20 mL), saturated aqueous solution of ammonium chloride (20 mL) and water (20 mL). Organic layer was dried over $MgSO_4$ and evaporated. Product was isolated with use of column chromatography (hexane - ethyl acetate in gradient 10-30% of ethyl acetate). Obtained solid was recrystallised (DCM/ methanol) to give 0.140 g (0.126 mmol, 38%) of **BEF-tBu**.

^{1}H NMR (400 MHz, $CDCl_3$): δ 1.32 (s, 1H), 1.47 (m, 38H), 2.35 (m, 4H), 4.04 (s, 8H), 6.57 (d, *J*=8.3 Hz, 4H), 7.42 (d, *J*=8.3 Hz, 4H), 7.49 (m, 4H), 7.63 (d, 7.7 Hz, 2H); ^{13}C NMR (100 MHz, $CDCl_3$): δ 28.0, 29.8, 34.5, 53.6, 54.4, 80.2, 81.9, 88.3, 91.2, 111.8, 112.1, 120.1, 123.1, 125.7, 131.1, 132.8, 140.1, 148.1, 148.4, 169.7, 172.5. Data were in agreement with those previously reported.[109]

2,5,8,11,14,17-Hexaoxanonadecan-19-yl 4-methylbenzenesulfonate (54)[186]

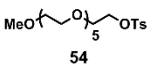

54

This known compound was prepared by analogy with a reported procedure.[166] To a cooled suspension of TsCl (4.1 g, 21.9 mmol) in DCM (5 mL) at 0 °C was added a solution of hexaethylene glycol monomethyl ether (5.0 g, 16.8 mmol) in DCM (5 mL) and Et_3N (4.7 mL, 33.6 mmol), under inert atmosphere. Reaction mixture was allowed to warm to 20 °C and was stirred for 16 h. After this time, it was poured into H_2O (20 mL) and extracted with EtOAc (50 mL), Et_2O (50 mL) and $CHCl_3$ (50 mL). The organic washings were combined, dried over $MgSO_4$ and evaporated to give 7.04 g (15.6 mmol, 93% yield) of compound **54** as a yellow oil.

^{1}H NMR (400 MHz, $CDCl_3$): δ 2.45 (s, 3H), 3.37 (s, 3H), 3.60–3.70 (m, 22H), 4.13–4.17 (m, 2H), 7.34 (d, *J*=8.1 Hz, 2H), 7.79 (d, *J*=8.1 Hz, 2H); ^{13}C NMR (62 MHz, $CDCl_3$): δ 21.7, 59.0, 68.7, 69.7, 70.6–70.7, 72.0, 128.1, 130.2, 133.3, 145.0; *m/z* ESI+ 473.2, $[M+Na]^+$, $C_{20}H_{34}NaO_9S^+$ requires 473.18 (100%). Data were in agreement with those previously reported.[186]

2,2'-((4-Iodophenyl)azanediyl)bis(ethan-1-ol) (55)[187]

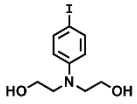

55

This known compound was prepared according to the literature procedure.[134] Iodine (10.4 g, 41.4 mmol) was added to a cooled solution of *N,N'*-phenyldiethanoloamine (2.5 g, 13.8 mmol) in dioxane and pyridine (1:1, 30 mL) at 0 °C. After 1 h of stirring at 0 °C the reaction mixture was allowed to warm to 20 °C and stirred for next 16 h. After this time, a saturated solution of $Na_2S_2O_3$ (15 mL) was added and the mixture was washed with EtOAc (20 mL). The organic phase was dried over $MgSO_4$ and evaporated. The crude product was dissolved in DCM and precipitated with hexane to give 3.47 g (11.3 mmol, 81% yield) of compound **55**.

^{1}H NMR (200 MHz, $CDCl_3$): δ 3.37–3.44 (m, 4H), 3.52–3.58 (m, 4H), 6.55 (d, *J*=9.1 Hz, 2H), 7.39 (d, *J*=9.1 Hz, 2H); ^{13}C NMR (50 MHz, $CDCl_3$): δ 53.7, 58.5, 75.8, 114.3, 137.6, 148.0; *m/z* ESI+ 330.0, $[M+Na]^+$, $C_{10}H_{14}INNaO_2^+$ requires 329.9 (100%). Data were in agreement with those previously reported.[187]

2,2'-((4-((Triisopropylsilyl)ethynyl)phenyl)azanediyl)bis(ethan-1-ol) (56)

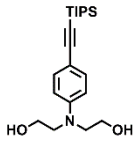

56

This novel compound was synthesized by adapting a reported procedure.[167] Compound **55** (0.80 g, 2.6 mmol), $Pd(OAc)_2$ (116 mg, 0.50 mmol), PPh_3 (270 mg, 1.0 mmol) and CuI (65 mg, 0.30 mmol) were placed in a Schlenk tube and the system was flushed with nitrogen. Distilled DIPA (12 mL) was added and reaction mixture was degassed by two freeze-thaw cycles. Ethynyltriisopropylsilane (1.6 mL, 7 mmol) was added and additional freeze-thaw cycle was run. Reaction was left stirring at 50 °C for 12 h. After this time, the reaction mixture was allowed to cool to 20 °C and EtOAc (20 mL) was added. The organic phase was washed with H_2O (20 mL), saturated solution of NH_4Cl (20 mL) and H_2O (20 mL). Organic layer was dried over $MgSO_4$ and evaporated. The product was isolated by column

chromatography on silica ($CHCl_3$ - MeOH in gradient 0–4% of MeOH) to give 740 mg (2.0 mmol, 78%) of compound **56**.

^{1}H NMR (400 MHz, $CDCl_3$): δ 1.27 (m, 21H), 3.54–3.57 (m, 4H), 3.78–3.82 (m, 4H), 3.99 (bs, 2H), 6.56 (d, *J*=8.5 Hz, 2H), 7.34 (d, *J*=8.5 Hz, 2H); ^{13}C NMR (100 MHz, CDCl3): δ 11.4, 18.7, 55.2, 60.6, 87.8, 107.9, 111.1, 111.9, 133.3, 147.5; *m/z* EI+ 361.24, $[M]^+$, $C_{21}H_{35}NO_2Si^+$ requires 361.24 (100%).

_N,N_-Di-(2,5,8,11,14,17,20-heptaoxadocosan-22-yl)-_N_-(4-((triisopropylsilyl)ethynyl) phenyl)-amine (57)

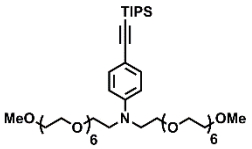

57

This novel compound was prepared by analogy with a reported procedure.[168] Compound **56** (1.25 g, 3.5 mmol) and NaH (0.63 g of 60% dispersion in mineral oil, 15.9 mmol) were suspended in THF (5 mL) and the reaction mixture was refluxed for 1 h under inert atmosphere followed by the addition of 2,5,8,11,14,17-hexaoxanonadecan-19-yl 4-methylbenzenesulfonate (4.70 g, 10.4 mmol) in THF (5 mL). After 48 h of refluxing, the mixture was allowed to cool to 20 °C and H_2O (10 mL) was added. Aqueous phase was extracted with DCM (50 mL); the organic layer was dried over $MgSO_4$ and evaporated. The product was isolated from the reaction mixture by column chromatography on silica (EtOAc – MeOH, in gradient 0–10% of MeOH) to give 1.90 g (2.07 mmol, 60%) of compound **57**.

^{1}H NMR (200 MHz, $CDCl_3$): δ 1.07 (m, 21H), 3.34 (s, 6H), 3.51–3.63 (m, 56H), 6.59 (d, *J*=9.3 Hz, 2H), 7.27 (d, *J*=9.3 Hz, 2H); ^{13}C NMR (100 MHz, $CDCl_3$): δ 11.4, 18.7, 50.9, 59.0, 68.4, 70.5, 70.5–70.6, 70.7, 71.9, 87.3, 108.3, 110.4, 111.3, 133.3, 147.6; *m/z* ESI+ 940.5, $[M+Na]^+$, $C_{47}H_{87}NNaO_{14}Si^+$ requires 940.6 (100%).

_N,N_-Di-(2,5,8,11,14,17,20-heptaoxadocosan-22-yl)-_N_-(4-ethynylphenyl)-amine (58)

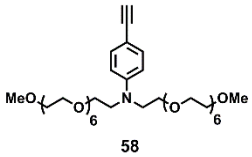

58

This novel compound was prepared by analogy with a reported procedure.[165] To a solution of compound **57** (2.2 g, 2.3 mmol) in THF (2 mL) a solution of TBAF (1.0 M in THF, 11.0 mL, 11.0 mmol) was added and the solution was stirred for 12 h at 20 °C. After this time, the solvent was evaporated and the compound was isolated from the mixture by column chromatography on silica (EtOAc – MeOH, in gradient 0–10% of MeOH) to give 1.5 g (1.9 mmol, 85%) of **58**.

^{1}H NMR (500 MHz, $CDCl_3$): δ 2.90 (s, 1H), 3.25 (s, 6H), 3.42–3.53 (m, 56H), 6.50 (d, *J*=8.0 Hz, 2H), 7.17 (d, *J*=8.0 Hz, 2H); ^{13}C NMR (125 MHz, $CDCl_3$): δ 50.8, 58.8, 68.3, 70.4, 70.4–70.5, 70.6, 71.8, 75.0, 84.6, 108.4, 111.2, 133.2, 147.9; *m/z* ESI+ 784.3, $[M+Na]^+$, $C_{38}H_{67}NNaO_{14}^+$ requires 784.4 (100%)

3,3'-(2,7-diiodo-9*H*-fluorene-9,9-diyl)dipropionic acid (59)[132]

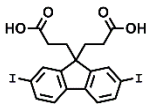

59

This known compound was prepared according to the literature procedure.[132] To a solution of compound **50** (5.0 g, 7.4 mmol) in DCM (100 mL) TFA (2.3 mL, 30.0 mmol) was added. The mixture was stirred for 2 h at room temperature and then a second portion of TFA (5.6 mL, 74 mmol) was added. The reaction was stirred another 2 h. After that solvent was evaporated. 3.8 g, (6.7 mmol, 91%) of desired compound **59** were isolated.

^{1}H NMR (400 MHz, DMSO-d_6): δ 1.30 (m, 4H), 2.30 (m, 4H), 7.68-7.70 (m, 2H), 7.74-7.76 (m, 2H), 7.94-7.96 (m, 2H), ^{13}C NMR (100 MHz, DMSO-d_6): δ 29.2, 33.8, 54.3, 94.7, 122.8, 132.5, 136.9, 139.8, 150.4, 174.1; *m/z* EI-MS+ 561.9135, $[M]^+$, $C_{19}H_{16}I_2O_4^+$, requires 561.9138 (100%). Reported in the literature NMR spectra of 3,3'-(2,7-diiodo-9*H*-fluorene-9,9-diyl)dipropionic acid were recorded in D_2O/NaOH at pD 10. Therefore identity of the compound **59** was confirmed by comparison with NMR spectra recorded for a genuine sample of 3,3'-(2,7-diiodo-9*H*-fluorene-9,9-diyl)dipropionic acid in DMSO-d_6. Spectra of the genuine sample and **59** were in agreement.

3,3'-(2,7-Diiodo-9*H*-fluorene-9,9-diyl)bis(propan-1-ol) (60)

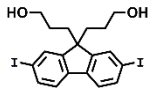

60

This novel compound was prepared by analogy with a reported procedure.[169] A solution of borane-THF complex (1.0 M, 56 mL, 56 mmol) was added slowly to a cooled to 0 °C solution of compound **59** (7.2 g, 12.8 mmol) in anhydrous THF (10 mL). After 2 h of stirring at 20 °C reaction mixture was poured into ice (500 mL) and precipitated solid was removed upon filtration. The solid was dissolved in THF and precipitated with Et_2O to give 6.00 g (11.2 mmol, 87% yield) of compound **60** as a white powder.

^{1}H NMR (400 MHz, DMSO-d_6): δ 0.59–0.65 (m, 4H), 1.96–2.00 (m, 4H), 3.10–3.14 (m, 4H), 7.66 (d, *J*=7.8 Hz, 2H), 7.71 (dd, *J*=1.3 Hz, *J*=7.8 Hz, 2H), 7.83 (d, *J*=1.3 Hz, 2H); ^{13}C NMR (50 MHz,

DMSO-d_6): δ 27.7, 35.7, 55.2, 61.2, 94.4, 122.6, 132.1, 136.3, 139.7, 152.4; *m/z* ESI+ 557.0, $[M+Na]^+$, $C_{19}H_{20}I_2NaO_2^+$ requires 556.9 (100%).

(((2,7-diiodo-9*H*-fluorene-9,9-diyl)bis(propane-3,1-diyl))bis(oxy))bis(*tert*-butyldimethylsilane) (61)

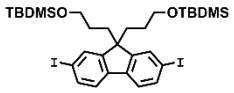

61

This novel compound was prepared by analogy with a reported procedure.[170] To a solution of 3,3'-(2,7-diiodo-9H-fluorene-9,9-diyl)bis(propan-1-ol) (**60**) (100 mg, 0.18 mmol) in DMF (4 mL) TBDMSCl (73 mg, 0.46 mmol) and imidazole (32 mg, 0.47 mmol) were added and the mixture was stirred at room temperature for 3.5 h. After that time, the solvent was evaporated and the product was isolated from the crude reaction mixture by use of column chromatography (PE – DCM; 1:1, v/v) to give 125 mg (0.16 mmol, 88 %) of **61** as a white solid.

^{1}H NMR (400 MHz, $CDCl_3$): δ 0.01 (s, 12H), 0.77–0.81 (m, 4H), 0.85 (s, 18H), 1.99–2.04 (m, 4H), 3.34 (t, *J*=6.3 Hz, 4H), 7.41 (d, *J*=8.4 Hz, 2H), 7.64–7.67 (m, 4H); ^{13}C NMR (100 MHz, $CDCl_3$): δ -5.0, 18.5, 26.0, 27.2, 36.2, 55.2, 62.9, 93.2, 121.7, 132.2, 136.4, 139.7. 152.2; *m/z* ESI+ 763.4, $[M]^+$, $C_{31}H_{49}I_2O_2Si_2^+$ requires 763.1 (100 %).

BEF-OTBDMS

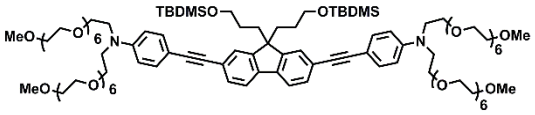

BEF-OTBDMS

This novel compound was synthesized by adapting a reported procedure.[108] To the predried under vacuum CuI (5.0 mg, 0.026 mmol), $Pd(OAc)_2$ (6.0 mg, 0.026 mmol), PPh_3 (13 mg, 0.050 mmol) and (((2,7-diiodo-9H-fluorene-9,9-diyl)bis(propane-3,1-diyl))bis(oxy))bis(*tert*-butyldimethylsilane) (**61**) (50 mg, 65 μmol), distilled DIPA (3.0 mL) was added and two freeze-thaw cycles were carried out. A suspension of acetylene **58** (110 mg, 0.14 mmol) in DIPA (1 mL) was added and additional freeze-thaw cycle was run. After 2 h of stirring at 50 °C reaction was diluted with DCM (50 mL) and crude mixture was washed with H_2O (20 mL) and NH_4Cl (20 mL). Organic layer was dried over $MgSO_4$ and evaporated to dryness. The final compound was isolated from the mixture with use of column chromatography on silica (EtOAc – MeOH, in gradient 0-25 % of MeOH). Compound was purified further by size exclusion chromatography (DCM as eluent) and 30 mg (0.015 mmol, 21 %) of yellow film were obtained.

^{1}H NMR (400 MHz, $CDCl_3$): δ 0.0 (s, 12H), 0.89–0.91 (m, 22H), 2.11–2.15 (m, 4H), 3.40 (t, *J*=6.4 Hz, 4H), 3.44 (s, 12 H), 3.58–3.62 (m, 8H), 3.64-3.74 (m, 104H), 6.74 (d, *J*=8.9 Hz, 4H), 7.44 (d, *J*=8.9 Hz, 4H), 7.50–7.53 (m, 4H), 7.67 (d, *J*=8.4 Hz, 2H); ^{13}C NMR (100 MHz, $CDCl_3$) δ: -5.3, 18.3, 26.0, 27.2, 36.4, 50.8, 54.4, 59.0, 63.2, 68.4, 70.5, 70.5, 70.6-70.7, 71.9, 88.3, 90.8, 110.0, 111.4, 119.7, 122.8, 125.7, 130.5, 132.9, 140.1, 147.6, 150.3; *m/z* MALDI-TOF$^+$ 2052.15, $[M+Na]^+$, $C_{107}H_{180}N_2O_{30}Si_2Na^+$ requires 2053.21 (100 %).

BEF-OH

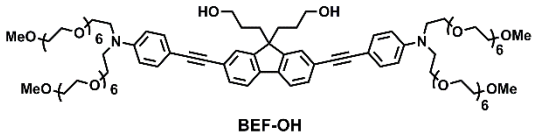

BEF-OH

Procedure 1: **BEF-OTBDMS** (15 mg, 70 μmol) was treated with 1.0 M solution of TBAF in THF (0.2 mL, 0.2 mmol) and stirred at room temperature for 5 h. After this time $CaCl_2$ was added, stirred for 5 minutes and removed by filtration. The solvent was evaporated to dryness and crude reaction mixture was purified by size exclusion chromatography (DCM as eluent). Further purification included isolation by HPLC (HPLC *method 1*). Obtained compound was sonicated in petroleum ether, microfiltered, dissolved in DCM and solvent was evaporated with stream of nitrogen. 1.2 mg (0.7 μmol, 9%) of pure product were obtained.

Procedure 2: This novel compound was synthesized by adapting a reported procedure.[108] The following solids were dried under vacuum: CuI (1 mg, 0.005 mmol), $Pd(OAc)_2$ (1 mg, 0.004 mmol) PPh_3 (2 mg, 0.008 mmol) and compound **60** (50 mg, 0.93 mmol). Distilled DIPA (0.5 mL) was added and two freeze-thaw cycles were carried out. A solution of compound **58** (157 mg, 0.21 mmol) in anhydrous MeCN (0.5 mL) was added and an additional freeze-thaw cycle was run. The progress of the reaction was monitored by HPLC (*method 1*). After 2 h of stirring at 20 °C the reaction mixture was diluted with DCM (50 mL) and the crude mixture was washed with H_2O (20 mL) and saturated aqueous solution of NH_4Cl (20 mL). The organic layer was dried over $MgSO_4$ and evaporated to dryness. The final compound was isolated from the mixture with use of reverse phase column chromatography (in gradient from 100% of H_2O (without TFA!) to 100% MeCN). **BEF-OH** was obtained in 33% yield (55 mg, 0.03 mmol).

^{1}H NMR (400 MHz, $CDCl_3$) δ 0.87–0.94 (m, 4H), 2.09–2.13 (m, 4H), 3.38 (m, 16H), 3.53–3.55 (m, 8H), 3.60–3.67 (m, 104H), 6.70 (d, *J*=8.5 Hz, 4H), 7.39 (d, *J*=8.5 Hz, 4H), 7.47–7.49 (m, 4H), 7.63 (d, *J*=8.2 Hz, 2H); *m/z* MALDI-TOF$^+$ 1825.08 $[M+Na]^+$, $C_{95}H_{152}N_2O_{30}Na^+$ requires 1825.04 (100%).

_N_-methylpryridinium iodide (62)[188]

62

This known compound was prepared using modified reaction conditions reported in the literature.[171] To the solution of pyridine (2.1 mL, 25.3 mmol) in THF (10 mL) methyl iodide (1.7 mL, 27.8 mmol) was added and reaction was stirred at room temperature for 3 h. After this time, solvent was decanted and remaining solid was sonicated with fresh THF (20 mL) and decanted once again. The procedure was repeated two times more and then remaining residues of solvent were evaporated to dryness. 5.26 g (25.0 mmol, 94 % yield) of **62** as a yellow solid was obtained and without further purification used in the next step.

^{1}H NMR (DMSO, 400 MHz), δ 4.36 (s, 3H), 8.11-8.17 (m, 2H), 8.56-8.61 (m, 1H), 8.98 (d, *J*=5.9 Hz, 2H); ^{13}C NMR (DMSO, 200 MHz), δ 48.3, 128.1, 145.4, 145.9. Data were in agreement with those previously reported.[188,189]

_N_-Methylpyridinium hexafluorophosphate (Pyr)[190]

Pyr

This known compound was prepared using modified reaction conditions reported in the literature.[171] Compound **62** (1.08 g, 4.88 mmol) was dissolved in a few drops of H_2O and precipitated with saturated solution of NH_4PF_6 in MeOH. Solvent was decanted and remaining solid was washed with fresh MeOH. Solvent was decanted again and solid was dried under vacuum. 380 mg (1.58 mmol, 33% yield) of **Pyr** as a white solid were obtained. ^{1}H NMR as for **62**. Data were in agreement with those previously reported.[190]

2,7-Diiodo-9*H*-fluorene-9,9-diyl)bis(propane-3,1-diyl) bis(4-acetylbenzoate) (63)

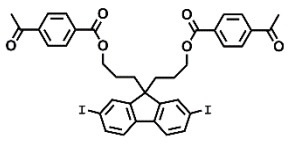

63

This novel compound was prepared using reaction conditions reported in the literature.[104] Compound **60** (300 mg, 0.56 mmol), 4-acetoxybenzoic acid (200 mg, 1.22 mmol), EDC (234 mg, 1.23 mmol) and DMAP (25 mg, 0.20 mmol) were dissolved in anhydrous DCM (5 mL) and stirred for 2 h at 20 °C. The mixture was diluted with H_2O and extracted with DCM (50 mL). The organic extracts were

combined and dried over $MgSO_4$ and evaporated to dryness. The residue was dissolved in $CHCl_3$ and passed through a silica plug with $CHCl_3$ as eluent. Product containing fractions were combined and evaporated in *vacuo*. The product was purified further by redissolving in MeOH and precipitating with Et_2O/hexane (1:1 v/v) to yield **63** as a white solid (54%, 250 mg, 0.30 mmol).

^{1}H NMR ($CDCl_3$, 400 MHz) *δ:* 1.04-1.16 (m, 4H), 2.13-2.17 (m, 4H), 2.65 (s, 6H), 4.07 (t, *J*=6.2 Hz, 4H), 7.47 (d, *J*=8.4 Hz, 2H), 7.72-7.73 (m, 4H), 8.02 (d, *J*=8.7 Hz, 4H), 8.06 (d, *J*=8.7 Hz, 4H); ^{13}C NMR ($CDCl_3$, 1200 MHz) *δ:* 22.1, 25.9, 30.6, 35.3, 53.6, 63.9, 92.5, 120.9, 127.3, 128.8, 130.8, 132.9, 135.9, 138.9, 139.2, 149.7, 164.5, 196.5; *m/z* EI$^+$ 826.0248, [M], $C_{37}H_{32}I_2O_6^+$ requires 826.0289 (100%).

BEF-Phen

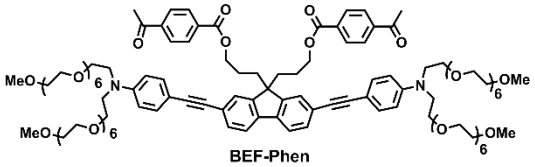

BEF-Phen

This novel compound was prepared using reaction conditions reported in the literature.[108] The following solids were dried under vacuum: CuI (0.9 mg, 0.005 mmol), $Pd(OAc)_2$ (1.1 mg, 0.005 mmol) PPh_3 (2.6 mg, 0.01 mmol) and compound **63** (74 mg, 0.09 mmol). Distilled DIPA (1 mL) was added and two freeze-thaw cycles were carried out. A solution of acetylene **58** (150 mg, 0.20 mmol) in anhydrous MeCN (2 mL) was added and additional freeze-thaw cycle was run. The progress of the reaction was monitored by TLC and HPLC (*method 3*). After 1 h of stirring at 20 °C, additional portion of CuI (0.9 mg, 0.005 mmol), $Pd(OAc)_2$ (1.1 mg, 0.005 mmol) PPh_3 (2.6 mg, 0.01 mmol) and acetylene **58** (50 mg, 0.07 mmol) in anhydrous MeCN (1 mL) were added. Once the reaction was completed the mixture was diluted with DCM (50 mL) followed by washing with H_2O (20 mL) and saturated aqueous solution of NH_4Cl (20 mL). The organic layer was dried over $MgSO_4$ and evaporated to dryness. The residue was redissolved in $CHCl_3$ and passed through the silica column eluting with $CHCl_3$/MeOH (95:5 v/v). The product was purified with use of size exclusion chromatography with $CHCl_3$ as eluent to yield **BEF-Phen** (31 mg, 0.015 mmol, 16 %).

^{1}H NMR ($CDCl_3$, 500 MHz) *δ:* 1.09-1.15 (m, 4H), 2.21-2.24 (m, 4H), 2.44 (s, 6H), 3.38 (s, 12H), 3.54-3.56 (m, 8H), 3.58-3.69 (m, 104H), 4.05-4.07 (m, 4H), 6.68 (d, *J*=8.9 Hz, 4H), 7.37 (d, *J*=8.9 Hz, 4H), 7.54 (m, 4H), 7.69 (d, *J*=8.1 Hz, 2H), 7.94 (d, *J*=8.5 Hz, 4H), 8.04 (d, *J*=8.5 Hz, 4H); ^{13}C NMR ($CDCl_3$, 125 MHz) *δ:* 22.2, 25.7, 35.4, 49.8, 53.3, 58.0, 64.1, 67.3, 69.6-69.7, 70.9, 87.1, 90.4, 108.6, 110.5, 119.2, 122.3, 124.4, 127.2, 128.8, 130.0 132.0, 133.0, 139.2, 146.8 148.2, 164.6, 196.5; *m/z* MALDI-TOF$^+$ 2093.23, [M], $C_{113}H_{164}N_4O_{34}^+$ requires 2094.12 (100%).

(2,7-Diiodo-9*H*-fluorene-9,9-diyl)bis(propane-3,1-diyl) bis(4-nitrobenzoate) (64)

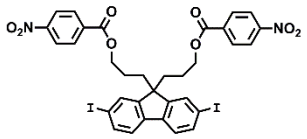

64

This novel compound was prepared using reaction conditions reported in the literature. [104] Compound **60** (178 mg, 0.33 mmol), *p*-nitrobenzoic acid (93 mg, 0.55 mmol), EDC (114 mg, 0.59 mmol) and DMAP (8 mg, 0.07 mmol) were dissolved in anhydrous MeCN and THF (1:1 v/v, 6 mL) and stirred overnight at 20 °C. The mixture was diluted with H_2O and extracted with $CHCl_3$ (50 mL). The organic extracts were combined, dried over $MgSO_4$ and evaporated to dryness. The product was isolated by column chromatography on silica with PE/$CHCl_3$ 4:1 v/v as eluent to give compound **64** as a white solid (21%, 60 mg, 0.072 mmol).

^{1}H NMR ($CDCl_3$, 400 MHz) δ: 1.04-1.11 (m, 4H), 2.14-2.18 (m, 4H), 4.07-4.10 (m, 4H), 7.49 (d, *J*=8.5 Hz, 2H), 7.72-7.64 (m, 4H), 8.13 (d, *J*=8.2 Hz, 4H), 8.30 (d, *J*=8.2 Hz, 4H); ^{13}C NMR ($CDCl_3$, 100 MHz) δ: 23.1, 36.2, 54.6, 65.4, 93.7, 122.0, 123.6, 130.7, 131.8, 131.5, 136.9, 139.9, 150.5, 150.6, 164.5; *m/z* EI$^+$ 831.9778, $[M]^+$, $C_{33}H_{26}I_2N_2O_8$ requires 831.9778 (100%).

BEF-NB

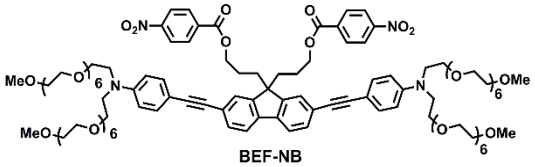

BEF-NB

This novel compound was prepared using modified reaction conditions reported in the literature.[108] The following solids were dried under vacuum: CuI (3.0 mg, 0.016 mmol), $Pd(OAc)_2$ (4.7 mg, 0.021 mmol), PPh_3 (11 mg, 0.042 mmol) and compound **64** (88 mg, 0.10 mmol). Distilled DIPA (1 mL) was added and two freeze-thaw cycles were carried out. A solution of acetylene **58** (160 mg, 0.21 mmol) in anhydrous MeCN (2 mL) was added and additional freeze-thaw cycle was run. The progress of the reaction was monitored by TLC and HPLC (*method 3*). After 1 h of stirring at 20 °C additional portion of CuI (3.0 mg, 0.016 mmol), $Pd(OAc)_2$ (4.7 mg, 0.021 mmol), PPh_3 (11 mg, 0.042 mmol) was added. After 18 h of stirring the reaction mixture was diluted with EtOAc (50 mL) and the crude mixture was washed with H_2O (20 mL) and saturated aqueous solution of NH_4Cl (20 mL). The organic layer was dried over $MgSO_4$ and evaporated to dryness. The residue was dissolved in $CHCl_3$ and passed through the silica column eluting with $CHCl_3$/MeOH (95:5 v/v). The product was purified with use of size exclusion chromatography with $CHCl_3$ as eluent to yield **BEF-NB** (33 mg, 0.016 mmol, 15% yield).

^{1}H NMR ($CDCl_3$, 400 MHz) *δ:* 1.04-1.07 (m, 4H), 2.12-16 (m, 4H), 3.30 (s, 12H), 3.46-3.48 (m, 8H), 3.51-3.62 (m, 104H), 3.97-4.00 (m, 4H), 6.61 (d, *J*=8.8 Hz, 4H), 7.27 (d, *J*=8.8 Hz, 4H), 7.42 (s, 2H), 7.45 (d, *J*=7.8 Hz, 2H), 7.61 (d, *J*=7.8 Hz, 2H), 8.04 (d, *J*=8.0 Hz, 4H), 8.13 (d, *J*=8.0 Hz, 4H); ^{13}C NMR ($CDCl_3$, 100 MHz) *δ:* 23.2, 36.4, 50.8, 54.2, 59.0, 65.5, 68.4, 70.5-70.7, 72.0, 87.9, 91.6, 109.3, 111.5, 120.2, 123.4, 123.5, 125.3, 130.6, 131.0, 132.8, 133.8, 135.5, 140.0, 147.9. 149.0, 150.5, 164.5; *m/z* MALDI-TOF$^+$ 2123.47, $[M+Na]^+$, $C_{109}H_{158}N_4O_{36}Na^+$ requires 2123.06 (100%).

2,7-Diiodo-9*H*-fluorene-9,9-diyl)bis(propane-3,1-diyldimethanesulfonate (65)

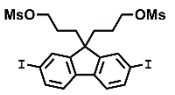

65

This novel compound was prepared using reaction conditions reported in the literature.[172] To a cooled (0 °C) solution of compound **60** (1.00 g, 1.87 mmol) in anhydrous DCM (10 mL), Et_3N (1.6 mL, 11.48 mmol) and methanesulfonyl chloride (580 μL, 7.50 mmol) were added dropwise. After 1 h of stirring at 20 °C the mixture was diluted with H_2O and extracted with $CHCl_3$ (50 mL). The organic extracts were combined, dried over $MgSO_4$ and evaporated to dryness. The product was isolated with use of column chromatography on silica with $CHCl_3$ as eluent to give **65** as a white solid (900 mg, 1.3 mmol, 70% yield).

^{1}H NMR ($CDCl_3$, 400 MHz) *δ* 0.94-1.00 (m, 4H), 2.04-2.09 (m, 4H), 2.89 (s, 6H), 3.89-3.93 (m, 4H), 7.42 (d, *J*=8.5 Hz, 2H), 7.64-7.67 (m, 4H); ^{13}C NMR ($CDCl_3$, 100 MHz) *δ* 23.6, 35.5, 37.4, 54.3, 69.8, 93.8, 122.0, 131.9, 137.0, 139.7, 150.2.

1,1'-((2,7-diiodo-9*H*-fluorene-9,9-diyl)bis(propane-3,1-diyl))bis(pyridin-1-ium) methanesulfonate (66)

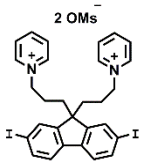

66

This novel ncompound was prepared using reaction conditions reported in the literature.[173] Compound **65** (200 mg, 0.28 mmol) was dissolved in anhydrous pyridine (5 mL) and heated for 15 h at 115 °C. The reaction was allowed to cool to 20 °C and solvent was evaporated to dryness. The residue was dissolved in MeCN and precipitated with THF. Solvent was decanted and precipitation procedure was repeated several times, to yield the product **66** as a fine red powder (120 mg, 0.14 mmol, 50%).

^{1}H NMR (DMSO-d_6, 400 MHz) δ 1.02-1.10 (m, 4H), 1.96-2.02 (m, 4H), 2.32 (s, 6H), 4.35-4.39 (m, 4H), 7.65-7.67 (m, 4H), 7.71 (d, *J*=8.0 Hz, 2H), 8.07-8.10 (m, 4H), 8.56-8.60 (m, 2H), 8.89 (d, *J*=6.0 Hz, 4H); ^{13}C NMR (DMSO-d_6, 100 MHz) *δ:* 26.4, 35.1, 40.7, 54.9, 61.2, 95.4, 123.3, 128.9, 132.5, 137.4, 140.1, 145.5, 146.4, 151.0; *m/z* ESI-MS+ 329.1, $[M]^{2+}$ $C_{29}H_{28}I_2N_2^{2+}$ requires 329.0 (100%).

BEF-Pyr

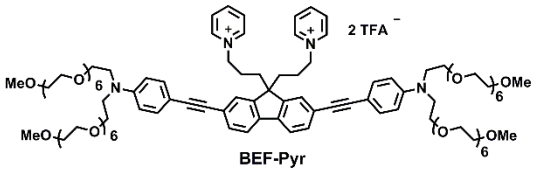

This novel compound was prepared using reaction conditions reported in the literature.[108] The following solids were dried under vacuum: CuI (1.3 mg, 0.007 mmol), $Pd(OAc)_2$ (1.5 mg, 0.007 mmol), PPh_3 (4 mg, 0.015 mmol) and compound **66** (60 mg, 0.07 mmol). Distilled DIPA (2 mL) was added and two freeze-thaw cycles were carried out. A solution of acetylene **58** (120 mg, 0.160 mmol) in anhydrous MeCN (3 mL) was added and additional freeze-thaw cycle was run. The progress of the reaction was monitored by HPLC (*method 1*). After 2 h of stirring at 20 °C the reaction mixture was diluted with $CHCl_3$ (50 mL) and the crude mixture was washed with H_2O (20 mL) and saturated aqueous solution of NH_4Cl (20 mL). The organic layer was dried over $MgSO_4$ and evaporated to dryness. The final compound was isolated from the crude mixture with use of reverse phase column chromatography (in gradient from 100% of H_2O (0.1% TFA v/v) to 100% MeCN). Product containing fractions were extracted with $CHCl_3$, organic washings were combined, dried over $MgSO_4$ and evaporated to dryness. Further purification required use of size exclusion chromatography with $CHCl_3$ as eluent to give **BEF-Pyr** (22 mg, 0.01 mmol, 14 %). The methanesulfonate counterion was replaced by the TFA anion during column chromatography with TFA-buffer.

^{1}H NMR ($CDCl_3$, 500 MHz) *δ:* 1.35-1.47 (m, 4H), 1.98-2.12 (m, 4H), 3.34 (s, 12H), 3.49-3.53 (m, 8H), 3.55-3.69 (m, 104H), 4.46-4.61 (m, 4H), 6.65 (d, *J*=8.5 Hz, 4H), 7.16 (s, 2H), 7.35 (d, *J*=8.5 Hz, 4H), 7.42 (d, *J*=7.8 Hz, 2H), 7.59 (d, *J*=7.8 Hz, 2H), 7.92-8.04 (m, 4H), 8.31-8.39 (m, 2H), 8.97-9.14 (m, 4H); ^{13}C NMR ($CDCl_3$, 125 MHz) *δ:* 26.7, 35.0, 51.2, 53.9, 59.4, 62.1, 68.8, 70.9-71.0, 71.1, 72.3, 88.5, 92.6, 109.8, 120.0, 120.8, 123.9, 125.7, 128.8, 131.6, 133.4, 139.9, 145.4, 145.5, 148.3, 148.8; ^{19}F NMR ($CDCl_3$, 376 MHz) *δ:* -75.4; *m/z* MALDI-TOF$^+$ 1926.49, $[M]^+$, $C_{105}H_{160}N_4O_{28}$ requires 1926.13 (100%).

3-Methyl-4-nitrobenzoic acid methyl ester (71)[191]

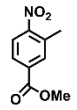

71

This known compound was prepared according to the literature procedure.[174] To 3-methyl-4-nitrobenzoic acid (5.0 g, 28.0 mmol) suspended in MeOH (50 mL) concentrated H_2SO_4 (0.5 mL) was added and reaction was heated at reflux for 24 h, cooled to room temperature and MeOH was removed in *vacuo.* The residue was dissolved in EtOAc (50 mL), washed with saturated $NaHCO_3$ (50 mL), H_2O (50 mL), dried over $MgSO_4$ and solvent was evaporated to dryness. The product **71** was obtained as white solid in 77 % yield (4.20 g, 21.5 mmol).

^{1}H NMR (400 MHz, $CDCl_3$) *δ:* 2.61 (s, 3H), 3.96 (s, 3H), 7.96-7.97 (m, 2H), 8.02 (s, 1H); ^{13}C NMR (100 MHz, $CDCl_3$) *δ:* 20.1, 52.7, 124.5, 128.0, 133.4, 133.7, 134.0, 151.8, 165.3. Data were in agreement with those previously reported.[191]

4-Nitro-3-(propionyloxymethyl) benzoic acid methyl ester (67)

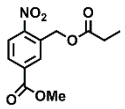

67

This novel compound was prepared by analogy with a reported procedure.[175] Compound **71** (1.4 g, 7.2 mmol) and NBS (1.4 g, 7.9 mmol) were suspended in CCl_4 (50 mL). The reaction mixture was heated to reflux followed by addition of benzoyl peroxide (0.35 g, 1.4 mmol). After 48 h of refluxing reaction was allowed to cool to room temperature, solvent was evaporated to dryness and residue was dissolved in EtOAc (30 mL). Organic phase was washed with 1:1 mixture of $NaHCO_3$ and $Na_2S_2O_3$ (50 mL), H_2O (50 mL), dried over $MgSO_4$ and solvent was evaporated to dryness. Without further purification crude benzyl bromide was dissolved in DMF (5 mL) and K_2CO_3 (1.9 g, 13.8 mmol), NaI (0.21 g, 1.4 mmol) and propionyl acid (1 mL, 13.4 mmol) were added. Reaction was heated at 80ºC for 1 h. After cooling to room temperature solvent was removed in *vacuo*, residue was dissolved in EtOAc (30 mL) and washed with brine (30 mL). Organic phase was dried over $MgSO_4$ and evaporated to dryness. The product was isolated from reaction mixture with use of column chromatography (eluent: hexane - EtOAc in gradient 0-15 % of EtOAc, v/v) to give 0.34 g of **67** as a light yellow solid (1.3 mmol, 18%).

^{1}H NMR (400 MHz, $CDCl_3$) *δ:* 1.21 (t, *J*=7.5 Hz, 3H), 2.47 (q, *J*=7.5 Hz, 2H), 3.99 (s, 3H), 5.52 (s, 2H), 8.12-8.14 (m, 2H), 8.25 (s, 1H); ^{13}C NMR (100 MHz, $CDCl_3$) *δ:* 9.0, 27.4, 52.9, 62.3, 125.1, 129.8, 130.4, 132.5, 134.5, 150.0, 164.9, 173.7.

3-Acetoxymethyl-4-nitrobenzoic acid methyl ester (69)

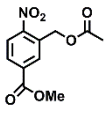

69

This novel compound was prepared using reaction conditions reported in the literature.[175] Compound **71** (2.00 g, 10.2 mmol) and NBS (2.00 g, 11.2 mmol) were suspended in CCl_4 (50 mL). The reaction mixture was heated to reflux followed by addition of benzoyl peroxide (0.50 g, 2.0 mmol). After 48 h of refluxing reaction was allowed to cool to room temperature, solvent was evaporated to dryness and residue was dissolved in EtOAc (30 mL). Organic phase was washed with 1:1 mixture of $NaHCO_3$ and $Na_2S_2O_3$ (50 mL), H_2O (50 mL), dried over $MgSO_4$ and solvent was evaporated to dryness. Without further purification crude benzyl bromide was dissolved in DMF (5 mL) and NaOAc (1.7 g, 20.7 mmol) was added. Reaction was heated at 70ºC for 24 h. After cooling to room temperature solvent was removed in *vacuo*, residue was dissolved in EtOAc (30 mL) and washed with brine (30 mL). Organic phase was dried over $MgSO_4$ and evaporated to dryness. The product was isolated from reaction mixture with use of column chromatography (DCM as eluent) to give 0.6 g (2.37 mmol, 23%) of **69** as a light yellow solid.

^{1}H NMR (400 MHz, $CDCl_3$) *δ:* 2.20 (s, 3H), 4.01 (s, 3H), 5.51 (s, 2H), 8.12-8.15 (m, 2H), 8.26 (s, 1H); ^{13}C NMR (100 MHz, $CDCl_3$) *δ:* 20.7, 52.9, 62.5, 125.1, 129.9, 130.4, 132.3, 134.5, 150.0, 165.0, 170.3.

4-Methoxy-2-nitrobenzaldehyde (73)[176]

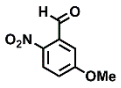

73

This known compound was prepared according to the literature procedure.[176] To a solution of 5-hydroxy-2-nitrobenzaldehyde (0.2 g, 1.2 mmol) in absolute EtOH (3 mL) dimethylsulfate (1.0 mL, 11 mmol) was added. The mixture was cooled to 0 °C and NaOH (0.24 g, 6 mmol) in H_2O (1 mL) was added dropwise. Reaction mixture was stirred at 50 °C for 2 days. After cooling down to room temperature, H_2O (10 mL) was added and reaction mixture was extracted 3 times with DCM (20 mL). The organic washings were combined, dried over $MgSO_4$ and evaporated to give yellow oil. The

product was purified by column chromatography (hexane - EtOAc in gradient 0-10 % of EtOAc) and 0.1 g (0.55 mmol, 46 %) of **73** as a yellow solid were obtained.

^{1}H NMR (400 MHz, $CDCl_3$) *δ:* 3.95 (s, 3H), 7.15 (dd, *J*=2.8 Hz, *J*=9.0 Hz, 1H), 7.30 (d, *J*=2.8 Hz, 1H), 8.15 (d, *J*=9.0 Hz, 1H), 10.48 (s, 1H); ^{13}C NMR (100 MHz, $CDCl_3$) *δ:* 56.3, 113.3, 118.6, 127.3, 134.3, 142.3, 164.0, 188.5. Data were in agreement with those previously reported.[176,192]

(4-Methoxy-2-nitrophenyl)methanol (74)[193]

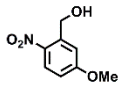

74

This known compound was prepared using modified reaction conditions reported in the literature.[177] To a cooled to 0 °C solution of compound **73** (100 mg, 0.55 mmol) in MeOH (1 mL) $NaBH_4$ (40 mg, 1.05 mmol) was added and reaction mixture was stirred for 1 h at room temperature. After this time solvent was evaporated and residue dissolved in H_2O. Solution was acidified to pH 4 with 2.0M HCl and extracted with EtOAc. Organic phase was dried over $MgSO_4$ and evaporated to give 70 mg (0.38 mmol, 70 % yield) of **74** which without further purification was used in the next step.

^{1}H NMR (400 MHz, $CDCl_3$) *δ:* 3.92 (s, 3H), 5.01 (s, 2H), 6.89 (dd, *J*=2.7 Hz, *J*=9.1 Hz, 1H), 7.22 (d, *J*=2.7 Hz, 1H), 8.18 (d, *J*=9.1 Hz, 1H). Data were in agreement with those previously reported.[193]

4-Methoxy-2-nitrobenzyl propionate (68)

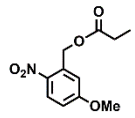

68

This novel compound was prepared by analogy with a reported procedure.[178] To a solution of compound **74** (0.2 g, 1.1 mmol) in DCM (2 mL) Et_3N (0.4 mL, 2.9 mmol) and propionyl chloride (0.16 mL, 1.8 mmol) were added and reaction was stirred for 1 h at room temperature. The mixture was diluted with DCM (10 mL) and organic phase was washed with H_2O (10 mL), dried over $MgSO_4$ and evaporated to dryness. Desired product was isolated with use of column chromatography (eluent: hexane- ethyl acetate in gradient 5-10 % of EtOAc) followed by precipitation (DCM/ PE) to give 77 mg (0.32 mmol, 30 %) of **68** as a white solid.

^{1}H NMR (400 MHz, $CDCl_3$) *δ:* 1.22 (t, *J*=7.5 Hz, 3H), 2.49 (q, *J*=7.5 Hz, 2H), 3.92 (s, 3H), 5.56 (s, 2H), 6.91 (dd, *J*=2.6 Hz, *J*=9.3 Hz, 1H), 7.05 (d, *J*=2.6 Hz, 1H), 8.22 (d, *J*=9.3 Hz, 1H); ^{13}C NMR (200 MHz, $CDCl_3$) *δ:* 9.1, 27.5, 55.9, 63.0, 112.4, 113.9, 128.0, 135.7, 140.2, 163.8, 173.6.

4-Methoxy-2-nitrobenzyl acetate (70)

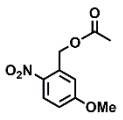

70

This novel compound was prepared by analogy with a reported procedure.[178] To a solution of compound **68** (60 mg, 0.32 mmol) in THF (2 mL), acetyl chloride (0.03 mL, 0.42 mmol), DMAP (5 mg, 0.04 mmol) and Et_3N (0.1 mL, 0.6 mmol) were added and reaction was stirred at 20 °C for 16 h. The solvent was evaporated to dryness and product was isolated from the reaction mixture by column chromatography (hexane - EtOAc in gradient 0-20 % of EtOAc, v/v) to give 50 mg (0.22 mmol, 68%) of **70** as a white solid.

^{1}H NMR (400MHz, $CDCl_3$) *δ:* 2.19 (s, 3H), 3.91 (s, 3H), 5.53 (s, 2H), 6.90 (dd, *J*=2.6 Hz, *J*=9.1 Hz, 1H), 7.04 (d, *J*=2.6 Hz, 1H), 8.20 (d, *J*=9.1 Hz, 1H); ^{13}C NMR (200MHz, $CDCl_3$) *δ:* 20.8, 55.9, 63.2, 112.4, 114.0, 128.1, 135.5, 140.2, 163.8, 170.2.

3-Formyl-4-nitrobenzoic acid (75)[194]

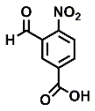

75

This known compound was synthesized by adapting a reported procedure.[49] To a suspension of methy-3-formyl-nitrobenzoate (0.70 g, 3.35 mmol) in H_2O (5 mL) conc. H_2SO_4 (0.5 mL) was added and the reaction mixture was stirred at 100 °C for 24 h. After this time reaction was allowed to cool, the precipitate was filtered, washed thoroughly with H_2O and dried. Compound **75** was obtained as a white powder in 61% yield (0.40 g, 2.0 mmol).

^{1}H NMR (250 MHz, DMSO-d_6) *δ:* 8.24 (d, *J*=8.1 Hz, 1H), 8.37–8.40 (m, 2H), 10.25 (s, 1H); ^{13}C NMR (62 MHz, DMSO-d_6) *δ:* 125.8, 131.1, 131.6, 135.6, 136.2, 152.0, 166.0, 190.1. Data were in agreement with those previously reported.[194]

Methyl 3-(hydroxymethyl)-4-nitrobenzoate (76)[195]

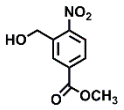

76

This compound was prepared using modified reaction conditions reported in the literature.[177] To the cooled to 0 ºC solution of methyl 3-formyl-4-nitrobenzoate (200 mg, 0.95 mmol) in MeOH (2 mL) $NaBH_4$ (35 mg, 0.93 mmol) was added and reaction was stirred for 1 h at 20 °C. After this time solvent was evaporated and water was added. Solution was acidified to pH 4 and extracted with EtOAc. Organic phase was dried over $MgSO_4$ and evaporated to give 180 mg (0.85 mmol, 9% yield) of **76** which without further purification was used in the next step.

^{1}H NMR (400 MHz, $CDCl_3$) *δ:* 3.98 (s, 3H), 5.03 (s, 2H), 8.08-8.13 (m, 2H), 8.44 (s, 1H); ^{13}C NMR (100 MHz, $CDCl_3$) *δ:* 52.8, 61.6, 124.8, 129.2, 130.4, 134.5, 137.4, 149.6, 165.3. No literature spectroscopy data was available for comparison.

Methyl 4-nitro-3-((tryptophyloxy)methyl)benzoate (NB-Trp)

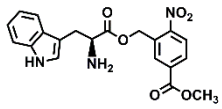

NB-Trp

This novel compound was prepared by analogy with a reported procedure.[104,179] To a solution of **76** (100 mg, 0.47 mmol) in DCM (5 mL) N_α-Fmoc-L-tryptophan (187 mg, 0.44 mmol), EDC (84 mg, 0.44 mmol) and DMAP (5 mg, 0.04 mmol) were added and reaction was stirred at room temperature. After 2 h the mixture was diluted with DCM (20 mL) and washed with H_2O (50 mL). Organic layer was dried over $MgSO_4$ and solvent was removed in *vacuuo.* The residue was dissolved in $CHCl_3$, passed through a silica plug and collected organic phase was evaporated to dryness. The crude product was dissolved in anhydrous MeCN (2 mL) and piperidine (420 μL, 4.25 mmol) was added. After 1 h of stirring at room temperature solvent was evaporated and compound purified by column chromatography (eluent: $CHCl_3$ – MeOH, 99:1, v/v) to give 80 mg of **NB-Trp** as a yellow powder (0.20 mmol, 42 %).

^{1}H NMR (400 MHz, $CDCl_3$) *δ:* 1.73 (bs, 2H), 3.09 (dd, *J*=7.7 Hz, *J*=14.3 Hz, 1H), 3.31 (dd, *J*=5.5 Hz, *J*=14.3 Hz, 1H), 3.92-3.97 (m, 4H), 5.43-5.52 (m, 2H),7.00-7.02 (m, 1H), 7.06-7.09 (m, 1H), 7.12-7.16 (m, 1H), 7.28 (d, *J*=8.3 Hz, 1H), 7.58 (d, J=7.7 Hz, 1H), 8.05-8.11 (m, 2H), 8.15 (s, 1H), 8.53 (bs, 1H); ^{13}C NMR (100 MHz, $CDCl_3$) *δ:* 30.9, 53.0, 55.2, 62.9, 110.7, 111.3, 118.5, 119.4, 122.1, 123.1, 125.1, 127.3, 130.0, 130.6, 131.8, 134.5, 136.2, 150.0, 164.9, 174.8; m/z ESI+ 398.2, $[M+H]^+$, $C_{20}H_{20}N_3O_6^+$ requires 398.1; 420.1, $[M+Na]^+$, $C_{20}H_{19}N_3NaO_6^+$ requires 420.1 (100 %).

(2,7-Diiodo-9*H*-fluorene-9,9-diyl)bis(propane-3,1-diyl) bis(3-formyl-4-nitrobenzoate) (77)

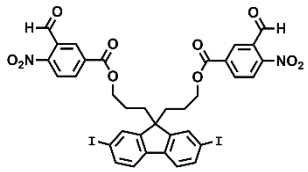

77

This novel compound was synthesized by adapting a reported procedure.[104] Compound **60** (200 mg, 0.37 mmol), **74** (160 mg, 0.82 mmol), EDC (156 mg, 0.81 mmol) and DMAP (9 mg, 0.07 mmol) were dissolved in anhydrous DCM (5 mL) and stirred for 2 h at 20 °C. The mixture was diluted with water and extracted with DCM (50 mL). The organic extracts were combined and dried over $MgSO_4$ and evaporated to dryness. The residue was dissolved in $CHCl_3$ and passed through a silica plug with $CHCl_3$ as eluent. The product containing fractions were combined and evaporated *in vacuo*. The product was further purified by dissolving in DCM and precipitating with PE to give compound **77** as a white solid in 75% yield (250 mg, 0.28 mmol).

^{1}H NMR (500 MHz, $CDCl_3$) *δ:* 1.10–1.16 (m, 4H), 2.18–2.20 (m, 4H), 4.15 (t, *J*=6.23 Hz, 4H), 7.52 (d, *J*=7.8 Hz, 2H), 7.73–7.77 (m, 4H), 8.21 (d, *J*=8.6 Hz, 2H), 8.36 (dd, *J*=1.6 Hz, *J*=8.6 Hz, 2H), 8.53 (d, *J*=1.6 Hz, 2H), 10.44 (s, 2H); ^{13}C NMR (125 MHz, $CDCl_3$) *δ:* 23.1, 36.1, 54.7, 65.9, 93.8, 122.2, 124.9, 131.0, 131.2, 131.8, 134.6, 135.2, 137.0, 140.0, 150.5, 151.7, 163.5, 187.1; *m/z* EI-MS+ 887.84, $[M]^+$, $C_{35}H_{26}I_2N_2O_{10}^+$ requires 887.96 (100%).

(2,7-Diiodo-9*H*-fluorene-9,9-diyl)bis(propane-3,1-diyl) bis(3-(hydroxymethyl)-4-nitrobenzoate) (78)

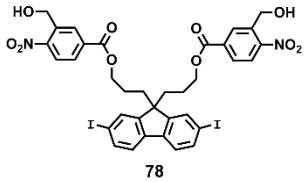

78

This novel compound was synthesized by adapting a reported procedure.[177] $NaBH_4$ (20 mg, 0.53 mmol) was added to a cooled solution of compound **77** (250 mg, 0.28 mmol) in MeOH (3 mL) at 0 °C, and reaction mixture was stirred at 20 °C. After 15 min DCM (3 mL) was added to keep the material in solution. After an additional 1 h of stirring, DCM was evaporated and reaction was poured into the beaker with ice (250 mL). Ice was allowed to melt and aqueous phase was extracted with EtOAc (50 mL) and $CHCl_3$ (50 mL). Organic extracts were combined, dried over $MgSO_4$ and evaporated to dryness. The residue was dissolved in DCM and precipitated with hexane to give 190 mg of compound **78** as a white foam (0.21 mmol, 76% yield).

^{1}H NMR (400 MHz, $CDCl_3$) *δ:* 1.02–1.12 (m, 4H), 2.14–2.19 (m, 4H), 4.08 (m, 4H), 5.03 (s, 4H), 7.47 (d, *J*=7.9 Hz, 2H), 7.69–7.72 (m, 4H), 8.00 (d, *J*=8.7 Hz, 2H), 8.11 (d, *J*=8.7 Hz, 2H), 8.37 (s, 2H); ^{13}C NMR (100 MHz, $CDCl_3$) *δ:* 23.2, 36.3, 54.6, 61.9, 65.4, 93.7, 122.0, 125.1, 129.4, 130.6, 131.8, 134.7, 136.9, 137.2, 139.9, 149.7, 150.7, 164.6; *m/z* EI-MS+ 891.87, $[M]^+$, $C_{35}H_{30}I_2N_2O_{10}^+$ requires 891.99 (100%).

(2,7-Diiodo-9*H*-fluorene-9,9-diyl)bis(propane-3,1-diyl)bis(((((methoxy)carbonyl)Fmoc-tryptophyl)oxy)methyl)-4-nitrobenzoate (79)

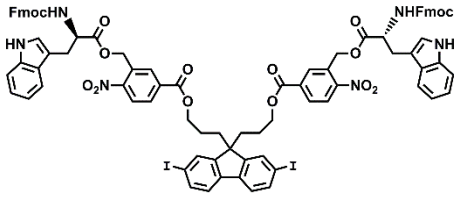

79

This novel compound was synthesized by adapting a reported procedure.[104] Compound **78** (100 mg, 0.11 mmol), N_α-Fmoc-L-tryptophan (95 mg, 0.22 mmo), DMAP (3 mg, 0.03 mmol) and EDC (42 mg, 0.22 mmol) were dissolved in DCM (3 mL) and stirred at 20 °C. After 2 days the reaction mixture was diluted with DCM (30 mL) and was washed with water (50 mL). Organic layer was dried over $MgSO_4$ and evaporated to dryness. Product was isolated with use of column chromatography on silica (eluent $CHCl_3$ – MeOH, in gradient 0–2% MeOH) to give 150 mg (0.09 mmol, 80% yield) of compound **79**.

^{1}H NMR (400 MHz, $CDCl_3$) *δ:* 0.87–0.94 (m, 4H), 1.92–1.96 (m, 4H), 3.85–3.92 (m, 4H), 3.85–3.92 (m, 4H), 4.05–4.09 (m, 2H), 4.23–4.31 (m, 4H), 4.69–4.74 (m, 2H), 5.30–5.36 (m, 6H), 6.86 (s,2H), 6.95–6.99 (m, 2H), 7.02–7.05 (m, 2H), 7.12–7.19 (m, 6H), 7.24–7.31(m, 6H), 7.39–7.47 (m, 6H), 7.57–7.58 (m, 4H), 7.63 (d, *J*=7.4 Hz, 4H), 7.87 (d, *J*=8.4 Hz, 2H), 7.91–7.98 (m, 4H), 8.07 (s, 2H); ^{13}C NMR (100 MHz, $CDCl_3$) *δ:* 23.1, 28.0, 36.1, 47.1, 54.5, 54.9, 63.4, 65.4, 67.1, 93.6, 109.6, 111.3, 118.4, 119.8, 119.9, 122.0, 122.4, 123.0, 125.2, 127.1, 127.5, 127.7, 130.0, 130.9, 131.3, 131.8, 134.5, 136.0, 136.9, 139.8, 141.3, 143.7, 143.9, 150.0, 150.6, 155.8, 164.1, 171.6.

BEF-NB(Fmoc)Trp (80)

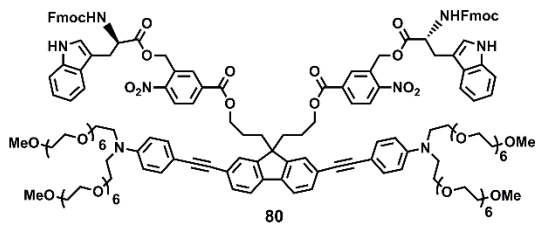

80

This novel compound was synthesized by adapting a reported procedure.[108] To the vacuum-dried CuI (0.5 mg, 0.003 mmol), $Pd(OAc)_2$ (0.6 mg, 0.003 mmol), PPh_3 (1.5 mg, 0.006 mmol), compound **79**

(100 mg, 0.058 mmol) and distilled DIPA (1.5 mL) was added and two freeze-thaw cycles were carried out. A solution of compound **58** (100 mg, 0.13 mmol) in anhydrous DCM (1 mL) was added and additional freeze-thaw cycle was run. The progress of the reaction was monitored by HPLC (*HPLC Method 4*). After 1 h of stirring at 20 °C the reaction mixture was diluted with DCM (50 mL) and crude mixture was washed with H_2O (20 mL) and NH_4Cl (20 mL). Organic layer was dried over $MgSO_4$ and evaporated to dryness. The major impurities were removed from the crude reaction mixture with use of the reverse phase column chromatography (in gradient from 100% of H_2O (0.1% TFA v/v) to 100% MeCN). Product containing fractions were combined and evaporated to dryness. **BEF-NB-(Fmoc)Trp (80)** was obtained a yellow film (50 mg, 0.017 mmol, 32% yield)

^{1}H NMR (400 MHz, DMSO-d_6) δ: 0.88–0.95 (m, 4H), 2.11–2.20 (m, 4H), 3.17–3.24 (m, 16H), 3.39–3.42 (m, 8H), 3.47–3.58 (m, 104H), 3.87–3.91 (m, 4H), 4.10–4.16 (m, 4H), 4.21–4.26 (m, 2H), 4.34–4.38 (m, 2H), 5.37 (s, 4H), 6.69 (d, *J*=8.8 Hz, 4H), 6.92–6.95 (m, 2H), 7.00–7.05 (m, 2H), 7.15 (s, 2H), 7.19–7.30 (m, 10H), 7.34–7.38 (m, 4H), 7.45 (d, *J*=8.3 Hz, 2H), 7.50 (d, *J*=7.9 Hz, 2H), 7.56–7.62 (m, 6H), 7.80–7.83 (m, 6H), 7.91 (d, *J*=7.9 Hz, 2H), 7.98 (d, *J*=8.3 Hz, 2H), 8.05–8.09 (m, 4H), 10.81 (s, 2H); *m/z* ESI MS+ 1489.70663, $[M+2H]^{2+}$, $C_{163}H_{204}N_8O_{44}^{2+}$ requires 1489.19970 (100%).

BEF-NB-Trp

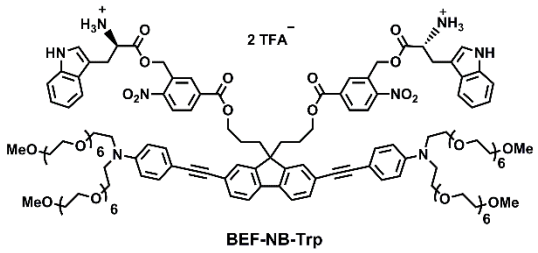

This novel compound was synthesized by adapting a reported procedure.[179] To the solution of **BEF-NB-(Fmoc)Trp (80)** (10 mg, 0.0033 mmol) in MeCN (0.25 mL) piperidine (30 μL, 0.35 mmol) was added and reaction was stirred at 20 °C for 2 h. After this time solvent was blew down by the stream of nitrogen and product was isolated from the crude reaction mixture by semi-preparative HPLC in TFA-buffered solvent system (*HPLC Method 4*). Product containing fractions were combined and freeze-dried to give **BEF-NB-Trp** in 10% yield (0.92 mg, 0.0003 mM).

^{1}H NMR (500 MHz, DMSO-d_6) δ: 0.93–1.00 (m, 4H), 2.20–2.28 (m, 4H), 3.19–3.26 (m, 16H), 3.47–3.58 (m, 112H), 3.99–4.05 (m, 4H), 4.31–4.37 (m, 2H), 5. 39 (d, *J*=13.9 Hz, 2H), 5.46 (d, *J*=13.9 Hz, 2H), 6.71 (d, *J*=8.4 Hz, 4H), 6.91–6.94 (m, 2H), 7.01–7.04 (m, 2H), 7.15 (m, 2H), 7.27–7.30 (m, 4H), 7.42 (d, *J*=7.7 Hz, 2H), 7.48 (d, *J*=8.1 Hz, 2H), 7.66 (s, 2H), 7.85 (d, *J*=7.7 Hz, 2H), 8.05–8.09 (m, 4H), 8.13 (m, 2H), 8.36 (bs, 6H), 10.97 (s, 2H); ; *m/z* ESI-MS+ 1267.1304, $[M]^{2+}$, $C_{133}H_{184}N_8O_{40}^{2+}$ requires 1267.1314 (100%).

Pyridin-4-ylmethyl 4-((*tert*-butoxycarbonyl)amino)butanoate (81)[109]

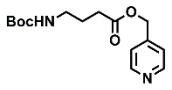

81

This compound was prepared according to the literature procedure.[109] 4-Pyridine methanol (130 mg, 1.19 mmol), Boc-GABA-OH (300 mg, 1.47 mmol), EDC (280 mg, 1.47 mmol) and DMAP (14 mg, 0.11 mmol) were dissolved in anhydrous THF and MeCN (4.0 mL, 1: 1, v/v). The mixture was stirred at 20 °C for 16 h. After this time, the mixture was diluted with H_2O (15 mL) and extracted with DCM (3 × 25 mL). The organic extracts were combined, dried over $MgSO_4$ and evaporated to dryness. The product was isolated by column chromatography on silica (eluent: $CHCl_3$) to yield 290 mg (0.98 mmol, 82% yield) of compound **81** as a white solid.

^{1}H NMR (400 MHz, $CDCl_3$) *δ:* 1.41 (s, 9H), 1.84 (quin, *J*=7.2 Hz, 2H), 2.45 (t, *J*=7.2 Hz, 2H), 3.14-3.19 (m, 2H), 4.74 (bs, 1H), 5.11 (s, 2H), 7.23 (d, *J*=5.9 Hz, 2H), 8.58 (d, *J*=5.9 Hz, 2H); ^{13}C NMR (100 MHz,$CDCl_3$) *δ:* 25.3, 28.4, 31.3, 39.7, 64.2, 79.2, 121.8, 144.8, 150.0, 156.0, 172.7; *m/z* ESI-MS+ 295.1, $[M+H]^+$, $C_{15}H_{23}N_2O_4^+$ requires 295.1 (100%). Data were in agreement with those previously reported.[109]

4-(((4-((*tert*-Butoxycarbonyl)amino)butanoyl)oxy)methyl)-1-methylpyridin-1-ium iodide (82)

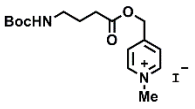

82

This novel compound was synthesized by adapting a reported procedure.[126] To the solution of compound **81** (250 mg, 0.85 mmol) in MeOH (3.0 mL) methyl iodide (310 μL, 5.0 mmol) was added dropwise and reaction was stirred at 60 °C over 16 h. After this time the mixture was allowed to cool to room temperature, the solvent was evaporated to dryness and product was purified by dissolving in THF and precipitating with Et_2O. The product **82** was obtained as a red foam in 68 % yield (250 mg, 0.58 mmol).

^{1}H NMR (400 MHz, DMSO-d_6) *δ:* 1.39 (s, 9H), 1.69 (quin, *J*=7.0 Hz, 2H), 2.50-2.54 (m, 2H, under DMSO-d_6), 2.94-3.00 (m, 2H), 4.33 (s, 3H), 5.43 (s, 2H), 6.90-6.93 (m, 1H), 8.08 (d, *J*=6.5 Hz, 2H), 8.95 (d, J=6.5 Hz, 2H); ^{13}C NMR (200 MHz, DMSO-d_6) *δ:* 25.2, 28.7, 31.0, 39.4, 48.1, 63.5, 78.0, 125.1, 145.7, 156.1, 156.2, 172.8; *m/z* ESI-MS+ 309.2, $[M]^+$, $C_{16}H_{25}N_2O_4^+$ requires 309.1 (100 %).

4-(((4-Ammoniobutanoyl)oxy)methyl)-1-methylpyridin-1-ium formate (Pyr-GABA)

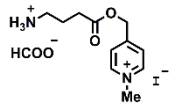

Pyr-GABA

This novel compound was prepared according to the adapted literature procedure.[180] Compound **82** (50 mg, 0.11 mmol) was dissolved in formic acid (1 mL) and stirred at room temperature for 3 h. Solvent was removed in *vacuo* and remaining residue dried under vacuum. The product, **Pyr-GABA**, was obtained in 95 % yield (40 mg, 0.10 mmol)

^{1}H NMR (400 MHz, D_2O) *δ:* 1.91 (quin, *J*=7.6 Hz, 2H), 2.60 (t, *J*=7.6 Hz, 2H), 2.96 (t, *J*=7.6 Hz, 2H), 4.25 (s, 3H), 5.35 (s, 2H), 7.89 (d, *J*=6.5 Hz, 2H), 8.24 (s, 1H), 8.64 (d, *J*=6.5 Hz, 2H);^{13}C NMR (200 MHz, DMSO-d_6) *δ:* 22.8, 30.5, 38.5, 48.0, 63.6, 125.1, 145.9, 156.6, 172.3; *m/z* ESI-MS+209.1, $[M-H]^+$, $C_{11}H_{17}N_2O_2^+$ requires 209.1 (100 %).

Pyridin-4-ylmethyl (*tert*-butoxycarbonyl)tryptophanate (84)

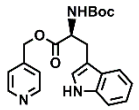

84

This novel compound was synthesized by adapting a reported procedure.[181] 4-Pyridine methanol (0.50 g, 4.6 mmol), EDC (1.07 g, 5.6 mmol), DMAP (56 mg, 0.46 mmol) and N_α-Boc-L-tryptophan (2.1 g, 6.9 mmol) were dissolved in anhydrous MeCN (5 mL) and mixture was stirred for 8 h. After this time, the solvent was evaporated, the mixture was dissolved in DCM (30 mL) and washed with H_2O (30 mL). The organic phase was dried over $MgSO_4$ and the solvent was evaporated to dryness. The product was isolated by column chromatography on silica (EtOAc as eluent) to yield 1.65 g (4.17 mmol, 90% yield) of compound **84** as a white solid.

^{1}H NMR (400 MHz, $CDCl_3$) *δ:* 1.44 (s, 9H), 3.28 (dd, *J*=6.3 Hz, *J*=14.5 Hz, 1H), 3.35 (dd, *J*=5.4 Hz, *J*=14.5 Hz, 1H), 4.72–4.77 (m, 1H), 5.02 (d, *J*=13.7 Hz, 1H), 5.08 (d, *J*=13.7 Hz, 1H), 5.14 (d, *J*=7.9 Hz, 1H), 6.93 (s, 1H), 7.00 (d, *J*=5.0 Hz, 2H), 7.09–7.13 (m, 1H), 7.18–7.22 (m, 1H), 7.33 (d, *J*=8.1 Hz, 1H), 7.56 (*d*, J=8.1 Hz, 1H), 8.35 (s, 1H), 8.51 (bs, 2H); ^{13}C NMR (100 MHz, $CDCl_3$) *δ:* 28.1, 28.4, 54.8, 64.8, 80.3, 109.3, 111.7, 118.6, 119.5, 122.0, 123.4, 127.5, 136.5, 145.1, 149.1, 155.6, 172.4; *m/z* ESI-MS+ 396.2, $[M+H]^+$, $C_{22}H_{26}N_3O_4^+$ requires 396.2 (100%).

1,1'-((2,7-Diiodo-9*H*-fluorene-9,9-diyl)bis(propane-3,1-diyl)bis(4-(((4-((*tert*-butoxycarbonyl) tryptophyl)oxy)methyl)pyridin-1-ium)propyl) methanesulfonate (83)

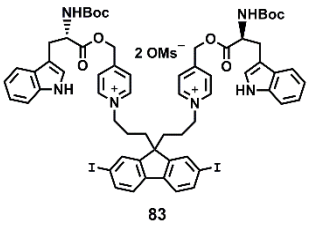

83

This novel compound was synthesized by adapting a reported procedure.[173] Compound **65** (250 mg, 0.36 mmol), **84** (426 mg, 1.08 mmol) and molecular sieves were placed in as flask and dried under vacuum. MeCN (5.0 mL) was added and the reaction mixture was heated at 100 °C under N_2 atmosphere. After 12 h the mixture was allowed to cool down to 20 °C and filtered. Collected liquid was evaporated to dryness. Resulting oil was dissolved in MeCN and product was precipitated with Et_2O. Precipitant was decanted and sonicated with Et_2O. The procedure of precipitation and sonication was repeated until the compound **83** formed red solid (320 mg, 0.22 mmol, 60% yield).

^{1}H NMR (500 MHz, DMSO-d_6) *δ:* 1.01–1.08 (m, 4H), 1.35 (s, 18H), 1.99–2.04 (m, 4H), 2.32 (s, 6H), 3.12 (dd, *J*=8.7 Hz, *J*=14.3 Hz, 2H), 3.18 (dd, *J*=6.5Hz, *J*=14.3 Hz, 2H), 4.30–4.40 (m, 6H), 5.31 (d, *J*=16.1 Hz, 2H), 5.38 (d, *J*=16.1 Hz, 2H), 6.94–6.97 (m, 2H), 7.00–7.03 (m, 2H), 7.20 (s, 2H), 7.30 (d, *J*=7.8 Hz, 2H), 7.49–7.52 (m, 4H), 7.66–7.77 (m, 10H), 8.78 (d, *J*=6.5 Hz, 4H), 10.89 (s, 2H); ^{13}C NMR (125 MHz, DMSO-d_6) *δ:* 26.0, 27.1, 28.5, 34.8, 40.3, 54.4, 55.3, 60.3, 63.7, 78.8, 94.7, 109.7, 112.0, 118.4, 118.8, 121.3, 122.8, 124.4, 125.0, 127.4, 132.1, 136.5, 136.9, 139.6, 144.5, 150.5, 155.8, 155.9, 172.6; *m/z* ESI-MS+ 645.3, $[M]^{2+}$, $C_{63}H_{68}I_2N_6O_8^{2+}$ requires 645.1 (100%).

BEF-Pyr-(Boc)Trp (85)

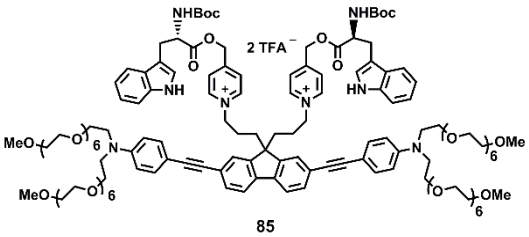

85

This novel compound was synthesized by adapting a reported procedure.[108] $Pd(OAc)_2$ (1.2 mg, 0.006 mmol), PPh_3 (2.8 mg, 0.01 mmol) and CuI (0.8 mg, 0.006 mmol) were placed in a Schlenk tube and dried under vacuum. Compound **83** (80 mg, 0.054 mmol) was dissolved in mixture of MeCN and CH_2Cl_2 (0.2 mL, 1:1, v/v) and transferred to the Schlenk tube. DIPA (0.2 mL) was added and the reaction mixture was degassed by two freeze-thaw cycles. A solution of compound **58** (94 mg, 0.12 mmol) in MeCN (0.1 mL) was added to the reaction mixture and additional freeze-thaw cycle was performed. Reaction was stirred at 20 °C and its progress was monitored by HPLC (*HPLC Method 1*).

After 2 h the mixture was diluted with EtOAc (20 mL), organic phase was washed with H_2O (20 mL), followed by saturated aqueous solution of NH_4Cl (20 mL) and H_2O (20 mL). Organic layer was dried over $MgSO_4$ and evaporated. Product was isolated with use of reverse phase column chromatography (gradient from 100% H_2O with 0.1% TFA to 100% acetonitrile) to give 50 mg (0.017 mmol, 33% yield) of **85** as an oil. It is assumed that methanefulfonate counterion was replaced with TFA anion during the column chromatography with TFA-buffer. NMR spectra confirmed the absence of methanesulfonate.

^{1}H NMR (500 MHz, DMSO-d_6) δ: 1.12–1.27 (m, 4H), 1.37 (s, 18H), 2.11–2.25 (m, 4H), 3.13–3.22 (m, 4H), 3.29 (s, 12H), 3.34–3.63(m, 112H), 4.38–4.50 (m, 6H), 5.32 (d, *J*=16.5 Hz, 2H), 5.38 (d, *J*=16.5 Hz, 2H), 6.79 (d, *J*=8.5 Hz, 4H), 6.97–7.00 (m, 2H), 7.05–7.08 (m, 2H), 7.23 (s, 2H), 7.34–7.39 (m, 6H), 7.51–7.59 (m, 8H), 7.77 (d, *J*=6.3 Hz, 4H), 7.90 (d, *J*=7.9 Hz, 2H), 8.88 (d, *J*=6.3Hz, 4H), 11.02 (s, 2H); ^{13}C NMR (125 MHz, DMSO-d_6) δ: 26.2, 27.0, 28.4, 35.3, 50.4, 54.1, 55.2, 58.4, 60.4, 63.6, 68.1, 69.9, 70.1–70.2, 70.3, 71.6, 78.9, 88.6, 92.1, 108.3, 109.6, 111.8, 118.3, 118.7, 121.0, 121.3, 122.9, 124.3, 124.9, 125.6, 127.3, 131.2, 132.8, 136.4, 139.8, 144.5, 148.3, 149.0, 155.8, 155.9, 172.6.

BEF-Pyr-Trp

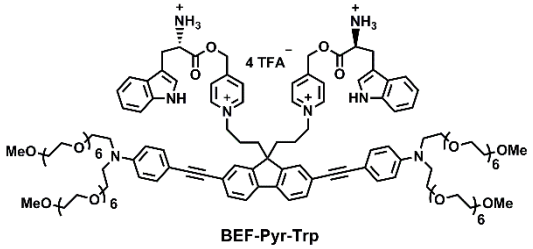

BEF-Pyr-Trp

This novel compound was synthesized by adapting a reported procedure.[181] Triisopropylsilane (0.1 mL) was added to a solution of **85** (15 mg, 0.005 mmol) in formic acid (1 mL) and reaction was stirred at 20 °C. The progress of the reaction was monitored by HPLC (*HPLC Method 1*) and after 2 h, the solvent was evaporated under a stream of nitrogen. **BEF-Pyr-Trp** was isolated from the crude reaction mixture by semi-preparative HPLC (*HPLC Method 1*). Product containing fractions were combined and freeze-dried. 1.08 mg of **BEF-Pyr-Trp** (0.0004 mmol, 8% yield) was obtained.

^{1}H NMR (500 MHz, DMSO-d_6) δ: 0.96–1.05 (m, 4H), 2.07–2.17 (m, 4H), 3.16 (s, 12H), 3.24 (under H_2O, 4H), 3.34–3.58 (m, 112H), 4.25–4.33 (m, 4H), 4.36–4.42 (m, 2H), 5.26 (d, *J*=16.7 Hz, 2H), 5.32 (d, *J*=16.7 Hz, 2H), 6.67 (d, *J*=8.7 Hz, 4H), 6.81–6.85 (m, 2H), 6.89–6.93 (m, 2H), 7.15–7.17 (m, 2H), 7.21 (d, *J*=8.4 Hz, 2H), 7.25 (d, *J*=8.7 Hz, 4H), 7.36 (d, *J*=7.8 Hz, 2H), 7.43 (d, *J*=8.1 Hz, 2H), 7.51 (s, 2H), 7.61 (d, J=6.7 Hz, 4H), 7.78 (d, *J*=8.1 Hz, 2H), 8.42 (bs, 6H), 8.68 (d, *J*=6.7 Hz, 4H), 10.95 (s, 2H); *m/z* ESI-MS+ 590.0792, $[M]^{4+}$, $C_{129}H_{186}N_8O_{32}^{4+}$ requires 590.0797 (100%).

1-butylpyridin-1-ium iodide (Bu-Pyr)[196]

Bu-Pyr

This known compound was synthesized by analogy with a reported procedure.[126] To the solution of pyridine (2.1 mL, 26.0 mmol) in MeOH (10.0 mL) 1-iodobutane (8.2 mL, 72.0 mmol) was addend dropwise and reaction was heated at 55ºC for 16 h. After this time solvent was evaporated and crude material dried under vacuum. No further purification was required and 6.15 g of yellow solid were obtained (23.4 mmol, 90 % yield).

^{1}H NMR (400 MHz, DMSO-d_6) *δ:* 0.90 (t, *J*=7.4 Hz, 3H), 1.29 (sext, *J*=7.4 Hz, 2H), 1.91 (quin, *J*=7.4 Hz, 2H), 4.65 (t, *J*=7.4 Hz, 2H), 8.16-8.22 (m, 2H), 8.61-8.67 (m, 1H), 9.16 (d, *J*=5.8 Hz,2H); ^{13}C NMR (100 MHz, DMSO-d_6) *δ:* 13.8, 19.2, 33.1, 60.9, 128.6, 145.2, 146.0; *m/z* ESI-MS+ 136.1, $[H]^+$, $C_9H_{14}N^+$ requires 136.1 (100 %). Full NMR spectroscopy data were not reported in ref. [196]. NMR spectra were in agreement with those reported for 1-butylpyridin-1-ium bromide.[197]

4-((((tert-Butoxycarbonyl)tryptophyl)oxy)methyl)-1-methylpyridin-1-ium iodide (86)

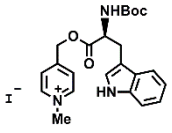

86

This novel compound was synthesized by adapting a reported procedure.[126] To the solution of compound **84** (500 mg, 1.26 mmol) in MeOH (1.5 mL) methyl iodide (120 µL, 1.90 mmol) was added dropwise and reaction was stirred at 55 °C over 72 h. After this time the mixture was allowed to cool to room temperature, the solvent was evaporated to dryness and product was purified by dissolving in THF and precipitating with Et_2O. Compound **86** was obtained as a yellow solid in 74 % yield (500 mg, 0.93 mmol).

^{1}H NMR (DMSO-d_6, 500 MHz), *δ:* 1.37 (s, 9H), 3.14 (dd, *J*= 8.6 Hz, J=14.5 Hz, 1H), 3.21 (dd, *J*=6.4 Hz, *J*=14.5 Hz, 1H), 4.33 (s, 3H), 4.39-4.43 (m, 1H), 5.35 (d, *J*=16.3 Hz,1H), 5.41 (d, *J*=16.3 Hz, 1H), 6.98-7.01 (m, 1H), 7.07-7.10 (m, 1H), 7.20-7.23 (m, 1H), 7.37 (d, *J*=8.1 Hz, 1H), 7.49-7.54 (m, 2H), 7.82 (d, *J*=6.4 Hz, 2H), 8.91 (d, *J*=6.4 Hz, 2H), 10.85 (s, 1H); ^{13}C NMR (DMSO-d_6, 250 MHz), *δ:* 27.1, 28.6, 48.0, 55.2, 63.7, 79.0, 109.7, 111.9, 118.4, 118.8, 121.4, 124.3, 124.6, 127.4, 136.4, 145.4, 155.5, 156.0, 172.5; *m/z* ESI-MS+ 410.2, $[M]^+$, $C_{23}H_{28}N_3O_4^+$ requires 410.2 (100 %).

4-(((2-ammonio-3-(1H-indol-2-yl)propanoyl)oxy)methyl)-1-methylpyridin-1-ium trifluoroacetate (Pyr-Trp)

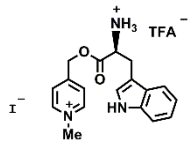

Pyr-Trp

This novel compound was synthesized by adapting a reported procedure.[182] Compound **86** (50 mg, 0.093 mmol) was dissolved in THF (1mL) and TFA (100 μL) was added dropwise. After 1 h of stirring at room temperature the solvent was blew down with the stream of nitrogen. Remaining oil was dissolved in THF and the product was precipitated with Et_2O to give 25 mg (0.046 mmol, 49 % yield) of **Pyr-Trp** as a yellow solid.

^{1}H NMR (DMSO-d_6, 400 MHz), *δ:* 3.31-3.41 (m, 2H), 4.34 (s, 3H), 4.48-4.54 (m, 1H), 5.41 (d, *J*=16.0 Hz, 1H), 5.47 (d, *J*=16.0 Hz, 1H), 6.99-7.01 (m,1H), 7.02-7.13 (m,1H), 7.25 (s, 1H), 7.39 (d, *J*=7.7 Hz, 1H), 7.51 (d, *J*=8.2 Hz, 1H), 7.79-7.84 (m, 2H), 8.67 (bs, 3H), 8.87-8.92 (m, 2H), 11.09 (s, 1H); ^{13}C NMR (DMSO-d_6, 100 MHz), *δ:* 27.0, 48.0, 53.3, 64.8, 106.9, 112.1, 118.4, 119.3, 121.8, 125.0, 125.4, 127.2, 136.8, 145.7, 154.4, 169.4; *m/z* ESI-MS+ 155.7, $[M]^{2+}$, $C_{18}H_{21}N_3O_2^{2+}$ requires 155.6 (100 %); 310.2, $[M\text{-}H]^+$, $C_{18}H_{20}N_3O_2^+$ requires 310.1 (100 %).

***tert*-Butyl 4-acetylbenzoate (87)**[198]

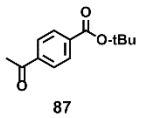

87

This known compound was prepared according to the adapted literature procedure.[183] 4-Acetylbenzoic acid (0.80 g, 4.87 mmol), Boc_2O (2.60 g, 11.92 mmol) and DMAP (0.22 g, 1.80 mmol) were dissolved in *t*-BuOH (20 mL) and stirred for 6 h at room temperature under inert atmosphere. Reaction mixture was diluted with H_2O (50 mL), extracted with $CHCl_3$ (150 mL) and organic washings were dried over $MgSO_4$ and evaporated to dryness. The product was purified by column chromatography on silica (cyclohexane : $CHCl_3$ in gradient 50-100 % of $CHCl_3$, v/v) to give 0.94 g (4.3 mmol, 90 %) of **87** as a white solid.

^{1}H NMR (400 MHz, $CDCl_3$) *δ:* 1.62 (s, 9H), 2.65 (s, 3H), 8.00 (d, *J*=8.3 Hz, 2H), 8.08 (d, *J*=8.3 Hz, 2H); ^{13}C NMR (250 MHz, DMSO-d_6) *δ:* 27.4, 28.1, 81.8, 128.7, 129.7, 135.3, 140.2, 164.6, 198.1. Data were in agreement with those previously reported.[198]

tert-Butyl 4-(2-bromoacetyl)benzoate (88)

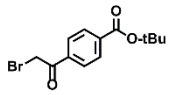

88

This novel compound was prepared according to the adapted literature procedure.[104] To the cooled to 0 ºC solution of compound **87** (400 mg, 1.8 mmol) in $CHCl_3$ (30 mL), a solution of bromine (100 µL, 1.9 mmol) in $CHCl_3$ (16 mL) was added dropwise. Reaction was stirred at room temperature until the color changed from intensively red to pale yellow. Crude mixture was washed with $NaHCO_3$, followed by washing with H_2O. Organic phase was dried over $MgSO_4$ and evaporated to dryness. The product was purified by column chromatography on silica (PE : DCM, 1:4, v/v) to give 345 mg (1.15 mmol, 64 %) of **88** as a white solid.

^{1}H NMR (400 MHz, $CDCl_3$) *δ:* 1.54 (s, 9H), 4.38 (s, 2H), 7.94 (d, *J*=8.4 Hz, 2H), 8.02 (d, *J*=8.4 Hz, 2H); ^{13}C NMR (250 MHz, $CDCl_3$) *δ:* 28.1, 31.1, 81.9, 128.7, 129.8, 136.5, 136.7, 164.5, 190.9; *m/z* ESI-MS+ 320.9, $[M+Na]^+$, $C_{13}H_{15}BrNaO_3$ requires 321.0 (100 %).

tert-Butyl 4-(2-(((tert-butoxycarbonyl)tryptophyl)oxy)acetyl)benzoate (89)

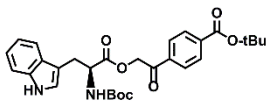

89

This novel compound was prepared according to the adapted literature procedure.[119] To a cooled to 13 ºC solution of compound **88** (15 mg, 0.05 mmol) in CH_3CN (0.1 mL) a solution of Boc-Trp-OH (23 mg, 0.075 mmol) in CH_3CN (0.6 mL) was added dropwise followed by addition of DBU (11 µL, 0.075 mmol). Reaction was stirred at room temperature for 16 h. The solvent was evaporated to dryness and the product was isolated with use of column chromatography on silica ($CHCl_3$: MeOH, in gradient 0-5 % of MeOH, v/v) to give 21 mg (0.04 mmol, 80 %) of **89** as a white solid.

^{1}H NMR (400 MHz, $CDCl_3$) *δ:* 1.33 (s, 9H), 1.54 (s, 9H), 3.27 (dd, *J*=6.2 Hz, *J*=14.9 Hz, 1H), 3.41 (dd, *J*=5.4 Hz, *J*=14.9 Hz, 1H), 4.70-4.76 (m, 1H), 4.99 (d, *J*=7.7 Hz, 1H), 5.16 (d, *J*=16.4 Hz, 1H), 5.35 (d, *J*=16.4 Hz, 1H), 7.02-7.07 (m, 1H), 7.08-7.14 (m, 2H), 7.27 (d, *J*=7.9 Hz, 1H), 7.53 (d, *J*=7.9 Hz, 1H), 7.82 (d, *J*=8.3 Hz, 2H), 7.99 (d, *J*=8.3 Hz, 2H), 8.13 (bs, 1H); ^{13}C NMR (100 MHz, $CDCl_3$) *δ:* 27.8, 28.1, 28.3, 54.2, 66.5, 79.9, 82.0, 109.9, 111.2, 118.7, 119.6, 122.1, 123.4, 127.6, 127.8, 129.8, 136.1, 136.6, 136.8, 155.3, 164.6, 171.9, 191.6; *m/z* ESI-MS- 521.0, $[M-H]^-$, $C_{29}H_{33}N_2O_{47}^-$ requires 521.22 (100 %).

4-(5-((1H-indol-3-yl)methyl)-6-oxo-5,6-dihydro-2H-1,4-oxazin-3-yl)benzoic acid (90)

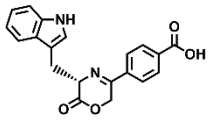

90

This novel compound was prepared according to the adapted literature procedure.[180] Compound **89** (10 mg, 0.019 mmol) was dissolved in formic acid (1 mL) and stirred at room temperature. After 6 h solvent was removed *in vacuo* and remaining solid was coevaporated with toluene. The product was obtained as white film in 100 % yield (6 mg, 0.019 mmol).

^{1}H NMR (400 MHz, DMSO-d_6) δ: 3.40 (dd, J=6.6 Hz, J=14.4 Hz, 1H), 3.46 (dd, J=5.0 Hz, J=14.4 Hz, 1H), 4.75-4.80 (m, 1H), 4.98 (dd, J=1.0 Hz, J=16.3 Hz, 1H), 5.35 (dd, J=3.0 Hz, J=16.3 Hz, 1H), 6.90-6.95 (m, 1H), 7.01-7.06 (m, 1H), 7.11 (d, J=2.3 Hz, 1H), 7.31 (d, J=8.1 Hz, 1H), 7.56 (d, J=8.0 Hz, 1H), 7.90 (d, J=8.3 Hz, 2H), 7.98 (d, J=8.3 Hz, 2H); ^{13}C NMR (100 MHz, DMSO-d_6) δ: 28.3, 60.7, 67.5, 110.2, 111.7, 118.7, 119.2, 121.3, 124.6, 127.8, 129.8, 133.3, 136.3, 138.3, 162.9, 163.5, 167.2, 169.5; *m/z* ESI-MS+ 349.0, $[M+H]^+$, $C_{20}H_{17}N_2O_4^+$ requires 349.1 (100 %).

***tert*-Butyl 4-(2-((3-(1H-indol-3-yl)propanoyl)oxy)acetyl)benzoate (91)**

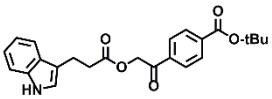

91

This novel compound was prepared with a modified literature procedure.[119] To the solution of compound **88** (45 mg, 0.15 mmol) in CH_3CN (0.3 mL) a solution of 3-indolepropionic acid (31 mg, 0.16 mmol) in CH_3CN (1.5 mL) was added dropwise, followed by the addition of DIPEA (27 µL, 0.16 mmol). Reaction was stirred for 16 h at 20 °C. The mixture was diluted with $CHCl_3$ (30 mL), washed with H_2O (40 mL), the organic layer was dried over $MgSO_4$ and evaporated to dryness. The product was isolated from the crude reaction mixture with use of column chromatography on silica ($CHCl_3$: MeOH, in gradient 0-5 % of MeOH, v/v) and further purified by dissolving n DCM and precipitating with PE to give 42 mg (0.10 mmol, 67 %) of **91** as a white solid.

^{1}H NMR (400 MHz, $CDCl_3$) δ: 1.52 (s, 9H), 2.80 (t, J=7.5 Hz, 2H), 3.08 (t, J=7.5 Hz, 2H), 5.22 (s, 2H), 6.92 (s, 1H), 7.00-7.05 (m, 1H), 7.07-7.12 (m, 1H), 7.24 (d, J=8.0 Hz, 1H), 7.51 (d, J=7.8 Hz, 1H), 7.81 (d, J=8.2 Hz, 2H), 7.97 (d, J=8.2 Hz, 2H); ^{13}C NMR (100 MHz, $CDCl_3$) δ: 20.5, 28.1, 34.5, 66.1, 82.0, 111.2, 114.7, 118.6, 119.3, 121.6, 122.0, 127.1, 127.6, 129.8, 136.3, 136.5, 137.0, 164.6, 172.7, 192.2; *m/z* ESI-MS$^+$ 430.0, $[M+Na]^+$, $C_{24}H_{25}NO_5Na^+$ requires 430.1 (100 %).

4-(2-((3-(1H-indol-3-yl)propanoyl)oxy)acetyl)benzoic acid (COOH-Phen-Ind)

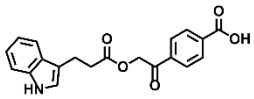

COOH-Phen-Ind

This novel compound was prepared according to the adapted literature procedure.[180] Compound **91** (10 mg, 0.024 mmol) was dissolved in formic acid (1 mL) and stirred at room temperature. After 2 h solvent was removed *in vacuo* and the residue was coevaporated with toluene to give 8 mg (0.023 mmol, 95 % yield) of **COOH-Phen-Ind** as a white film.

^{1}H NMR (400 MHz, DMSO-d_6) *δ:* 2.83 (t, *J*=7.5 Hz, 2H), 3.03 (t, *J*=7.5 Hz, 2H), 5.52 (s, 2H), 6.97-7.01 (m, 1H), 7.05-7.10 (m, 1H), 7.18 (s, 1H), 7.34 (d, *J*=7.9 Hz, 1H), 7.53 (d, *J*=7.8 Hz, 1H), 8.04-8.11 (m, 4H), 10.82 (s, 1H); ^{13}C NMR (100 MHz, DMSO-d_6) *δ:* 20.6, 34.5, 67.0, 111.8, 113.3, 118.5, 118.7, 121.4, 122.8, 127.3, 128.4, 130.1, 135.7, 136.6, 137.4, 166.9, 172.6, 193.3; *m/z* ESI-MS$^-$ 350.1, $[M-H]^-$, $C_{20}H_{16}NO_5^-$ requires 350.1 (100 %).

***tert*-Butyl 4-(2-((4-((*tert*-butoxycarbonyl)amino)butanoyl)oxy)acetyl)benzoate (92)**

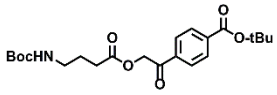

92

This novel compound was prepared according to the adapted literature procedure. [120] To a cooled to 13 ºC solution of compound **88** (15 mg, 0.05 mmol) in THF (0.1 mL) a solution of Boc-GABA-OH (10 mg, 0.05 mmol) in THF (0.6 mL) was added dropwise followed by addition of DBU (9 µL, 0.06 mmol). To aid solubilisation CH_3CN (0.5 mL) was added and reaction was stirred at room temperature overnight. Crude reaction mixture was evaporated to dryness and the product was isolated with use of column chromatography on silica ($CHCl_3$ - MeOH, in gradient 0 – 1 % of MeOH, v/v) to give 18 mg (0.043 mmol, 85 %) of **92** as a white solid.

^{1}H NMR (400 MHz, $CDCl_3$) *δ:* 1.37 (s, 9H), 1.54 (s, 9H), 1.84 (quin, *J*=7.0 Hz, 2H), 2.48 (t, *J*=7.3 Hz, 2H), 3.13-3.19 (m, 2H), 4.69 (bs, 1H), 5.29 (s, 2H), 7.87 (d, *J*=8.4 Hz, 2H), 8.01 (d, *J*=8.4 Hz, 2H); ^{13}C NMR (100 MHz, $CDCl_3$) *δ:* 25.2, 28.1, 28.4, 31.1, 39.7, 66.0, 79.1, 82.0, 127.5, 129.8, 136.6, 136.9, 156.0, 164.5, 172.6, 191.9; *m/z* ESI-MS$^-$ 420.0, $[M-H]^-$, $C_{22}H_{30}NO_7^-$ requires 420.2 (100 %).

4-(2-(4-(*tert*-Butoxycarbonyl)phenyl)-2-oxoethoxy)-4-oxobutan-1-aminium formate (tBu-Phen-GABA)

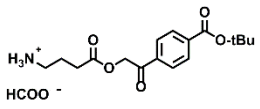

tBu-Phen-GABA

This novel compound was prepared according to the adapted literature procedure.[180] Compound **92** (23 mg, 0.054 mmol) was dissolved in formic acid (1 mL) and stirred at 20 °C. After 0.5 h solvent was removed *in vacuo* and remaining residue was coevaporated with toluene to give. 18 mg (0.049 mmol, 90 % yield) of **tBu-Phen-GABA** as a yellow film.

^{1}H NMR (500 MHz, DMSO-d_6) *δ:* 1.58 (s, 9H), 1.87 (quin, *J*=7.4 Hz, 2H), 2.60 (t, *J*=7.4 Hz, 2H), 2.86 (t, *J*=7.4 Hz, 2H), 5.55 (s, 2H), 8.05-8.09 (m, 4H), 8.39 (s, 1H); *m/z* ESI-MS+ 322.2, $[M]^+$, $C_{17}H_{24}NO_5^+$ requires 322.1 (100 %).

4-(2-(4-Carboxyphenyl)-2-oxoethoxy)-4-oxobutan-1-aminium formate (COOH-Phen-GABA)

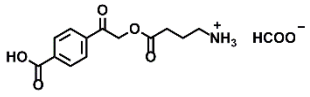

COOH-Phen-GABA

This novel compound was prepared according to the adapted literature procedure.[180] Compound **92** (18 mg, 0.042 mmol) was dissolved in formic acid (1 mL) and stirred at room temperature overnight. Solvent was removed *in vacuo* and remaining residue was coevaporated with toluene to give 8 mg (0.025 mmol, 60 % yield) of the product as a yellow film.

^{1}H NMR (400 MHz, CH_3COOH-d_3) *δ:* 2.32-2.68 (m, 2H under the solvent peak), 3.10-3.21 (m, 2H), 3.62-3.75 (m, 2H), 5.87-6.06 (m, 2H), 8.48-8.59 (m, 2H), 8.65-8.76 (m, 2H); ^{13}C NMR (100 MHz, CH_3COOH-d_3) *δ:* 22.8, 30.8, 39.6, 67.1, 128.3, 130.8, 134.5, 138.3, 170.1, 173.0, 193.07; *m/z* ESI-MS+ 266.1, $[M]^+$, $C_{13}H_{16}NO_5^+$ requires 266.1 (100 %).

2-(4-Methoxyphenyl)-2-oxoethyl 4-((*tert*-butoxycarbonyl)amino)butanoate (93)

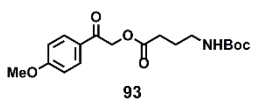

93

This novel compound was prepared according to the adapted literature procedure.[119] To a solution of 2-bromo-1-(4-methoxyphenyl)ethan-1-one (100 mg, 0.43 mmol) in MeCN (0.9 mL) a solution of Boc-GABA-OH (88 mg, 0.43 mmol) in MeCN (5 mL) was added followed by the addition of DBU (76 µL, 0.50 mmol) and reaction was stirred at room temperature for 16 h. Solvent was evaporated to dryness

and product was isolated from reaction mixture with use of column chromatography on silica ($CHCl_3$ – MeOH, in gradient 0-10 % MeOH, v/v) to give 100 mg of **93** as a white solid (0.28 mmol, 65 %).

^{1}H NMR (400 MHz, $CDCl_3$) *δ:* 1.35 (s, 9H), 1.81 (quin, *J*=7.0 Hz, 2H), 2.45 (t, *J*=7.3 Hz, 2H), 3.10-3.17 (m, 2H), 3.78 (s, 3H), 4.82-4.90 (bs, 1H), 5.22 (s, 2H), 6.86 (d, *J*=8.6 Hz, 2H), 7.80 (d, *J*=8.6 Hz, 2H); ^{13}C NMR (100 MHz, $CDCl_3$) *δ:* 25.2, 28.4, 31.1, 39.7, 55.2, 65.7, 79.0, 114.0, 127.0, 130.0, 156.0, 14.0, 172.7, 190.6; *m/z* EI-MS+ 351.1, [M], $C_{18}H_{25}NO_6$ requires 351.1 (100 %).

4-(2-(4-Methoxyphenyl)-2-oxoethoxy)-4-oxobutan-1-aminium formate (OMe-Phen-GABA)

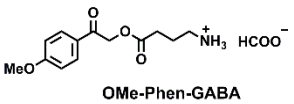

OMe-Phen-GABA

This novel compound was prepared according to the adapted literature procedure.[180] Compound **93** (35 mg, 0.01) was dissolved in formic acid (1 mL) and stirred at room temperature overnight. Solvent was removed *in vacuo* and remaining residue was coevaporated with toluene to give 29 mg (0.097 mmol, 97 % yield) of **OMe-Phen-GABA**.

^{1}H NMR (400 MHz, D_2O) *δ:* 2.00 (quin, J=7.3 Hz, 2H), 2.66 (t, *J*=7.3 Hz, 2H), 3.06 (t, *J*=7.3 Hz, 2H), 3.86 (s, 3H), 5.45 (s,2H), 7.04 (d, J=8.7 Hz, 2H), 7.91 (d, J=8.7 Hz, 2H), 8.33 (bs, 1H); ^{13}C NMR (200 MHz, D_2O+DMSO-d_6) *δ:* 22.2, 30.5, 55.9, 66.8, 114.7, 126.5, 130.8, 164.5, 170.4, 174.0, 194.3; *m/z* ESI-MS+ 252.1, $[M]^+$, $C_{13}H_{18}NO_4^+$ requires 252.1 (100 %).

2-(4-Hydroxyphenyl)-2-oxoethyl 4-((*tert*-butoxycarbonyl)amino)butanoate (94)[119]

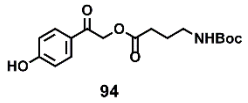

94

This known compound was prepared according to the literature procedure. [119] To a solution of 2-bromo-1-(4-hydroxyphenyl)ethan-1-one (100 mg, 0.46 mmol) in THF (1 mL) a solution of Boc-GABA-OH (203 mg, 0.49 mmol) in THF (2 mL) was added followed by the addition of DBU (76 μL, 0.50 mmol) and reaction was stirred at 20 °C for 16 h. Solvent was evaporated to dryness and product was isolated from reaction mixture with use of column chromatography on silica ($CHCl_3$ – MeOH, in gradient 0-5 % MeOH, v/v) to give 20 mg of **94** as a white solid (0.059 mmol, 12 %).

^{1}H NMR (400 MHz, $CDCl_3$) *δ:* 1.64 (s, 9H), 1.94 (quin, *J*=7.0 Hz, 2H), 2.58 (t, *J*=7.2 Hz, 2H), 3.24-3.27 (m, 2H), 5.39 (s, 2H), 7.97 (d, *J*=8.4 Hz, 2H), 8.12 (d, *J*=8.4 Hz, 2H). Neither NMR nor MS spectroscopic data are reported in the literature for comparison.

4-(2-(4-Hydroxyphenyl)-2-oxoethoxy)-4-oxobutan-1-aminium trifluoroacetate (OH-Phen-GABA)[119]

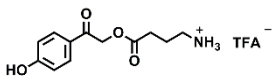

OH-Phen-GABA

This known compound was prepared according to the literature procedure. [119] Compound **94** (20 mg, 0.059 mmol) was dissolved in TFA (1 mL) and stirred at room temperature for 3 h. Solvent was removed by blowing down with stream of nitrogen and remaining residue was coevaporated with toluene. The residue was dissolved in H_2O followed by extraction with EtOAC and liofilization to give 12 mg (0.034 mmol, 57 % yield) of **OH-Phen-GABA**.

^{1}H NMR (400 MHz, D_2O) *δ:* 1.92 (quin, *J*=7.3 Hz, 2H), 2.58 (t, *J*=7.3 Hz, 2H), 2.9 (t, *J*=7.3 Hz, 2H), 5.40 (s, 2H), 6.88 (d, *J*=8.7 Hz, 2H), 7.81 (d, *J*=8.7 Hz, 2H); ^{13}C NMR (100 MHz, $CDCl_3$) *δ:* 22.0, 30.4, 38.6, 66.7, 115.8, 125.7, 131.0, 162.2, 174.3, 190.8; *m/z* ESI-MS+ 238.1, $[M]^+$, $C_{12}H_{16}NO_4^+$ requires 238.1 (100 %). Neither NMR nor MS spectroscopic data are reported in the literature for comparison.

(2,7-Diiodo-9*H*-fluorene-9,9-diyl)bis(propane-3,1-diyl) bis(4-(2-bromoacetyl)benzoate) (99)

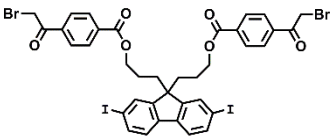

99

This novel compound was prepared by analogy with a reported procedure.[104] To the cooled to 0 °C solution of compound **63** (550 mg, 0.66 mmol) in $CHCl_3$ (11 mL), a solution of bromine (72 µL, 1.39 mmol) in $CHCl_3$ (5 mL) was added dropwise. Reaction was stirred at 20 °C until the color changed from intensively red to pale yellow. Crude mixture was washed with $NaHCO_3$, followed by washing with H_2O. Organic phase was dried over $MgSO_4$ and evaporated to dryness. The product was purified by column chromatography on silica (DCM : MeOH in gradient 0% to 5% of MeOH) to give 556 mg (0.56 mmol, 85%) of compound **99** as a white solid.

^{1}H NMR (400 MHz, $CDCl_3$) *δ:* 0.96–1.03 (m, 4H), 2.05–2.09 (m, 4H),4.00 (t, *J*=6.3 Hz, 4H), 4.38 (s, 4H), 7.39 (d, *J*=8.6 Hz, 2H), 7.64–7.65 (m, 4H), 7.97–8.02 (m, 8H); ^{13}C NMR (100 MHz, $CDCl_3$) *δ:* 23.2, 30.6, 36.3, 54.6, 65.0, 93.6, 122.0, 129.0, 130.0, 131.8, 134.6, 136.9, 137.1, 139.9, 150.7, 165.2, 190.8; *m/z* EI-MS+ 983.8 $[M]^+$, $C_{37}H_{30}Br_2I_2O_6^+$ requires 983.8 (100%).

(2,7-Diiodo-9*H*-fluorene-9,9-diyl)bis(propane-3,1-diyl)bis(4-(2-((3-(1H-indol-3-yl) propanoyl)oxy)acetyl)benzoate) (100)

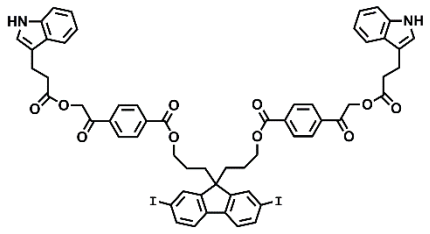

100

This novel compound was prepared by analogy with a reported procedure.[119] To a solution of compound **99** (100 mg, 0.1 mmol) in THF (0.5 mL) a solution of 3-indolepropionic acid (38 mg, 0.2 mmol) in THF (2.0 mL) was added followed by DBU (32 μL, 0.21 mmol). After 16 h of stirring at 20 °C the solvent was evaporated *in vacuo* and the product was isolated from the crude reaction mixture with use of the column chromatography ($CHCl_3$ – MeOH, 99:1 v/v). Compound **100** was obtained as white solid in 58% yield (70 mg, 0.058 mmol).

^{1}H NMR (400 MHz, $CDCl_3$) *δ:* 0.94–1.04 (m, 4H), 2.03–2.10 (m, 4H), 2.83 (t, *J*=7.7 Hz, 4H), 3.10 (t, *J*=7.6 Hz, 4H), 3.99 (t, *J*=6.2 Hz, 4H), 5.25 (s, 4H), 6.97 (s, 2H), 7.01–7.07 (m, 2H), 7.09–7.14 (m, 2H), 7.27 (d, *J*=8.2 Hz, 2H), 7.40 (d, *J*=7.9, 2H), 7.54 (d, *J*=7.7 Hz, 2H), 7.62–7.67 (m, 4H), 7.89 (d, *J*=8.2 Hz, 4H), 7.99 (d, *J*=8.2 Hz, 4H); ^{13}C NMR (100 MHz, $CDCl_3$) *δ:* 20.5, 23.2, 34.5, 36.3, 54.6, 65.0, 66.1, 93.6, 111.1, 114.8, 118.7, 119.4, 121.5, 121.9, 122.1, 127.2, 127.8, 130.0, 131.8, 134.6, 136.3, 136.9, 137.4, 140.0, 150.7, 165.3, 172.7, 192.1; *m/z* MALDI TOF$^+$ 1201.4, $[M+H]^+$, $C_{59}H_{51}I_2N_2O_{10}^+$, requires 1201.1 (100%).

BEF-Phen-Ind

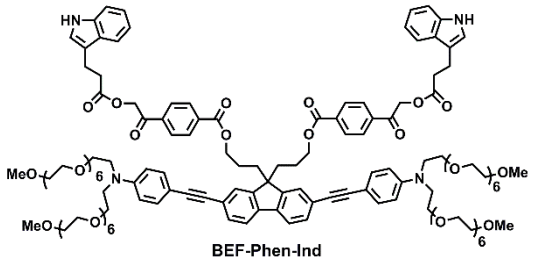

BEF-Phen-Ind

This novel compound was synthesized by adapting a reported procedure.[108] To vacuum-dried CuI (1.1 mg, 0.006 mmol), $Pd(OAc)_2$ (1.2 mg, 0.005 mmol) and PPh_3 (3.0 mg, 0.011 mmol), compound **100** (70 mg, 0.058 mmol) in DCM (1 mL) and distilled DIPA (1.0 mL) was added and two freeze-thaw cycles were carried out. A solution of compound **58** (93 mg, 0.122 mmol) in DCM (1 mL) was added and additional freeze-thaw cycle was run. The progress of the reaction was monitored by HPLC (*HPLC Method 2*). After 2 h of stirring at 20 °C the reaction mixture was diluted with $CHCl_3$ (50 mL)

and crude mixture was washed with H_2O (20 mL) and NH_4Cl (20 mL). The organic layer was dried over $MgSO_4$ and evaporated to dryness. The crude reaction mixture was dissolved in MeCN and passed through a pre-packed reverse phase column with MeCN as eluent. The organic phase was collected and solvent was removed *in vacuo* to give 180 mg of the crude reaction mixture. 10 mg of the crude mixture were purified with use of semi-prep HPLC to give 0.6 mg of **BEF-Phen-Ind** as a yellow oil (7% yield calculated for the 10 mg of purified crude, 0.0002 mmol).

^{1}H NMR (400 MHz, $CDCl_3$) *δ:* 0.92–1.00 (4H, m), 2.25–2.33 (m, 4H), 2.82 (t, *J*=7.7 Hz, 4H), 3.01 (t, *J*=7.6 Hz, 4H), 3.22 (s, 12H), 3.39–3.42 (under H_2O, m, 8H), 3.47–3.59 (m, 104 H), 3.99–4.04 (m, 4H), 5.36 (s, 4H), 6.72 (d, *J*=8.7 Hz, 4H), 6.97–7.00 (m, 2), 7.06–7.09 (m, 2H), 7.16–7.19 (m, 2H), 7.29–7.34 (m, 6H), 7.49–7.53 (m, 4 H), 7.69 (s, 2H), 7.89 (d, *J*=7.8 Hz, 2H), 8.00–8.04 (m, 8H), 10.83 (s, 2H); *m/z* MALDI TOF$^+$ 2468.81, $[M]^+$, $C_{135}H_{182}N_4O_{38}^+$ requires 2468.25 (100%); 2491.92, $[M+Na]^+$, $C_{135}H_{182}N_4O_{38}Na^+$ requires 2491.24 (100%); 2507.90, $[M+K]^+$, $C_{135}H_{182}N_4O_{38}K^+$ requires 2507.21 (100%).

7.3 Electrochemical measurements

Voltammetric measurements were conducted with an Autolab Eco-Chemie PGSTAT12 instrument using the following electrodes: a glassy carbon working electrode, $Ag/AgNO_3$ as a reference electrode (double-frit design, inner solution 0.1 M Bu_4NPF_6/0.002 M $AgNO_3$ in acetonitrile, outer solution 0.1 M Bu_4NPF_6 in THF) and a Pt counter electrode. The chamber containing the electrolyte solution (0.1 M Bu_4NPF_6 in THF) was degassed by bubbling with N_2. Potentials are reported with the ferrocene/ferrocenium (Fc/Fc^+) as the internal standard. A scan rate of 0.1 V s^{-1} and a step potential of 0.10 V were used in cyclic voltammetry measurements.

7.4 One-photon photolysis

One-photon photolysis of was carried out with a broad source of light Rayonet RMR-600 (300–400 nm, with peak at 350 nm), while wavelength dependent uncaging experiments were performed with use of and JobinYvon Ltd. Fluoromax2 spectrometer (340 nm, 360 nm, 380 nm, 400 nm, 420 nm, with 5 nm band width).

7.4.1 Actinometry

One-photon uncaging quantum yield was determined with use of Equation 7, according to which quantum yield of uncaging ϕ_u is defined as a ratio of number of molecules uncaged to the number of photons absorbed by the irradiated solution.[148]

$$\phi_u = \frac{kcVN_A}{f(1-10^{-A})} \qquad (7)$$

Equation 7. Equation used in calculating one-photon uncaging quantum yield ϕ_u where k - GABA release rate constant, c - concentration of the photolysed solution, V- volume of the photolysed solution, N_A – Avogadro number, f - number of photons administrated, A - absorption of the irradiated solution at the photolysis wavelength.

The number of molecules released per second, $kcVN_A$, was determined by following the progress of reaction by HPLC. The number of photons absorbed by the solution was calculated considering the number of administrated photons f and absorbance A of the sample. The photon flux of the light source was measured with ferric oxalate actinometry.

Ferric oxalate actinometry protocol[146]

All procedures were carried out in the dark. Ferric oxalate solution (0.5 mL, 0.006 M, prepared by dissolving potassium ferric oxalate trihydrate ($K_3[Fe(C_2O_4)_3]\cdot 3H_2O$, 300 mg) in H_2SO_4 (0.05 M, 100 mL)) was placed in a quartz cuvette and irradiated (with the Rayonet RMR-600 for 10 s, or with the JobinYvon Ltd. Fluoromax2 spectrometer for 120 s) while an identical control sample was kept in the dark. Irradiated ferric oxalate solution (0.2 mL) and a control sample (0.2 mL) were transferred to the cuvettes containing a mixture of buffered 0.1% phenanthroline solution (0.9 mL, prepared by dissolving 22.5 g of $CH_3CO_2Na\cdot 3H_2O$ and 0.100 g of phenanthroline in 100 mL of 0.5 M H_2SO_4) and H_2O (0.9 mL). Samples were kept in the dark for 1 h to allow the complexation to occur and their absorbance at 510 nm was measured. The irradiation time was chosen to ensure that the photoconversion of ferric oxalate does not exceed 5% and that the absorption of the $Fe(phen)_3^{2+}$ complex is within 0.5–1.

Upon exposure to light potassium ferric oxalate ($K_3[Fe(C_2O_4)_3]$) is converted to Fe^{2+} and as the quantum yield ϕ_R of formation of Fe^{2+} is well-known for a range of wavelengths (222–500 nm) the photon flux f irradiating the solution can be calculated with use of Equation 8,

$$f = \frac{no.\ molesFe^{2+}}{\phi_R t(1-10^{-A})} \qquad (8)$$

where ϕ_R is the quantum yield of the ferric oxalate conversion at the irradiation wavelength, t (s) is the irradiation time, $(1-10^{-A})$ is the fraction of light absorbed by the ferric oxalate solution while A is the absorption of 0.006 M solution at the irradiation wavelength. Formation of the colored $Fe(phen)_3^{2+}$complex (ε_{510} = 11,100 M^{-1} cm^{-1}) allows to quantify amount of Fe^{2+} generated during the irradiation by measuring the absorption of irradiated and non-irradiated sample (Equation 9).[147]

$$no.molesFe^{2+} = \frac{V_1 V_3 \Delta A(510\ nm)}{10^3 V_2 l\varepsilon\ (510\ nm)} \qquad \mathbf{(9)}$$

Where V_1 (mL) is the irradiated volume, V_2 (mL) is the aliquot of the irradiated solution transferred to the solution of buffered phenanthroline, V_3 (mL) is the final volume of the complexation solution, l (cm) is the optical path length of the quartz cuvette used for irradiation, ΔA (510 nm) is the difference

in absorbance between the irradiated solution and control stored in the dark, and ε (510 nm) is the extinction coefficient of the complex ($Fe(phen)_3^{2+}$) at 510 nm.

The calculated value of the photon flux was expressed in $E \cdot s^{-1}$ and was converted to photons$\cdot s^{-1}$ by multiplying the obtained value with the Avogadro number. The photon flux determined for Rayonet RMR-600 was $1.89 \pm 0.04 \times 10^{16}$ photons$\cdot s^{-1}$ and for JobinYvon Ltd. Fluoromax2 spectrometer at 360 nm was $3.3 \pm 0.5 \times 10^{15}$ photons$\cdot s^{-1}$.

7.4.2 Wavelength-dependent uncaging of BEF-Pyr-Trp

Fluorescence cuvette (10 mm path length) was filled with citric acid/ sodium citrate buffer (pH 3.0, 3 mL) and150 μL of the buffer were removed and replaced with 150 μL of the **BEF-Pyr-Trp** stock solution in H_2O +0.1% TFA/acetonitrile, (3:2, v/v) (due to the susceptibility of **BEF-PyrTrp** to decomposition we used fractions collected upon semi-preparative HPLC purification as stock solutions and stored them at –80 °C). The concentration (1.35–1.75 μM) was set such that A = 0.15–0.18 (for sample of 90% purity by HPLC and ε_{380} = 90 000 M^{-1} cm^{-1}). After measuring the absorbance the sample was split into 3 batches: *1* - 400 μL, which was photolyzed immediately at 350 nm in Rayonet-RMR 600 (10 min); *2* - 400 μL, which was kept in dark and used as control sample, *3* - 2200 μL, which was placed in the fluorometer and photolyzed at one of the following wavelengths: 340 nm, 360 nm, 380 nm, 400 nm, 420 nm. 35 μL aliquots of the control and photolyzed solution were removed after following time: 0, 150 s, 300 s, 600 s, 900 s, 1200 s, 1800 s, 2800 s, 3800 s, placed in HPLC vials and stored in the liquid nitrogen then analyzed one by one by HPLC with *method 1*.

Release of tryptophan was monitored and quantified at 220 nm, while depletion of starting material **BEF-Pyr-Trp** was quantified at 375 nm. HPLC chromatograms were transferred to Origin and integrated. Amount of released tryptophan was quantified with reference to the calibration curve, which was prepared for concentrations 1.24–6.20 μM with use of *HPLC method 1*.

7.4.3 Uncaging quantum yield of BEF-Pyr-Trp

Photolysis was carried out at 360 nm according to the protocol described in 7.4.2

7.4.4 Uncaging quantum yield of of BEF-Phen-Ind

A solution of **BEF-Phen-Ind** (17 μM in H_2O, 3 mL, 80% pure sample by HPLC, absorption of the solution A = 2.0, ε = 90 000 M^{-1} cm^{-1}) was split into 2 portions: 1 mL was kept in the dark whilst 2 mL were photolyzed at 360 nm with Ryonet-RMR 600. Every minute 30 μL aliquots were taken from the photolyzed reaction mixture and the control sample, placed in vials and stored in liquid nitrogen. After 10 minutes of irradiation samples were analyzed one by one by HPLC with use of *HPLC method 1*. Release of 3-indolepropionic acid was monitored and quantified at 220 nm, while depletion of starting material **BEF-Phen-Ind** was quantified at 375 nm. Amount of released 3-indolepropionic acid

was quantified with reference to the calibration curve that was prepared for concentrations 1.4–6.9 μM and 4.1–20.7 μM using *HPLC method 1*.

7.5 The composition of buffer solutions

Buffers used in stability experiments were prepared according to the following procedures.[184] All solutions were prepared in 100 mL scale.

Citric acid/ sodium citrate, pH 3.0

Prepared from 82 mL of 0.1 M citric acid (obtained upon dissolving 4.20 g of citric acid monohydrate, $C_6H_8O_7 \times H_2O$, in 200 mL of H_2O) and 18 mL of 0.1 M trisodium citrate (obtained upon dissolving 2.94 g of trisodium citrate dehydrate, $C_6H_5O_7Na_3 \times 2H_2O$, in 100 mL of H_2O).

Citric acid/ sodium citrate, pH 5.0

Prepared from 35 mL of 0.1 M citric acid (obtained upon dissolving 4.20 g of citric acid monohydrate, $C_6H_8O_7 \times H_2O$, in 200 mL of H_2O) and 65 mL of 0.1 M trisodium citrate (obtained upon dissolving 2.94 g of trisodium citrate dehydrate, $C_6H_5O_7Na_3 \times 2H_2O$, in 100 mL of H_2O).

PBS, Phosphate buffered saline, Na_2HPO_4 / NaH_2PO_4, pH 7.4

Prepared from 4.0 mL of 0.2 M Na_2HPO_4 (obtained upon dissolving 3.65 g of $Na_2HPO_4 \times 2H_2O$ in 100 mL of H_2O), 0.95 mL of 0.2 M NaH_2PO_4 (obtained upon dissolving 3.12 g of $NaH_2PO_4 \times 2H_2O$ in 100 mL of H_2O) and 95.05 mL of H_2O.

$NaHCO_3$-aCSF, pH 7.4

Prepared from 10 mL of solution A (obtained upon dissolving 0.29 of $CaCl_2 \times 2H_2O$, 1.8 g of glucose, 0.49 g of $MgCl_2 \times 6H_2O$, 0.22 g KCl, 7.37 g of NaCl, 0.19 g of $NaH_2PO4 \times 2H_2O$ in 100 mL of H_2O), 11 mL of solution B (obtained upon dissolving 2.0 g of $NaHCO_3$ in 100 mL of H_2O) and 79 mL of H_2O.

HEPES-aCSF, pH 7.4

Prepared from 10 mL of solution A (obtained upon dissolving 8.47 g of NaCl, 0.22 g KCl, 0.29 g of $CaCl_2 \times 2H_2O$, 1.8 g of glucose, 0.49 g of $MgCl_2 \times 6H_2O$ in 100 mL of H_2O), 10 mL of solution B (obtained upon dissolving 3.57 g of HEPES in 100 mL of H_2O) and 80 mL of H_2O. pH was adjusted to 7.4 with 1.0 M NaOH.

Sodium carbonate/sodium bicarbonate, pH 9.2

Prepared from 10 mL of 0.1 M Na_2CO_3 (obtained upon dissolving 2.11 g of anhydrous Na_2CO_3 in 200 mL of H_2O) and 90 mL of 0.1 M $NaHCO_3$ (obtained upon dissolving 1.68 g of anhydrous $NaHCO_3$ in 200 mL of H_2O).

7.6 Electrophysiology

Experiments were carried out with rat cortical cultures (DIV 14 – 28). Cultures were placed in a chamber perfused with HEPEs-based aCSF (in mM: 145 NaCl, 15 HEPES, 10 glucose, 3 KCl, 2 $CaCl_2$, 2 $MgCl_2$, pH 7.4 (adjusted with NaOH) and osmolarity set to 330 mosmol L^{-1}). All measurements were performed at room temperature. Whole-cell voltage-clamp recordings were acquired using a Multiclamp700b. Recording pipettes were filled with the following internal solution (in mM): 140 CsCl, 0.2 EGTA, 10 HEPES, 2 MgATP, 0.3 Na2GTP, 5 QX-314, pH 7.2 (adjusted with NaOH) and osmolarity set to 290 mosmol L^{-1}. A second patch pipette contained 0.01 – 2 mM of **BEF-Pyr-GABA** and was located close to the recorded neurons for local puffing. Alexa 594 (20 μM) was added to the recording solution to identify the locations and select region of interest for photomanipulation. Neurons were visualized with fluorescent images *via* 800 nm laser scanning. Two-photon irradiation was performed at 720 nm and uncaging was initiated with the laser every 6 s with a duration of 2 – 5 ms and 5 mW of the beam power (300 fs, Ti:sapphire laser). Uncaging was activated with a TTL trigger input, which synchronizes voltage clamp recordings and uncaging. A series of TTL were generated by the imaging laser and recorded as reference of voltage clamp recordings. All of the neurons were recorded at holding potential –70 mV.

References

[1] B. P. Bean, The action potential in mammalian central neurons, *Nat. Rev. Neurosci*., 2007, **8**, 451.

[2] A. Oleinick, F. Lemaître, M. G. Collignon, I. Svir and C. Amatore, Vesicular release of neurotransmitters: converting amperometric measurements into size, dynamics and energetics of initial fusion pores, *Faraday Discuss*., 2013, **164**, 33.

[3] K. A. Korzycka, P. M. Bennett, E. Jose Cueto-Diaz, G. Wicks, M. Drobijev, M. Blanchard-Desce, A. Rebane and H. L, Anderson, Two-photon sensitive protecting groups operating via intramolecular electron transfer: uncaging of GABA and tryptophan, *Chem. Sci*., 2015, **6**, 2419.

[4] T. Fehrentz, M. Schönberger and D. Trauner, Optochemical genetics, *Angew. Chem. Int. Ed.*, 2011, **50**, 12156.

[5] D. F. Owens and A. R. Kriegstein, Is there more to GABA than synaptic inhibition?, *Nat. Rev. Neurosci*., 2002, **3**, 715.

[6] M. Farrant and Z. Nusser, Variations on an inhibitory theme: phasic and tonic activation of GABA-a receptors, *Nat. Rev. Neurosci.,* 2005, **6**, 215.

[7] B. Bettler, K. Kaupmann, J. Mosbacher and M. Gassmann, Molecular Structure and Physiological Functions of GABA-B Receptors, *Physiol. Rev.*, 2004, **84**, 835.

[8] R. H. Kramer, J. J. Chambers and D. Trauner, Photochemical tools for remote control of ion channels in excitable cells, *Nat. Chem. Biol*., 2005, **7**, 360.

[9] R. H. Kramer, D. L Fortin and D. Trauner, New photochemical tools for controlling neuronal activity, *Curr. Opin. Neurobiol*., 2009, **19**, 544.

[10] L. Sjulson and G. Miesenböck, Photocontrol of neural activity: biophysical mechanisms and performance *in vivo*, *Chem. Rev.*, 2008, **108**, 1588.

[11] E. Pastrana, Optogenetics: controlling cell function with light, *Nat. Methods*, 2011, **8**, 24.

[12] L. Fenno, O. Yizhar and K. Deisseroth, The development and application of optogenetics, *Annu. Rev. Neurosci*., 2011, **34**, 389.

[13] G. C. R. Ellis-Davies, Caged compounds: photorelease technology for control of cellular chemistry and physiology, *Nat. Methods*, 2007, **4**, 619.

[14] G. C. R. Ellis-Davies, Are caged compounds still useful? In *Photosensitive Molecules for Controlling Biological Function, Neuromethods*, J. J. Chambers and R. H. Kramer, Eds., Humana Press, 2011, Vol. 55.

[15] G. C. R. Ellis-Davies, Neurobiology with caged calcium, *Chem. Rev*., 2008, **108**, 1603.

[16] J.A. Barltrop and P. Schofield, Photosensitive Protecting Groups, *Tetrahedron Lett*., 1962, **3**, 697.

[17] H. Kaplan, B. Forbush III and J. F. Hoffman, Rapid photolytic release of adenosine 5'-triphosphate from a protected analogue: utilization by the Na:K pump of human red blood cell ghosts, *Biochemistry*, 1978, **17**, 1929.

[18] P. Klán, T. Šolomek, C. G. Bochet, A. Blanc, R. Givens, M. Rubina, V. Popik, A. Kostikov and J. Wirz, Photoremovable protecting groups in chemistry and biology: reaction mechanisms and efficacy, *Chem. Rev.*, 2013, **113**, 119

[19] A. P. Pelliccioli and J. Wirz, Photoremovable protecting groups: reaction mechanism and applications, *Photochem. Photobiol. Sci.*, 2002, **1**, 441.

[20] C. G. Bochet, Photolabile protecting groups and linkers, *J. Chem. Soc., Perkin Trans. 1*, 2002, 125.

[21] J. E. T. Corrie, T. T. Furuta, R. Givens, A. L. Yousef and M. Goeldner, Photoremovable protecting groups used for the caging of biomolecules. In *Dynamic Studies in Biology: Phototriggers, Photoswitches and Caged Biomolecules*, M. Goeldner and R. S. Givens, Eds., Wiley-VCH Verlag GmbH & Co. KGaA: Weinheim, FRG, 2005.

[22] R. S. Givens, P. G. Conrad, A. L. Yousef, I.-I. Lee, Photoremovable protecting groups. In *CRC Handbook of Organic Photochemistry and Photobiology*, 2nd ed., W. Horspool, F. Lenci, Eds., CRC Press: Boca Raton, FL, 2004, pp.69/1-69/3.
[23] C. Sundararajan and D. E. Falvey, Photoremovable protecting groups based on electron transfer chemistry, *Photochem. Photobiol. Sci.*, 2004, **3**, 831.
[24] H. Yu, J. Li, D. Wu, Z. Qiua and Y. Zhang, Chemistry and biological applications of photo-labile organic molecules, *Chem. Soc. Rev.*, 2010, **39**, 464.
[25] G. Mayer and A. Heckel, Biologically active molecules with a "light switch", *Angew. Chem. Int. Ed.*, 2006, **45**, 4900.
[26] C. Brieke, F. Rohrbach, A. Gottschalk, G. Mayer and A. Heckel, Light-controlled tools, *Angew. Chem. Int. Ed.*, 2012, **51**, 8446.
[27] S. Stolik, J. A. Delgado, A. Perez and L. Anasagasti, Measurement of the penetration depths of red and near infrared light in human "ex vivo" tissues, *J. Photochem. Photobiol. B, Biol.*, 2000, **57**, 90.
[28] M. Pawlicki, H. A. Collins, R. G. Denning and H. L. Anderson, Two-photon absorption and the design of two-photon dyes, *Angew. Chem. Int. Ed.*, 2009, **48**, 3244.
[29] W. Denk, Two-photon scanning photochemical microscopy: Mapping ligand-gated ion channel distributions, *Proc. Natl. Acad. Sci. USA*, 1994, **91**, 6629.
[30] D. Warther, S. Gug, A. Specht, F. Bolze, J.-F. Nicoud, A. Mourot and M. Goeldner, Two-photon uncaging: New prospects in neuroscience and cellular biology, *Bioorg. Med. Chem.*, 2010, **18**, 7753.
[31] G. C. R. Ellis-Davies, Two-photon microscopy for chemical neuroscience, *ACS. Chem. Neurosci.*, 2011, **2**, 185.
[32] M. Matsuzaki, G. Ellis-Davies, T. Nemoto, Y. Miyashita, M. Iino and H. Kasai, Dendritic spine geometry is critical for AMPA receptor expression in hippocampal CA1 pyramidal neurons, *Nat. Neurosci.*, 2001, **4**, 1086.
[33] J. Noguchi, A. Nagaoka, S. Watanabe, G. C. R. Ellis-Davies, K. Kitamura, M. Kano, M. Matsuzaki and H. Kasai, *In vivo* two-photon uncaging of glutamate revealing the structure–function relationships of dendritic spines in the neocortex of adult mice, *J. Physiol.*, 2011, **589**, 2447.
[34] M. Matsuzaki, T. Hayama, H. Kasai and G. C. R. Ellis-Davies, Two-photon uncaging of γ-aminobutyric acid in intact brain tissue, *Nat. Chem. Biol.*, 2010, **6**, 255.
[35] E. M. R. Verde, L. Zayat, R. Etchenique and R. Yuste, Photorelease of GABA with visible light using an inorganic caging group, *Front. Neural Circuits*, 2008, **2**, 2.
[36] S. Kantevari, M. Matsuzaki, Y. Kanemoto, H. Kasai and G. C. R. Ellis-Davies, Two-color, two-photon uncaging of glutamate and GABA, *Nat. Methods*, 2010, **7**, 123.
[37] J. M. Amatrudo, J. P. Olson, H. K. Agarwal and G. C. R. Ellis-Davies, Caged compounds for multichromic optical interrogation of neural systems, *Eur. J. Neurosci.*, 2015, **41**, 4.
[38] S. Yao and K. D. Belfield, Two-Photon Fluorescent Probes for Bioimaging, *Eur. J. Org. Chem.*, 2012/17; doi: 10.1002/ejoc.201290042
[39] G. Bort, T. Gallavardin, D. Ogden and P. I. Dalko, From one-photon to two-photon probes: "caged" compounds, actuators, and photoswitches, *Angew. Chem. Int. Ed.*, 2013, **52**, 4526.
[40] T. M. Dore and H. C. Wilson, Chromophores for the delivery of bioactive molecules with two-photon excitation. In *Photosensitive molecules for controlling biological function, Neuromethods*, J. J. Chambers and R. H. Kramer, Eds., Humana Press, 2011, Vol **55**, p 57-92.
[41] G. S. He, L.-S. Tan, Q. Zheng and P. N. Prasad, Multiphoton absorbing materials: molecular designs, characterizations, and applications, *Chem. Rev.*, 2008, **108**, 1245.
[42] M. Albota, D. Beljonne, J.-L. Brédas, J. E. Ehrlich, J.-Y. Fu, A. A. Heikal, S. E. Hess, T. Kogej, M. D. Levin, S. R. Marder, D. McCord-Maughon, J. W. Perry, H. Röckel, M. Rumi, G. Subramaniam, W. W. Webb, X.-L. Wu, Ch. Xu, Design of organic molecules with large two-photon absorption cross sections, *Science*, 1998, **281**, 1653.
[43] S. Gug, F. Bolze, A. Specht, C. Bourgogne, M. Goeldner and J.-F. Nicoud, Molecular Engineering of Photoremovable Protecting Groups for Two-Photon Uncaging, *Angew. Chem. Int. Ed.*, 2008, **47**, 9525, doi: 10.1002/anie.200803964

[44] G. C. R. Ellis-Davies, A chemist and biologist talk to each other about caged neurotransmitters, *Beilstein J. Org. Chem*., 2013, **9**, 64.
[45] D. D. Shi, F. F. Trigo, M. F. Semmelhack and S. S.-H. Wang, Synthesis and biological evaluation of bis-CNB-GABA, a photoactivatable neurotransmitter with low receptor interference and chemical two-photon uncaging properties, *J. Am. Chem. Soc*., 2014, **136**, 1976.
[46] A. Specht, F. Bolze, J.-F. Nicoud and M. Goeldner, Characterization of one- and two-photon photochemical uncaging efficiency. In *Chemical Neurobiology: Methods and Protocols, Methods in Molecular Biology*, M. R. Banghart, Ed., Humana Press, 2013, Vol. 995, p 79-87.
[47] P. Anstaett, A. Leonidova and G. Gasser, Caged phosphate and the slips and misses in determination of quantum yields for ultraviolet-A induced photouncaging, *ChemPhysChem*., 2015, **16**, 1857.
[48] N. I. Kiskin, R. Chillingworth, J. A. McCray, D. Piston and D. Ogden, The efficiency of two-photon photolysis of a "caged" fluorophore, *o*-1-(2-nitrophenyl)ethylpyranine, in relation to photodamage of synaptic terminals, *Eur. Biophys. J.*, 2002, **30**, 588.
[49] I. Aujard, C. Benbrahim, M. Gouget, O. Ruel, J.-B. Baudin, P. Neveu and L. Jullien, *o*-Nitrobenzyl photolabile protecting groups with red-shifted absorption: syntheses and uncaging cross-sections for one- and two-photon excitation, *Chem. Eur. J.*, 2006, **12**, 6865.
[50] G. Papageorgiou and J. E. T. Corrie, Effects of aromatic substituents on the photocleavage of 1-acyl-7-nitroindolines, *Tetrahedron*, 2000, **56**, 8197.
[51] J. Morrison, P. Wan, J. E. T. Corrie and G. Papageorgiou, Mechanisms of photorelease of carboxylic acids from 1-acyl-7-nitroindolines in solutions of varying water content, *Photochem. Photobiol. Sci.*, 2002, **1**, 960.
[52] O. D. Fedoryak, J.-Y. Sul, P. G. Haydon and G. C. R. Ellis-Davies, Synthesis of a caged glutamate for efficient one- and two-photon photorelease on living cells, *Chem. Commun*., 2005, 3664.
[53] G. C. R. Ellis-Davies, M. Matsuzaki, M. Paukert, H. Kasai and D. E. Bergles, 4-Carboxymethoxy-5,7-dinitroindolinyl-Glu: an improved caged glutamate for expeditious ultraviolet and two-photon photolysis in brain slices, *J. Neurosci.*, 2007, **27**, 6601.
[54] G. Papageorgiou and J. E. T. Corrie, Synthesis of an anionically substituted nitroindoline-caged GABA reagent that has reduced affinity for GABA receptors, *Tetrahedron*, 2007, **63**, 9668.
[55] F. F. Trigo, G. Papageorgiou, J. E.T. Corrie, D. Ogden, Laser photolysis of DPNI-GABA, a tool for investigating the properties and distribution of GABA receptors and for silencing neurons in situ, *J. Neurosci. Methods.*, 2009, **181**, 159.
[56] A. Specht, J.-S. Thomann, K. Alarcon, W. Wittayanan, D. Ogden, T. Furuta, Y. Kurakawa and M. Goeldner, New photoremovable protecting groups for carboxylic acids with high photolytic efficiencies at near-UV irradiation. Application to the photocontrolled release of L-glutamate, *ChemBioChem.*, 2006, **7**, 1690.
[57] N. Gagey, P. Neveu, C. Benbrahim, B. Goetz, I. Aujard, J.-B. Baudin and L. Jullien, Two-photon uncaging with fluorescence reporting: evaluation of the *o*-hydroxycinnamic platform, *J. Am. Chem. Soc.*, 2007, **129**, 9986.
[58] N. Gagey, P. Neveu and L. Jullien, Two-photon uncaging with the efficient 3,5-dibromo-2,4-dihydroxycinnamic caging group, *Angew. Chem. Int. Ed.*, 2007, **46**, 2467.
[59] T. Furuta, S. S. Wang, J. L. Dantzker, T. M. Dore, J. W. Bybee, E. M. Callaway, W. Denk and R. Y. Tsien, Brominated 7-hydroxycoumarin-4-ylmethyls: photolabile protecting groups with biologically useful cross-sections for two photon photolysis, *Proc. Natl. Acad. Sci. USA*, 1999, **96**, 1193.
[60] V. R. Shembekar, Y. Chen, Ba. K. Carpenter and G. P. Hess, A protecting group for carboxylic acids that can be photolyzed by visible light, *Biochemistry*, 2005, **44**, 7107.
[61] E. Fino, R. Araya, D. S. Peterka, M. Salierno, R. Etchenique and R. Yuste, RuBi-Glutamate: two-photon and visible-light photoactivation of neurons and dendritic spines, *Front. Neural Circuits*, 2009, **3**, 2.
[62] M. Salierno, E. Marceca, D. S. Peterka, R. Yuste and R. Etchenique, A fast ruthenium polypyridine cage complex photoreleases glutamate with visible or IR light in one and two photon regimes, *J. Inorg. Biochem.*, 2010, **104**, 418.

[63] Y. Zhu, C. M. Pavlos, J. P. Toscano and T. M. Dore, 8-Bromo-7-hydroxyquinoline as a photoremovable protecting group for physiological use: mechanism and scope, *J. Am. Chem. Soc.*, 2006, **128**, 4267.

[64] O. D. Fedoryak, T. M. Dore. Brominated hydroxyquinoline as a photolabile protecting group with sensitivity to multiphoton excitation, *Org. Lett.*, 2002, **4**, 3419.

[65] M. J. Davis, C. H. Kragor, K. G. Reddie, H. C. Wilson, Y. Zhu and T. M. Dore, Substituent effects on the sensitivity of a quinoline photoremovable protecting group to one- and two-photon excitation, *J. Org. Chem.*, 2009, **74**, 1721.

[66] M. Petit, C. Tran, T. Roger, T. Gallavardin, H. Dhimane, F. Palma-Cerda, M. Blanchard-Desce, F. C. Acher, D. Ogden and P. I. Dalko, Substitution effect on the one- and two-photon sensitivity of DMAQ "caging" groups, *Org. Lett*., 2012, **14**, 6366.

[67] L. Donato, A. Mourot, C. M. Davenport, C. Herbivo, D. Warther, J. Léonard, F. Bolze, J.-F. Nicoud, R. H. Kramer, M. Goeldner and A. Specht, Water-soluble, donor–acceptor biphenyl derivatives in the 2-(*o*-nitrophenyl)propyl series: highly efficient two-Photon uncaging of the neurotransmitter-aminobutyric acid at λ=800 nm, *Angew. Chem. Int. Ed.*, 2012, **51**, 1840.

[68] J. P. Olson, H.-B. Kwon, K. T. Takasaki, C. Q. Chiu, M. J. Higley, B. L. Sabatini and G. C. R. Ellis-Davies, Optically selective two-photon uncaging of glutamate at 900 nm, *J. Am. Chem. Soc.*, 2013, **135**, 5954.

[69] J. M. Amatrudo, J. P. Olson, G. Lur, C. Q. Chiu, M. J. Higley and G. C. R. Ellis-Davies, Wavelength-selective one- and two-photon uncaging of GABA, *ACS Chem. Neurosci.*, 2014, **5**, 64.

[70] Y. Sakamoto, S. Boinapally, C. Katan and M. Abe, Synthesis and photochemical reactivity of caged glutamates with π-extended coumarin chromophore as a photolabile protecting group *Tetrahedron Lett.*, 2013, **54**, 7171.

[71] C. Bao, G. Fan, Q. Lin, B. Li, S. Cheng, Q. Huang and L. Zhu, Styryl conjugated coumarin caged alcohol: Efficient photorelease by either one-photon long wavelength or two-photon NIR excitation, *Org. Lett*., 2012, **14**, 572.

[72] S. Boinapally, B. Huang, M. Abe, C. Katan, J. Noguchi, S. Watanabe, H. Kasai, B. Xue and T. Kobayashi, Caged glutamates with π-extended 1,2-dihydronaphthalene chromophore: design, synthesis, two-photon absorption property, and photochemical reactivity, *J. Org. Chem*., 2014, **79**, 7822.

[73] A. Specht, F. Bolze, L. Donato, C. Herbivo, S. Charon, D. Warther, S. Gug, J.-F. Nicoud and M. Goeldner, The donor–acceptor biphenyl platform: A versatile chromophore for the engineering of highly efficient two-photon sensitive photoremovable protecting groups, *Photochem. Photobiol. Sci.*, 2012, **11**, 578.

[74] S. Gug, S. Charon, A. Specht, K. Alarcon, D. Ogden, B. Zietz, J. Léonard, S. Haacke, F. Bolze, J.-F. Nicoud and M. Goeldner, Photolabile glutamate protecting group with high one and two-photon uncaging efficiencies, *ChemBioChem.*, 2008, **9**, 1303.

[75] F. Bolze, J.-F. Nicoud, C. Bourgogne, S. Gug, X. H. Sun, M. Goeldner, A. Specht, L. Donato, D. Warther, G. F. Turi and A. Losonczy, Two-photon uncaging: the chemist point of view, *Opt. Mater.*, 2012, **34**, 1664.

[76] S. Picard, E. Genin, G. Clermont, V. Hugues, O. Mongin and M. Blanchard-Desce, Octupolar chimeric compounds built from quinoline caged acetate moieties: a novel approach for 2-photon uncaging of biomolecules, *New. J. Chem.*, 2013, **37**, 3899.

[77] L. Porrés, O. Mongin, C. Katan, M. Charlot, T. Pons, J. Mertz and M. Blanchard-Desce, Enhanced two-photon absorption with novel octupolar propeller-shaped fluorophores derived from triphenylamine, *Org. Lett.*, 2004, **6**, 47.

[78] P. Dunkel, C. Tran, T. Gallavardin, H. Dhimane, D. Ogden and P. I. Dalko, Quinoline-derived two-photon sensitive quadrupolar probes, *Org. Biomol. Chem*., 2014, **12**, 9899.

[79] C. Tran, T. Gallavardin, M. Petit, R. Slimi, H. Dhimane, M. Blanchard-Desce, F. C. Acher, D. Ogden and P. I. Dalko, Two-photon "caging" groups: effect of position isomery on the photorelease properties of aminoquinoline-derived photolabile protecting groups, *Org. Lett*., 2015, **17**, 402.

[80] J. R. Lakowicz, *Principles of fluorescence spectroscopy*, 3rd ed., Springer: New York, 2006, p 277-284, 341-348, 443-453.
[81] P. Suppan, *Chemistry and light* (in Polish), Wydaw. Naukowe PWN: Warszawa, 1997, p 79-83, translated by J. Prochorow.
[82] S. E. Braslavsky, E. Fron, H. B. Rodrıguez, E. San Roman, G. D. Scholes, G. Schweitzer, B. Valeur and J. Wirz, Pitfalls and limitations in the practical use of Förster's theory of resonance energy transfer, *Photochem. Photobiol. Sci.*, 2008, **7**, 1444.
[83] D. Wöll, J. Smirnova, W. Pfleiderer and U. E. Steiner, Highly efficient photolabile protecting groups with intramolecular energy transfer, *Angew. Chem. Int. Ed.*, 2006, **45**, 2975.
[84] D. Wöll, S. Laimgruber, M. Galetskaya, J. Smirnova, W. Pfleiderer, B. Heinz, P. Gilch and U. E. Steiner, On the mechanism of intramolecular sensitization of photocleavage of the 2-(2-nitrophenyl)propoxycarbonyl (NPPOC) protecting group, *J. Am. Chem. Soc*., 2007, **129**, 12148.
[85] G. Papageorgiou, D. Ogden and J. E. T. Corrie, An antenna-sensitized nitroindoline precursor to enable photorelease of L-glutamate in high concentrations, *J. Org. Chem.*, 2004, **69**, 7228.
[86] G. Papageorgiou, D. Ogden and J. E. T. Corrie, An antenna-sensitised 1-acyl-7-nitroindoline that has good solubility properties in the presence of calcium ions and is suitable for use as a caged L-glutamate in neuroscience, *Photochem. Photobiol. Sci*., 2008, **7**, 423.
[87] M. C. Pirrung, T. M. Dore, Y. Zhu and V. S. Rana, Sensitized two-photon photochemical deprotection, *Chem. Commun*., 2010, **46**, 5313.
[88] S. Picard, E. J. Cueto-Diaz, E. Genin, G. Clermont, F. Acher, D. Ogden and M. Blanchard-Desce, Tandem triad system based on FRET for two-photon induced release of glutamate, *Chem. Commun.*, 2013, **49**, 10805.
[89] E. J. Cueto Díaz, S. Picard, V. Chevasson, J. Daniel, V. Hugues, O. Mongin, E. Genin and M. Blanchard-Desce, Cooperative dyads for two-photon uncaging, *Org. Lett*., 2015, **17**, 102.
[90] H. Lemmetyinen, N. V. Tkachenko, A. Efimov and M. Niemi, Photoinduced intra- and intermolecular electron transfer in solutions and in solid organized molecular assemblies, *Phys. Chem. Chem. Phys*., 2011, **13**, 397.
[91] H. Imahoria, Y. Morib, Y. Matanoa, Nanostructured artificial photosynthesis, *J. Photochem. Photobio. C: Photochem. Rev.*, 2003, **4**, 51.
[92] M. R. Wasielewski, Photoinduced electron transfer in supramolecular systems for artificial photosynthesis, *Chem. Rev.*, 1992, **92**, 435.
[93] R. A. Marcus, On the theory of chemiluminescent electron transfer reactions, *J. Chem. Phys*., 1965, **43**, 2654.
[94] J. W. Leon and D. G. Whitten, Photofragmentation in linked donor-acceptor molecules. Intramolecular single electron transfer induced cleavage of a 1,2-diamine, *J. Am. Chem. Soc*., 1993, **115**, 8038.
[95] C. Costentin, M. Robert and J.-M. Savéant, Electron transfer and bond breaking: recent advances, *Chem. Phys*., 2006, **324**, 40.
[96] IUPAC. Compendium of Chemical Terminology, 2nd ed. (the "Gold Book"). Compiled by A. D. McNaught and A. Wilkinson. Blackwell Scientific Publications, Oxford (1997). XML on-line corrected version: http://goldbook.iupac.org (2006-) created by M. Nic, J. Jirat, B. Kosata; updates compiled by A. Jenkins. ISBN 0-9678550-9-8.
[97] J. R. Miller, L. T. Calcaterra and G. L. Closs, Intramolecular long-distance electron transfer in radical anions. The effects of free energy and solvent on the reaction rates, *J. Am. Chem. Soc*., 1984, **106**, 3047.
[98] M. N. Paddon-Row, Investigating long-range electron-transfer processes with rigid, covalently linked donor-(norbornylogous bridge)-acceptor systems, *Acc. Chem. Res*., 1994,**27**, 18.
[99] S. S. Isied, M. Y. Ogawa and J. F. Wisharts, Peptide-mediated intramolecular electron transfer: long-range distance dependence, *Chem. Rev.*, 1992, **92**, 381.
[100] W. B. Davis, M. R. Wasielewski and M. A. Ratner, Electron transfer rates in bridged molecular systems: a phenomenological approach to relaxation, *J. Phys. Chem. A*, 1997, **101**, 6158.
[101] A. K. Felts, W. T. Pollard and R. A. Friesner, Multilevel redfield treatment of bridge-mediated long-range electron transfer: a mechanism for anomalous distance dependence, *J. Phys. Chem.*, 1995, **99**, 2929.

[102] R. A. Marcus, Electron transfer reactions in chemistry. Theory and experiment, *Rev. Mod. Phys.*, 1993, **65**, 599.
[103] G. Grampp, The Marcus inverted region from theory to experiment, *Angew. Chem. Int. Ed. Engl*., 1993, **32**, 691.
[104] K. Lee and D. E. Falvey, Photochemically removable protecting groups based on covalently linked electron donor-acceptor systems, *J. Am. Chem. Soc*., 2000, **122**, 9361.
[105] C. Sundararajan and D. E. Falvey, Photolytic release of carboxylic acids using linked donor−acceptor molecules: direct versus mediated photoinduced electron transfer to *N*-alkyl-4-picolinium esters, *Org. Lett*., 2005, **7**, 2631.
[106] J. Wang, PhD Thesis, Georgia Institute of Technology, 2007, thesis advisor: S. R. Marder.
[107] Y. Lu, F. Hasegawa, S. Ohkuma, T. Goto, S. Fukuhara, Y. Kawazu, K. Totani, T. Yamashita and T. Watanabe, Highly efficient two-photon initiated polymerization in solvent by using a novel two-photon chromophore and co-initiators, *J. Mater. Chem*., 2004, **14**, 1391.
[108] O. Mongin, L. Porrès, M. Charlot, C. Katan and M. Blanchard-Desce, Synthesis, fluorescence, and two-photon absorption of a series of elongated rodlike and banana-shaped quadrupolar fluorophores: a comprehensive study of structure–property relationships, *Chem. Eur. J.*, **2007**, 13, 1481.
[109] Philip M. Bennett, PhD Thesis, University of Oxford, 2013, thesis advisor: H. L. Anderson.
[110] C. P. Andrieux, A. Le Gorande and J.-M. Savéant, Electron transfer and bond breaking. Examples of passage from a sequential to a concerted mechanism in the electrochemical reductive cleavage of arylmethyl halides, *J. Am. Chem. Soc*., 1992, **114**, 6892.
[111] L. Álvarez-Griera, I. Gallardo and G. Guirado, Estimation of nitrobenzyl radicals reduction potential using spectro-electrochemical techniques, *Electrochim. Acta*, 2009, **54**, 5098.
[112] R. Labrecque, J. Mailhot, B. Daoust, J.-M. Chapuzet and J. Lessard, Electrolabile protecting groups for ketones: the electrochemical reductive cleavage of 1,3-dioxolanes and 1,3-dioxanes containing nitro or halo groups, *Electrochim. Acta*, 1997, **42**, 2089.
[113] J. M. Chapuzet, C. Gru, R. Labrecque and J. Lessard, The electrochemical reductive cleavage of a *p*-nitro-1,3-dioxolane and a *p*-nitro-1,3-dioxane in basic aqueous ethanol at Hg: electrolabile protecting groups of ketones, *J. Electroanal. Chem*., 2001, **507**, 22.
[114] H. L. S. Maia, M.-J. Medeiros, M.-I. Montenegro, D. Pletche, The cathodic cleavage of the 4-nitrobenzyloxycarbonyl group from amine derivatives in aprotic conditions, *J. Chem. Soc. Perkin Trans. II*, 1988, 409.
[115] A. Banerjee and D. E. Falvey, Protecting groups that can be removed through photochemical electron transfer: mechanistic and product studies on photosensitized release of carboxylates from phenacyl esters, *J. Org. Chem.*, 1997, **62**, 6245.
[116] A. Banerjee, K. Lee, Q. Yu, A. G. Fang and D. E. Falvey, Protecting group release through photoinduced electron transfer: wavelength control through sensitized irradiation, *Tetrahedron Lett.* 1998, **39**, 4635.
[117] A. Banerjee, K. Lee and D. E. Falvey, Photoreleseable protecting groups based on electron transfer chemistry. Donor sensitized release of phenacyl groups from alkohols, phosphates and diacids, *Tetrahedron*, 1999, **55**, 12699.
[118] K. Stensrud, J. Noh, K. Kandler, J. Wirz, D. Heger and R. S. Givens, Competing pathways in the photo-favorskii rearrangement and release of esters: studies on fluorinated *p*-hydroxyphenacyl-caged GABA and glutamate phototriggers, *J. Org. Chem*., 2009, **74**, 5219.
[119] R. S. Givens, A. Jung, C.-H. Park, J. Weber and W. Bartlett, New photoactivated protecting groups. 7. *p*-Hydroxyphenacyl: a phototrigger for excitatory amino acids and peptides, *J. Am. Chem. Soc*., 1997, **119**, 8369.
[120] R. S. Givens, J. F. W. Weber, P. G. Conrad, G. Orosz, S. L. Donahue and S. A. Thayer, New phototriggers 9: *p*-hydroxyphenacyl as a C-terminal photoremovable protecting group for oligopeptides, *J. Am. Chem. Soc*., 2000, **122**, 2687.
[121] R. Garner and G. T. Young, Amino-acids and peptides. Part XXXIII. Synthesis of Val5-angiotensin-II by the picolyl ester method, *J. Chem. Soc. C*, 1971, 50.
[122] R. Camble, R. Garner and G. T. Young, Novel facilitation of peptide synthesis, *Nature*, 1968, **217**, 247.

[123] S. Wieditz and H. Schafer, The picolyl group, an electroactive protection group for alkohols, *Acta. Chem. Scand. B*, 1983, **37**, 475.
[124] D. R. Corbin, D. F. Eaton and V. Ramamurthy, Use of polar picolyl protecting groups in peptide synthesis, *J. Org. Chem.*, 1988, **53**, 5386.
[125] M. I. Montenegro, The electrochemical cleavage of protecting groups, *Electrochim. Acta*, 1986, **31**, 607.
[126] C. Sundararajan and D. E. Falvey, C-O Bond fragmentation of 4-picolyl- and *N*-methyl-4-picolinium esters triggered by photochemical electron transfer, *J. Org. Chem*., 2004, **69**, 5547.
[127] C. Sundararajan and D. E. Falvey, Photorelease of carboxylic and amino acids from *N*-methyl-4-picolinium esters by mediated electron transfer, *Photochem. Photobiol. Sci.*, 2006, **5**, 116.
[128] J. B. Borak and D. E. Falvey, Ketocoumarin dyes as electron mediators for visible light induced carboxylate photorelease, *Photochem. Photobiol. Sci*., 2010, **9**, 854.
[129] C. Sundararajan and D. E. Falvey, Photorelease of carboxylic acids, amino acids, and phosphates from *N*-alkylpicolinium esters using photosensitization by high wavelength laser dyes, *J. Am. Chem. Soc.*, 2005, **127**, 8000.
[130] J. B. Borak and D. E. Falvey, A new photolabile protecting group for release of carboxylic acids by visible-light-induced direct and mediated electron transfer, *J. Org. Chem*., 2009, **74**, 3894.
[131] J. E. Raymond, A. Bhaskar, T. Goodson, N. Makiuchi, K. Ogawa and Y. Kobuke, Synthesis and two-photon absorption enhancement of porphyrin macrocycles, *J. Am. Chem. Soc*., 2008, **130**, 17212.
[132] J. J. Michels, M. J. O'Connell, P. N. Taylor, J. S. Wilson, F. Cacialli and H. L. Anderson, Synthesis of conjugated polyrotaxanes, *Chem. Eur. J*., 2003, **9**, 6167.
[133] Y. Cheng, L. Zhao, Y. Lic and T. Xu, Design of biocompatible dendrimers for cancer diagnosis and therapy: current status and future perspectives, *Chem. Soc. Rev*., 2011, **40**, 2673.
[134] C. Monnereau, E. Blart and F. Odobel, A cheap and efficient method for selective para-iodination of aniline derivatives, *Tetrahedron Lett.*, 2005, **46**, 5421.
[135] F. Terenziani, A. Painelli, C. Katan, M. Charlot and M. Blanchard-Desce, Charge instability in quadrupolar chromophores: symmetry breaking and solvatochromism, *J. Am. Chem. Soc*., 2006, **128**, 15742.
[136] J. Olmsted, Calorimetric determinations of absolute fluorescence quantum yields, *J. Phys. Chem.*, 1979, **83**, 2581.
[137] C. Katan, M. Charlot, O. Mongin, C. Le Droumaguet, V. Jouikov, F. Terenziani, E. Badaeva, S. Tretiak and M. Blanchard-Desce, Simultaneous control of emission localization and two-photon absorption efficiency in dissymmetrical chromophores, *J. Phys. Chem. B*, 2010, **114**, 3152.
[138] A. I. Ciuciu, K. A. Korzycka, W. J. M. Lewis, P. M. Bennett, H. L. Anderson and L. Flamigni, Model dyads for 2PA uncaging of a protecting group via photoinduced electron transfer, *Phys. Chem. Chem. Phys*., 2015, **17**, 6554.
[139] A. Weller, Photoinduced electron transfer in solution: exciplex and radical ion pair formation free enthalpies and their solvent dependence, *Z. Phys. Chem. NF*, 1982, **133**, 93.
[140] S. R. Greenfield, W. A. Svec, D. Gosztola and M. R. Wasielewski, Multistep photochemical charge separation in rod-like molecules based on aromatic imides and diimides, *J. Am. Chem. Soc*., 1996, **118**, 6767.
[141] D. D. Tanner, J. J. Chen, L. Chen and C. Luelo, Fragmentation of substituted acetophenones and halobenzophenone ketyls. Calibration of a mechanistic probe, *J. Am. Chem. Soc.*, 1991, **113**, 8074.
[142] A. Rosspeintner and E. Vauthey, Bimolecular photoinduced electron transfer reactions in liquids under the gaze of ultrafast spectroscopy, *Phys. Chem. Chem. Phys*., 2014, **16**, 25741.
[143] A. Harriman, Further comments on the redox potentials of tryptophan and tyrosine, *J. Phys. Chem.*, 1987, **91**, 6102.
[144] I. M. Kovach, I. H. Pitman and T. Higuchi, Amino acid esters of phenols as prodrugs: synthesis and stability of glycine, β-aspartic acid, and α-aspartic acid esters of *p*-acetamidophenol, *J. Pharm. Sci*., 1981, **70**, 881.

[145] R. W. Hay and L. Main, Catalysis by aromatic aldehydes and carbon dioxide of the hydrolysis of the *p*-nitrophenyl esters of L-leucine, glycine and L-β-phenylalanine, *Aust. J. Chem.*, 1968, **21**, 155.
[146] H. J. Kuhn, S. E. Braslavsky and R. Schmidt, Chemical actinometry, *Pure Appl. Chem.*, 1989, **61**, 187.
[147] M. Montalti, A. Credi, L. Prodi and M. T. Gandolfi, Chemical actinometry. In *Handbook of Photochemistry*, Taylor & Francis Group: Florida, 2006, p 601–604.
[148] J. Goedhart and T. W. J. Gadella, Photolysis of caged phosphatidic acid induces flagellar excision in *Chlamydomonas*, *Biochemistry*, 2004, **43**, 4263.
[149] R. S. Givens, K. Stensrud, P. G. Conrad II, A. L. Yousef, C. Perera, S. N. Senadheera, D. Heger and J. Wirz, *p*-Hydroxyphenacyl photoremovable protecting groups — robust photochemistry despite substituent diversity, *Can. J. Chem.*, 2011, **89**, 364.
[150] K. F. Stensrud, D. Heger, P. Sebej, J. Wirz and R. S. Givens, Fluorinated photoremovable protecting groups: the influence of fluoro substituents on the photo-Favorskii rearrangement, *Photochem. Photobiol. Sci*., 2008, **7**, 614.
[151] C.-H. Park and R. S. Givens, New photoactivated protecting groups. 6. *p*-Hydroxyphenacyl: a phototrigger for chemical and biochemical probes, *J. Am. Chem. Soc*., 1997, **119**, 2453.
[152] K. Monnier, G. Schmitt, B. Laude, M.-F. Mercier, M. M. Kubicki and M. Jannin, Étude de la stéréochimie de la réaction de cycloaddition dipolaire-1,3 de quelques 5-phényl-3,6-dihydro-2*H*-1,4-oxazin-2-ones avec les *N*-méthyl et *N*-phénylmaléimides, *Can. J. Chem*., 1995, **73**, 181.
[153] G. Papageorgiou and J. E. T. Corrie, Synthesis and properties of carbamoyl derivatives of photolabile benzoins, *Tetrahedron*, 1997, **53**, 3917.
[154] P. G. Conrad II, R. S. Givens, J. F. W. Weber and K. Kandler, New phototriggers[1]: extending the *p*-hydroxyphenacyl π−π* absorption range, *Org. Lett*., 2000, **2**, 1545.
[155] J. B. Edson, L. P. Spencer and J. M. Boncella, Photorelease of primary aliphatic and aromatic amines by visible-light-induced electron transfer, *Org. Lett*., 2011, **13**, 6156.
[156] F. M. Rossi, M. Margulis, C.-M. Tang and J. P. Y. Kao, *N*-Nmoc-L-glutamate, a new caged glutamate with high chemical stability and low pre-photolysis activity, *J. Biol. Chem.*, 1997, **272**, 32933.
[157] A. Barberis, J. W. Mozrzymas, P. I. Ortinski and S. Vicini, Desensitization and binding properties determine distinct α1β2γ2 and α3β2γ2 $GABA_A$ receptor-channel kinetic behavior, *Eur. J. Neurosci*., 2007, **25**, 2726.
[158] D. J. Maconochie, J. M. Zempel and J. H. Steinbach, How quickly can $GABA_A$ receptors open?, *Neuron*, 1994, **12**, 61.
[159] M. V. Jones and G. L. Westbrook, Desensitized states prolong $GABA_A$ channel responses to brief agonist pulses, *Neuron*, 1995, **15**, 181.
[160] R. O. Schoenleber and B. Giese, Photochemical release of amines by C,N-bond cleavage, *Synlett*, 2003, 501.
[161] C. A. M. Seidel, A. Schulz and M. H. M. Sauer, Nucleobase-specific quenching of fluorescent dyes. 1. Nucleobase one-electron redox potentials and their correlation with static and dynamic quenching efficiencies, *J. Phys. Chem*., 1996, **100**, 5541.
[162] V. V. Pavlishchuka and A. W. Addison, Conversion constants for redox potentials measured versus different reference electrodes in acetonitrile solutions at 25 °C, *Inorg. Chim. Acta*, 2000, **298**, 97.
[163] J. E. Raymond, A. Bhaskar, T. Goodson, N. Makiuchi, K. Ogawa and Y. Kobuke, Synthesis and two-photon absorption enhancement of porphyrin macrocycles, *J. Am. Chem. Soc*., 2008, **130**, 17212.
[164] F. Tancini1, Y.-L. Wu, W. B. Schweizer, J.-P. Gisselbrecht, C. Boudon, P. D. Jarowski, M. T. Beels, I. Biaggio and F. Diederich, 1,1-Dicyano-4-[4-(diethylamino)phenyl]buta-1,3-dienes: Structure–Property Relationships, *Eur. J. Org. Chem*., 2012, 2756.
[165] A. Elangovan, Y.-H. Wang and T.-I. Ho, Sonogashira coupling reaction with diminished homocoupling, *Org. Lett*., 2003, **5**, 1841.
[166] C. Gentilini, M. Boccalon and L. Pasquato, Straightforward synthesis of fluorinated amphiphilic thiols, *Eur. J. Org. Chem*., 2008, 3308.

[167] V. Hrobáriková, P. Hrobarik, P. Gajdos, I. Fitilis, M. Fakis, P. Persephonis and P. Zahradnık, Benzothiazole-based fluorophores of donor-π-acceptor-π-donor type displaying high two-photon absorption, *J. Org. Chem*., 2010, **75**, 3053.
[168] C. B. Nielsen, M. Johnsen, J. Arnbjerg, M. Pittelkow, S. P. McIlroy, P. R. Ogilby and M. Jørgensen, Synthesis and characterization of water-soluble phenylene-vinylene-based singlet oxygen sensitizers for two-photon excitation, *J. Org. Chem.*, 2005, **70**, 7065.
[169] N. M. Yoon, C. S. Pak, H. C. Brown, S. Krishnamurthy and T. P. Stocky, Selective reductions. XIX. Rapid reaction of carboxylic acids with borane-tetrahydrofuran. Remarkably convenient procedure for the selective conversion of carboxylic acids to the corresponding alcohols in the presence of other functional groups, *J. Org. Chem*., 1973, **38**, 2786.
[170] T. J. Donohoe, A. Ironmonger and N. M. Kershaw, Synthesis of (–)-(Z)-deoxypukalide: application of ring closing metathesis to the construction of complex aromatic heterocylic natural products, *Angew. Chem. Int. Ed*., 2008, **47**, 7314.
[171] A. Pace, P.Pierro, S. Buscemi, N. Vivona and E. Clennan, Photooxidations of alkenes in fluorinated constrained media: fluoro-organically modified NaY as improved reactors for singlet oxygen "ene" reactions, *J. Org. Chem*., 2007, **72**, 2644.
[172] T. Terasaka, T. Kinoshita, M. Kuno, N. Seki, K. Tanaka and I. Nakanishi, Structure-based design, synthesis, and structure-activity relationship studies of novel non-nucleoside adenosine deaminase inhibitors, *J. Med. Chem*., 2004, **47**, 3730.
[173] A. Boccia, V. Lanzilotto, V. Di Castro, R. Zanoni, L. Pescatori, A. Arduinib and A. Secchi, Preparation, reactivity and controlled release of SAMs of calix[4,6]arenes and calix[6]arene-based rotaxanes and pseudorotaxanes formed on polycrystalline Cu, *Phys. Chem. Chem. Phys.*, 2011, **13**, 4452.
[174] C. S. Hawes, R. Babarao, M. R. Hill, K. F. White, B. F. Abrahams and P. E. Kruger, Hysteretic carbon dioxide sorption in a novel copper(II)-indazole-carboxylate porous coordination polymer, *Chem. Commun.*, 2012, **48**, 11558.
[175] S. H. Lee, M. J. Kim, S.-H. Lee, J. Kim, H.-J. Park and J. Lee, Thiazolylmethyl ortho-substituted phenyl glucoside library as novel C-aryl glucoside SGLT2 inhibitors, *Eur. J. Med. Chem*., 2011, **46**, 2662.
[176] X.-D. Xiong, W.-X. Chen, Y.-Y. Kuang and F.-E. Chen, A novel and practical synthesis of 2-amino-5-hydroxypropiophenone, *Org. Prep. Proc. Int*., 2009, **41**, 423.
[177] P. Chand, Y. S. Babu , S. Bantia, N. Chu, L. B. Cole, P. L. Kotian, W. G. Laver, J. A. Montgomery, V. P. Pathak, S. L. Petty, D. P. Shrout, D. A. Walsh and G. M. Walsh, Design and synthesis of benzoic acid derivatives as influenza neuraminidase inhibitors using structure-based drug design, *J. Med. Chem.*, 1997, **40**, 4030.
[178] A. Blanc and C. G. Bochet, Wavelength-controlled orthogonal photolysis of protecting groups, *J. Org. Chem.*, 2002, **67**, 5567.
[179] C. J. MacNevin, F. Atif, I. Sayeed, D. G. Stein and D. C. Liotta, Development and screening of water-soluble analogues of progesterone and allopregnanolone in models of brain injury, *J. Med. Chem.*, 2009, **52**, 6012.
[180] J. W. Lampe, C. K. Biggers, J. M. Defauw, R. J. Foglesong, S. E. Hall, J. M. Heerding,. W. Darges, J. E. Davis, F. R. Hubbard and M. L. Stamper, Synthesis and protein kinase inhibitory activity of balanol analogues with modified benzophenone subunits, *J. Med. Chem*., 2002, **45**, 2624.
[181] S. S. Agasti, C.-C. You, P. Arumugama and V. M. Rotello, Structural control of the monolayer stability of water-soluble gold nanoparticles, *J. Mater. Chem*., 2008, **18**, 70.
[182] Y. Yamada, A. Akiba, S. Arima, C. Okada, K. Yoshida, F. Itou, T. Kai, T. Satou, K. Takeda and Y. Harigaya, Synthesis of linear tripeptides for right-hand segments of complestatin, *Chem. Pharm. Bull.*, 2005, **53**, 1277.
[183] K. Takeda, A. Akiyama, H. Nakamura, S. Takizawa, Y. Mizuno, H. Takayanagi, Y. Harigaya, Dicarbonates: convenient 4-dimethylaminopyridine catalyzed esterification reagents, *Synthesis*, 1994, 1063.
[184] R. M. C. Dawson, D. C. Elliot, W. H. Elliot; K. M. Jones, *Data for biochemical research*, 3rd ed., Oxford Science Publ., 1986.

[185] A. N. Albertsen, S. E. Maurer, K. A. Nielsena and P.-A. Monnard, Transmission of photo-catalytic function in a self-replicating chemical system: in situ amphiphile production over two protocell generations, *Chem. Commun*., 2014, **50**, 8989.
[186] J. Bertran-Vicente, R. A. Serwa, M. Schümann, P. Schmieder, E. Krause and C. P. R. Hackenberger, Site-specifically phosphorylated lysine peptides, *J. Am. Chem. Soc*., 2014, **136**, 13622.
[187] W. K. Bell, B. M. Rawlings, B. K. Long, R. C. Webb, B. K. Keitz, L. Häußling and C. G. Willson, Poling and crosslinking processes in NLO polymers, *J. Polym. Sci. A Polym. Chem*., 2014, **52**, 2769.
[188] V. Somoza, M. Lindenmeier, E. Wenzel, O. Frank, H. F. Erbersdobler and T. Hofmann, Activity-guided identification of a chemopreventive compound in coffee beverage using in vitro and in vivo techniques, *J. Agric. Food Chem*., 2003, **51**, 6861.
[189] H. Chaumeil, P. Jacques, V. Diemer, D. Le Nouën, C. Carré, A ^{13}C NMR study of pyridinium phenoxide series with increasing sterical hindrance reveals the dramatic influence of torsion on their structure, *J. Mol. Struct*., 2011, **1002**, 70.
[190] P. Bolduc, A. Jacques and S. K. Collins, Efficient macrocyclization achieved via conformational control using intermolecular noncovalent π-cation/arene interactions, *J. Am. Chem. Soc*., 2010, **132**, 12790.
[191] A. B. Powell and S. S. Stahl, Aerobic oxidation of diverse primary alcohols to methyl esters with a readily accessible heterogeneous Pd/Bi/Te catalyst, *Org. Lett*., 2013, **15**, 5072.
[192] R. Manetsch, L. Zheng, M. T. Reymond, W.-D. Woggon and J.-L. Reymond, A catalytic antibody against a tocopherol cyclase inhibitor, *Chem. Eur. J*., 2004, **10**, 2487.
[193] C. Kong, N. Jana and T. G. Driver, Rh_2(II)-Catalyzed selective aminomethylene migration from styryl azides, *Org. Lett*., 2013, **15**, 824.
[194] N. Brauer, B. Buchmann, U. Klar, A. T. Laak, G. Langer, B. Lindenthal, A. Rotgeri, 2,5-Disubstituierte 2H-indazole als EP2-rezeptor-antagonisten, Ger. Offen. DE 102009049662A1, April 14 2011.
[195] D. H. Young, Use of certain amides as probes for detection of antitubulin activity and resistance monitoring, U.S. Patent, 6,500,405, Dec 31 2002.
[196] A. R. Katritzky and Z. Dega-Szafran, Proton and carbon-13 NMR studies of 1-substituted pyridinium salts, *Magn. Reson. Chem*., 1989, **27**, 1090.
[197] B. M. Khadilkar and G. L. Rebeiro, Previous article next article table of contents microwave-assisted synthesis of room-temperature ionic liquid precursor in closed vessel, *Org. Proc. Res. Dev*., 2002, **6**, 826.
[198] R. W. Jr. Heidebrecht, T. A. Miller, K. J. Wilson, D. J. Witter, J. Grimm, Hydroxyalkylarylamide derivatives, Pat. Appl., WO 2007087130 A2, August 2 2007.
[199] W. Denk, J. H. Strickler, W. W. Webb, Two-photon laser scanning fluorescence microscopy, *Science*, 1990, **248**, 73.
[200] G. Papageorgiou, D. C. Ogden, A. Barth and J. E. T. Corrie, Photorelease of carboxylic acids from 1-acyl-7-nitroindolines in aqueous solution: rapid and efficient photorelease of L-glutamate, *J. Am. Chem. Soc*., 1999, **121**, 6503.
[201] G. Papageorgiou, D. Ogden, G. Kelly and J. E. T. Corrie, Synthetic and photochemical studies of substituted 1-acyl-7-nitroindolines, *Photochem. Photobiol. Sci*., 2005, **4**, 887.
[202] N. S. Makarov, M. Drobizhev and A. Rebane, Two-photon absorption standards in the 550-1600 nm excitation wavelength range, *Optics Express*, 2008, **16**, 4029.
[203] J. D. Wilkinson, G. Wicks, A. Nowak-Król, Ł. G. Łukasiewicz, C. J. Wilson, M. Drobizhev, A. Rebane, D. T. Gryko and H. L. Anderson, Two-photon absorption in butadiyne-linked porphyrin dimers: torsional and substituent effects, *J. Mater. Chem. C*, 2014, **2**, 6802.